CGRP family of G protein-coupled receptors and their signalling in human cardiovascular cells

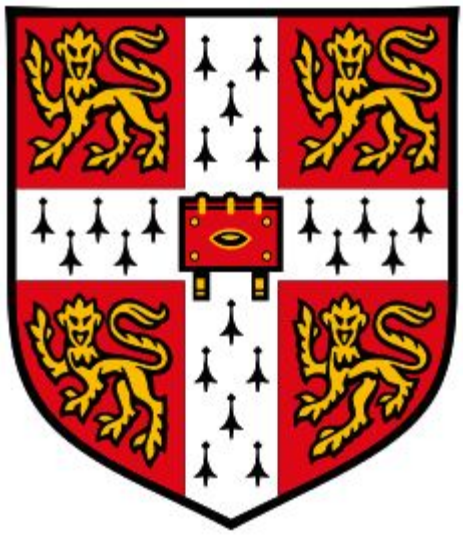

Ashley James Clark

Department of Pharmacology

University of Cambridge

This thesis is submitted for the degree of Doctor of Philosophy

Trinity Hall September 2020

CGRP family of G protein-coupled receptors and their signalling in human cardiovascular cells

This thesis is the result of my own work and includes nothing which is the outcome of work done in collaboration except as declared in the Preface and specified in the text. It is not substantially the same as any that I have submitted, or, is being concurrently submitted for a degree or diploma or other qualification at the University of Cambridge or any other University or similar institution except as declared in the Preface and specified in the text. I further state that no substantial part of my thesis has already been submitted, or, is being concurrently submitted for any such degree, diploma or other qualification at the University of Cambridge or any other University or similar institution except as declared in the Preface and specified in the text. It does not exceed the prescribed word limit for the relevant Degree Committee (Faculty of Biology).

Ashley J. Clark

CGRP family of G protein-coupled receptors and their signalling in human cardiovascular cells

The aim of this body of work has been to further understanding of the signalling and functional properties of a unique family of cell surface receptors known as G protein-coupled receptors (GPCRs), and one of their subclasses: The CGRP receptor family. These receptors are crucial for transducing information from the extracellular to intracellular space. While much pharmacological research has gone into understanding the signalling and function of GPCRs in recombinant systems, there is a very little knowledge of these receptors in their native environment and at endogenous expression levels. Nor is there direct evidence for potentially controversial phenomena such as signalling bias in endogenous cells. This provided the impetus to address the need for a better understanding of the pharmacology of endogenous human calcitonin receptor-like receptor (CLR) in its native cellular environment. Therefore, primary human cardiovascular cells, gene editing techniques, and a host of intracellular assays were used to study the signalling properties of this GPCR family, revolving around the CLR, to attempt to uncover how these receptors function endogenously. Through the research presented here, it is shown that the CLR, when stimulated by endogenous agonists activates a whole host of signalling pathways to bring about differing physiological effects. In doing so it has revealed unique roles for calcitonin-gene related peptide (CGRP), adrenomedullin (AM), and the little-understood peptide adrenomedullin 2 (AM2). All of which are dependent on the presence of a group of GPCR accessory proteins known as receptor activity-modifying proteins (RAMPs). These proteins are not only crucial for CLR function, but this dissertation demonstrates the remarkable way in which they govern and dictate the intracellular signalling of the CGRP family of peptides endogenously. Beyond this, the G protein and accessory protein involvement in certain signalling cascades, the spatiotemporal aspects to CGRP peptide signalling, and the functional outcomes of signalling in cell organoid models are all explored. It is the author's belief that this work adds a great deal to the understanding of the CLR, and more generally takes a step forward in the understanding of endogenous GPCR signalling bias.

Ashley J. Clark

“Don’t adventures ever have an end? I suppose not. Someone else always has to carry on the story.”

- J.R.R. Tolkien, The Fellowship of the Ring

Table of Contents

Acknowledgments

There are many people, too many to list here, who I would like to thank for making it possible to complete this thesis. From support staff to principal investigators, I am truly grateful to everyone who made it possible for me to conduct this research.

The first person I would like to thank directly is my supervisor Dr. Graham Ladds, for his endless help and guidance from the first time I stepped into the lab, to becoming the scientist I am today. This guidance extended beyond purely the scientific, to for instance, encouragement to attend scientific conferences that not only helped me truly understand my research and its context within the field, but were fantastic and unforgettable experiences in themselves. I would also like to my industrial supervisor Dr. Mark Wigglesworth for his help and advice as well as providing invaluable access to research equipment within AstraZeneca; that otherwise would not have been possible without him. As well as everyone at AstraZeneca who helped me learn how to navigate their facilities and use their equipment. I would like to thank the entire Ladds laboratory and the many people who have been a member during my time there. Some of whom were Mathew Harris, Dewi Safitri, and Ho Yan Yeung; they were lovely people to work with and good friends. I would like to thank the many collaborators the Ladds laboratory has both within the University of Cambridge and beyond. One in particular was Prof. David Poyner, with whom it was a pleasure to work and share my research.

Lastly, I would like to thank my family and loved ones, most of all my mother, sister, and Sally, as without their support none of this would have been possible. As well as my dog Boris, the best friend a person could wish for, right up to the end.

List of Publications

Clark, A.J., R. Thompson, I. Winfield, M. Wigglesworth, G. Ladds "Physiological consequences of RAMP-mediated agonist bias at the calcitonin receptor-like receptor" *pA_2 online BPS Pharmacology 2017*

Routledge, S. J., J. Simms, **A. J. Clark**, H. Y. Yeung, M. J. Wigglesworth, I. M. Dickerson, P. Kitchen, G. Ladds, and D. R. Poyner. 2020. "Receptor component protein, an endogenous allosteric modulator of family B G protein coupled receptors." *Biochim Biophys Acta Biomembr* 1862 (3):183174. doi: 10.1016/j.bbamem.2019.183174.

Clark, A.J., G. Ladds. 2020. "Adrenomedullin/Intermedin" *Encyclopedia of Molecular Pharmacology* 67383_0_En, (Chapter 5055-1).

Clark A. J., N. Mullooly, D. Safitri, D. R. Poyner, D. Giani, M. Wigglesworth, G. Ladds. "CGRP-receptor family reveals endogenous GPCR agonist bias and its significance in primary human cardiovascular cells" *submitted to Nature, preprint uploaded to BioRxiv.org: https://biorxiv.org/cgi/content/short/2020.12.21.423730v1*

Abbreviations

AC – adenylyl cyclase

AM – adrenomedullin

AMYR – amylin receptor

AM_1R – adrenomedullin receptor

AM2 – adrenomedullin 2

AM_2R – adrenomedullin 2 receptor

CALCR – gene encoding the calcitonin receptor protein (CTR)

CALCRL– gene encoding the calcitonin receptor-like receptor protein (CLR)

cAMP – cyclic adenosine monophosphate

cGMP – cyclic guanosine monophosphate

CGRP – calcitonin gene related peptide

CGRPR – calcitonin gene related peptide receptor

CLR – calcitonin receptor-like receptor

CRISPR – clustered regularly interspaced short palindromic repeats

CTR – calcitonin receptor

DAG – diacylglycerol

DNA – deoxyribonucleic acid

ECM – extracellular matrix

EC50 – agonist concentration required to produce a half-maximal response

Emax – maximum response achieved by a ligand

EPAC – exchange protein directly activated by cAMP

ERK – extracellular signal-regulated kinase

FSK – forskolin

GAPDH – glyceraldehyde 3-phosphate dehydrogenase

GC – guanylyl cyclase

GDP – guasosine diphosphate

GPCR – G protein-coupled receptor

GRK – GPCR kinases

GTP – guanosine triphosphate

HCM – human cardiac myocyte

HUVEC – human umbilical vein endothelial cell

HUAEC – human umbilical artery endothelial cell

IP_3 – inositol (1,4,5)-trisphosphate

NO – nitric oxide

NOS – nitric oxide synthase

MOI – multiplicity of infection

PDE – phosphodiesterase

PIP_2 – phosphatidyl inositol (4,5)-bisphosphate

PIP_3 – phosphatidyl inositol (3,4,5)-trisphosphate

PI3K – phosphoinositide 3-kinase

PKA – protein kinase A

PKC – protein kinase C

PLA_2 – phospholipase A_2

PLC – phospholipase C

PM – plasma membrane

PMA – phorbol 12-myristate 13-acetate

PTX – pertussis toxin

qRT-PCR – quantitative reverse transcription polymerase chain reaction

RAMP – receptor activity-modifying protein

RNA – ribonucleic acid

RCP – receptor component protein

SB – stimulation buffer

sgRNA – single-guide RNA

VEGF – vascular endothelial growth factor

VSMC – vascular smooth muscle cell

List of Figures

List of Tables

Preface

This thesis is the result of my own work and includes nothing which is the outcome of work done in collaboration except as declared in the preface and specified in the text:

Additional repeats for a select number of experiments were performed by: Dewi Safitri (University of Cambridge) (**Figure 3.14**, **Figure 3.18D**), and Rachel Thompson (University of Cambridge) (**Figure 3.11**, **Table 3.8**).

This thesis is not the same as any work that has already been submitted before for any degree or qualification. Parts of this thesis have been published as per the list of publications section.

This thesis does not exceed the prescribed word limit of the Degree Committee for the Faculty of Biology

Word count: approximately 44,500

Abstract

The aim of this body of work has been to further understanding of the signalling and functional properties of a unique family of cell surface receptors known as G protein-coupled receptors (GPCRs), and one of their subclasses: The CGRP receptor family. These receptors are crucial for transducing information from the extracellular to intracellular space. While much pharmacological research has gone into understanding the signalling and function of GPCRs in recombinant systems, there is a very little knowledge of these receptors in their native environment and at endogenous expression levels. Nor is there direct evidence for potentially controversial phenomena such as signalling bias in endogenous cells. This provided the impetus to address the need for a better understanding of the pharmacology of endogenous human calcitonin receptor-like receptor (CLR) in its native cellular environment. Therefore, primary human cardiovascular cells, gene editing techniques, and a host of intracellular assays were used to study the signalling properties of this GPCR family, revolving around the CLR, to attempt to uncover how these receptors function endogenously. Through the research presented here, it is shown that the CLR, when stimulated by endogenous agonists activates a whole host of signalling pathways to bring about differing physiological effects. In doing so it has revealed unique roles for calcitonin-gene related peptide (CGRP), adrenomedullin (AM), and the little-understood peptide adrenomedullin 2 (AM2). All of which are dependent on the presence of a group of GPCR accessory proteins known as receptor activity-modifying proteins (RAMPs). These proteins are not only crucial for CLR function, but this dissertation demonstrates the remarkable way in which they govern and dictate the intracellular signalling of the CGRP family of peptides endogenously. Beyond this, the G protein and accessory protein involvement in certain signalling cascades, the spatiotemporal aspects to CGRP peptide signalling, and the functional outcomes of signalling in cell organoid models are all explored. It is the author's belief that this work adds a great deal to the understanding of the CLR, and more generally takes a step forward in the understanding of endogenous GPCR signalling bias.

Chapter 1. General Introduction

Cell Surface Receptors

Cell surface receptors provide the interface between cells, the building blocks of life, and the outside world. There are multiple families including: Ligand-gated ion channels or ionotropic (e.g. cys-loop receptors), Catalytic or enzyme-linked receptors (e.g. Receptor tyrosine kinases), and lastly the largest and most diverse is the G protein-coupled receptor (GPCR) or metabotropic receptor family (e.g. muscarinic acetylcholine receptors) (Lefkowitz 2004). Cell surface receptors can come into contact with the external environment, internal environment, and very often the extracellular matrix (ECM). Which is a non-cellular network made up of collagens, elastin, fibronectin, and other glycoproteins. The matrix components provide a complex network for cells to reside in tissues by binding each other, matrix proteins and cell adhesion receptors (Theocharis et al. 2016). The molecules that can bind and invoke a reaction in cell surface receptors are broad and include: peptide hormones, neurotransmitters, cytokines, adhesion molecules and growth factors. The role of cell surface receptors is to then transduce signals into cells from the extracellular environment, which ultimately regulates a huge array of cellular functions, such as: survival, growth, migration, differentiation, and the maintenance of homeostasis.

G protein-coupled receptors

GPCRs or 7 transmembrane receptors, are, as mentioned above, the largest family of cell surface receptors (Lefkowitz 2007). These are characterised by their seven membrane-spanning domains, and a brief overview of this architecture is as follows: A GPCR contains one continuous polypeptide starting with an extracellular domain comprised of the N-terminus flowing into seven hydrophobic

transmembrane domains connected by three protruding extracellular loops and three intracellular loops, followed by an intracellular domain created by the C terminus (Alexander et al. 2019). It is thought GPCRs comprise over 1% of the human genome (Bjarnadottir et al. 2006, Smith et al. 2018). Which codes for approximately 800 distinct GPCRs; roughly 350 are non-sensory and the targets of most pharmacological intervention, the rest are sensory, with about 400 olfactory receptors, 33 for taste and a small amount of light and pheromone sensing receptors (Alexander et al. 2019). GPCRs regulate almost all physiological functions and are implicated in the pathogenesis of a huge range of diseases: such as diabetes, heart disease, and Parkinson's to name a few. Their importance in these disease states is such that approximately 35% of currently prescribed drugs target GPCRs making them the most heavily targeted protein family for therapeutics (Sriram and Insel 2018). Although it wasn't until cloning of the mammalian β2 adrenoceptor or adrenergic receptor and comparison with the visual rhodopsin and its 7-transmembrane structure that it was first realised they were part of a much larger family of receptors (Dixon et al. 1986). Cloning of other adrenergic, serotonin and muscarinic cholinergic receptors further confirmed the existence of this family of receptors (Dohlman et al. 1991). They have been multiple attempts to classify them into different subgroups or families, based on distinctive features. Although they all share the 7 stretches of 25-35 mostly hydrophobic amino-acids that reside in the plasma membrane. The main vertebrate families based on phylogenetic analysis of the human genome are: Glutamate, Rhodopsin, Adhesion, Frizzled/Taste2, and Secretin (Schioth and Fredriksson 2005). Family A or the rhodopsin family is the largest and contains the first member (rhodopsin) to be crystallised (Palczewski et al. 2000). They have characteristically short N termini and the NSxxNPxxY motif in transmembrane 7. As for the metabotropic glutamate receptors or family C they have relatively long N termini and a 'Venus fly trap' binding domain for glutamate. The adhesion family of receptors (Family B2), were first discovered through bioinformatic studies (Fredriksson et al. 2002, Bjarnadottir et al. 2004). Their N-termini are rigid, highly glycosylated structures, and some contain a GPCR proteolytic domain. Then there is the frizzled family (Family F), first confirmed as a family of GPCRs by (Slusarski et al. 1997). They are amongst the most highly conserved GPCRs, and

contain common features such as IFL in transmembrane 2 and SxKTL in transmembrane 7. There are also the taste 2 sensory receptor subfamilies. Lastly, there is secretin or Family B named after the first receptor discovered in this family. It has 18 members coded by 15 genes (**Table 1.1**), and it is some of the members of this family that will be the focus of this thesis: Family B GPCRs have long N-terminal domain or extracellular domain (ECD) (100-160 amino acids), suitable for binding the carboxy-terminal segment of large peptide ligands (Wootten et al. 2017). This ECD is the first stage of the proposed 'two-domain model' of binding unique to the class. The family B GPCRs also have very similar transmembrane domains, despite the class Bs only sharing 20-45% sequence homology (de Graaf et al. 2017). Moreover, many of the structures have been solved by X-ray crystallography and cryogenic electron microscopy (Cryo-EM); the calcitonin gene related peptide (CGRP) receptor is the most recent example (Liang et al. 2018). This family has been implicated in many human diseases; two of which are obesity and type 2 diabetes, and for this reason they have been the a target for much drug design (Archbold et al. 2011), although this has not been without its challenges (Hoare 2005) with non-peptide targeting proving difficult up until very recently (Zhao et al. 2020). In this study they found a non-peptide agonist for the glucagon-like peptide-1 (GLP-1) receptor that could activate the receptor through a novel agonist binding site.

Family B GPCRs	Ligands
GCGR	Glucagon, Oxyntamodulin
GIP	GIP
GLP-1	GLP-1, Exendin , Liraglutide, Glucagon
GLP-2	GLP-2, Teduglutide
Secretin	Secretin, VIP
GHRH	GHRH, D-Ala^2-GHRH
PAC_1	PACAP-27, PHM
$VPAC_1$	VIP, PACAP-27, PG 99-465
$VPAC_2$	VIP, PACAP-27, BAY55-9837
PTH1	PTH, PTHrP, TIP
PTH2	PTH, PTHrP, TIP
CRF_1	CRF, Urocortin 1, Sauvagine
CRF_2	CRF, Urocortin 1, Sauvagine, Urocortin 3
CLR	CGRP, Adrenomedullin, Adrenomedullin 2
CGRP	CGRP, Adrenomedullin, Adrenomedullin 2
AM_1	CGRP, Adrenomedullin, Adrenomedullin 2
AM_2	CGRP, Adrenomedullin, Adrenomedullin 2
CT	Calcitonin, Amylin, CGRP
AMY_1	CGRP, Amylin
AMY_2	Amylin

Table 1.1. Family B GPCR members. All 18 members of the GPCRs in the Family B classification system, separated into five subfamilies based on similarities in their physiological roles.

GPCR activation and signalling

GPCRs perform their functions through initiating signalling cascades; in order to do this they need to be activated, (although this can happen constitutively (Zhang et al. 2014)) it is predominately achieved through binding ligands that act as agonists. There are a huge variety of possible agonists including: small molecules, peptides, large peptide hormones, large protein domains, neurotransmitters, photons, odorants and ions (Alexander et al. 2017). The receptors themselves are allosteric proteins (DeVree et al. 2016), meaning they exist in multiple conformational states and the

above agonists can change their confirmation through binding to the extracellular face of the receptor. This triggers a series of events whereby the receptor undergoes a conformational change, this then opens the transducer binding site and influences intracellular protein engagement with the receptor (Hilger et al. 2018, Kenakin 2017). Just as there are many molecules capable of interacting with GPCRs at their extracellular face, there is also a huge variety of intracellular proteins that can engage with the receptor from inside the cell. Some of which are: G proteins, arrestins, PDZ-domain-containing scaffolds, and those without such as A kinase anchor proteins (AKAPs) and Receptor activity modifying proteins (RAMPs) (Dunn and Ferguson 2015, Peterson and Luttrell 2017), and these will be explored in more detail below starting with G proteins.

G protein activation and signalling

G proteins are the canonical GPCR interacting proteins. They are heterotrimeric meaning that they are composed of 3 subunits: Gα, Gβ, and Gγ. Although Gβ and Gγ are obligate heterodimers. Their canonical activation pathway involves agonist binding first, this then induces a conformational change in the receptor. This in turn promotes a conformational change in the G proteins, importantly this causes guanine exchange factor (GEF) activity to catalyse the release of guanosine diphosphate (GDP) and replacement with guanosine triphosphate (GTP) on the Gα subunits, which is aided by a much greater concentration of GTP in cells relative to GDP (Oldham and Hamm 2008). This destabilises the complex and leads to Gα and Gβγ subunits dissociating and activating a host of possible signalling pathways specific to each G protein which will be discussed further separately. There are 16 Gα proteins, 5Gβ, and 13 Gγ subunits (Wootten et al. 2018) producing many different combinations. The 16 Gα proteins are further categorised into four major families (**Table 1.2**). Furthermore, there are a series of subtype-specific residues in each of the families of Gα proteins around the protein core (Flock et al. 2017). These residues create a selectivity barcode enabling selective G protein binding by the specific GPCR-agonist combination. This barcode can also be read differently by different GPCRs as

they may bind the same positions in the GPCR but a receptor can have distinct residues in that position (Flock et al. 2017).

Gα subunits			
$G\alpha_{s/olf}$	$G\alpha_{i/o}$	$G\alpha_{q/11}$	$G\alpha_{12/13}$
α_s	α_{i1}, α_{i2}, α_{i3}	α_q	α_{12}
α_{sXL}	α_o	α_{11}	α_{13}
α_{olf}	α_t	α_{14}	
	α_z	$\alpha_{15/16}$	
	α_{gust}		

Table 1.2. Gα subunit classification. All 16 member of the Gα family of proteins divided into classes broadly based on their function.

There are multiple effectors regulated by G proteins These can include adenylyl cyclase (AC), guanylyl cyclase (GC), phosphodiesterases (PDEs), phospholipase A2 (PLA2), phospholipase C (PLC), phosphoinosite 3-kinases (PI3Ks). These are capable of directly or indirectly modulating levels of second messengers such as cyclic adenosine monophosphate (cAMP), cyclic guanosine monophosphate (cGMP), diacylglycerol (DAG), inositol trisphosphate (IP_3), phosphatidylinositol 4,5-bisphosphate (PIP_2), Phosphatidylinositol (3,4,5)-trisphosphate (PIP_3), and calcium. G proteins also modulate extracellular signal-regulated protein kinases 1 and 2 ($ERK_{1/2}$), and ion channel activity (Marinissen and Gutkind 2001). Each in turn can trigger distinct signalling cascades. Some of which are shown in (**Figure 1.1).** The most well-studied of these pathway is the $G\alpha_s$ mediated pathway. Once activated this itself then activates a family of enzymes known as the adenylyl cyclases (ACs). These belong to the Class III nucleotidyl cyclase family (along with the guanylyl cyclases, that convert GTP to cGMP). There are 10 adenylyl cyclase isoforms, the first nine are bound to the membrane and AC10 is soluble (Willoughby and Cooper 2007). Once activated by $G\alpha_s$ they convert ATP into cAMP, however they can be regulated by other proteins and molecules such as calcium bound to calmodulin, this is capable of stimulating AC1 and AC8, and calcium alone inhibits AC5 and AC6. PKA and PKC are also

known to modulate adenylyl cyclases (Halls and Cooper 2017). cAMP itself can activate a myriad of downstream effects by activating effectors such as protein kinase A (PKA) and the cAMP- and the cAMP-regulated exchange factor for Rap1 (EPAC), or cAMP response element–binding protein (CREB) leading to gene regulation, regulation of metabolism, positive inotropy in the heart, gluconeogenesis or lipolysis (Ravnskjaer et al. 2016, Boularan and Gales 2015). It is thought that adenylyl cyclases can also exist in lipid rafts (Pike et al. 2002) these compartmentalise cAMP signalling enabling localised and distinct signalling events, within these rafts many other proteins can co-localise with a host of other proteins including A kinase anchoring proteins (AKAPs), PKA, PKC, and phosphodiesterases – the enzymes that degrade cAMP. Together this can create signalling micro-domains (Ayling et al. 2012). The next family to mention is the $G\alpha_{i/o}$, defined by their ability to inhibit adenylyl cyclases and their sensitivity to inhibition by pertussis toxin (PTX). It is important to note that it is not simply $G\alpha$ subunits that trigger signalling cascades. The $G\beta\gamma$ subunit also has many important roles such as stimulating small GTPases such as Ras to activate MAPKs, they can also regulate K^+ channels (e.g. in the heart via M2 muscarinic receptors), and phosphatidylinositol 3-kinase (PI3K) (Neves et al. 2002).

The $G_{q/11}$ pathway, and α subunits are made up of the members described in (**Table 1.2**), of these $G\alpha_q$ and $G\alpha_{11}$ are the most ubiquitously expressed and share 88% amino-acid sequence homology (Mizuno and Itoh 2009). They are activated in the same manner as the previous G proteins, but activate a unique signalling cascade: $G\alpha_{q/11}$ binds and activates phospholipase C (PLC) at the plasma membrane (**Figure 1.1**). This then hydrolyses phosphatidylinositol-4,5-bisphosphate (PIP_2) into diacylglycerol and inositol 1,4,5 trisphosphate (IP_3). DAG itself can then activate protein kinase C which has a number of phosphorylation targets. But the most well studied continuation of this pathway is through IP_3; this diffuses into the cell to the IP_3 receptor on the endoplasmic reticulum (ER) membrane (Kamato et al. 2017). This receptor acts as a channel allowing calcium release into the cytosol from these ER stores, the response is then enhanced by calcium mediated calcium release to produce a wave of calcium before it is quickly taken back up into the ER by store operated calcium entry (SOCE)

(Thillaiappan et al. 2019). Lastly there is the $G\alpha_{12}$ and $G\alpha_{13}$ G protein family. The α subunits have 70% amino-acid sequence homology (Singer et al. 1994) and are ubiquitously expressed. As for the downstream pathways, these are much less well understood. Having said that, it has been established that they can regulate the activation of RhoGTPases (Aittaleb et al. 2010). In order to do so they must first activate their effectors; proteins belonging to a family known as RH domain containing guanine nucleotide exchange factors for Rho (RH–RhoGEFs). Examples of these known to be regulated by $G\alpha_{12}$ and $G\alpha_{13}$ include: p115RhoGEF, PDZ–RhoGEF and LARG (Fukuhara et al. 2000, Kourlas et al. 2000). RhoGTPases belong to the RAS family of monomeric (as opposed to heterotrimeric G proteins) GTP binding proteins with a slow rate of innate GTPase activity so are bound to GTP or GDP depending on their state of activation. They can then lead to the regulation of many processes such as gene expression and actin cytoskeleton rearrangement (Sit and Manser 2011). $G\alpha_{12}$ and $G\alpha_{13}$ themselves are regulated by kinases, PKC is a kinase has been heavily implicated in their phosphorylation and regulation it was initially thought only $G\alpha_{12}$ was regulated by PKC (Kozasa and Gilman 1996), before it was shown that $G\alpha_{13}$ is also inhibited by PKC (Offermanns et al. 1996).

It is also important to acknowledge that there is a temporal aspect to the above GPCR signalling, in the example of the parathyroid receptor (PTHR) there is short and long term signalling, which appears physiologically relevant as short term signalling appears to cause rapid calcium mobilisation at the bone surface whereas long term signalling seems to lead to bone growth (Hanyu et al. 2012). There is also evidence that sustained β- adrenenoreceptor signalling leads to upregulation of the PCK1 gene (Tsvetanova and von Zastrow 2014). In the canonical model of GPCR signalling these second messengers then lead to kinase activation (GRKs, PKA, PKC) and negative feedback to the receptor by β-arrestin recruitment to the phosphorylated receptor, G protein uncoupling, and recruitment of endocytic machinery (Pavlos and Friedman 2017).

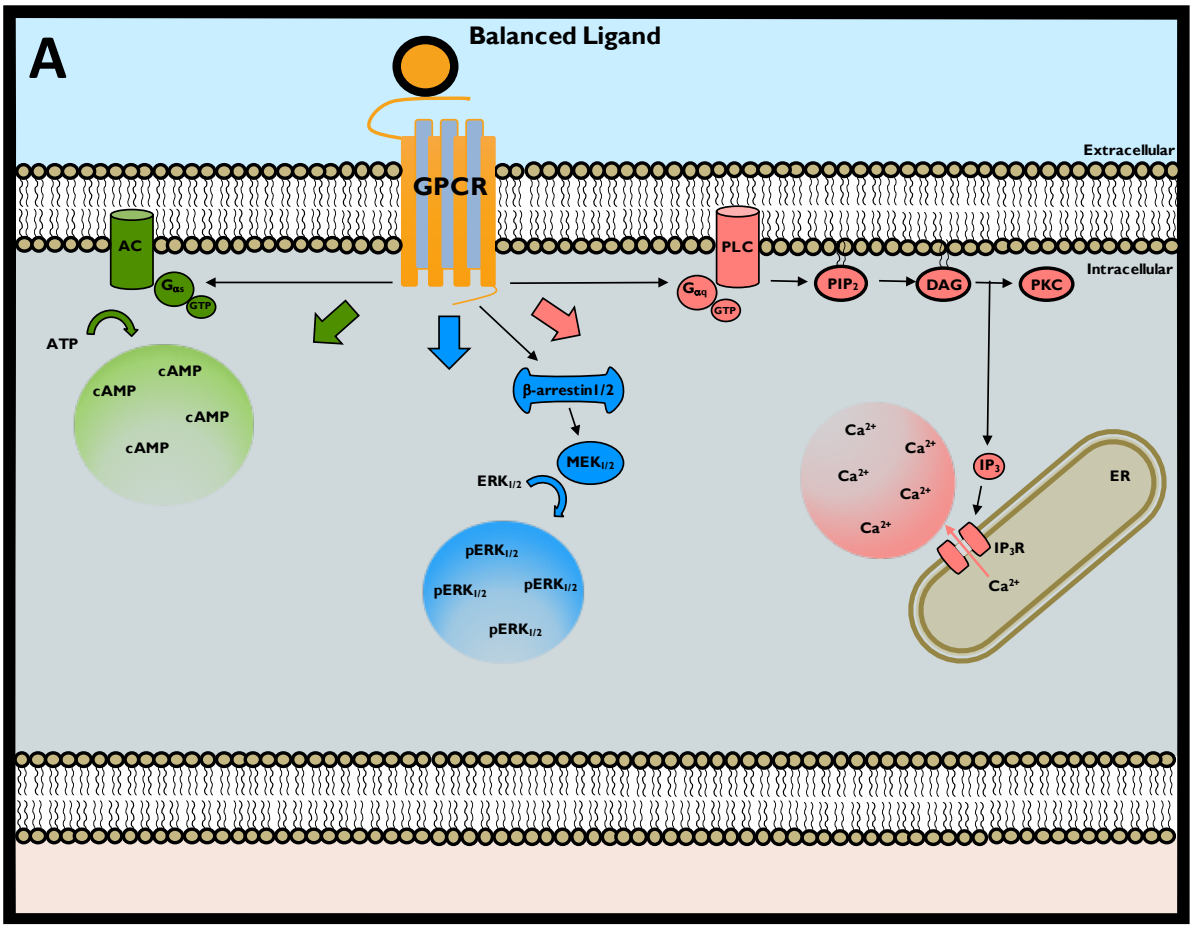

Figure 1.1. Typical signal transduction pathways downstream of a GPCR Schematic representation of a ligand stimulating GPCR activation; capable of recruiting Gα, Gq, and β-arrestin and their subsequent second messenger signaling pathways represented here by cAMP, calcium, and $pERK_{1/2}$ respectively. Also shown is the inherent amplification possible from the stimulation of a single GPCR producing a wave of second messenger production intracellularly.

G protein-independent signalling

Arrestins, briefly mentioned above, act as negative regulators of G protein signalling, there are two non-visual arrestins in humans: β-arrestin1 and β-arrestin2. Interestingly, they also act as scaffolds for G protein independent signalling, primarily for the activation of mitogen-activated protein kinases such as ERK1/2 (MAPKs) (**Figure 1.1**), AKT, SRC, nuclear factor-κB (NF-κB) Kinases

(Ranjan et al. 2017). Moreover, it is now known they undergo conformational changes upon GPCR binding, and the extent of these changes leads to different outcomes (Lee et al. 2016).

GPCR Internalisation and Termination

In the canonical GPCR activation scheme, receptors are phosphorylated, often by GRKs (Benovic et al. 1986). They can also be phosphorylated by protein kinase A (PKA) and Protein Kinase C (PKC), they then phosphorylate serine and threonine residues on the carboxyl tail or in the third intracellular loop of the agonist bound receptor. This results in β-arrestin binding which prevents further G protein recruitment thus terminating signalling. It is thought this is achieved by binding similar regions to the G proteins in the intracellular core thus sterically hindering them. β-arrestins then mediated receptor internalisation via clathrin coated pits and degradation or recycling (Goodman et al. 1996, Oakley et al. 1999). Other proteins involved in this process include clathrin adaptor protein 2 (AP2) which aids in clathrin coated pit formation, and dynamin that cuts the clathrin coated pit off from the remainder of the plasm membrane (both of which are targeted by inhibitors later in this dissertation). A major component of this process is the activity of the regulators of G protein signalling (RGS) proteins mentioned above, the shorten the length of time that GTP is bound to a G protein (and therefore how long it is activated) through stimulating GTP hydrolysis. There are over 20 members of the RGS protein family (Coleman et al. 1994). Although this termination pathway can proceed as above for some receptors, the picture is much more complex than the original model for others; with some receptors having been shown to bind G proteins and β-arrestins at the same time and forming a 'super-complex' (Thomsen et al. 2016); this can be attributed to the recently observed biphasic engagement of β-arrestins by receptors (Shukla et al. 2014) where it was shown that the N-terminal domain of the arrestin interacts with the phosphorylated C-terminal tail of the GPCR first. Then a second weaker interaction is possible which involves the finger loop of the arrestin inserting into the receptor core. This interaction is thought to occlude G protein binding. This provides a possible explanation for

another recently observed phenomenon: GPCRs capable of mediating signalling from multiple subcellular locations; including the golgi membranes and endosomes (Eichel and von Zastrow 2018, Yarwood et al. 2017). This demonstrates their signalling goes beyond purely the plasma membrane, and distinct pools of plasma membrane or intracellular cAMP/pERK$_{1/2}$ have been detected providing evidence for a spatial as well as temporal elements to GPCR signalling.

GPCR Signalling bias

Signalling bias or biased agonism is a concept that describes the ability of individual ligands acting at the same GPCR to trigger different conformations leading to distinct levels of effector recruitment, patterns of signalling, and potentially unique physiological outcomes (**Figure 1.2**). An appreciation for this phenomenon first began when G protein independent β-arrestin mediated signalling was discovered (Wei et al. 2003, Violin and Lefkowitz 2007). From there ligand bias was then demonstrated between G proteins and β-arrestin mediated signalling (Violin and Lefkowitz 2007). Whereby different ligands had a preference for activating different pathways through the same receptor (**Figure 1.2**). Whereas, traditionally GPCRs were considered to switch between "on" and "off" conformations; known as the two-state model, it is now largely defunct. Due to the understanding that receptors can exist in a multitude of confirmations, and that these can be influenced by ligands. Crucially, ligands can be described in terms of two innate properties: affinity and efficacy. The former describes their ability to bind a receptor and the latter describes their ability to elicit a functional consequence. Antagonists for example possess an affinity for a receptor but no efficacy, whereas agonists possess both, and it is now known both affinities and their efficacies can vary at a single GPCR (Wisler et al. 2014). Importantly, bias is a relative term, and is usually in reference to a 'balanced ligand' at the signalling pathways or a single endogenous agonist for the receptor in studies of synthetic biased agonists (Smith et al. 2018). If we take the ligand from (**Figure 1.1**) as an example of a balanced ligand then (**Figure 1.2**) shows three different examples of possible biased ligands at that receptor.

Furthermore, there are subtle differences in types of bias: ligand encoded bias is generated by the ligand and the conformational changes it induces in the GPCR: preferentially recruiting one G protein over another, or G proteins vs β-arrestins. Observed as an increased potency in dose-response analysis of one pathway and decreased potency at another (relative to the balanced agonist). Biased receptors are those that stimulate one pathway over another despite stimulation by the balanced agonist; this can be different receptors in the same family, or a receptor containing mutations that means it recruits certain effectors less well (Kliewer et al. 2019). Then there is system bias where, expression or overexpression of certain proteins such as GRKs, G proteins or β-arrestins can bias a system towards a certain response, demonstrating that some bias can be tissue specific. It is important to

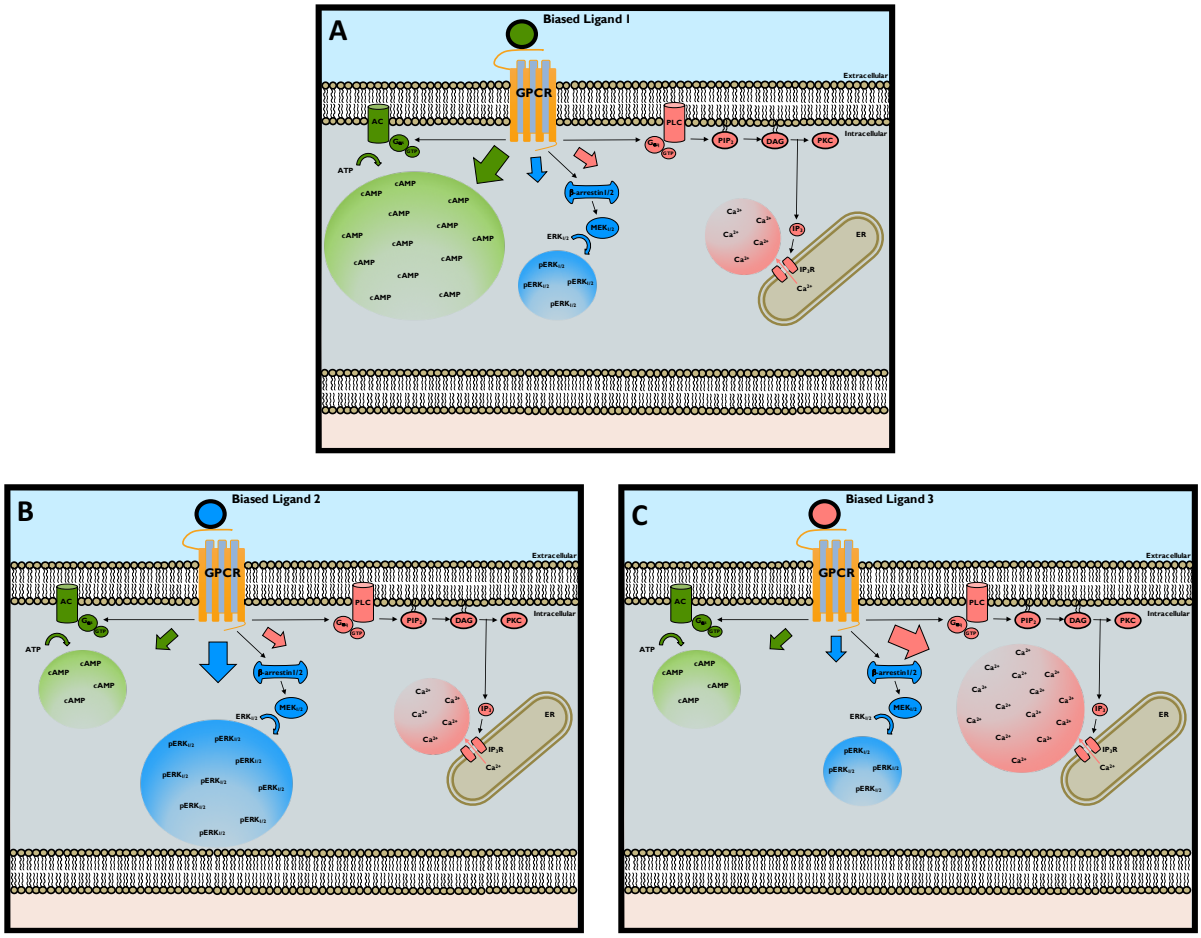

Figure 1.2. Representation of GPCR signalling bias. Schematic representation of a ligand stimulating GPCR activation; capable of recruiting Gα, Gq, and β-arrestin and their subsequent signaling pathways represented here by cAMP, calcium, and $pERK_{1/2}$ respectively. GPCR activation and signalling bya ligand biased towards cAMP (**A**), calcium (**B**), or $pERK_{1/2}$ (**C**) signalling relative to a balanced ligand represented schematically in Figure 1.1.

distinguish between ligand bias and system bias (Onaran et al. 2014). This can be achieved using methods such as quantifying bias - bias can be quantified through adapting the operational model of pharmacological agonism (Black and Leff 1983, Kenakin 2017), and through the generation of bias plots (Gregory et al. 2010).

Biased agonism created renewed interest in GPCRs as therapeutic targets, by providing a way to theoretically design ligands to produce desired outcomes, while minimising unwanted side effects through the same GPCR. Rather than simply activating or antagonising the receptor (Rajagopal et al. 2010, Davenport et al. 2020). An important example of bias and its therapeutic implications comes from the μ-opioid receptor. Morphine acts through this receptor to produce potent analgesic effects. However, alongside these it also causes undesirable side effects including respiratory depression and constipation. A trailblazing mouse knockout study suggested that the adverse effects and morphine tolerance were mediated by β-arrestin 2 signalling and receptor regulation, whereas the beneficial analgesic effects were thought to be G protein driven (Raehal et al. 2005). Thus, paving the way for the development of biased agonists at the μ-opioid receptor, and providing a potential example of how signalling bias can be therapeutically beneficial. Oliceridine is one G protein biased agonist, with reduced β-arrestin recruitment, currently under clinical trail evaluation. Compared to morphine this drug showed equivalent levels of analgesia with reduced side effects (Singla et al. 2019), crucially when examined specifically there was a reduction in negative respiratory side effects (Ayad et al. 2020) However, the development of biased agonists is not without its challenges and controversies; a recent study of another G protein biased agonist in mice still demonstrated respiratory depression despite being G protein biased (Hill et al. 2018). Furthermore, a recent study using β-arrestin recruitment deficient mutations of the μ-opioid receptor in mice showed increased analgesia but no reduction in respiratory side effects (Kliewer et al. 2019). Although this does not entirely refute the original findings, with multiple studies still supporting the evidence that reducing β-arrestin 2 recruitment does reduce tolerance (Raehal et al. 2011). Most recently a study that produced their

own β-arrestin 2 knockout mice recorded morphine evoking negative side effects such as constipation and respiratory depression (Kliewer et al. 2020) suggesting all negative side effects cannot be attributed to β-arrestins. Overall this seems to suggest that signalling bias observed in recombinant and mouse studies and how they reflect the outcomes seen in humans is not as fully understood as previously thought; and observations may well have been simplified too heavily down to a binary choice between G proteins and β-arrestins. Therefore, these reports demonstrate further study of the underlying signalling bias is needed. As well as highlighting the perils and limitations of extrapolating from rodent studies to human.

The calcitonin receptor-like receptor

In 1993, The calcitonin receptor-like receptor (CLR), originally classified as CRLR, was first identified and cloned in mammalian systems (Chang et al. 1993, Njuki et al. 1993). It is a member of the aforementioned family B GPCRs (**Table 1.1**), it is most closely related to the calcitonin receptor, and is endogenously activated by peptide ligands (McLatchie et al. 1998). These ligands are calcitonin gene related peptide (CGRP), adrenomedullin (AM) and adrenomedullin 2 (AM2); all members of the CGRP superfamily of peptides (calcitonin and amylin are the other members that do not activate CLR). As with most GPCRs it primarily couples to G proteins, in heterologous systems it has been shown to activate G_s, $G_{i/o}$, $G_{q/11/14}$ (Hay et al. 2018). These are able to regulate effectors such as adenylyl cyclase and PL C to generate intracellular second messengers including cAMP and Ca^{2+}, which then activate their respective intracellular signalling cascades. There is also much evidence of CLR recruitment of β-arrestins, internalisation and recycling (Hilairet et al. 2001, Kuwasako et al. 2000, Gingell et al. 2020). The CLR has been implicated in many diseases such as osteoporosis and renal cell carcinoma (Nikitenko et al. 2013).

Receptor activity-modifying proteins

The CLR is unique in that it forms obligate heterodimers with Receptor activity-modifying proteins (RAMPs) in order to traffic and form a functional receptor at the plasma membrane (McLatchie et al. 1998, Muff et al. 1998). RAMPs are small membrane spanning proteins, all have a large extracellular N terminus, a single transmembrane domain and a small intracellular C-terminal domain that regulate the function of certain GPCRs. There are three members of the family; RAMP1, RAMP2, and RAMP3 - and amino acid alignment shows 31% homology between them all (Barbash et al. 2017). They are widely expressed in humans, RAMP1 is expressed in the brain, pancreas and gastrointestinal tract, while RAMP2 is more highly expressed in the lungs (McLatchie et al. 1998). Most work has focused on the interaction of RAMPs with Family B GPCRs as such at least 9 of the 18 Family B GPCRs have recognised RAMP interactions (Hay and Pioszak 2016). With a further two known receptor-RAMP interactions outside of Family B (Serafin et al. 2020), as Family B make up a very small proportion of the GPCR family as a whole yet at least half interact with RAMPs it is likely that a huge range of GPCR-RAMP interactions are yet to be discovered; this is supported by predictions from co-evolution studies (Barbash et al. 2019). Returning to RAMP interactions with the CLR specifically, it is one of the most heavily studied receptor-RAMP interaction in heterologous systems, and the RAMPs form three individual receptors in combination with the CLR: CLR-RAMP1 named the 'CGRP Receptor', CLR-RAMP2 the 'AM_1 Receptor' and CLR-RAMP3 the 'AM_2 Receptor' (McLatchie et al. 1998). Of the three the CLR-RAMP1 is the only one to have had its structure resolved (Liang et al. 2018) (**Figure 1.3**), moreover it is currently the only receptor bound to a RAMP to have its structure published at this resolution.

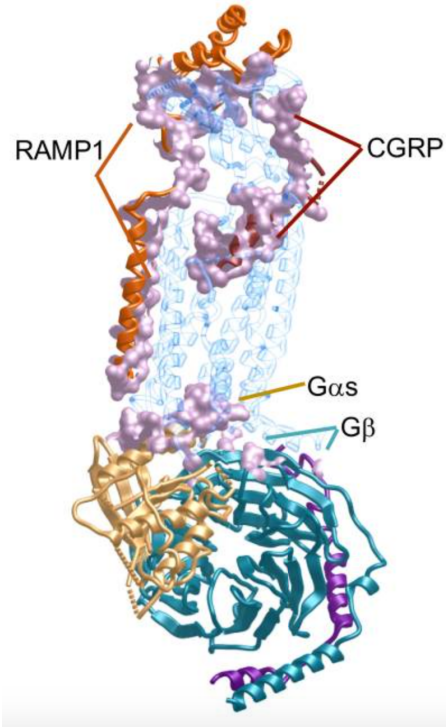

Figure 1.3. Calcitonin receptor-like receptor. CGRP–CLR–RAMP1–Gs cryo-EM structure illustrating the extent of CLR interactions with other proteins in the -structure. Figure from (Liang et al. 2018).

CGRP peptide family

CGRP overview

Calcitonin Gene-Related Peptide or CGRP is a 37 amino acid peptide – the main α-form is produce by alternative RNA processing of the calcitonin gene and was first discovered in 1982 (Amara et al. 1982). There is also a β-form, produced from a different gene but thought to be a duplication of the gene for the α-form, it differs by only three amino-acids and they both have similar roles. The key difference is that the α-form is found systemically whereas the β-form is found in the enteric system (Zaidi et al. 1990, Alevizaki et al. 1986). When CGRP is discussed in the literature, and here, it is in reference to the major α-form unless otherwise stated. CGRP is predominantly known physiologically

as a potent vasodilator (Brain et al. 1985), as well as having roles in pain regulation, in the peripheral and central nervous system, and in the cardiovascular system (Rosenfeld et al. 1983).

CGRP Pharmacology

The receptor through which CGRP predominately acts and has been most well studied in relation to CGRP is CLR-RAMP1 or the CGRP receptor. It is worth also noting that when the calcitonin receptor (CTR) is co -expressed in heterologous studies produces the amylin 1 receptor which has a high affinity receptor for CGRP (as well as amylin) (Walker et al. 2015). Although it is not known whether this has any physiological relevance (Gingell et al. 2019). Research has also suggested that receptor component protein (RCP) is essential to CLR-RAMP function (Evans et al. 2000), but there is controversy over how universal this protein's function is, as it is also a component of RNA polymerase III (Hu et al. 2002). It is also important to note that CLR-RAMP2 and CLR-RAMP3, while generally considered as AM receptors also bind and respond to CGRP (Weston et al. 2016, Qi et al. 2013) in co-expression models but again the relevance of this is yet to be fully explored. As for the pharmacology of the CGRP acting at the CGRP receptor, first and foremost it is a G_s-coupled receptor capable of potent stimulation of cAMP accumulation. There are many co-expression studies reporting a host of potencies, however a recent study (Hay et al. 2018) compiled these for the studies of the human CGRP receptor providing an average pEC_{50} of 9.61. CGRP is also capable of causing cAMP recruitment, as alluded to above, at other members of the receptor family with the rank order of potencies: CGRP>AMY_1>AMY_3>AMY_2>CTR>AM_2>AM_1. It has also been demonstrated that GCRP can couple to $G_{q/11}$ and elicit calcium mobilisation with a potency of 8.19 in a HEK-293 cell line (Weston et al. 2016). CGRP could also mobilise calcium at the CLR-RAMP2 and CLR-RAMP3 receptors. In the same publication CGRP mediated cAMP accumulation showed little sensitivity to pertussis toxin (PTX) at the CLR-RAMP1 but there was a strong effect on CGRP responses at CLR-RAMP2 and RAMP3 suggesting that CGRP can signal through $G_{i/o}$ proteins at the CLR-RAMP2 and CLR-RAMP3 but not CLR-RAMP1.

There are also reports of CGRP being able to stimulate the MAPK pathway (Kawase et al. 1999), as well as protecting cells from oxidative stress via $ERK_{/12}$ and p38 MAPKs (Schaeffer et al. 2003), although it remains uncertain which receptor CGRP acted through. Then there is the topic of bias, and CGRP provides a good example with the above work suggesting that CGRP at the CGRP receptor is strongly biased towards G_s coupling in a HEK-293 cell line (Weston et al. 2016). In terms of internalisation, a recent co-expression study demonstrated robust internalisation of CLR-RAMP1 in response to CGRP (Gingell et al. 2020). Moreover, there is evidence that this internalisation does not terminate signalling, as continued CGRP signalling from endosomes has been observed (Yarwood et al. 2017), in this study inhibitors of clathrin were shown to prevent this signalling suggesting that CGRP mediated CLR-RAMP1 internalisation is β-arrestin and clathrin driven.

CGRP Physiology

CGRP levels circulating in the plasma are relatively low which is likely due to the fast metabolic breakdown of the circulating peptide (Kraenzlin et al. 1985). Endothelial cells are known producers of CGRP (Doi et al. 2001) although its exactly role remains unclear. It is also often found at sensory never endings, where it is released in response to neuron signal transmission and depolarisation; from vesicles alongside substance P via the typical calcium stimulated exocytosis mechanism (Matteoli et al. 1988). A potential mediator of CGRP release in this nerve fibres are transient receptor potential vanilloid 1 (TRPV1) channels, they are important pain transducers and the connection to CGRP release has been demonstrated *in vitro* and *in vivo* (Quallo et al. 2015, Van der Schueren et al. 2008). CGRP levels change in physiological and pathophysiological conditions; firstly, in pregnancy where it is a proposed vascular regulator (Dong et al. 2002). As well as in the cardiovascular disease and hypertension; in these scenarios whether it has a contributory or protective role is still a source of confusion, although it is proposed to play a protective role in heart failure (Brain and Grant 2004). However, CGRP's role in migraine is clearer cut. Where it has been a major target for successful

therapeutic intervention. Firstly, with small molecule antagonists such as Olcegepant (Olesen et al. 2004) and then with monoclonal antibodies, the first of which to be approved was Erenumab (Goadsby et al. 2017). Even more recently small molecule positive modulators have been identified for the CLR including the CGRP receptor with great therapeutic potential (Hendrikse et al. 2020).

Systemic administration of CGRP in healthy human causes vasodilation (Gennari and Fischer 1985), what is more in the microvasculature it is the most potent vasodilator known (Brain et al. 1985). Yet administration in humans also has a positive chronotropic and ionotropic effect on the heart (Gennari and Fischer 1985). Studies in small mammals suggest this is mediated by a combination of direct effects on the heart muscle and sympathetic nerve activity. However, in the brain, when CGRP is directly injected into the ventricular system this caused vasoconstriction (Fisher et al. 1983). This suggests different actions of CGRP in different cell types and organ systems. Looking at the overall picture; in complete genetic knockout studies in mice where CGRP has been removed an increase in baseline blood pressure was observed in one study (Gangula et al. 2000), whereas in another there was no effect on the cardiovasculature (Lu et al. 1999). Even more confusingly clinical trials of small molecule CGRP antagonists for conditions such as migraine have shown no adverse cardiovascular effects (Petersen et al. 2005), including long term studies into the safety of the monoclonal antibody Erenumab (Ashina et al. 2019). Even in a study of patients with stable angina acute CGRP inhibition did not produce a significant difference (Depre et al. 2018) in this specific scenario, however, much further work is needed to ascertain whether chronic CGRP depletion would negatively affect patients with cardiovascular disease. Although good for drug discovery in non-cardiovascular related disease, more work is needed to marry the cardiovascular effects of CGRP with the seemingly contradictory clinical trial results. In terms of cardiac disease CGRP plays a protective role. It has been shown to protect against heart failure (Li et al. 2013) and improve cardiac performance in heart failure patients (Gennari et al. 1990). This has been demonstrated in multiple human studies confirming that CGRP has a beneficial effect on the failing heart; because there is an anticipated increase in cardiac output

coupled with a decrease in vascular resistance (Anand et al. 1991). However, CGRP's half life is short and the effects are lost shortly after halting administration. Therefore, there has been recent work attempting to evaluate CGRP analogues which may have future therapeutic benefit (Sheykhzade et al. 2018).

It is thought that CGRP mediates its vasodilatory effects through a combination of effects and pathways in endothelial and smooth muscle cells (SMCs) but that endothelial cells are not essential as vasodilation can be observed in SMCs without endothelial cells present in a study using bovine derived cells (Crossman et al. 1990). Although there is the caveat that the evidence presented for this is compiled from a combination of different animal model: CGRP is thought to increase cAMP in endothelial cells and SMCs, but without directly increasing cGMP in either. This activates PKA which phosphorylates ATP-sensitive potassium channels in the SMCs and leads to direct vasodilation (Nelson et al. 1990). In the (rat) endothelial cells cAMP release was observed, and so was nitric oxide (NO) production and this was thought to diffuses into SMCs to cause cGMP production and relaxation of the aorta, as the pan nitric oxide synthase (NOS) inhibitor - N omega-Nitro-L-arginine methyl ester hydrochloride (L-NAME) based inhibition of NO production also inhibited cGMP production and relaxation (Gray and Marshall 1992). It was also concluded that cAMP increases caused NO production, although there was no evidence linking the two. This suggests that the picture is incomplete and further work is needed to elucidate the signalling mechanisms for vasodilation, and which receptors are involved, especially in humans where the evidence is limited to systemic administration of the peptide and our understanding of the mechanisms involved are based on studies in animal tissue.

Adrenomedullin overview

Adrenomedullin (AM) is another member of the CGRP superfamily of peptides which exerts its effects through the CLR. The peptide has a multitude of different biological activities, foremost among them is AM's potent activity as a vasodilator (Kato and Kitamura 2015). It also plays a key regulatory role in the cardiovascular and lymphatic system, as well as in angiogenesis, and vascular homeostasis. AM was first discovered in 1993 (Kitamura et al. 1993). AM is a 52 amino-acid length peptide. The human AM gene is located on chromosome 11 and contains 4 exons and 3 introns. It is translated into the 185 amino acid long precursor prepro-AM which is eventually converted into mature AM. It contains a few residues which are highly conserved and found in all members of the CGRP peptide family: these are two N-terminal cysteines forming a disulphide-bonded ring structure and a threonine within this structure (Wimalawansa 1997). There is also an N-terminal extension, shared with AM2, although it seems to be of limited physiological significance as truncation of it has little effect on binding, signalling, and internalisation compared to the wild-type peptide (Schonauer et al. 2015, Santiago et al. 1995).

Adrenomedullin pharmacology

AM like CGRP and AM2 acts at the Class B GPCR – the CLR. It is also suggested that it may have some activity at the calcitonin and amylin receptors, amylin receptors are formed by the dimerization of CTR with either RAMP1 or RAMP2 (Hay et al. 2018). When considering the pharmacology of the human AM at the human receptors formed by the CLR (CLR-RAMP1/2/3). Most work primarily considers AM and the CLR simply as a G_s-coupled receptor (Poyner et al. 2002) and considers cAMP accumulation as a measure of its activity. With that in mind AM is known to activate all three receptors with potency at AM_1 (CLR-RAMP2) and AM_2 (CLR-RAMP3) significantly higher than at the CGRP (CLR-

RAMP1) receptor. This is based on the study combining multiple co-expression studies using the human receptor. The rank order of pEC_{50} values is AM_2 (9.36)>AM_1(9.19)>CGRP(8.09) (Hay et al. 2018), suggesting AM is not actually most potent at the receptor that takes its name but that it is slightly more potent at CLR-RAMP3. Despite these very similar potencies and cognate ligand the two adrenomedullin receptors (AM_1 and AM_2) are pharmacologically distinct receptors (Hay et al. 2003).

The signalling bias of AM through pathways beyond purely cAMP has recently been documented (Weston et al. 2016). There is evidence of this at the CGRP receptor where AM elicits a comparatively weak cAMP response (G_s). However, it has been shown that AM in fact also signals through $G_{i/o}$ proteins at the CGRP receptor. Providing an explanation for the weak cAMP signal induced. In the same publication, there was also evidence of AM evoking $G_{q/11}$ coupling to the CLR (Weston et al. 2016). Thus far these results have only been shown in overexpression systems and need demonstrating in the native system in order to determine the physiological relevance of AM and AM2's biased signalling.

In terms of internalisation and receptor recycling, research suggests AM can drive the internalisation of CGRP, AM1, and AM2 receptors (Nikitenko et al. 2006). Furthermore, it is likely to be β-arrestin driven (Hilairet et al. 2001) and when AM internalises with AM_1 it likely stays bound throughout the internalisation and degradation process (Schonauer et al. 2015). More evidence that the internalisation is β-arrestin driven comes from a very recent co-expression study documenting robust β-arrestin recruitment by AM at the CLR-RAMP2 receptor (Hendrikse et al. 2020). Although further work is needed to elucidate the precise differences in signalling between the peptide-receptor combinations in cellular systems where the receptors are endogenously expressed.

Adrenomedullin physiology

AM is widely expressed in the human body; systems of note where it is found are the cardiovascular, placenta, reproductive and blood (Eto et al. 2003, Ichiki et al. 1994). Although circulating levels are generally low (as with CGRP) due to its short half-life, it can be elevated physiologically and pathophysiologically (Lewis et al. 1998). AM is mainly (and highly) synthesised and released from endothelial cells suggesting a likely auto/paracrine role in the cardiovascular system (Sugo et al. 1994).

In terms of AM's physiology AM is involved in lymphangiogenesis and the control of lymphatic vascular function through stabilising the lymphatic endothelial barrier and sustaining vascular permeability (Klein and Caron 2015). AM is also expressed alongside CLR and RAMP2 in osteoblasts and promotes bone growth and mineralisation (Naot and Cornish 2008). There is a large increase in circulating AM in healthy pregnant women and it plays a part in multiple processes including immune regulation, decidualisation, implantation and placentation (Matson and Caron 2014). With the caveat that its role is still not yet completely understood. AM, like CGRP, is a potent vasodilator (Kato and Kitamura 2015), work performed in a rat model suggested that this is mediated by NO release from endothelial cells and its subsequent well documented actions on vascular smooth muscle cells (Feng et al. 1994) however, it is not clear whether it is via a cAMP-dependent or -independent method (Tsuruda et al. 2019). It is thought AM plays multiple roles in endothelial cells, another of which is regulating endothelial barrier function (Temmesfeld-Wollbrück et al. 2007). It is thought to cause barrier stabilisation and protect against infection mediated junctional protein disappearance. All brought about initially through cAMP production (Hocke et al. 2006). In the heart, and cardiac myocytes, AM is also synthesised, however its exact role is a source of much controversy (Bisping et al. 2007). Some report that AM is a positive inotrope acting in the same cAMP driven manner as β-adrenoreceptor agonists in humans (Bisping et al. 2007). While others report it having negative

inotropic effects on the human heart (Mukherjee et al. 2002, Perret et al. 1993). Nevertheless, AM is widely acknowledged to be cardioprotective through regulating cell proliferation as it has an antiapoptotic effect on endothelial cells, reportedly in a cAMP-independent manner via NO (Sata et al. 2000). AM can also increase cardiac output by causing vasodilation of coronary vessels and decreasing vascular resistance (Nagaya et al. 2000). The potent vasodilatory effects of AM are important in the lung circulation and can decrease vascular resistance in pulmonary hypertension as well as protecting against hypoxic pulmonary damage (Nagaya and Kangawa 2004). Therefore it is accepted that in the multiple disease states where AM levels are increased it is playing a protective role (Perez-Villa et al. 2004) Several clinical trials have been performed using AM in patients, due to the potential protective effects AM might provide in multiple disease states. Three examples include trails using AM in patients with pulmonary hypertension (Nagaya et al. 2000), heart failure (Nagaya et al. 2000), and myocardial infarction (Kataoka et al. 2010). The possible use of AM as a therapy option comes with the advantages and disadvantages often associated with peptide drugs; such as high potency and low toxicity, but also low bioavailability and stability.

Adrenomedullin 2 Overview

Adrenomedullin 2 (AM2) or intermedin (From here on referred to solely as adrenomedullin 2) was first discovered in 2004 (Roh et al. 2004, Takei et al. 2004) and is the final member of the CGRP superfamily of peptides to be addressed in detail here, as well as the least well understood (Hay et al. 2018). This peptide hormone is again, as with the others, an agonists at, and exerts its physiological effects through, the CLR (Hay et al. 2005). Physiologically, AM2 has effects on the cardiovascular system, adipose tissue, macrophages and the kidney, it can also activate the sympathetic nervous system (Hong et al. 2012). AM2 is a 53 amino acid peptide. The human AM2 gene is found on chromosome 22 and codes for prepro-AM2 which is 148 amino acid residues in length before it is converted into mature AM2, interestingly mature AM2 shares only 87% sequence identity with

mature AM2 in rodents (Roh et al. 2004). Mature AM21-53 can also be cleaved into AM21-47 and AM21-40 (Morimoto et al. 2007). Currently antibodies cannot distinguish between them and the prominence of each *in vivo* remains uncertain. As does the physiological and pharmacological relevance of these cleavage fragments. AM2 shares the conserved residues with the other members of the CGRP superfamily but is most closely related to AM as they both have a unique N-terminal extension (Hong et al. 2012), despite having only limited sequence homology (28%).

Adrenomedullin 2 pharmacology

Although as stated previously it is the least well studied of the peptides, AM2 as with AM and CGRP before has activity at all three of the CLR based receptors (measured in terms of cAMP) (Hay et al. 2005). It also appears be most potent at activating the AM2 receptor: Here referring to a compilation of multiple co-expression studies using the human receptor the rank order of potencies at each receptor are AM_2(9.01)>CGRP(8.23)>AM_1(7.91) (Hay et al. 2018). Therefore, when comparing the peptides with each other they have similar potencies at the CGRP and AM1 receptor, with the main difference being AM's significantly greater potency at the AM2 receptor. But as discussed above the potency of AM at the AM_2 receptor has been estimated as 9.36. So AM2 is not the most potent ligand acting at the AM_2 receptor. Moreover, even if it was the most potent in these studies it is still not clear which receptor AM2 exerts its activity through, especially as AM2 appears to have a large amount of cardiovascular functions as mentioned below yet there is very little RAMP3 expression in this region (Bell and McDermott 2008). Therefore, much more work is needed to understand which receptor AM2 exerts its effects through physiologically, and what relevance the above potencies have in this.

AM2 is also capable of eliciting signalling bias at human receptors in overexpression systems: There is evidence for $G_{i/o}$ coupling at all three CLR based receptors in response to AM2 in certain immortalised cell lines (Weston et al. 2016) as well as a small amount of $G_{q/11}$ and $G_{i/o}$ coupling in all three CLR-

RAMP combinations. Looking at these responses from the perspective of the AM_2 receptor the PTX sensitivity was cell-line dependent and therefore the G_i coupling varied and was not definitive. But in terms of G_q coupling and calcium release the receptor produced a detectable signal in response to CGRP, AM and AM2.

Adrenomedullin 2 physiology

AM2 is much like the other CGRP family members in that it is widely expressed throughout the body (Morimoto et al. 2007), and particularly high expression levels are seen in the hypothalamus, pituitary, heart, GI tract, kidney and circulation. It is believed to play a protective role in the renal and cardiovascular systems; inhibiting ER stress, inflammation and oxidative stress (Takei et al. 2004). Rodent studies confirm the vasodilatory effects of AM2; showing that it can increase blood flow and decrease vascular resistance in many organs including the heart, lungs, liver and kidneys. Intriguingly, it has even been suggested that it does so more potently than AM (Jolly et al. 2009). Although it is unclear which of the CLR-RAMP combinations it is acting through (Takei et al. 2004). In another rodent study AM2 reportedly exerts this effect through increasing endothelial nitric oxide production (Yang et al. 2006). As with AM, AM2 can stabilise vascular junctions through its actions on endothelial cells, as well as help prevent apoptosis (Aslam et al. 2012, Chen et al. 2006). Multiple different animal studies report that AM2 has a positive inotropic effect on the heart (Charles et al. 2006, Fujisawa et al. 2007), moreover it has been suggested that this is mediated through an increase in intracellular calcium and PKC activation (Dong et al. 2006). However, AM2 is not universally accepted as a positive inotrope, with another rodent study reporting that AM2 has a negative inotropic effect on the heart, and that it is mediated by NO release (Pires et al. 2012).

Equally, AM2 is elevated in pregnancy and has a hypotensive effect, while low AM2 levels are associated with pre-eclampsia (Chauhan et al. 2016). In the case of cardiac disease AM2 levels are

increased during myocardial infarction as well as acute coronary syndrome in humans (Bell et al. 2016). Multiple studies have suggested that it plays a protective role in these conditions (Chen et al. 2013), particularly during ischaemic cardiac injury, and this has been demonstrated consistently in rat models, firstly in isolated myocytes (Bell et al. 2008) and later in whole organism studies (Wei et al. 2015).

Aims

While specific aims will be outlined subsequently in individual chapters there are some clear overarching aims of this body of work. The first is to explore the extent of CLR signalling bias where it is endogenously expressed. Much work as outlined above has profiled the signalling of this receptor using overexpression in immortalised cell lines. This work aims to explore the signalling in a more physiologically relevant system. Then a further aim will be to assess how RAMPs influence this signalling; when distinct primary cell systems are established that express different CLR-RAMP combinations, their signalling will be studied and compared. These endogenous expression systems will be used to explore the involvement of CLR and its ligands in some physiological outcomes further downstream of the receptor's second messenger signalling pathways then later the work will go even further and see whether this is involved in the functional outcomes in cell organoid models. It will also be explored whether there are spatiotemporal aspects to the signalling of the receptors in the endogenous setting and whether this can be observed, as well as seeing whether different endogenous ligands evoke different spatiotemporal responses in the same receptor and cell system. Then finally gene editing techniques will be used to interrogate whether the contrasting signalling responses from the CLR ligands, seen in different primary cell lines is related to the differing RAMP expression in these cell lines, i.e. if the RAMP expression changes to what extent will the receptor signalling.

Chapter 2. Material and Methods

Materials

Peptide ligands and compounds

Human αCGRP, adrenomedullin (1-52), AM2/intermedin, calcitonin, amylin and adrenomedullin (22-52) (all Bachem UK Ltd, St. Helens, UK) are dissolved in water containing 0.1% Bovine Serum Albumin (BSA), to a 1 mM concentration and stored as 7 µl aliquots. VEGF, acetylcholine and isoproterenol (Sigma-Aldrich UK, Gillingham, UK) are dissolved in water + 0.1% BSA at 1 mM. 3-Isobutyl-1-methylxanthine (IBMX) is from Sigma-Aldrich. Olcegepant (BIBN-4096) (Tocris Biosciences, Bristol, UK) is made to a 1 mM stock in Dimethyl Sulphoxide (DMSO). Ionomycin (Cayman Biosciences, Cambridge, UK) is dissolved in absolute ethanol, forskolin and phorbol 12-myristate 13-acetate (PMA) (Sigma-Aldrich) are dissolved in DMSO all at 10 mM. YM-254890 (Alpha Laboratories), ESI-09 (Sigma-Aldrich), Rp-8-Br-cAMPs (Santa Cruz Biotechnology) are dissolved in DMSO at 10 mM. PTX was purchased in solution (ThermoFisher Scientific, Waltham, MA, USA). Barbadin (Aobious, Gloucestershire, UK), dynasore (Sigma-Aldrich), Pitstop 2 (Sigma-Aldrich), Compound 101 (Sigma-Aldrich) are dissolved in DMSO at 10 mM.

All other general laboratory reagents are analytical grade and purchased from Sigma-Aldrich unless otherwise stated.

Media and solutions

DMEM (– glutamate and + non-essential amino acids) growth medium is supplemented with 10% heat inactivated Fetal Bovine Serum (FBS). Endothelial Cell Growth Media (ECGM), Cardiac Myocyte Growth Media (CMGM) and Smooth Muscle Cell Growth Media (SMCGM) are all supplied as complete media (Promocell, Heidelberg, Germany). All media combined with 1% antibiotic antimycotic solution (100x Sigma) upon opening and before use in cell culture.

Phosphate buffered saline (PBS) is made by dissolving a tablet (Sigma-Aldrich) in 200 mL distilled water and is autoclaved. Sterile Hank's balanced salt solution (HBSS) is purchased with and without calcium (Lonza).

Oligonucleotides

Listed here are all oligonucleotides (**Table 2.1**) used for all RT-PCR demonstrating gene expression in later chapters.

Oligonucleotides	**Sequence**	**Amplicon size (bp)**
Human		
GAPDH	5' - TGCACCACCAACTGCTTAGC- 3'	87
	5' - GGCATGGACTGTGGTCATGAG- 3'	
$G\alpha_s$	5' - CGACGACACTCCCGTCAAC- 3'	177
	5' - CCCGGAGAGGGTACTTTTCCT- 3'	
$G\alpha i_1$	5' - TTAGGGCTATGGGGAGGTTGA- 3'	186
	5' - GGTACTCTCGGGATCTGTTGAAA- 3'	

$G\alpha i_2$	5’ - TACCGGGCGGTTGTCTACA- 3’	89
	5’ - GGGTCGGCAAAGTCGATCTG- 3’	
$G\alpha i_3$	5’ - ATCGACCGCAACTTACGGG- 3’	229
	5’ - AGTCAATCTTTAGCCGTCCCA- 3’	
$G\alpha_{11}$	5’ - GGCTTCACCAAGCTCGTCTAC- 3’	172
	5’ - CACTGACGTACTGATGCTCG- 3’	
$G\alpha_{12}$	5’ - CCGCGAGTTCGACCAGAAG- 3’	245
	5’ - TGATGCCAGAATCCCTCCAGA- 3’	
$G\alpha_{13}$	5’ - CAGCAACGCAAGTCCAAGGA- 3’	220
	5’ - CCAGCACCCTCATACCTTTGA- 3’	
$G\alpha_{14}$	5’ - GAGCGATGGACACGCTAAGG- 3’	168
	5’ - TCCTGTCGTAACACTCCTGGA- 3’	
$G\alpha_{15}$	5’ - CCAGGACCCCTATAAAGTGACC- 3’	126
	5’ - GCTGAATCGAGCAGGTGGAAT- 3’	
$G\alpha_o$	5’ - GGAGCAAGGCGATTGAGAAAA- 3’	169
	5’ - GGCTTGTACTGTTTCACGTCT- 3’	
$G\alpha_z$	5’ - GGTCCCGGAGAATTGACCG- 3’	175
	5’ - ATGAGGGGCTTGTACTCCTTG- 3’	
$G\alpha_q$	5’ - TGGGTCAGGATACTCTGATGAAG- 3’	144
	5’ - TGTGCATGAGCCTTATTGTGC- 3’	
CTR	5’ - CCTATCACCCAATAGAGCCCAAG - 3’	91
	5’ - TGCATTCGGTCATAGCATTTGTA - 3’	
CLR	5’ - ACCAGGCCTTAGTAGCCACA - 3’	298
	5’ - ACAAATTGGGCCATGGATAA - 3’	
RAMP1	5’ - CTGCCAGGAGGCTAACTACG - 3’	298

	5’ - GACCACGATGAAGGGGTAGA - 3’	
RAMP2	5’ - GGGGGACGGTGAAGAACTAT - 3’	227
	5’ - GTTGGCAAAGTGGATCTGGT - 3’	
RAMP3	5’ - AACTTCTCCCGTTGCTGCT - 3’	353
	5’ - GACGGGTATAACGATCAGCG - 3’	
β-arrestin-1	5’ - AAAGGGACCCGAGTGTTCAAG - 3’	159
	5’ - CGTCACATAGACTCTCCGCT - 3’	
β-arrestin-2	5’ - TCCATGCTCCGTCACACTG - 3’	82
	5’ - ACAGAAGGCTCGAATCTCAAAG - 3’	
RCP	5’ - AGAGCAGCGTAAAGAAAGTGG - 3’	129
	5’ - CTGACAATTTCAGGACTCTGGTG - 3’	

Table 2.1. Oligonucleotides used in RT-PCR. Oligonucleotides for use in RT-PCR are acquired from PrimerBank and synthesised by Sigma-Aldrich.

Methods

Cell culture

HEK-293S cells and HEK-293S ΔCTR/CLR/RAMPs (formerly MedImmune now AstraZeneca, Cambridge), and PC3 cells were cultured in 25 cm^2 flasks, in the DMEM + 10% FBS. The cells were passaged approximately every 4 days depending on confluency with a final volume of 10 ml produced from 1 ml of the previous cell culture and 9 ml of the growth medium. The cells were grown in an incubator (37 °C, humidified 95% air, 5% CO_2) between passaging. Primary cell lines; HUVECs and

HUAECs (PromoCell) were cultured in (ECGM) (PromoCell), and Cardiac Myocytes (human) were grown in CMGM, and Human Vascular Smooth Muscle Cells were grown in SMCGM. Cells were grown in 25 cm^3 flasks or 75 cm^3 flasks depending on cell density required. They were passaged every 4 days and split at a 1/5 dilution and used from passage 1-6. All cells grown with 1% antibiotic antimycotic solution (Sigma). The cells were grown in an incubator (37 °C, humidified 95% air, 5% CO_2) between passaging.

For cryo-storage and recovery all cells irrespective of cell-type are grown to approximately 90% confluency in a 25 cm^3 flask, harvested and re-suspended in 1 ml of their respective culture media + 10% DMSO. The cell solution is transferred to a cryogenic vial and frozen gradually in polystyrene protective packaging to -80°C. Following this cells are transferred to liquid nitrogen where they can be stored long term. For removal from cryo-storage vials containing cells can be taken out and stored on dry ice for a maximum of 10 min before being quickly thawed in a 37 °C water bath. 1 ml containing vials then have the cell solution removed and placed in 9ml complete media pre-warmed to 37 °C. The resulting 10 ml of cell solution is centrifuged (1400 RPM, 4 min). Cells are then re-suspended in 5ml pre-warmed complete cell media and transferred to a 25 cm^3 flask for growth in an incubator (37 °C, humidified 95% air, 5% CO_2) and passaging as above.

Bacterial transformation and DNA purification

Escherichia coli (*E. coli*) are transformed with plasmids containing genes for Ampicillin resistance and the CLR (or a RAMP) according to laboratory protocol: *E. coli* cells are defrosted and left on ice for 30min. Then 10 µl ligation buffer and 1 µl plasmid DNA are added to the cells and they are returned to ice for 5 min. The cells are heat shocked in a 42°C water bath for 2 min, before returning to ice again for 5 min. After 30 min recovery the cells are added to 100 ml LB (Luria Bertani Broth) with 2 µl ampicillin added to kill any bacteria that did not take up and express the plasmid DNA. The bacteria

are then grown in a shaking incubator for 24 h. Following incubation, the plasmid DNA is purified using a QIAGEN plasmid maxi kit according to the manufacturer's protocol using manufacturer's reagents. Following this the concentration of the DNA is then determined using a NanoDrop Lite Spectrophotometer (Thermo Scientific).

Cell transfection

From HEK-293 cell stock dilutions of 1/2, 1/4, 1/6 and 1/8 are made in DMEM up to a final volume of 2ml in 6 well cell culture plates The different dilutions spaced out cell growth so transfections and therefore assays could take place on different days. After incubation of usually 24 h for 1/4 and 48 h for 1/8, the cells had achieved optimal confluency (about 80%) for transfection. To individual wells on the plate a 75 µl solution of DNA preparation is added. This is composed of 2 µg DNA (1 µg CLR, 1 µg RAMP), 6 µl Fugene HD (Promega) and serum free DMEM making up the volume (the presence of serum reduces transfection efficiency (Jacobsen et al. 2004)). Fugene is the reagent used to transfer plasmids across the plasma membrane. It is used at a 3:1 Fugene:DNA ratio as per the manufacturers' instructions. 10 min after it is made, the DNA preparation is added to a well containing cells. Then the cells are incubated (48 h, 37 °C, humidified 95% air, 5% CO_2) to achieve optimum transfection. Constructs used are pcDNA3.1-FLAG-RAMP1, pcDNA3.1-FLAG-RAMP2, pcDNA3.1-FLAG-RAMP3 and pcDNA3.1-cmyc-CLR-GFP (Weston et al. 2016)

RNA extraction and RT-PCR

First cells are grown to confluency in a 6 well plate. All RNA extraction steps are performed in a fume hood where possible, and all surfaces and equipment sterilised with 70% ethanol. Prior to RNA extraction cell media is removed and cells are washed twice (PBS, 500 µl). Approximately $2x10^5$ cells are used per extraction (RNAqueous-4PCR kit, Ambion). They are then lysed with 350 µl Lysis/Binding

Solution and a sterile scrapper. An equal volume (350 µl) of 64% ethanol is added and the solution mixed before being transferred to a filter cartridge inside a collection tube. This is spun in a microcentrifuge (12,500 rpm, 1 min). The cartridge is then washed with 700 µl wash solution 1 and 2 x 500 µl wash solution 2/3 (spun between each wash). The cartridge is transferred to a fresh collection tube for RNA elution with 50 µl preheated (70-80°C) elution solution (0.1 mM EDTA). 1 µl DNase 1 and 0.1vol (5 µl) 10X DNase 1 buffer is added (30 min, 37°C) to remove possible contamination from genomic DNA. Finally, DNase inactivation reagent 0.1vol (5.6 µl) is added (1 min, RT) then the solution is spun (10,000 rpm, 30 secs) and supernatant collected. Purity of RNA samples quantified using NanoDrop Lite spectrophotometer (Thermo Scientific), samples with yields over 100 ng/µl and with $A_{260/280}$ vaules over 1.9 used.

Complementary DNA is synthesised using a QuantiTect reverse transcription kit (Qiagen). Template RNA is diluted such that 1 µg is added to RNase-free water and 2 µl gDNA wipeout buffer and made up to 14 µl. This is incubated in a heat block (2 min, 42 °C). Meanwhile mastermix is made up on ice: 1 µl reverse transcriptase, 4 µl RT buffer, 1 µl RT primer mix. This is then combined with the template RNA and incubated (15 min, 42 °C), before RT is inactivated by incubation (15 min, 95°C). The cDNA is then available to perform real-time PCR with oligonucleotides previously published and verified for genes of interest, synthesised and supplied by Sigma Aldrich (UK), sequences recorded in appendices.

Electrophoresis is performed on a 2% agarose (in TAE) gel. The Image is captured using G Box iChemi gel documentation system utilising GeneTools analysis software (Syngene) densitometry analysis performed using GeneTools. mRNA levels of the genes of interest normalised to GAPDH expression.

Intracellular signalling assays

Where inhibitors are used, the conditions and concentrations remain constant across all assays. YM-254890 the $G_{q/11/14}$ inhibitor is applied (100 nM) as a pre-treatment 30 min before the assay start (Takasaki et al. 2004). ESI-09 the non-selective EPAC1/2 inhibitor and pre-treatment is also required (100 μM, 15 min)(Almahariq et al. 2013). Rp-8-Br-cAMPs the PKA inhibitor has pre-treatment conditions of (100 μM, 15 min) (Schwede et al. 2000). PTX inactivates $G\alpha_i$ proteins and requires (200 ng/ml, 16 h, 37 °C) pre-treatment conditions (Weston et al. 2016). The GPCR internalisation inhibitors have the following pre-treatment conditions: Barbadin (100 μM, 30 min) (Beautrait et al. 2017), dynasore (80 μM, 30 min) (Macia et al. 2006), Pitstop 2 (100 μM, 30 min) (Beautrait et al. 2017), Compound 101 (100 μM, 30 min) (Thal et al. 2011, Lowe et al. 2015).

Preparation of peptide ligands

As with many of the assays subsequently described in this section a range of stimulating ligand concentrations is needed to perform dose response experiments. To perform ligand dilutions or a serial dilution: stock solutions of ligand are 10^{-3}M, these are made to 10^{-4}M by a 1/10 dilution in H_2O + BSA (0.1%). Then 2 μl of each dilution is added to the first well of each ligand's respective column on the 96 well plate. On this plate where the ligand dilution series is made, the same is done for the positive control, in the case of cAMP this is forskolin, this is added as 8 μl aliquots in the first well. This is alongside 92 μl SB (see below) in the case of cAMP in each of these first wells, and 98 μl SB in each of the first wells containing ligand. After this all wells have 90 μl SB added. Then 10 μl is taken out of the first well in each column and mixed with the subsequent well, and so on all the way down the column to create a dilution series.

Measurement of intracellular cAMP accumulation

cAMP assays (PerkinElmer, Beaconsfield, UK) are performed according to manufacturer's protocol and (Weston et al. 2016), in detail; First stimulation buffer (SB) is prepared: 0.02 g (0.1%) of BSA and 10 µl IBMX (a phosphodiesterase inhibitor) are added to 20 ml of PBS (phosphate-buffered saline) warmed to 37°C. All in a 20 ml universal tube, it is then vortexed.

Antibody solution is then prepared by creating a 1/100 dilution of the Alexa Fluor 647-anti cAMP antibody is made in SB. Cells are later resuspended in this solution. Cell preparation is carried out under a fume hood with all equipment cleaned with ethanol to generate a sterile environment and minimise the risk of infection in cell culture. Cells have their media aspirated off and 500 µl of 0.05% Trypsin-EDTA is added to each individual well where cells are grown in a 6 well plate. The cells are subsequently returned to the incubator for 10 minutes to trypsinise. 500 µl of media is then added to each well, the cells are thoroughly dislodged through repeated pipetting, and added to 1.5 µl Eppendorf tubes. The cells are centrifuged (1000rpm, 5 min) to form a pellet so than the trypsin containing media can be removed. The cells are washed and re-suspended in 500 µl PBS and centrifuged two further times before final resuspension in PBS. A 10 µl aliquot of each cell suspension is added to a haemocytometer. It is used to count the number of cells in a given area, under the microscope, to calculate the number of cells/µl. This process is also carried out for $pERK_{1/2}$ assays.

Cells are resuspended in the antibody solution so as to produce a concentration of the final solution such that a 5 µl aliquot will contain 2000 cells. A 5 µl aliquot is added to each well of the 384 well white the 384-well Optiplate. To plate cells for a cAMP assay, the antibody and cell solution is added in 5 µl aliquots to each well. In the first column forskolin is added in 5 µl aliquots in descending concentrations from 10^{-4} M to 10^{-11} M. To the subsequent columns each of the 3 ligands and any other stimulating conditions are added individually in 5 µl aliquots in concentrations descending from 10^{-6}

M to 10^{-13} M. The Optiplate is covered in foil to reduce light exposure. Then incubated on a shaker plate (room temperature, 30min). This stimulation time varied depending on the cell type used. All HEK-293 cell experiments had an 8 min stimulation time, and all primary cells 30 min.

If antagonist studies are being performed they diluted alongside the stimulating agonists and added to the cells in the form of co-stimulation.

2500 µl of detection buffer (DB) is usually made up for an assay as per manufacturers' suggestion and protocol: This provides approximately enough for up to 12 columns on the 384 well Optiplate allowing for pipetting error. The DB is made in a small universal tube (10 ml) wrapped in foil to prevent light interference. 2460 µl of cAMP Detection buffer is added along with 20 µl of Eu-SA and 20 µl of b-cAMP. The Eu-SA is taken from 2 µl Eu-W8044 labelled streptavidin diluted in 34 µl detection buffer (generating a 1 in 18 dilution). b-cAMP is made from 4 µl Biotin-cAMP diluted 1 in 6 in 20 µl detection buffer. The final 2500 µl volume of DB for the assay is incubated (room temperature, 15 min).

After the 30 min incubation period 10 µl of detection buffer is added to all wells before the Optiplate is again covered in foil and incubated on the shaker plate (room temperature, 60 min). Following the incubation period, the Optiplate is immediately read by the Mithras LB 940 multimode microplate reader (Berthold technologies, Harpenden, UK). Light pulses from the plate reader at 340 nm excite the Eu-chelate molecules bound to biotin-cAMP, itself bound to the antibody. Energy is transferred to the Alexa molecules which emit light at 665 nm, and this is detected by the plate reader. As intracellular cAMP is produced this competes for antibody binding and reduces the fluorescence intensity detected.

In order to perform the time course experiments all conditions are kept consistent except for the stimulation time, detection buffer is added at each different time point to freeze or end the assay from 0 min post stimulation up to 30. Experiments are also performed at 4°C to assess the influence of temperature on these time course assays. This was achieved by pre-cooling all equipment a 4°C

cold room, and subsequently performing the assay steps in a 4°C cold room rather than at the standard room temperature.

Measurement of intracellular calcium signalling

All cell lines were plated at 20,000 cells/well on fibronectin coated (40 min, 100 µl, 10 µg/ml, exposure 24 h prior to cell plating) Costar 96 well black clear-bottom plates, and cultured as previously described.

On the day of the assay cells media is removed from cells and the cells are loaded with 10µM and 40µl per well Fluo-4/AM (Fluo-4/AM assay kit, Invitrogen). Cell preparation is carried out under a fume hood with all equipment cleaned with ethanol to generate a sterile environment and minimise the risk of infection in cell culture. Loading takes place in the dark at room temperature for 1 hour. Cells are then washed twice with Hank's Balance Salt Solution (HBSS) (Lonza, Slough, UK), then are left in 100 µl/well Calcium-free HBSS for the duration of the assay. In wells where I attempt to inhibit $G\alpha_{q/11}$ signalling cells are wells are pre-treated with 100nM YM-254890 (as above) in calcium free HBSS (Ligands are made up exactly as described above but in Calcium free HBSS such that a 20µl volume can be added to 100 µl cells during the assay over a concentration range of 1 pM to 1 µM). All assays are performed using the BD Pathway 855 Bioimaging Systems (BD Biosciences, San Jose, CA, USA). Which injects ligands into individual wells of the 96 well plate prior to the fluorophore being excited at a wavelength of 494 nm and emission being recorded at 516 nm. The fluorophore fluo-4 is an analogue of fluo-3, and the fluo-4 AM ester is cleaved upon cell entry so it does not leave and only measures intracellular calcium, which it binds to in order to increase fluorescence output upon cell stimulation. With Images taken every second for 2 minutes so that calcium transients in the cytoplasm of the cells in each well can be imaged. Peak responses in each treatment are then normalised to the positive control (10 µM ionomycin).

Measurement of intracellular nitric oxide

As with calcium assays all cell lines were plated at 20,000 cells/well on fibronectin coated (40 min, 100 µl, 10 µg/ml, exposure 24 h prior to cell plating) Costar 96 well black clear-bottom plates. On the day of the assay cells are loaded with 40µl, 10µM DAF-FM diacetate (ThermoFisher Scientific) This dye theoretically records intracellular nitric oxide as upon entering the cells the diacetate is cleaved by esterases trapping the dye inside the cells (Falcone et al. 2008). Loading takes place in the dark (room temperature, 30 min). Cells are then washed with HBSS (Lonza) and remain in that for the duration of the assay. All assays are performed using the BD Pathway 855 Bioimaging Systems (BD Biosciences). Which injects ligands into individual wells of the 96 well plate prior to the Fluorophore being excited at a wavelength of 494 nm and emission is recorded at 516nm(Falcone et al. 2008). With Images taken every second for 2 minutes so that nitric oxide transients in the cytoplasm of the cells in each well can be observed.

An alternative single end point nitric oxide assay involved: Primary cells were cultured as above. 24 hours prior to assay cells were plated on Costar 96 well black clear bottom plates at 40,000 cells/well. The assay was performed according to manufacturer's protocol. Briefly; cells pre-incubated with NO dye and assay buffer 1 (Fluorometric Nitric Oxide Assay Kit, Abcam, UK) for 30 min at 37°C in 5% CO_2. Any inhibitors requiring 30 min pre-treatment (YM-254890/L-NAME/DMSO control) were added at this point. Ligand stimulation occurred immediately after this for 15 min at 37°C C in 5% CO_2. Stain and ligand solution were removed, assay buffer II was added, and wells were read immediately. The absorbance was measured using a Mithras LB940 microplate reader with an excitation/emission of 540/590 nm. Endothelial cell responses were normalised to 10 µM acetylcholine (Holton et al. 2010) or HCM responses were normalised to 10 µM Isoproterenol (Vaniotis et al. 2013, Gauthier et al. 1998).

Measurement of intracellular phospho-$ERK_{1/2}$ (Thr202/Tyr204)

Primary cells were grown to 100% confluency in 6 well plates, HEK-293 cells were grown to the same level, including a transfection step (as above). On the day of the experiment media was replaced with serum free media 4 h prior to cell harvesting. Tyrpsin-EDTA was used to dissociate the cells and they are spun down, counted and re-suspended HBSS with 0.1% BSA as previously described in the cAMP accumulation assay section. Ligands are also diluted in HBSS-BSA (as in above assays and described in detail in cAMP assay section). Cells are then plated on 384 well plates in 8 µl aliquots at a density of 35,000 cells/well. Next Ligands are added (4 µl) for 5 min stimulation at room temperature in this range 10^{-4} M to 10^{-11} M, ligands are diluted as described above. Cells are then lysed as per manufacturer's instructions with 4µl of lysis buffer (Cisbio phosphor-$ERK_{1/2}$ cellular assay kit) for 30 min shaking at room temperature. The 2 specific antibodies; one labelled with Eu3+-Cryptate (the donor) and the other is labelled with d2 (the acceptor) are pre-mixed in 1:1 ratio. Then 4 µl is added to each well and the plate incubated for a further 4 h. Then fluorescence emissions were read at 665 nm and 620 nm using a Mithras LB940 microplate reader.

In order to perform the time course experiments all conditions are kept consistent except for the stimulation time, detection buffer is added at each different time point to freeze or end the assay from 0 min post stimulation up to 60. As in the cAMP accumulation time course assays.

Measurement of cell proliferation

All cell lines were cultured and trypsinised as above in order to be seeded at a density of 2500 cells/well in a clear flat bottom 96-well plate (Corning, NY, USA) and incubated at 37°C in 5% CO2. After 24 h, cells were exposed to ligands and control: the dilution series is performed as explained in extensive detail above but in complete endothelial cell growth media (HUVECs and

HUAECs) or myocyte growth media (HCMs) rather than H_2O+BSA (cAMP) or HBSS+BSA ($ERK_{1/2}$ and calcium) so that cells can continue to be incubated and grow over a period of up to 10 days. Cells were incubated for a further 72 h at 37°C in 5% CO_2. After 72 h incubation, 5 µl of Cell Counting Kit – 8 (CCK-8)(Sigma) was added to each well cells were then incubated for another 2 h at 37°C in 5% CO_2 and in the dark as per (Safitri et al. 2020): The active compound is 2-(2-methoxy-4-nitrophenyl)-3-(4-nitrophenyl)-5-(2,4-disulfophenyl)-2H-tetrazolium, monosodium salt, or WST-8 which is reduced by cellular dehydrogenases when the electron carrier 1-Methoxy PMS is present, to an orange formazan dye. The absorbance of each well was measured using a Mithras LB940 microplate reader with an excitation of 450 nm. The absorbance measured from formazan is directly proportional to the number of viable cells.

Statistical analysis

All data analysis was performed in GraphPad Prism 8.4 (GraphPad Software). For cAMP assays data analysis, the raw fluorescence data from an assay it is interpolated to the standard curve using the inbuilt GraphPad function. This generates a new set of values which accounts for variability in the plate reader and assay kit. These interpolated values are then normalized to the forskolin values, with the highest (100 µM) and lowest (10 pM) values providing the maximum and minimum levels of cAMP production, and accounting for day to day variation in cellular responses but retains the variance for control values. Then the data could be analysed using the nonlinear regression (curve fit) function to produce concentration-response curves for agonist stimulation. Where he means of individual experiments were combined to generate the curves shown. In the case of calcium and nitric oxide (time resolved) assays images are stacked, corrected for background fluorescence and peak intensity measured in the region of interest using ImageJ. Data were then exported to Prism to plot fluorescence time courses and generate dose-response curves. All calcium responses are normalised to calcium release from intracellular stores driven by 10 µM Ionomycin (Yoshida and Plant 1992). For

data generated in the $ERK_{1/2}$ assay the fluorescence reading at 665 nm is divided by the 620 nm reading and the result multiplied by 1000 for every individual well. The resulting data were then further analysed in GraphPad Prism 8.4, where values are normalised to $ERK_{1/2}$ phosphorylation caused from cells in response to 100 µM phorbol 12-myristate 13-acetate (PMA). Cell proliferation was calculated as a percentage of number of cells treated with vehicle alone. Data were fitted to obtain concentration–response curves using either the three-parameter logistic equation - used to obtain values of E_{max} and pEC_{50} or the operational model of receptor agonism was used where necessary to obtain efficacy (τ and equilibrium disassociation constant (K_A) values (Black and Leff 1983, Baltos et al. 2016, Qin et al. 2017). All statistical tests are performed in GraphPad Prism, and outlined in the legend of each table or figure where they are used, but briefly: Statistical differences were analysed using one-way ANOVA followed by Dunnett's *post-hoc* (for comparisons amongst more than two groups) or unpaired Student's t test with Welch's correction (for comparison between two groups) with a p value < 0.05 considered the threshold for significance. Values are reported in tables are means +/- SEM. Bias factors; $\Delta\Delta(\tau/K_a)$ were calculated for each ligand at each pathway and from this generated signalling bias plots. This is done by taking the logarithm of the τ/K_a and plotting the ratios of each pathway to one another on a logarithmic scale. Correlations between pEC50 values were assessed by scatter plot and Pearson's correlation coefficient (r) was calculated with 95% confidence interval.

iCell myocyte specific cell culture and functional assays

iCell myocyte cell culture

Monolayer (2D)

iCell Cardiomyocytes (Cellular Dynamics, Madison, WI, USA) were stored in liquid nitrogen until use and thawed according to the manufacturer's instructions as outlined above in the cell culture section. Wells to be used of an E-Plate CardioECR 48 (ACEA Biosciences, Inc. San Diego, CA, USA) are coated in gelatine (50 µl, 0.1%) (Sigma-Aldrich) 2 hours before plating. Thawed cells are diluted in pre-warmed iCell CM plating medium and then plated at 30,000 plateable cells/well in 100 µl plating media. Cells were allowed to adhere at room temperature for 15 min. Then placed in a humidified incubator with 5% CO_2 at 37°C. Plating media is replaced with iCell cardiomyocyte maintenance 48 h after seeding. Medium change was then performed every other day for 12 days. After this time spontaneous cell beating will have stabilised and then Cells were assayed after this.

Organoid (3D)

iCell Cardiomyocytes (Cellular Dynamics, Madison, WI, USA) were thawed according to the manufacturer's instructions and re-suspended in plating media at (2000 cells/µl). Human Cardiac Fibroblasts (Promocell, Germany) were routinely cultured according to supplier recommendations in Fibroblast growth media and re-suspended at the required density (500 cells/50 µl) in plating media. Spheroids were seeded by combining Cardiomyocytes (2000/well) and fibroblasts (500/well) with 1 ul/6x10E^4 cells Gold/iron oxide nanoparticle reagent (Nanoshuttle-PL, n3D Biosciences, USA), and then plated in 100 µl plating media in ultra-low attachment 96 well plates (Corning). Cultures were

incubated at 37°C 5% CO_2 in an humidified incubator. Plating media is replaced with iCell cardiomyocyte maintenance media 24 h after seeding. Then 50% is replaced every 2 days afterwards. After plating the spheroids then self-assemble and were able to be transferred to 96 well sensor plates (NSP-96 CardioEcyte96 sensor plates 0.6 mm, Nanion Technologies GmbH, Germany). Before transfer a sensor plate is coated with 10 µg/ml fibronectin and was aligned with neodymium magnet plate (AstraZeneca, Cambridge, UK) this helped magnetically guide the spheroids to settle themselves and position exactly above the central sensing electrode located in the well base when they are transferred: Spheroids are transferred using a multi-channel manual pipettor equipped with wide-bore tips to allow for spheroid transfer into the tip without disruption. Contents were carefully pipetted directly onto the central sensor electrode area. Visual inspection with a microscope is used to assess whether spheroids are positioned above the central sensing electrode. Only spheroids that settle within the boundary of the central sensor electrode area can be assayed. 2 days after transfer to sensor plates Impedance assays can then be performed on the CardioExcyte96 platform (Nanion Technologies).

Measurement of beat rate determined by cellular impedance recordings

Monolayer (2D)

Complete media change performed on the day of the experiment, at least 4 h prior to compound addition. Ligands/control are diluted (as described previously) in 50 ul iCell maintenance media, 50 µl is removed and ligand/control are added to return the volume per well to 100 µl. Recording is begun immediately on the xCELLigence RTCA CardioECR system (ACEA Biosciences, Inc.) and Impedance data were collected providing beat rates for the spontaneously beating cardiomyocytes. Readings were

taken every minute. Data were then exported to GraphPad Prism Software for graphing and statistical analysis. Data are representative of at least 3 independent experiments.

Organoid (3D)

Complete media change performed on the day of the experiment, at least 4 h prior to compound addition; ensuring 200 µl/well volumes. This becomes 250 µl with ligand/control addition (50 µl compound added in Maintenance media). Immediately after ligand/control addition Sensor plates are loaded onto a CardioEcyte96 platform (Nanion Technologies) (Doerr et al. 2015). Impedance data were then collected with reading sweeps taken every minute. Data were then exported to Prism (GraphPad Software) for graphing and statistical analysis. Data are representative of at least 3 independent experiments.

Measurement of intracellular calcium signalling in iCell myocytes

Cells are thawed and cultured as above in Cell Carrier ultra plates (PerkinElmer) coated in gelatine (50 µl 0.1%)(Sigma-Aldrich). Complete media change performed on the day of the experiment, at least 4 h prior to compound addition. Replacing media with 50 µl of maintenance media. 30min prior to compound addition remove 25 µl of media and add 25 µl Ca5 dye (FLIPR Calcium 5 Explorer Assay Kit, Molecular Devices). Cells incubated at 37°C 5% CO_2 until ligand/control addition. Ligand/control then added in 50 µl media and cells imaged on FLIPR Tetra System (Molecular Devices).

Quantitative RT-PCR

Cardiomyocytes were thawed and suspended as above in iCell plating medium and plated in a 24 well plate (pre-coated in gelatine) at 100,000 cells/well. Plating media is replaced with iCell maintenance 48 h after seeding. Medium change was then performed every other day for 12 days.

Media is then removed and cells are washed in PBS. RNA is extracted and gDNA eliminated using QIAGEN RNA extraction kit as per manufacturer's instructions. The yield and quality of RNA was assessed by measuring absorbance at 260 and 280 nm (Nanodrop ND-1000 Spectrophotometer, NanoDrop technologies LLC). RNA was used immediately for the preparation of cDNA using the Multiscribe reverse transcriptase. For the preparation of cDNA 100 ng of RNA was reverse transcribed using Taq-man reverse transcription kit (Life Technology, MA, USA) according to manufacturer's instructions. Reactions were performed on a thermal Cycler as following: 25°C, 10 min; 48°C, 30 min; 95°C, 5 min. cDNA was stored at -20°C.

For each independent sample, qPCR was performed in triplicate using TaqMan Gene Expression assays according to manufacturer's instructions (Life Technologies, MA, USA) for GAPDH (Hs02786624_g1), CALCR (Hs01016882_m1), CALCRL (Hs00907738_m1), RAMP1 (Hs00195288_m1), RAMP2 (Hs01006937_g1), RAMP3 (Hs00389131_m1) and plated onto fast microAmp plates containing 2 µl cDNA, 1 µl Taq-man probe, 10 µl Taq-man fast universal master mix (Applied Biosystems) and 10 µl ddH_2O. PCR reactions were performed on ABI 7900 HT real time PCR system. The program involved initial heating at 5°C for 2 min and denaturation at 95°C for 10 min, fluorescence was then detected over 40 cycles (95 for 15 s 60 for 1 min). Data are expressed as relative expression of the gene of interest to the reference gene GAPDH where: $Relative\ expression = 2^{-((Cq\ of\ gene\ of\ interest) - (Cq\ of\ ACTB))}$. For some genes no mRNA was detected. This is indicated in the figure legends (Ostrovskaya et al. 2019).

iCell specific statistical analysis

Raw impedance data were analysed using xCELLigence® RTCA CardioECR Data Analysis software (for 2D experiments). The software enables the assessment of cardiac cell beating and beat rate data to be generated this is defined as the number of beats per unit time and is expressed as beats/min, and

processed into graph format in GraphPad Prism. Impedance and from a sensor plate experiment were processed using Nanion CardioExcyte Control software (for 3D experiments). Beat detection and therefore beat rate was calculated for each sweep. This was then exported and processed into graph format in GraphPad Prism. Data are mean ± S.E.M. and statistical significance was calculated using unpaired Student's t test with Welch's correction.

CRISPR-cas9 cell generation, imaging and analysis

Immunofluorescence

This is the overarching protocol so where it differs it is outlined in the respective section. Cells were seeded in Cell Carrier Ultra 96 well plate (Perkinelmer, Boston) at a cell density of 160,000 cells/well and maintained at 37°C in 5% CO_2 with relevant cell culture media. Cells were washed twice with PBS, fixed with 4% paraformaldehyde (PFA) in PBS (10 min, RT) then washed three times with PBS. The cells were permeabilized with 0.05% Tween 20 in PBS (60 min, RT), and then incubated with 10% goat serum in PBS (60 min, RT). The cells were then incubated in primary antibody for RAMP1, or RAMP2 protein (Discovery Antibodies) (diluted at various manufacturer recommended concentrations in PBS/0.05% Tween/3% BSA) at 4°C, overnight and protected from light (other primary antibodies described in the sections they were used). The cells were washed three times with PBS and incubated with AlexaFluor 488 donkey anti-rabbit / AlexaFluor 568 goat anti-rabbit (Invitrogen, 1/500) (1hr, RT) protected from light. Cells were washed three times with PBS, then nuclei were stained with Hoechst (Invitrogen) (1/2000 in PBS, 10min, RT). Multi-wavelength analysis of results is performed on the CV7000 following a repeat of the 3x wash in PBS w/o Mg^{2+} or $Ca^{2+}{}_i$ and immediately imaged at 20x magnification (Cell Voyager 7000S, Yokogawa).

Kill curve generation

To generate a kill curve first cells at 90% confluency were harvested from flasks with Trypsin, then plated in cell carrier ultra 96 well plate at 10,000 cells per well and incubated 24 hours, 37°C 5% CO_2. 24 h later cells were treated with Puromycin and Blasticidin (stock at 10mg/ml) in the dosing regime ranging from 0 µg/ml to 30 µg/ml as outlined in the Results section. Cells are then Incubated for 72 hours 37°C 5% CO_2. 72 h later cell culture media was changed containing fresh antibiotic. 48 h after this cells were fixed and permeabilised in their plates as above. Cells are washed three times in PBS and then incubated in 1:2000 dilution of Hoechst (Invitrogen) in PBS + 0.05% Tween20 + 3% BSA for 1 hour protected from light. The cells were stored at 4°C prior to imaging on CV7000 as outlined previously.

CRISPR-cas9 genome engineering and MOI optimisation in HUVECs

HUVECs with the RAMP2 gene knocked out or the control HPRT1 gene knocked out were generated by CRISPR/Cas9 homology directed repair (Ran et al. 2013). The sgRNA sequences that were designed and manufactured targeting RAMP2 were (5'-CGCTCCGGGTGGAGCGCGCCGG-3'), (5'-TCCGGGTGGAGCGCGCCGGCGG-3'), and (5'-CCCGCGTCTCCCTAGGACCCGA-3') for Cas9 targeting to the human RAMP2 gene (Sigma-Aldrich). Positive control virus targeting HPRT1 gene was purchased 'off the shelf' from (Sigma-Aldrich). All guides were delivered in the LV01 vector (U6-gRNA:ef1a-puro-2A-Cas9-2A-tGFP) vector provided by (Sigma-Aldrich).

An optimal MOI of transduction had to be established to do this - cells at 90% confluency were harvested from flasks with Trypsin, then plated in cell carrier ultra 96 well plate at 10,000 cells per well and incubated 24 hours, 37°C 5% CO_2. Such that 24 h later cells were approximately 70% confluent. Media is removed from the cells 24 h later and media containing Polybrene (110 µl, 8

μg/ml) and virus. The concentration of virus varied to achieve an MOI range of 0.01 to 10. An amount was taken from the stock of pooled virus with a titre of 5533333 TU/ml ranging from 0.02 μl/well to 18 μl/well to achieve the desired MOI. Virus is stored at -70°C at all times. The amount of time it is removed from storage was kept to a minimum to reduce the chance of degradation as well as keeping samples on ice until application to cell samples. Following viral application cells are incubated for 24 hours 37°C 5% CO2. The following day media is removed and replaced with media containing puromycin (1 μg/ml) (Thermo Fisher Scientific) for 3 days to select for transduced cells. At this time media is changed again. In the control well that did not have viral addition upon media change no living cells remained, confirmed antibiotic selection. cells were fixed and permeabilised as above. The cells were then incubated in primary antibody for cas9 protein (Cell signalling technology) 7A9-3A3, diluted 1/700 in PBS/0.05% Tween/3% BSA) at 4°C, overnight and protected from light. Cells are washed three times in PBS and then incubated in 1:2000 dilution of Hoechst (Invitrogen) in PBS + 0.05% Tween20 + 3% BSA for 1 hour protected from light. The cells were stored at 4°C prior to imaging to imaging on CV7000 as outlined previously.

Once an optimal viral MOI was determined CRISPR-cas9 engineered cells could be generated for assays and sequencing, an overview of the process is shown in in (**Figure 2.1**) In detail:

More than one cell line was generated, as a control HPRT1 KO cell line was needed alongside the RAMP2 KO HUVECs; described below is the generation of RAMP2 KO using the virus pool at an MOI of 10: HUVEC cells were seeded in 6 well plates at a cell density of 160,000 cells/well and maintained at 37°C in 5% CO_2 with Complete Endothelial Cell Growth Media containing 100 μg/ml streptomycin (Sigma-Aldrich). 24 h after seeding pooled virus containing sgRNA/Cas9 constructs containing an MOI of 10, ensuring that each cell is infected by several lentivirus and increasing the likelihood of achieving KO. Transduction was performed in media containing 8 μg/ml Polybrene (Sigma-Aldrich). Cells were cultured for 24 h then treated with Puromycin (1 μg/ml) (Thermo Fisher Scientific) for 3 days to select for transduced cells. Cells then cultured in fresh media containing puromycin and expanded before

cells were collected for genotyping by Sanger sequencing (described below), qRT-PCR, and functional assays (described previously). All data shown were from cells expanded from these colonies.

Sequencing of genomic loci was performed by first extracting Genomic DNA from virally transduced HUVEC cells by: collecting approximately 10,000 cells, washing in PBS (sigma-Aldrich) and then lysing with DirectPCR Lysis Reagent (Viagen Biotech) containing Proteinase K (Qiagen) at 0.4 mg/ml. The lysate was incubated at 55°C for 4 h; 85°C, for 10 min; 12°C for 12 h. PCR reaction was then set up in (20 µl) as follows: 2x Flash Phusion PCR Master Mix (Thermo Fisher) (20 µl), forward primer (5'- AATTCGGGGAGCGATCCTG -3') (Eurogentec)(1 µl)(10 µm). reverse primer (5'-GAGACCCTCCGAAAATAGGC -3') (Eurogentec) (1 µl)(10 µm). DNA (100 ng/µl)(1 µl), ddH2O (7 µl). The product was amplified by PCR using the following program: 98°C, 1min; 35x (98°C, 10secs; 55°C, 10 s; 72°C, 15 s), 72°C, 1 min; 4°C, hold. PCR clean-up was performed prior to sequencing using the Illustra GFX PCR DNA and Gel-band Purification Kit (Illustra, now Sigma) according to manufacturer's instructions. Editing of RAMP2 gene was confirmed by Sanger sequencing (Eurofins, Camberley, UK) with the raw traces displayed the results section and online TIDE analysis also reported in the results section.

RAMP reintroduction in RAMP KO HUVECs

In HUVECs cells where RAMP2 KO was confirmed RAMP1 expression achieved through transduction of virus containing RAMP1 MISSION TRC3 Open Reading Frame (ORF) plasmid (pLX_304) (Sigma-Aldrich) into RAMP2 KO-HUVECs. HUVEC cells were seeded in 6 well plates at a cell density of 160,000 cells/well and maintained at 37°C in 5% CO_2 with Complete Endothelial Cell Growth Media containing 100µg/ml streptomycin (Sigma, US). 24 h after seeding, virus containing the ORF construct was transduced into cells in media containing 8 µg/ml Polybrene. Cells were cultured for 24 h then treated with blasticidin (5 µg/ml) (ThermoFisher Scientific) for 6 days to select for transduced cells.

Cells were collected for genotyping by qRT-PCR and expanded for functional assays methods for both outlined previously. All 'HUVEC RAMP1' data shown were from cells expanded from these colonies and grown in blasticidin.

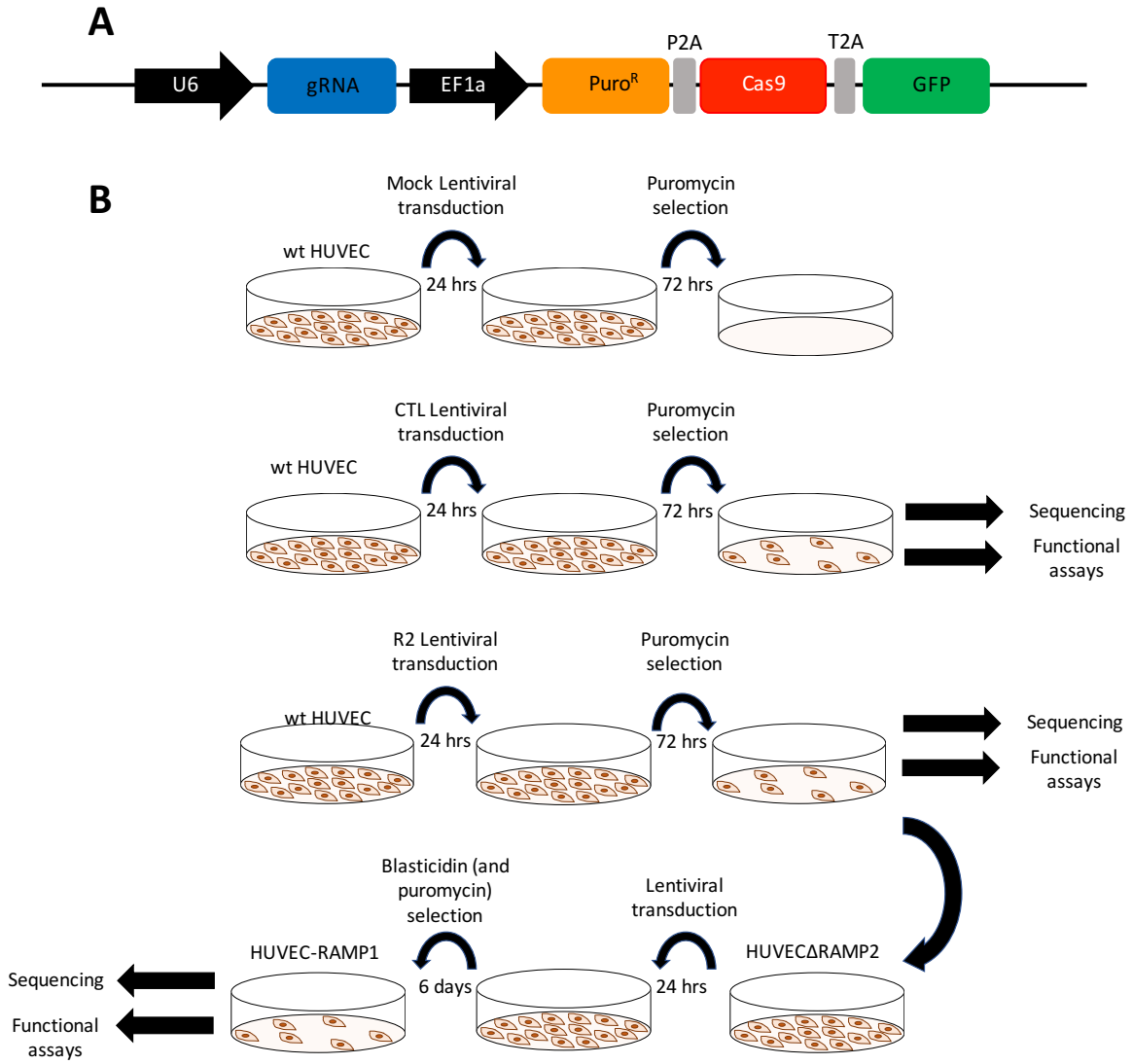

Figure 2.1. CRISPR-cas9 workflow. Schematic representation of the gRNA sequence targeting the 1st exon of the WT RAMP2 gene in the lentiviral vector expressing gRNA, puromycin resistance, GFP and cas9 supplied by (Sigma-Aldrich) (**A**). Schematic the workflow for generation of gene edited HUVEC cell pools (**B**).

Chapter 3. Identification and Characterisation of CLR Signalling in a Primary Cell Model.

Aims and Hypothesis

The overall aim of the thesis was to study endogenous agonist bias at the CLR. As a result the first aspect of the study was to identify a primary cell model that could be grown in cell culture and used over multiple passages to study CLR signalling and function in its endogenous environment. Due to the unique requirement of CLR to dimerise with a RAMP in order to traffic and function it was imperative that a cell line was identified that only expressed a single RAMP: (RAMP1, RAMP2 or RAMP3). To enable the receptor activity observed to be purely attributed to one CLR-RAMP complex, and thus further our understanding of that complex, rather than there being question marks over where the signalling comes from. Further to this it was also important to identify a cell model not expressing CTR, as the only other receptor known to bind and respond to the CGRP family peptides. In the literature HUVECs have been used for a long time as a good primary model for endothelial cell function at early passage numbers (Jaffe et al. 1973, Onat et al. 2011), and having recorded responsiveness to AM in an angiogenesis study (Fernandez-Sauze et al. 2004). Which promisingly suggested there may be some endogenous CLR. However, there were no studies exploring the GPCR pharmacology in these cells, specifically for the CLR mediated agonist bias in these cells. Therefore, the first step in this study was to determine the CGRP family receptor composition of the cell line in question. Following successful identification of the CLR in this cell line the aim was to identify the expression of proteins relevant to GPCR signalling. As well as establish the primary cell model in a variety of intracellular signalling assays and profile the signalling responses that the endogenous peptides could elicit through the CLR. Depending on the RAMP present it was established whether the cognate ligand vs the other two produced different signalling responses (if any) in the second messenger, and physiological response pathways.

On top of a desire to consider endogenous receptor activity in a more 'human' cell line. An issue which is often not considered is that most commonly used immortalised cell lines already express one or more RAMPs and quite often the CTR as it is believed to be important for cell line growth/ survival (Findlay 2006). In the literature experiments are usually performed on receptor RAMP complexes that are overexpressed in these cells (Hay et al. 2018). However, the background expression in them is often overlooked/left unexplored (Weston et al. 2016). Moreover, even when the cell line in question is the same as another it is often said that that no one 'HEK' line, for instance, is the same. The laboratory was fortunate to be gifted a HEK-293 line which did not express the CTR, CLR and RAMPs (Medimune, now AstraZeneca, Cambrdige). It was thought pertinent to replicate the literature co-expression studies of CLR and RAMPs to see if the same signalling patterns could be observed in these HEK-293 cells with a 'clean background'. These results here could then be viewed in light of the pharmacological studies performed in the primary cell system.

Then returning to primary cells and having established HUVECs as a good and novel model of endogenous CLR/RAMP2 function the aim was to identify another primary cell line expressing only CLR/RAMP2 and look at the signalling bias that the CGRP peptide family could elicit to determine whether the patterns of signalling and rank orders of potency observed were unique to CLR/RAMP2 in HUVECs or whether they appeared in other primary cells expressing the same receptor. Endothelial cells seemed a good starting point and HUAECs were the cells identified as model cells. Finally, an aim was to find a primary cell line expressing CLR/RAMP1, to establish how the CGRP family peptides signalled in a line expressing this receptor naturally, and what this would mean for the more physiological outcomes.

Results

HUVEC CGRP family Receptor Expression Profile

RT-PCR was performed in HUVECs using oligonucleotides for the CLR-related components of interest. This was done alongside a housekeeping gene (GAPDH) for reference and normalisation purposes. The mRNA expression was observed for the CTR and CLR receptors as well as the three RAMPs. The results are shown here as relative expression (**Figure 3.1**) generated from densitometry analysis of the PCR gel (**Supplemental Figure 8.1**). The data showed that the HUVECs expressed CLR and RAMP2, and crucially the presence of the CTR, RAMP1 or RAMP3 were not detected at the mRNA level. These data suggested that HUVECs may be a suitable model for the study of the endogenous CLR-RAMP2.

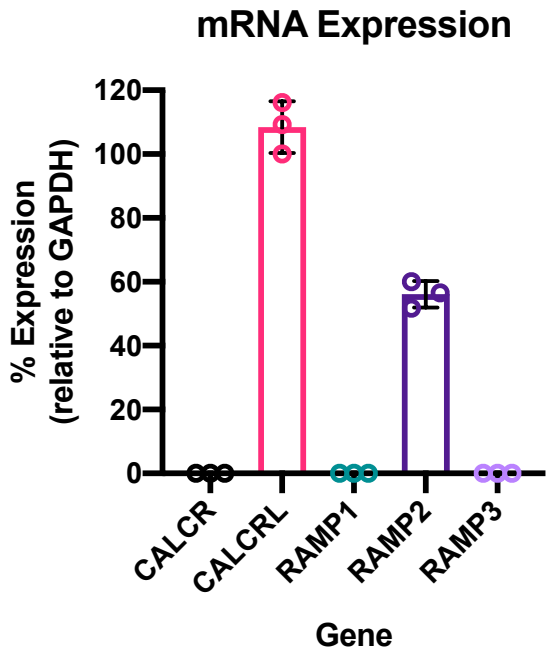

Figure 3.1. Calcitonin family Receptor expression in HUVECs. mRNA Expression of CALCR, CALCRL, RAMP1, RAMP2, and RAMP3 genes in HUVECs as determined by RT-PCR. Data represent mean + S.E.M. of 3 independent experiments relative to GAPDH expression. Where no expression was detected values are reported as 0.

Measurement of CLR-mediated Intracellular cAMP accumulation

Given the initial result promised the potential expression of a single receptor/RAMP complex. The next step was to determine whether there was any functional receptor in this these cells. In order to achieve this cAMP accumulation was used as CLR has been suggested to be a G_s-coupled receptor in the literature (McLatchie et al. 1998). To assess whether HUVECs were suitable for this assay it had to first be determined whether they produced a detectable amount of cAMP in this system. To do so forskolin was used; a direct activator of adenylyl cyclase over a concentration range of (100 pM-100 μM) using multiple passages (between P1 and P6) (**Figure 3.2**). This shows that there is a dose-dependent relationship between the concentration of forskolin added and the concentration of cAMP measured. These data confirm that these cells had all the apparatus necessary to measure cAMP accumulation in response to ligand stimulation. Therefore, it could be seen whether there was a detectable cAMP response when a GPCR shown to be present at the mRNA level (CLR) was stimulated with ligands known to activate it (CGRP, AM and AM2).

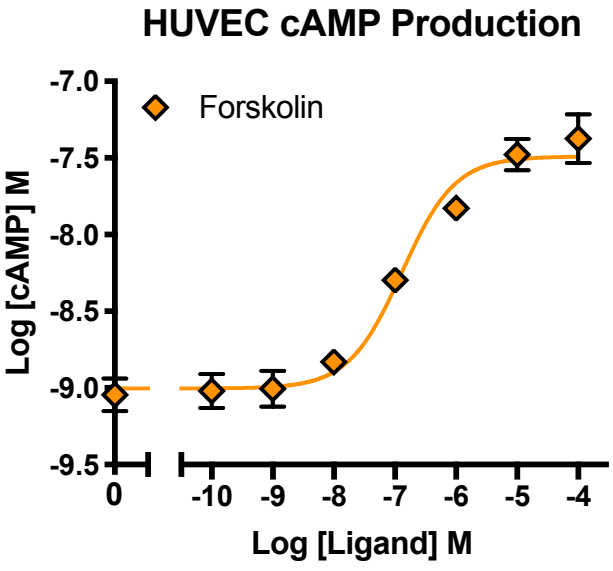

Figure 3.2: **cAMP Production in HUVECs.** Characterisation of cAMP accumulation in response to stimulation by forskolin over a concentration range of 100 pM to 100μM. Data are analysed using a three-parameter non-linear regression curve. All values represent mean + S.E.M. calculated from 4 Independent experiments.

CGRP family peptides mediated cAMP production in HUVECs

While the RT-PCR showed the presence of CLR and RAMP2 this was not enough evidence to prove that there was a functional receptor complexes at the surface of the cells. Therefore pharmacological investigation of the CLR-RAMP2 complex was performed using cAMP accumulation as a readout in response to CGRP, AM and AM2 the three peptides known to bind the CLR and produce a functional response (**Figure 3.3**). It was apparent that all 3 agonists were able to produce a functional cAMP-mediated response. In contrast a negative control was provided by both calcitonin and amylin as neither of which were able to produce a functional response above baseline in the HUVECs confirming, as anticipated from the RT-PCR data, that no functional CTR was present in these cells (**Figure 3.3A**).

In terms of the specific responses observed to CGRP, AM and AM2, based on previous research (Weston et al. 2016, Hay et al. 2018) with CLR/RAMP2 co-expressed in HEK-293 cells it was anticipated that AM would be the most potent ligand at eliciting a cAMP response, with both CGRP and AM2 significantly less potent than AM and indeed this proved to be the case in the HUVECs (AM>AM2>CGRP)(**Table 3.1**)(**Figure 3.3B**). Whereas In HEK-293 cells CGRP was the next potent and AM2 the least, this is the other way around in HUVECs with AM2 very clearly more potent than CGRP (**Figure 3.3**). This is demonstrated in their pEC50 values, AM2 is almost 10-fold less potent than AM and CGRP almost 100-fold, producing a very weak cAMP response (**Figure 3.3C**). Application of the operational model of agonism (Black and Leff 1983) enabled operation parameters to be determined (**Table 3.1**). These parameters will subsequently be used to provide an analysis of the signalling bias present in endothelial cells.

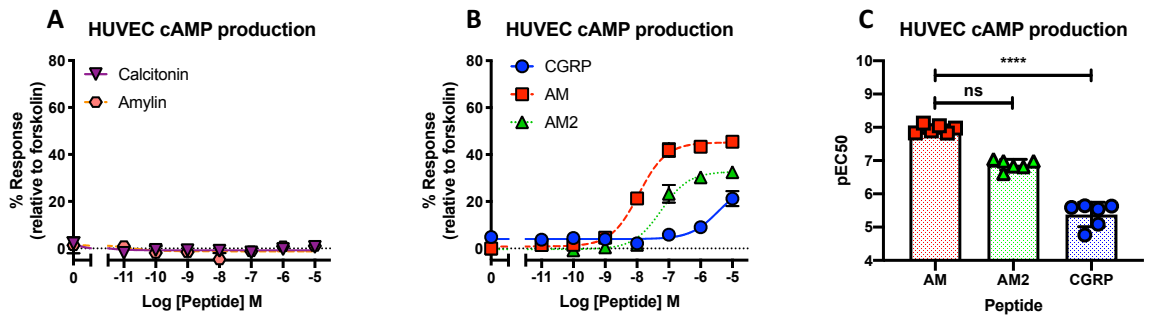

Figure 3.3. cAMP signalling in HUVECs in response to the calcitonin peptide family and CGRP peptide family. Characterisation of cAMP accumulation in response to stimulation by Calcitonin and Amylin in HUVECs relative to 100μM forskolin (**A**). Characterisation of cAMP accumulation in response to stimulation by CGRP, adrenomedullin (AM) and adrenomedullin 2 (AM2) in HUVECs relative to 100 μM forskolin (**B**). Data are analysed using a three-parameter non-linear regression curve. Individual pEC50 values + S.E.M. are the plotted for HUVECs (**C**). All values are calculated from 6 individual data sets. Statistical significance compared to the cognate ligand (AM) and determined using one-way ANOVA with Dunnett's post-hoc test, (*, p<0.05; **, p<0.01; ***, p<0.001; ****, p<0.0001).

	cAMP					
	CGRP		AM		AM2	
pEC50	5.46****	0.39	7.95	0.07	7.24	0.11
Emax	27.14*	6.75	45.17	1.17	32.75	1.21
pKa	5.61****	0.25	7.67	0.09	6.99****	0.14
logτ	-0.51***	0.09	-0.10	0.02	-0.33	0.03
n	6		6		6	

Table 3.1. cAMP signalling in HUVECs in response to the CGRP peptide family. Characterisation of cAMP accumulation in response to stimulation by CGRP, AM and AM2 in HUVECs relative to 100 μM forskolin. Data are analysed using a three-parameter non-linear regression curve, and are presented here as mean ± S.E.M. of n individual data sets. pEC50: negative logarithm of the agonist concentration required to produce a half-maximal response. Emax: maximal response to ligands expressed as a percentage of forskolin. pKa: negative logarithm of the equilibrium dissociation constant for each ligand generated using the operational model of agonism (Black and Leff 1983). Logτ: coupling efficiency parameter of the ligand (Black and Leff 1983). Statistical significance compared to the cognate ligand (AM) and determined using one-way ANOVA with Dunnett's post-hoc test, (*, p<0.05; **, p<0.01; ***, p<0.001; ****, p<0.0001).

CGRP family peptides mediated pERK$_{1/2}$ activation in HUVECs

The next signalling pathway downstream of GPCRs to consider in exploring and profiling the signalling of this peptide family in HUVECs is ERK$_{1/2}$ phosphorylation. First a commonly used positive control was established: PMA (Verin et al. 2000) could produce a measurable response in these cells (**Figure 3.4A**). From there the dose-response that could be produced by CGRP, AM and AM2 was profiled (**Figure 3.4B**), and how distinct they were from each other through statistical analysis of the differences between each ligand induced response compared to the cognate ligand for the receptor (AM) (**Table 3.2**). It was found that both CGRP and AM2 had significantly different potencies (**Figure 3.3C**). Surprisingly not only was the CGRP response the most significantly different but it was more potent than the cognate ligand for the receptor at ERK$_{1/2}$ phosphorylation. With a pEC50 of 7.71±0.10 (**Table 3.2**) this makes CGRP more than ten times more potent at eliciting ERK$_{1/2}$ phosphorylation than AM (pEC50: 6.36±0.12) and over 100 times more potent than AM2 (pEC50: 5.45±0.20). Again application of the operational model of agonism (Black and Leff 1983) has enabled operation parameters to be determined (**Table 3.2**).

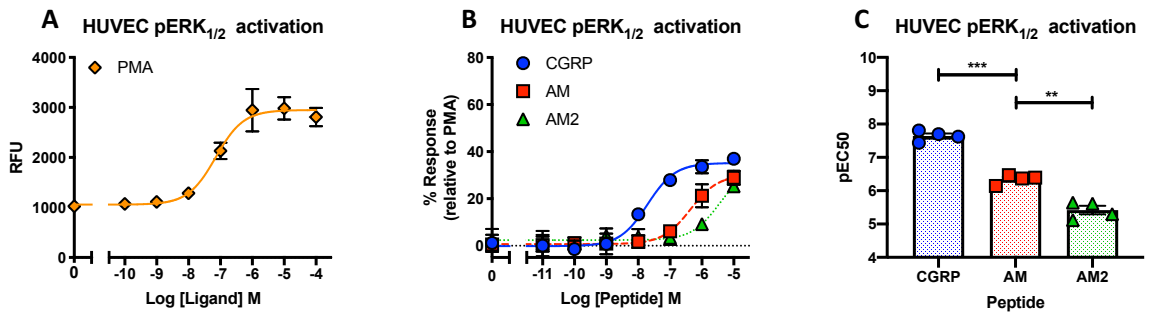

Figure 3.4. $ERK_{1/2}$ signalling in HUVECs in response to the calcitonin peptide family and CGRP peptide family. Characterisation of $pERK_{1/2}$ activation in response to stimulation by PMA over a concentration range of 100 pM to 100 μM (**A**). Characterisation of $pERK_{1/2}$ activation in response to stimulation by CGRP, AM and AM2 in HUVECs relative to 100 μM PMA (**B**). Data are analysed using a three-parameter non-linear regression curve. Individual pEC50 values + S.E.M. are then plotted for HUVECs. All values are calculated from 4 individual data sets. Statistical significance compared to the cognate ligand (AM) and determined using one-way ANOVA with Dunnett's post-hoc test, (*, p<0.05; **, p<0.01; ***, p<0.001; ****, p<0.0001).

	$pERK_{1/2}$					
	CGRP		AM		AM2	
pEC50	7.71***	0.10	6.36	0.12	5.45**	0.20
Emax	35.17	1.13	30.16	1.75	33.30	4.59
pKa	7.46***	0.10	6.18	0.13	5.41**	0.19
logτ	-0.28	0.02	-0.38	0.04	-0.35	0.08
n	4		4		4	

Table 3.2. $ERK_{1/2}$ signalling in HUVECs in response to the calcitonin peptide family and CGRP peptide family. Characterisation of $pERK_{1/2}$ activation in response to stimulation by CGRP, AM and AM2 relative to 100 μM PMA. Data are analysed using a three-parameter non-linear regression curve, and are presented here as mean ± S.E.M. of n individual data sets. pEC50: negative logarithm of the agonist concentration required to produce a half-maximal response. Emax: maximal response to ligands expressed as a percentage of PMA. pKa: negative logarithm of the equilibrium dissociation constant for each ligand generated using the operational model of agonism (Black and Leff 1983). Logτ: coupling efficiency parameter of the ligand (Black and Leff 1983). Statistical significance compared to the cognate ligand (AM) and determined using one-way ANOVA with Dunnett's post-hoc test, (*, p<0.05; **, p<0.01; ***, p<0.001; ****, p<0.0001).

CLR-mediated signalling in a clean background HEK-293 cell line

Initially the signalling response of un-transfected HEK-293S's vs the 'clean background' (i.e. those without background CTR/CLR/RAMP expression) HEK-293S's were looked at to see if there was a difference in background expression (**Figure 3.5**). Using calcitonin and CGRP there was a clear difference; in the un-transfected HEK-293S cells that had not undergone receptor KO both ligands produced a potent response (**Figure 3.5.A**) whereas in the 'clean background' HEK-293S cells only a very small response was observable above baseline at the highest concentration (Figure 3.5.B). Then the CLR and three RAMPs were individually over-expressed in this clean background cell line and profiled the signalling of CGRP, AM and AM2 through cAMP production and then directly compare this to the responses observed in primary human cells. As well as $ERK_{1/2}$ signalling to potentially inform the understanding of the primary cell $ERK_{1/2}$ signalling (**Figure 3.4**). The rank order of potencies produced in the cAMP assays for CLR-RAMP2 (**Figure 3.6B**) corresponded with the cAMP data produced in HUVECs. Interestingly AM2 again was more potent than CGRP contrasting with the previous literature reports (**Table 3.3**) (Weston et al. 2016). Across the board the CGRP responses are less potent than those seen in the literature. The increased CGRP potency seen in the literature may be related to the strong CGRP response recorded in un-transfected HEK-293S cells that did not have no background CLR/CTR expression. While only an example this demonstrated the importance of a clean background in these pharmacological studies. In the $ERK_{1/2}$ phosphorylation experiments, the peptides were in general less potent than at cAMP accumulation with the notable exception of AM in the CLR-RAMP1 expressing cells (**Figure 3.6A**). Here it was more potent at $pERK_{1/2}$ than at cAMP accumulation. The responses produced by CGRP, AM and AM2 were also less distinct from each other shown by a lack of significance compared to the cognate ligand (**Table 3.3**). In contrast to cAMP

signalling, where in all cases apart from CLR-RAMP3 the pEC50s were significantly different from the cognate ligand (**Table 3.3**).

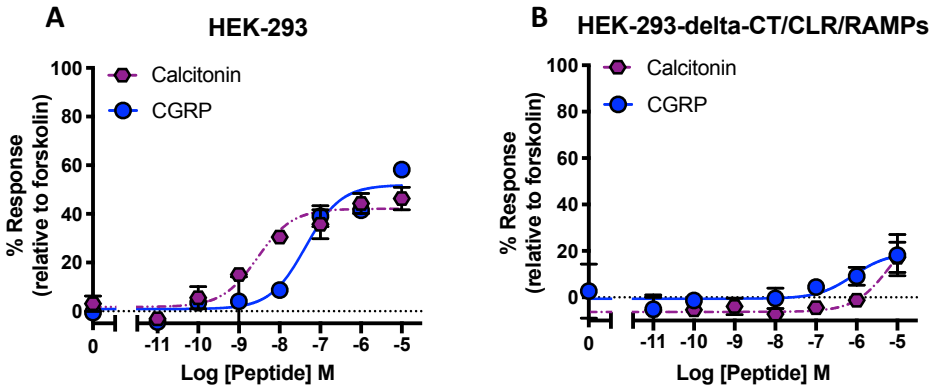

Figure 3.5. cAMP signalling in HEK-293 cells in response to calcitonin and CGRP. Characterisation of cAMP accumulation in response to stimulation by calcitonin and CGRP in HEK 293S and HEK 293 CTR, CLR and RAMP knockout cells, relative to 100 μM forskolin (**A**). Characterisation of cAMP accumulation in response to stimulation by CGRP in HEKs relative to 100 μM forskolin (**B**). Data are analysed using a three-parameter non-linear regression curve. All values are calculated from 3 individual data sets.

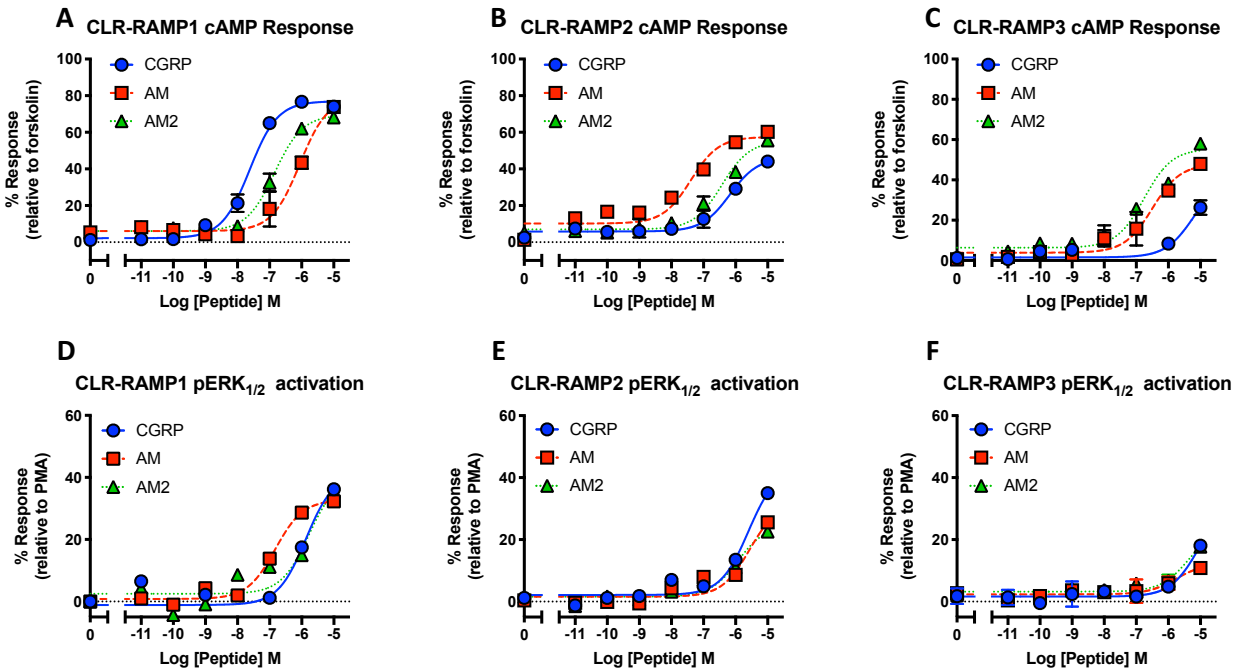

Figure 3.6. cAMP and $ERK_{1/2}$ signalling in HEK-293 cells co-expressing CLR-RAMP1, CLR-RAMP2 and CLR-RAMP3 in response to the CGRP peptide family. Characterisation of cAMP and $ERK_{1/2}$ in response to stimulation by CGRP, AM and AM2 in HEKs relative to 100μM forskolin(**A-F**). Data are analysed using a three-parameter non-linear regression curve. Individual pEC50 values + S.E.M. are the plotted for HEKs. All values are calculated from 3 individual data sets.

		cAMP					
		CGRP		**AM**		**AM2**	
CLR-RAMP1	pEC50	7.62	0.07	6.05****	0.12	6.84**	0.07
	Emax	76.99	1.77	79.14	4.83	69.48	1.78
	pKa	6.98	0.09	5.40***	0.20	6.35*	0.08
	Logτ	0.51	0.04	0.54	0.13	0.32	0.04
	n	3		3		3	
		CGRP		**AM**		**AM2**	
CLR-RAMP2	pEC50	6.17**	0.12	7.17	0.11	6.42**	0.13
	Emax	46.24*	2.65	58.84	1.91	55.31	3.02
	pKa	5.93**	0.14	6.85	0.12	6.11*	0.15
	Logτ	-0.12	0.05	0.03	0.04	0.03	0.06
	n	3		3		3	
		CGRP		**AM**		**AM2**	
CLR-RAMP3	pEC50	5.22	0.65	6.50	0.19	6.59	0.20
	Emax	41.18	23.24	47.84	3.72	53.91	4.23
	pKa	5.00	0.82	6.23	0.21	6.29	0.23
	Logτ	-0.17	0.42	-0.07	0.07	0.01	0.08
	n	3		3		3	
		$pERK_{1/2}$					
		CGRP		**AM**		**AM2**	
CLR-RAMP1	pEC50	5.88	0.35	6.82	0.13	5.74	0.44
	Emax	41.21	8.96	32.83	1.70	41.01	10.60
	pKa	5.65	0.39	6.65	0.13	5.52	0.50
	Logτ	-0.14	0.16	-0.33	0.04	-0.19	0.20
	n	3		3		3	
		CGRP		**AM**		**AM2**	
CLR-RAMP2	pEC50	5.60	0.22	5.56	0.35	5.92	0.24
	Emax	43.16	6.04	32.04	7.52	24.81	3.40
	pKa	5.36	0.25	5.40	0.39	5.81	0.26
	Logτ	-0.14	0.11	-0.35	0.15	-0.51	0.08
	n	3		3		3	
		CGRP		**AM**		**AM2**	
CLR-RAMP3	pEC50	5.06	0.43	5.77	0.31	5.36	0.42
	Emax	32.28	14.64	12.25	1.95	24.04	7.11
	pKa	4.90	0.53	5.73	0.32	5.26	0.46
	Logτ	-0.34	0.30	-0.95	0.10	-0.56	0.19
	n	3		3		3	

Table 3.3. cAMP signalling in HEK-293 cells co-expressing CLR-RAMP1, CLR-RAMP2 and CLR-RAMP3 in response to the CGRP peptide family and CGRP peptide family. Characterisation of cAMP accumulation in response to stimulation by CGRP, AM and AM2 in HEK-293S relative to 100 μM forskolin. Data are analysed using a three-parameter non-linear regression curve, and are presented here as mean ± S.E.M. of n individual data sets. pEC50: negative logarithm of the agonist concentration required to produce a half-maximal response. Emax: maximal response to ligands expressed as a percentage of forskolin. pKa: negative logarithm of the equilibrium dissociation constant for each ligand generated using the operational model of agonism (Black and Leff 1983). Logτ: coupling efficiency parameter of the ligand (Black and Leff 1983). Statistical significance compared to the cognate ligand (CLR-RAMP1: CGRP, CLR-RAMP2: AM, CLR-RAMP3: AM2) and determined using one-way ANOVA with Dunnett's post-hoc test, (*, p<0.05; **, p<0.01; ***, p<0.001; ****, p<0.0001).

CGRP family peptide signalling and receptor expression in HVSMCs

In the initial search for a cell line expressing a single receptor/RAMP complex the possibility of using vascular smooth muscle cells (HVSMCs) was explored as a model alongside profiling HUVEC receptor expression, cAMP and $pERK_{1/2}$ responses, the same experiments were performed in HVSMCs. The cAMP and $ERK_{1/2}$ assays performed promisingly suggested that there was functional CLR at the surface (**Figure 3.7A,B**). These data showed that in the HVSMCs that CGRP was the most potent peptide at cAMP accumulation, AM the least, but in the $ERK_{1/2}$ phosphorylation the most and least potent peptides were AM and AM2 respectively. Unfortunately, the RT-PCR showed that both RAMP1 and RAMP2 are expressed (**Figure 3.7C**). While this does not mean to say both are translated, the current paucity in well regarded antibodies (Hay et al. 2018) (and indeed later optimisation experiments potentially confirming this (**Supplemental Figure 8.10**)) meant that this was not possible at the time to easily assess with certainty whether only RAMP1 was expressed at the cell surface despite the fact that CGRP was the most potent mediator of cAMP in this cell type (**Table 3.4**). Moreover, with both RAMPs transcribed there are no guarantees that certain conditions or forms of stimulation might stimulate translation of the other RAMP. Given this uncertainty it was concluded that it was necessary to choose a suitable model cell line with a 'clean' expression pattern from the mRNA level onwards. To provide as much certainty as possible about what receptor complex is producing the observed effects. This led to future work focusing on HUVECs as well as HUAECs and HCMs as will be detailed later on in this chapter.

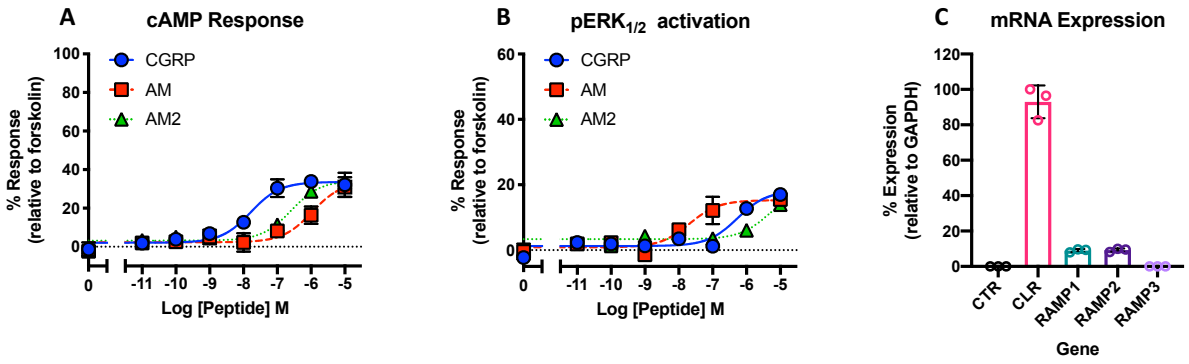

Figure 3.7. cAMP signalling, $ERK_{1/2}$ activation and receptor expression in HVSMCs. Characterisation of cAMP accumulation in response to stimulation by CGRP, AM and AM2 in HVSMCs relative to 100 μM forskolin (**A**). Characterisation of $pERK_{1/2}$ activation in response to stimulation by CGRP, AM and AM2 in HVSMCs relative to 100 μM PMA (**B**). mRNA Expression of CALCR, CALCRL, RAMP1, RAMP2, and RAMP3 genes relative to GAPDH in HVSMCs. Determined by RT-PCR (**C**). Data are analysed using a three-parameter non-linear regression curve. All values are calculated from at least 3 individual data sets.

	cAMP					
	CGRP		AM		AM2	
pEC50	7.79	0.11	5.97	0.16	6.59	0.11
Emax	33.61	1.21	33.72	3.00	34.37	1.51
pKa	7.60	0.11	5.79	0.15	6.45	0.13
logτ	-0.33	0.03	-0.33	0.05	-0.32	0.04
n	4		4		4	

	$pERK_{1/2}$					
	CGRP		AM		AM2	
pEC50	6.27	0.22	7.69	0.29	5.33	0.43
Emax	18.16	2.00	15.28	1.57	18.80	5.38
pKa	6.16	0.25	7.52	0.27	5.56	0.32
logτ	-0.70	0.07	-0.80	0.05	-0.75	0.11
n	3		3		3	

Table 3.4. cAMP signalling and ERK activation in HVSMCs. Characterisation of cAMP accumulation in response to stimulation by CGRP, AM and AM2 in HVSMCs relative to 100 μM forskolin. Characterisation of $pERK_{1/2}$ activation in response to stimulation by CGRP, AM and AM2 in HVSMCs relative to 100 μM PMA. Data are analysed using a three-parameter non-linear regression curve, and are presented here as mean ± S.E.M. of n individual data sets.

Antagonising CGRP, AM and AM2-mediated cAMP accumulation in HUVECs

The evidence thus far suggests that HUVECs could be the best model going forward as the CLR and a single RAMP - RAMP2 are expressed (**Figure 3.1**), and that they produce a functional CLR-RAMP2 receptor at the cell surface. However, in order to prove beyond doubt that all cAMP responses produced by the CGRP family of peptides were due to CLR-RAMP2 receptor signalling attempts were made to antagonise the response using a known antagonist of the CLR-RAMP2 receptor (Hay et al. 2003): AM22-52. A cleaved version of full length adrenomedullin peptide with no intrinsic agonist ability. Experiments were also performed to attempt to antagonise the cAMP responses with Olcegepant: the clinically approved antagonist of the CLR-RAMP1 receptor (Petersen et al. 2005)**.** **Figure 3.8** shows that AM22-52 was able to significantly antagonise the responses from all three ligands. It has reduced the potency of AM and AM2 as shown. The change in CGRP pEC50 was not significant however this may be related to the error produced by curve fitting to a very small response, and indeed the reduction in response is confirmed by a significant drop in Emax ($p<0.01$). In contrast to the effects seem with AM22-52. Olcegepant did not significantly alter any of the responses (**Figure 3.8**) demonstrating that no signalling responses are occurring through CLR-RAMP1, in alignment with previous results showing no RAMP1 expression (**Figure 3.1**).

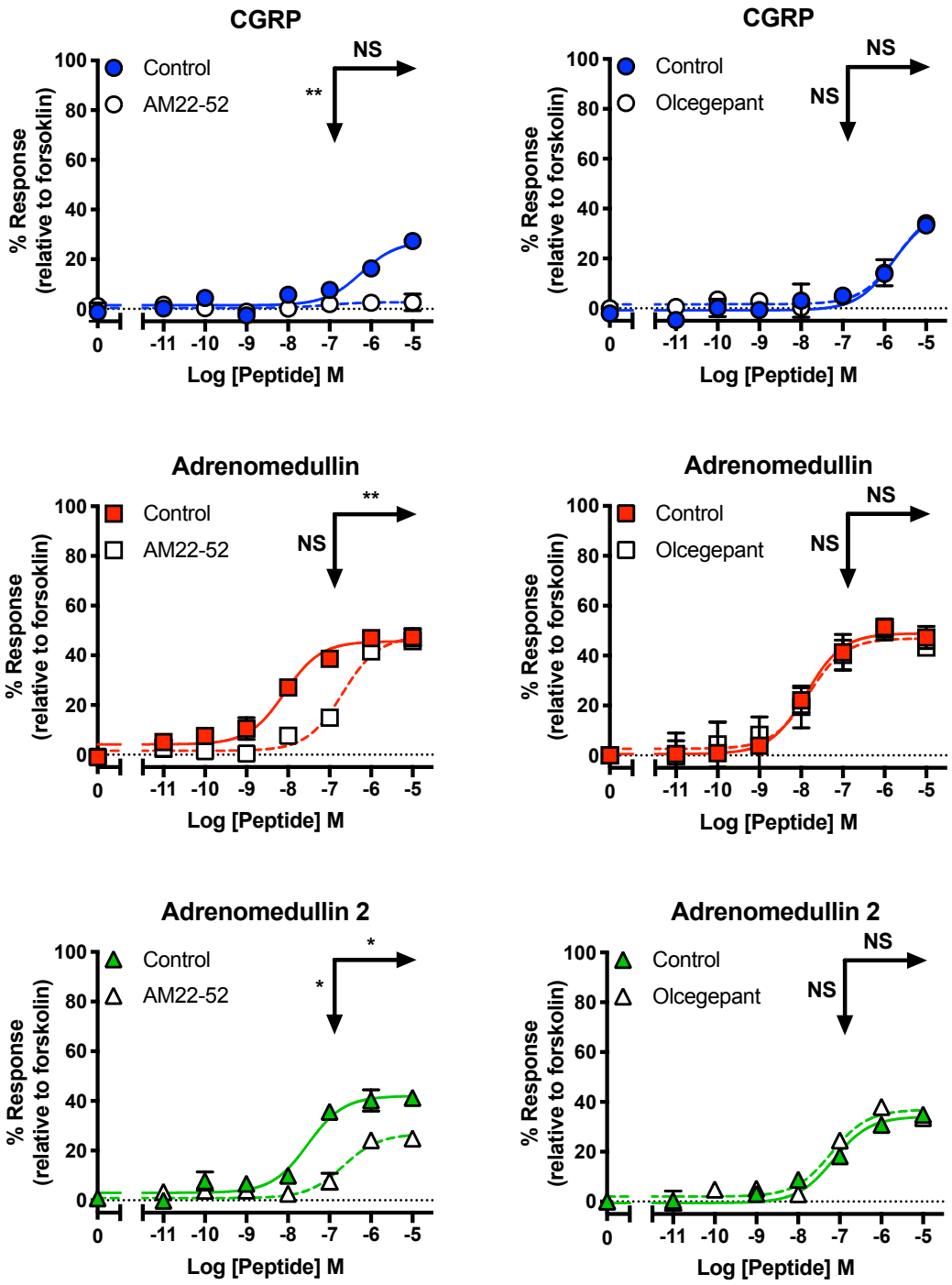

Figure 3.8. Antagonism of cAMP signalling in HUVECs with CLR-RAMP2 and CLR RAMP1 antagonists. Characterisation of cAMP accumulation in response to stimulation by CGRP, adrenomedullin (AM) and adrenomedullin 2 (AM2) in HUVECs in the presence and absence of 100 nM AM22-52 or Olcegepant respectively. All relative to 100 μM Forskolin. Data are analysed using a three-parameter non-linear regression curve. Statistical significance determined compared to control using an unpaired t test with Welch's correction: *, $p<0.05$; **, $p<0.01$; ***, $p<0.001$. NS denotes no statistical significance observed. All values are calculated from at least 3 individual data sets. Horizontal arrows show pEC50, and Vertical arrows show Emax statistical significance.

	AM22-52					
	CGRP		AM		AM2	
pEC50	7.08	1.81	6.69**	0.11	6.67*	0.24
Emax	2.71**	1.71	47.68	2.16	26.74*	2.67
pEC50 (c)	6.24	0.28	8.08	0.13	7.52	0.16
Emax (c)	27.36	4.60	45.66	1.74	42.02	2.15
n	3		3		3	

	Olcegepant					
	CGRP		AM		AM2	
pEC50	5.70	0.18	7.82	0.12	7.20	0.14
Emax	38.74	4.93	46.90	1.72	36.91	1.82
pEC50 (c)	5.79	0.20	7.88	0.15	7.15	0.17
Emax (c)	40.54	4.58	48.93	2.43	34.14	2.17
n	6		6		6	

Table 3.5. Antagonism of cAMP signalling in HUVECs with CLR-RAMP2 and CLR-RAMP1 antagonists. Characterisation of cAMP accumulation in response to stimulation by CGRP, AM, and AM2 in HUVECs in the presence and absence of 100 nM AM22-52 or Olcegepant respectively. All relative to 100 μM forskolin. (c) represents control treated data. Data are analysed using a three-parameter non-linear regression curve, and are presented here as mean ± S.E.M. of n individual data sets. Statistical significance determined compared to each individual control using an unpaired t test with Welch's correction: *, $p<0.05$; **, $p<0.01$; ***, $p<0.001$.

Exploring the effect of primary cell passage number on signalling

The above results are taken from experiments on cells from P1-6 only due to the suggestion that outside of this range HUVECs can lose the expression of certain proteins (Jersmann et al. 2001). It was explored whether the cAMP response to the peptides and therefore GPCR signalling would change over passage numbers beyond those suggested as the optimal limit by the literature. The following experiments were performed from passage 3 to 14. After which the cells went into senesce and would not grow any further. The results show that for CGRP and AM induced cAMP signalling the responses do not significantly differ over passage number between results up to passage 6 and results after passage 6 (**Figure 3.9**). This suggests that the cellular signalling machinery and receptor expression levels do not significantly change up until the cells enter senescence after passage 14. However, there were two cases of AM2 EC50s differing significantly from the early passage data, at passage 11 and 1 2(**Table 3.6**). Although the Emax data does not differ and the AM2 potencies at subsequent passages are not significantly altered. Suggesting these are isolated differences and not part of a wider trend. As there is no other statistical evidence for the signalling changing in a meaningful way. This suggests that the CLR-RAMP2 G_s function of the cells remains consistent. There were some isolated differences observed in the AM2 data but overall there were no observable trends or deviations. Although future work was performed at passages only up to 6 to remain in line with literature evidence that these cells become less 'endothelial like' at later passages it has been demonstrated that it is possible, if necessary, to explore cAMP signalling dynamics at later passages with some level of confidence that the results will not differ from those seen at earlier passages.

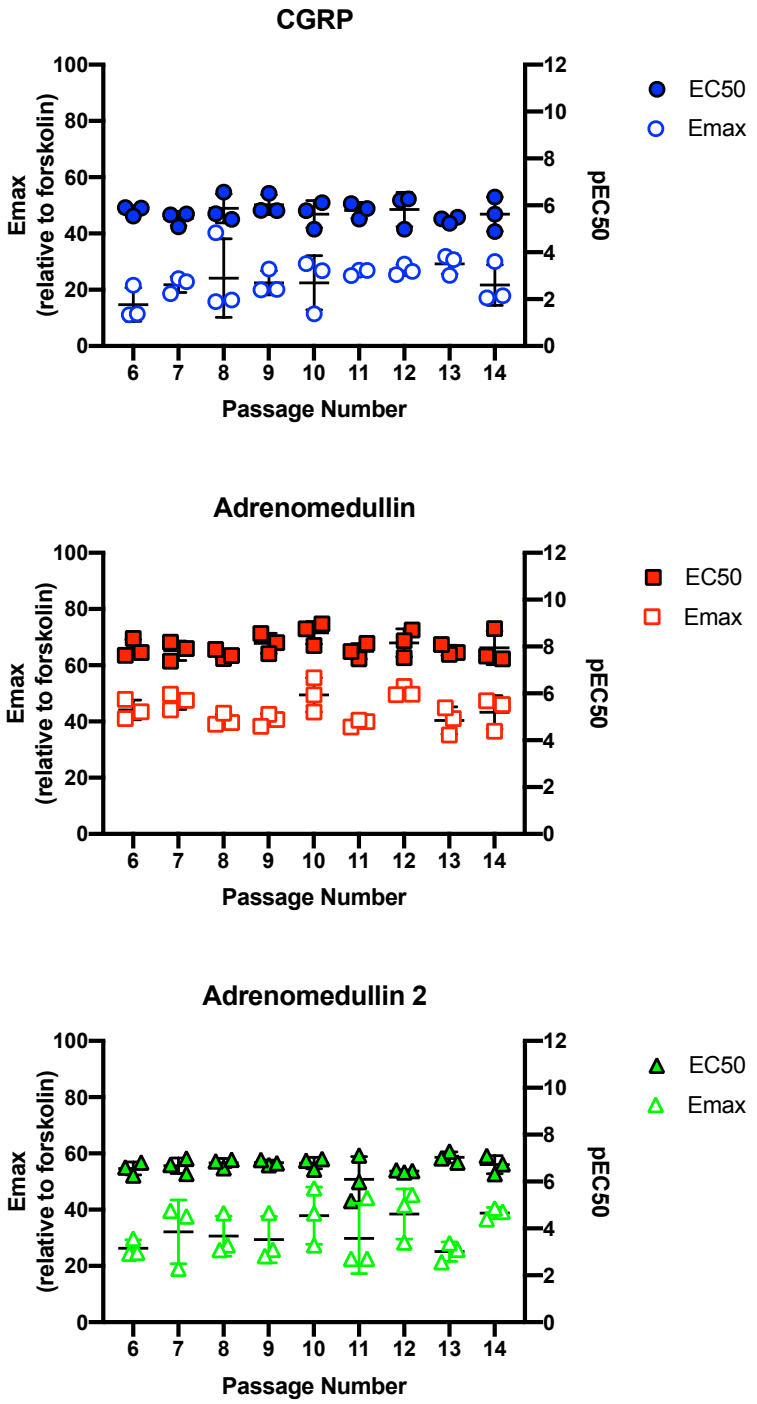

Figure 3.9. CGRP family peptide cAMP signalling in HUVECs beyond passage 6. Characterisation of cAMP accumulation in response to stimulation by CGRP, adrenomedullin (AM) and adrenomedullin 2 (AM2) in HUVECs relative to 100 μM forskolin across multiple passages. Data are analysed using a three-parameter non-linear regression curve, and pEC50/Emax values are plotted from 3 individual data sets

Passage	pEC50	S.E.M.	CGRP Emax	S.E.M.	n
6	5.78	0.12	14.72	3.44	3
7	5.44	0.18	21.80	1.62	3
8	5.87	0.35	24.15	8.06	3
9	6.03	0.25	22.49	2.46	3
10	5.62	0.33	22.50	5.58	3
11	5.79	0.19	26.28	0.61	3
12	5.83	0.42	27.03	1.12	3
13	5.38	0.08	29.24	2.08	3
14	5.62	0.42	21.67	4.17	3

Passage	pEC50	S.E.M.	AM Emax	S.E.M.	n
6	7.91	0.22	44.12	2.00	3
7	7.82	0.24	47.10	1.62	3
8	7.66	0.12	40.52	1.23	3
9	8.13	0.25	40.53	1.24	3
10	8.59	0.28	49.45	3.51	3
11	7.80	0.19	39.50	0.72	3
12	8.16	0.34	50.54	0.95	3
13	7.83	0.13	40.39	2.80	3
14	7.94	0.41	43.29	3.42	3

Passage	pEC50	S.E.M.	AM2 Emax	S.E.M.	n
6	6.56	0.16	26.28	1.73	3
7	6.67	0.19	32.12	6.55	3
8	6.79	0.11	30.61	4.11	3
9	6.81	0.06	29.39	4.77	3
10	6.79	0.14	37.90	5.87	3
11	6.09**	0.56	29.75	7.22	3
12	6.44*	0.03	38.46	5.14	3
13	7.03	0.14	25.09	1.99	3
14	6.72	0.22	38.80	1.15	3

Table 3.6 CGRP family peptide cAMP signalling in HUVECs beyond passage 6. Characterisation of cAMP accumulation in response to stimulation by CGRP, adrenomedullin (AM) and adrenomedullin 2 (AM2) in HUVECs relative to 100 μM forskolin across multiple passages. Data are analysed using a three-parameter non-linear regression curve, and are presented here as mean ± S.E.M. of n individual data sets. Statistical significance compared to the mean + S.E.M. of CGRP, AM and AM2 for pEC50 and Emax from **Table 1.1** and determined using one-way ANOVA with Dunnett's post-hoc test (*, p<0.05; **, p<0.01; ***, p<0.001, p<0.001 ****).

CGRP family peptide mediated intracellular calcium release in HUVECs

i[Ca^{2+}] mobilisation was the next commonly measured second messenger utilised by GPCRs that was aimed to measure in HUVECs in response to CGRP, AM and AM2. First a positive control (ionomycin) was used to determine whether it was possible to observe i[Ca^{2+}] mobilisation in these cells. This was possible as seen in **Figure 3.10A** and provided a positive control for assessing GPCR induced calcium release. From there the dose-dependency that could be produced by CGRP, AM and AM2 was profiled (**Figure 1.11B**). Dose-response curves were generated by normalising the peak fluorescence produced to ionomycin (**Supplemental Figure 8.3**). Then how distinct CGRP, AM and AM2 responses were from each other was determined through statistical analysis of the differences between each ligand induced response compared to the cognate ligand for the receptor (AM) (**Figure 1.11C**). Strikingly, AM2 here produces the most potent response and an even more significantly higher maximal level of calcium release, relative to the comparatively modest level produced by the cognate ligand (AM). In contrast to AM and AM2, CGRP was able to stimulate effectively no calcium release from internal stores. Again application of the operational model of agonism (Black and Leff 1983) has enabled operation parameters to be determined (**Table 3.7**).

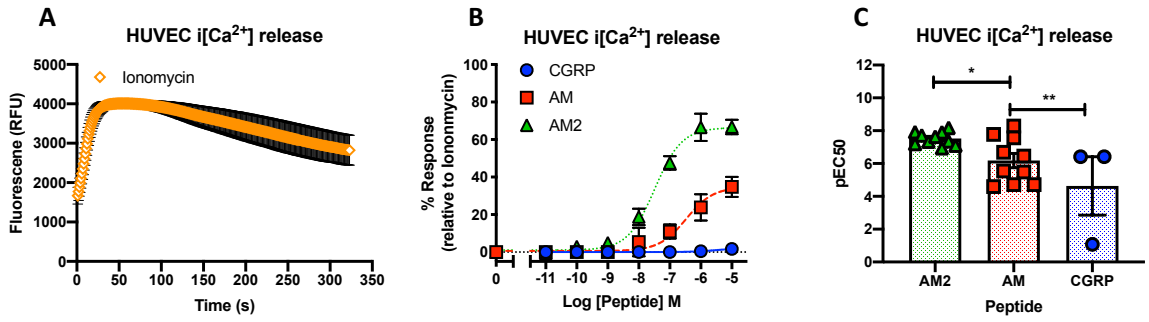

Figure 3.10. Intracellular calcium signalling in HUVECs in response to the CGRP peptide family. Characterisation of i[Ca^{2+}] release in response to stimulation by Ionomycin at 10 μM (**A**). Characterisation of i[Ca^{2+}] release in response to stimulation by CGRP, adrenomedullin (AM) and adrenomedullin 2 (AM2) in HUVECs relative to 100 μM ionomycin (**B**). Data are analysed using a three-parameter non-linear regression curve. Individual pEC50 values + S.E.M. are then plotted for HUVECs (**C**). All values are calculated from at least 3 individual data sets. Statistical significance compared to the cognate ligand (AM) and determined using one-way ANOVA with Dunnett's post-hoc test, (*, p<0.05; **, p<0.01; ***, p<0.001; ****, p<0.0001).

	Calcium					
	CGRP		AM		AM2	
pEC50	5.44**	0.33	6.47	0.26	7.48*	0.10
Emax	2.26****	0.54	34.72	3.71	66.36***	2.66
pKa	5.44	0.34	6.29	0.27	7.03*	0.10
logτ	-1.63****	0.10	-0.28	0.07	0.29****	0.05
n	3		10		10	

Table 3.7. Intracellular calcium signalling in HUVECs in response to the CGRP peptide family. Characterisation of i[Ca^{2+}] release in response to stimulation by CGRP, AM and AM2 relative to 10 μM ionomycin. Data are analysed using a three-parameter non-linear regression curve, and are presented here as mean ± S.E.M. of n individual data sets. pEC50: negative logarithm of the agonist concentration required to produce a half-maximal response. Emax: maximal response to ligands expressed as a percentage of ionomycin. pKa: negative logarithm of the equilibrium dissociation constant for each ligand generated using the operational model of agonism (Black and Leff 1983). Logτ: coupling efficiency parameter of the ligand (Black and Leff 1983). Statistical significance compared to the cognate ligand (AM) and determined using one-way ANOVA with Dunnett's post-hoc test, (*, p<0.05; **, p<0.01; ***, p<0.001; ****, p<0.0001).

CGRP family peptide signalling in HUVECs from a single donor

All HUVEC experiments described previously were performed using HUVECs from pooled donors as standard. The signalling responses of CGRP, AM and AM2 were profiled in HUVECs from a single donor to assess whether the same patterns of responses could be seen across all three signalling pathways. In the case of cAMP the same rank order of potencies was observed (AM>AM2>CGRP)(**Figure 3.11A**), although the difference between AM and AM2 pEC50 is accentuated in the single donor cells with it now being significant. For $ERK_{1/2}$ phosphorylation CGRP is again the most potent relative to the other two peptides (**Figure 3.11B**). However, when comparing AM with AM2 while AM2 is still the least potent it is not significantly so in these single donor HUVECs. When measuring intracellular calcium mobilisation, no response was recorded to CGRP in these cells so curve fitting could not be achieved with the data and thus the pEC50/Emax values are reported as zero (**Figure 3.11C**). This differs only slightly to the pooled donor case as the responses were very close to zero, however for those data it was possible to fit a curve and report pEC50/Emax values. For the other two peptides the trends observed were also very similar to the pooled donor responses; as AM2 was significantly more potent than AM, as was the maximal response. Overall In the three pathways measured it is apparent that CGRP, AM and AM2 produces very similar patterns of responses relative to each other in the single donor case as they do when cells are pooled together from multiple donors (**Table 3.8**). Therefore, it was concluded that signalling we observed in cells pooled from multiple donors is reflective of the signalling that occurs in cells from individual donors.

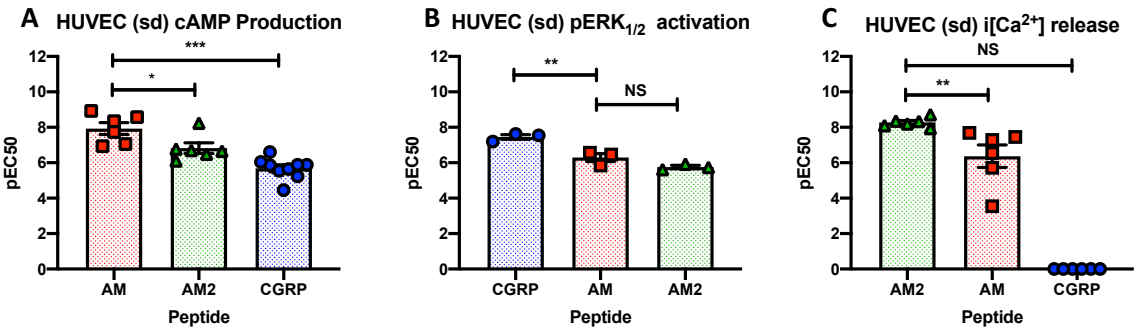

Figure 3.11. CGRP family peptide cAMP, $ERK_{1/2}$ and calcium signalling in single donor HUVECs. Characterisation of cAMP accumulation (**A**), $pERK_{1/2}$ activation (**B**) and $i[Ca^{2+}]$ release (**C**) in response to stimulation by CGRP, adrenomedullin (AM) and adrenomedullin 2 (AM2) in HUVECs relative to forskolin (100 μM), PMA (100 μM) and ionomycin (10 μM) respectively. Data are analysed using a three-parameter non-linear regression curve, and pEC50 values are plotted from at least 3 individual data sets.

	cAMP					
	CGRP		AM		AM2	
pEC50	5.68***	0.20	7.93	0.34	6.82*	0.30
Emax	17.85****	4.83	42.19	1.61	35.40	1.10
n	6		6		9	

	$pERK_{1/2}$					
	CGRP		AM		AM2	
pEC50	7.45**	0.13	6.29	0.22	5.76	0.09
Emax	36.24	2.18	28.20	2.07	26.54	2.72
n	3		3		3	

	Calcium					
	CGRP		AM		AM2	
pEC50	N/D	N/D	6.37	0.64	8.27**	0.11
Emax	N/D	N/D	38.87	2.80	47.61***	4.22
n	6		6		6	

Table 3.8. CGRP family peptide cAMP, $ERK_{1/2}$ and calcium signalling in single donor HUVECs. Characterisation of cAMP accumulation, $pERK_{1/2}$ activation and $i[Ca^{2+}]$ release in response to stimulation by CGRP, AM and AM2 in HUVECs relative to forskolin (100 μM), PMA (100 μM) and ionomycin (10 μM) respectively. Data are analysed using a three-parameter non-linear regression curve, and are presented here as mean ± S.E.M. of n individual data sets. Statistical significance compared to the cognate ligand (AM) and determined using one-way ANOVA with Dunnett's post-hoc test, (*, p<0.05; **, p<0.01; ***, p<0.001; ****, p<0.0001).

Optimisation of nitric oxide measurements and CGRP family peptide nitric oxide signalling in HUVECs

There was no precedent in publications from our lab for the determination of nitric oxide (NO) production in cells. So, it was attempted to optimise an assay for this purpose. First using DAF-FM, the NO binding agent, on a BD pathway system using published methods (Falcone et al. 2008), however, this was not successful (**Figure 3.12**): An observable response from known positive controls for NO release in the HUVECs could not be measured over this time range first using acetyl choline (ACh) as it GPCR-ligand observed to stimulate NO production in HUVECs (Falcone et al. 2008) (**Figure 3.12A**). As this was unsuccessful, other potential positive controls were tested to rule out the possibility that ACh was the issue (**Figure 3.12 B-D**). This assay is intended to detect concentration dependent NO fluxes in real time. However, for each compound tested the fluorescence detected remained stable over time. Moreover, for compounds over the concentration range used, purely looking at the baseline fluorescence of the cells treated with different concentrations there is no detectable concentration dependent effects: This is shown by attempts to apply a non-linear curve fit to the data (**Figure 3.12 E,F**). It was possible that either insufficient NO was produced over the time range used or that the assay was not sensitive enough. As it was not practical to measure NO in real time for longer periods, and cells may die being outside of an incubator for much longer. The research direction moved to find an assay that could detect more high throughput endpoint NO production.

Therefore, it attempted to optimise an alternative end point assay, with much greater success. This assay required ligand stimulation time optimisation; the manufacturer recommended doing so with L-Arginine which was done alongside ACh (**Figure 3.13A**). 15 min was decided upon as the optimum stimulation time as it was at this point that ACh, positive control for GPCR mediated NO, provided the greatest level of raw fluorescence (**Figure 3.13A**). From here the dose-response relationship of the positive control ACh and NO production was explored (**Figure 3.13B**). As it was

indeed possible to determine dose dependent GPCR-mediated NO production with this assay then it was investigated whether the ligands of interest could stimulate NO production and how they compared to each other. All three ligands could cause NO production in HUVECs in a dose dependent manner (**Figure 3.13C**). In terms of pEC50 the rank order of potency is AM2>AM>CGRP (**Figure 3.13D**), however, they are close enough such that there was a non-significant difference between them (**Table 3.9**). The significant differences were observable between AM2 and the cognate ligand for peptides. the Emax and Log tau, the AM2 in particular was much greater than was observed for the other peptides.

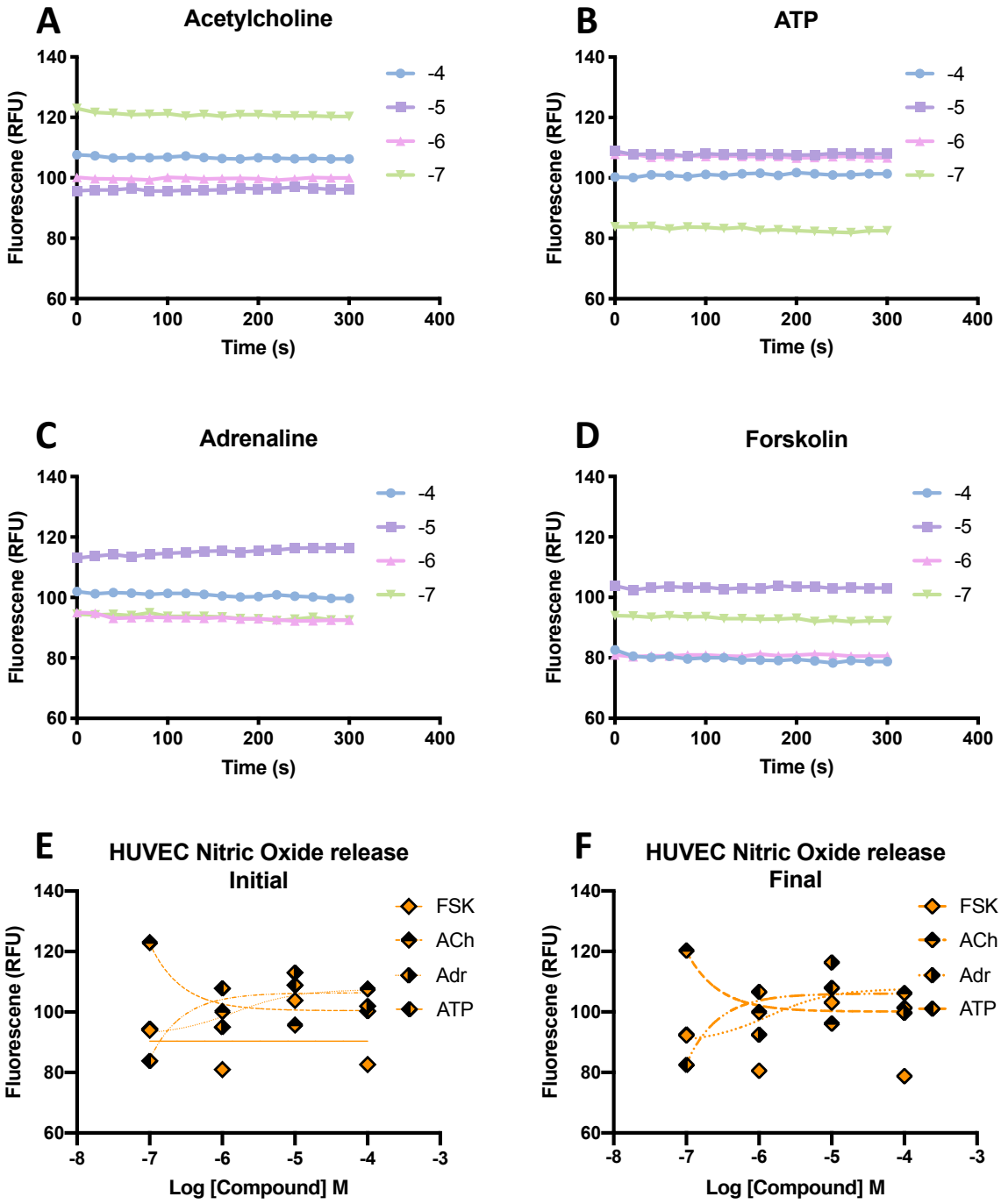

Figure 3.12. Optimisation of detection of nitric oxide release in HUVECs. Characterisation of nitric oxide release in response to stimulation by acetylcholine, ATP, forskolin and adrenaline respectively with continuous fluorescence recording for 5min after stimulation (**A-D**). Multiple concentrations were used and displayed as 10^X M. Data are analysed using a three-parameter non-linear regression curve (**E-F**).

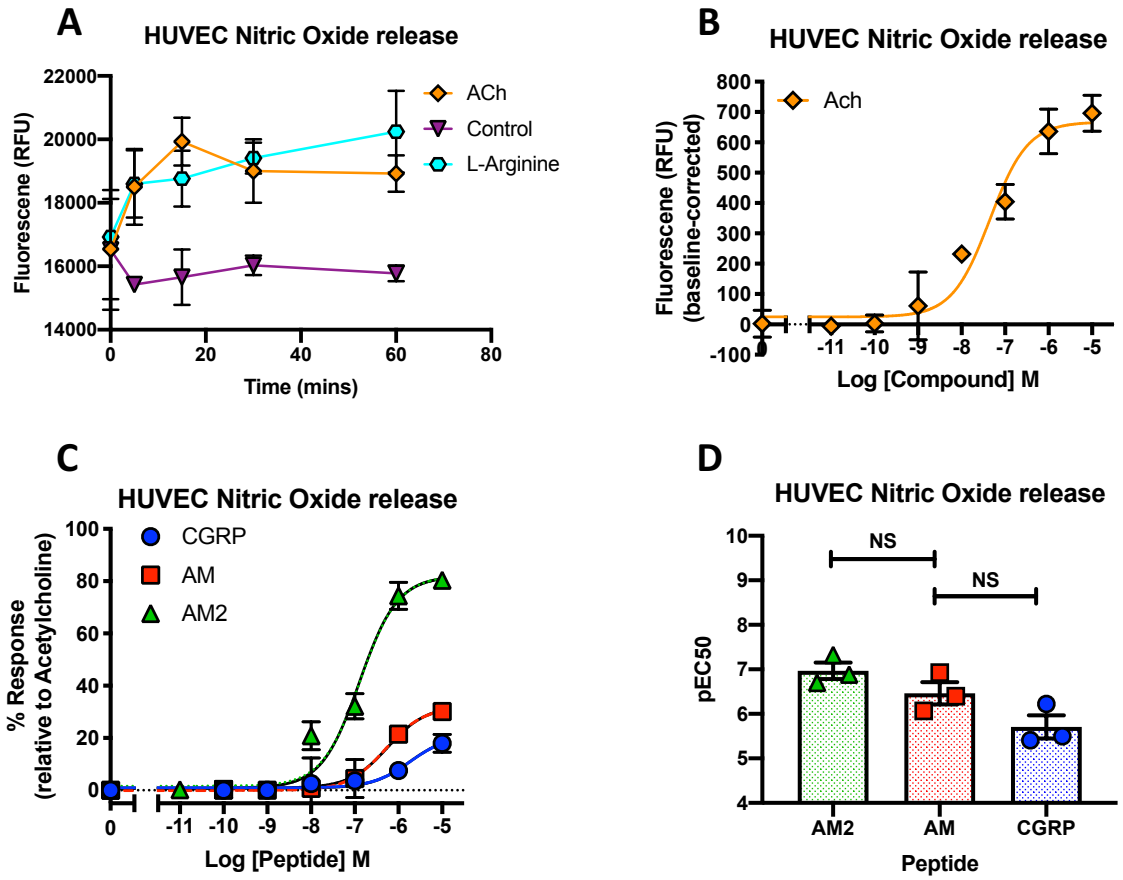

Figure 3.13. Nitric oxide signalling in HUVECs in response to the CGRP peptide family. Characterisation of NO release in response to stimulation by ACh (100 μM), vector control, and L-Arginine at multiple time points up to 60min (**A**). NO release in response to stimulation by ACh over a concentration range of 100pM to 100 μM (**B**). NO release in response to stimulation by CGRP, AM and AM2 in HUVECs relative to 100 μM ACh (**C,D**). Data are analysed using a three-parameter non-linear regression curve. Individual pEC50 values + S.E.M. are then plotted. All values are calculated from at least 3 individual data sets.

	NO					
	CGRP		AM		AM2	
pEC50	5.73	0.23	6.29	0.24	6.88	0.14
Emax	21.13	2.89	31.92	4.25	82.10***	4.62
pKa	5.64	0.52	6.08	0.31	6.15	0.15
logτ	-0.59	0.18	-0.33	0.11	0.65**	0.09
n	3		3		3	

Table 3.9. Nitric oxide signalling in HUVECs in response to the CGRP peptide family. Characterisation of Nitric oxide release in response to stimulation by CGRP, AM and AM2 relative to 100 μM ACh. Data are analysed using a three-parameter non-linear regression curve, and are presented here as mean ± S.E.M. pEC50: negative logarithm of the agonist concentration required to produce a half-maximal response. Emax: maximal response expressed as a percentage of NO. pKa: negative logarithm of the equilibrium dissociation constant for each ligand generated using the operational model (Black and Leff 1983). Logτ: coupling efficiency parameter of the ligand (Black and Leff 1983). Statistical significance compared to the cognate ligand (AM) and determined using one-way ANOVA with Dunnett's post-hoc test, (*, $p<0.05$; **, $p<0.01$; ***, $p<0.001$).

CGRP family peptide mediated proliferation in HUVECs

With the continued desire to discover whether agonism bias is observable in terms of physiological responses to CLR stimulation. A well-documented proliferation assay was utilised (Safitri et al. 2020) to observe the effects of CGRP, AM and AM2 on cell proliferation, and how they differed from one another. The assay involves the addition of formazan dye and the absorbance measured from this is directly proportional to the number of viable cells. Initially it was demonstrated that VEGF could produce the expected pro-proliferative effect in HUVECs (**Figure 3.14A**). Intriguingly forskolin provided the anti-proliferative control showing strong inhibition of cell proliferation. With these controls established CGRP, AM and AM2 effects were then explored. Here it was observed that CGRP was strikingly pro-proliferative (**Figure 3.14B**). While there was a dose-response relationship detectable for AM and AM2 in the pro-proliferative direction the maximal levels of proliferation achieved were 106.9% and 103.7% respectively (**Table 3.10**) and therefore only marginally over 100%. Where 100% represents the level of cell growth achieved by control treated cells over the time window. Unsurprisingly there was a powerful level of significance in the difference between the Emax of CGRP and AM the cognate ligand. Given the very strong potency of CGRP at the $pERK_{1/2}$ pathway and the well documented connection between $pERK_{1/2}$ and cell proliferation it was hypothesised that this and the proliferation response seen for CGRP are likely directly connected. Also given the strong anti-proliferative effects seen for forskolin it is interesting to observe that CGRP, the least potent peptide at initiating cAMP accumulation is then the most potent at stimulating cell proliferation, which cAMP appears to inhibit. While there is no obvious explanation for why AM and AM2 have little to no proliferative effects, it may be a case of different pathways 'balancing each other out' as AM for example is a potent stimulator of cAMP. So from the above forskolin evidence it might suggest that AM could also have anti-proliferative effects. On the other hand, AM is a reasonably potent inducer of $ERK_{1/2}$ phosphorylation, so taking this evidence with the CGRP $ERK_{1/2}$ and proliferation response

seen it may be assumed that AM could also produce strong proliferative responses. Therefore, taking the evidence together it might not be surprising that the level of cell proliferation seen in AM treated cells does not differ greatly from the control. These data suggest that ultimately signalling bias does follow through to physiological outcomes to some degree.

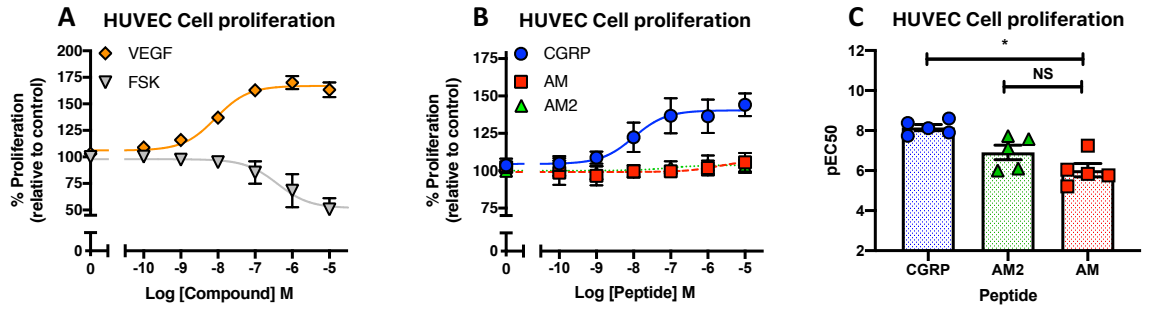

Figure 3.14. Cell proliferation in HUVECs in response to the CGRP peptide family. Characterisation of cell proliferation in response to stimulation by VEGF and forskolin over a concentration range of 100 pM to 100 μM 48 h prior to detection and relative to vector control treated cells (**A**). Characterisation of cell proliferation in response to stimulation by CGRP, AM, and AM2 in HUVECs 48 h prior to detection and relative to vector control treated cells (**B**). Data are analysed using a three-parameter non-linear regression curve. Individual pEC50 values + S.E.M. are then plotted for HUVECs (**C**). All values are calculated from 5 individual data sets. Statistical significance compared to the cognate ligand (AM) and determined using one-way ANOVA with Dunnett's post-hoc test, (*, p<0.05; **, p<0.01; ***, p<0.001; ****, p<0.0001).

	Proliferation					
	CGRP		AM		AM2	
pEC50	8.00*	0.19	5.73	0.68	7.06	0.90
Emax	140.39****	2.13	106.90	3.47	103.74	1.43
pKa	7.69	0.19	5.69	0.70	7.03	0.90
logτ	0.02**	0.06	-0.95	0.22	-1.29	0.20
n	5		5		5	

Table 3.10. Cell proliferation in HUVECs in response to the CGRP peptide family. Characterisation of Cell proliferation in response to stimulation by CGRP, AM and AM2 in HUVECs 48 h prior to detection and relative to vector control treated cells. Data are analysed using a three-parameter non-linear regression curve, and are presented here as mean ± S.E.M. of n individual data sets. pEC50: negative logarithm of the agonist concentration required to produce a half-maximal response. Emax: maximal response to ligands expressed as a percentage of VEGF. pKa: negative logarithm of the equilibrium dissociation constant for each ligand generated using the operational model of agonism (Black and Leff 1983). Logτ: coupling efficiency parameter of the ligand (Black and Leff 1983). Statistical significance compared to the cognate ligand (AM) and determined using one-way ANOVA with Dunnett's post-hoc test, (*, p<0.05; **, p<0.01; ***, p<0.001; ****, p<0.0001).

CLR/CTR receptor expression and CGRP family peptide signalling in HUAECs

The next question pondered was if the patterns of signalling bias were inherent to endothelial cells, and to address this question HUAECs were used. HUAECs are another human derived primary cell line, again endothelial but now arterial rather than from umbilical vein as HUVECs are. Using RT-PCR the receptor composition of these cells was uncovered. Analogous to HUVECs, HUAECs express CLR and RAMP2, and had no detectable CTR, RAMP1 or RAMP3 expression (**Figure 3.15A**). Providing a similar starting point in terms of expression to the HUVECs. The next step was to profile the signalling of CGRP, AM and AM2 in the five previously established pathways. The first was cAMP accumulation, in this the rank order of potency was AM>AM2>CGRP (**Figure 3.15D**). The result showing AM as the most potent, and producing the greatest response in terms of Emax, aligns well with literature reports of CLR-RAMP2 expression, as well as previously reported results here expressing CLR-RAMP2 in a HEK-293 cell line and results here from HUVECs endogenously expressing CLR/RAMP2. Giving strong evidence that this is another CLR/RAMP2 primary cell line. Allowing for direct comparisons with the HUVECs. Interestingly the potencies of all 3 peptides were slightly lower, as was the Emax for each e.g. AM – pEC50:7.95±0.09 vs 7.12±0.16 and Emax: 45.17±1.17 vs 24.97±1.51. Suggesting that the peptides/receptor signals less strongly in HUAECs when compared to HUVECs. Moving to intracellular calcium release; AM2 produced by far the most potent response (pEC50: 7.92±0.14) (**Table 3.11**), next was AM (pEC50 5.92±0.17), but when comparing the maximal responses, they were very similar; AM2 was 50.11±3.22 compared to 50.35±4.95 for AM. These are followed by CGRP which could only elicit a very small calcium response (**Figure 3.15B**), as in HUVECs. In terms of $pERK_{1/2}$ production the rank order of potencies was CGRP>AM>AM2 (**Figure 3.15C**) exactly mirroring the HUVECs scenario although the potency of CGRP was slightly less at a pEC50 of 7.06±0.18 vs 7.71± in the HUVECs. Following this the NO release assays were performed and a rank order of potency of AM2>AM>CGRP

was observed (**Figure 3.15E**). This again showed a striking role for AM2 in this pathway as it did in the HUVECs, here it has the greatest potency and Emax (7.00±0.18 and 71.48±4.88 respectively). Lastly in the 72 h proliferation assay forskolin suppressed proliferation showing cAMP has a negative influence on proliferation, AM and AM2 produced little to no positive or negative response (Emax: 102.63±1.30 and 107.69±1.03) in contrast to CGRP which stimulated a potent and large (7.55±0.19 and 146.65±2.99) response over baseline control cell growth modelled here as 100% growth (**Figure 3.15F**).

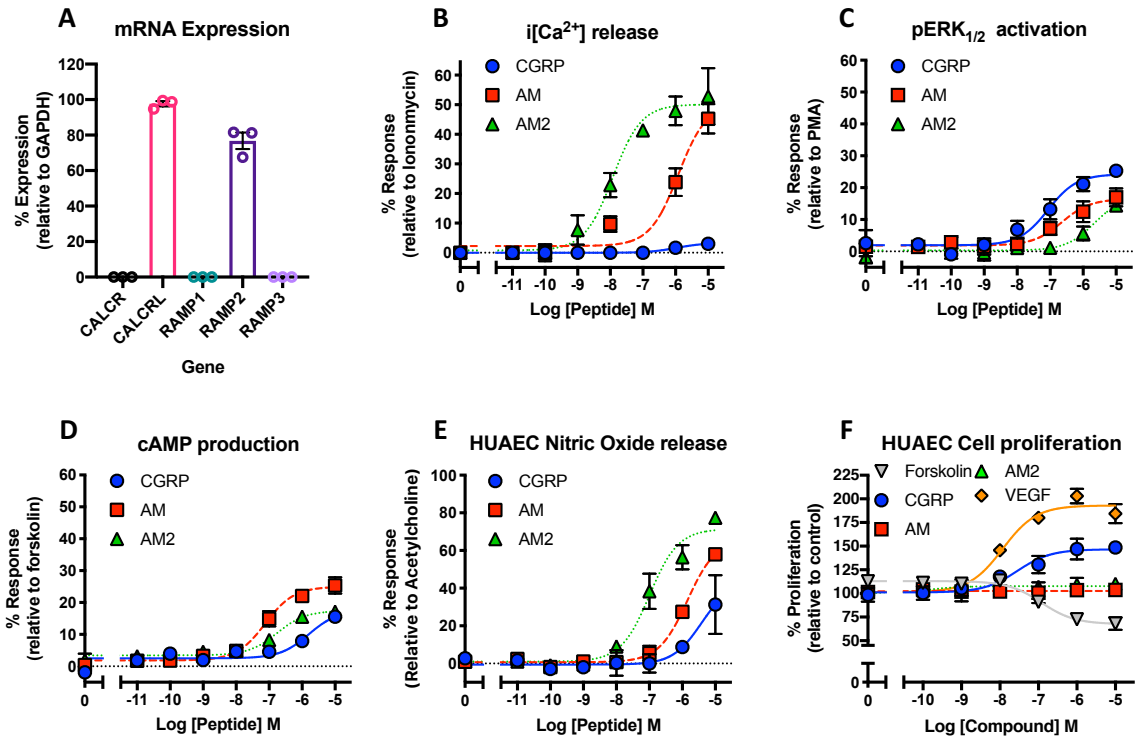

Figure 3.15: Receptor expression, and CGRP family Peptide signalling bias in HUAECs. Expression of CALCR, CALCRL, RAMP1, RAMP2, and RAMP3 genes in HUAECs determined by RT-PCR (**A**). Data represent mean + SEM of three independent experiments relative to GAPDH expression. ND = not detected in all three samples. Characterisation of cAMP accumulation relative to forskolin (100 μM) (**B**). Characterisation of intracellular calcium mobilisation (**C**) relative to ionomycin (10 μM). Characterisation of total nitric oxide production (**D**) relative to acetylcholine (100 μM). Intracellular $ERK_{1/2}$ phosphorylation (**E**) relative to PMA (10 μM). Characterisation of cell proliferation (**F**) relative to vector treated control. All pathways measured in response to stimulation by CGRP, adrenomedullin (AM) and adrenomedullin 2 (AM2), with the addition of forskolin (FSK) and VEGF for cell proliferation. Data are analysed using a three-parameter non-linear regression curve. All data represent mean + SEM of at least three independent experiments. Data are analysed using a three-parameter non-linear regression curve.

		HUAEC					
		CGRP		**AM**		**AM2**	
cAMP	pEC50	5.80***	0.27	7.12	0.16	6.76	0.20
	Emax	17.51*	2.46	24.97	1.51	17.46*	1.21
	pKa	5.72***	0.28	6.95	0.14	6.78	0.21
	Logt	-0.74*	0.09	-0.52	0.03	-0.75*	0.05
	n	10		10		10	
		CGRP		**AM**		**AM2**	
iCa	pEC50	5.96	0.14	5.92	0.17	7.92****	0.14
	Emax	3.36****	0.29	50.35	4.95	50.11	3.22
	pKa	5.95	0.14	5.65	0.19	7.61****	0.13
	Logt	-1.46****	0.04	-0.01	0.08	-0.01	0.05
	n	3		10		10	
		CGRP		**AM**		**AM2**	
pERK	pEC50	7.06	0.18	6.64	0.15	5.65*	0.21
	Emax	24.23*	1.62	16.48	0.94	17.59	2.44
	pKa	6.99	0.13	6.66	0.21	5.43*	0.33
	Logt	-0.52	0.03	-0.75	0.05	-0.67	0.12
	n	3		3		3	
		CGRP		**AM**		**AM2**	
NO	pEC50	5.43	0.39	5.85	0.09	7.00*	0.18
	Emax	43.25	13.02	66.07	2.63	71.48	4.88
	pKa	5.10	0.56	5.41	0.30	6.47	0.14
	Logt	-0.09	0.28	0.28	0.13	0.40	0.07
	n	3		3		3	
		CGRP		**AM**		**AM2**	
Growth	pEC50	7.55	0.19	11.45	3.48	9.93	0.52
	Emax	146.65****	2.99	102.63	1.30	107.69	1.03
	pKa	7.44	0.39	11.27	6.72	9.73	1.44
	Logt	-0.35	0.07	-1.76	0.72	-1.27	0.20
	n	3		3		3	

Table 3.11. pEC50, Emax, pKA, and log tau values for cAMP accumulation, i[Ca^{2+}] mobilisation and $ERK_{1/2}$ activation signalling pathways, nitric oxide release and cell proliferation physiological responses in HUAECs. Data are analysed using a three-parameter non-linear regression curve, and are presented here as mean ± S.E.M. of n individual data sets. pEC50: negative logarithm of the agonist concentration required to produce a half-maximal response. Emax: maximal response to ligands expressed as a percentage of positive control. pKa: negative logarithm of the dissociation constant for each ligand generated using the operational model of agonism (Black and Leff 1983). Logτ: coupling efficiency parameter of the ligand (Black and Leff 1983). Statistical significance compared to the cognate ligand (AM) and determined using one-way ANOVA with Dunnett's post-hoc test, (*, p<0.05; **, p<0.01; ***, p<0.001; ****, p<0.0001).

Receptor expression and CGRP family peptide signalling in human cardiac myocytes

RT-PCR was performed to ascertain which of the genes for the CTR, CALCR/CLR receptor and the accessory proteins RAMP1/2/3 were expressed at the mRNA level in HCMs. Of these genes, only CLR and RAMP1 were expressed at a detectable level in the HCMs (**Figure 3.16A**). In the majority of recombinant studies the CLR/RAMP1 is known as the 'CGRP receptor' and has been considered primarily a Gαs coupled receptor. Therefore, an intracellular cAMP accumulation assay was again used to assess whether function receptor is formed and as the mRNA suggested that there was no functional response detected to the CTR ligands calcitonin or amylin (**Figure 3.16B**). However, CGRP, AM and AM2 stimulation showed that functional receptor is formed in these HCMs (**Figure 3.16C**). Moreover, there was a strong concentration dependent increases in cAMP in response to all three of CGRP, AM and AM2 in demonstrating the CLR/RAMP1 in HCMs can couple to Gαs to produce a detectable response. Adding confidence to the building evidence that the CLR/RAMP1 receptor is formed in these cells, and as CGRP is the most potent ligand at cAMP accumulation followed by AM2, and AM is the least potent, this is consistent with expectations based on data from transfected systems and the previously reported observations in HEK-293 cells here (**Figure 3.5**). What is more statistical analysis confirmed the significance of difference between the pEC50 of AM and AM2 each compared to CGRP (**Table 3.12**)(p109).

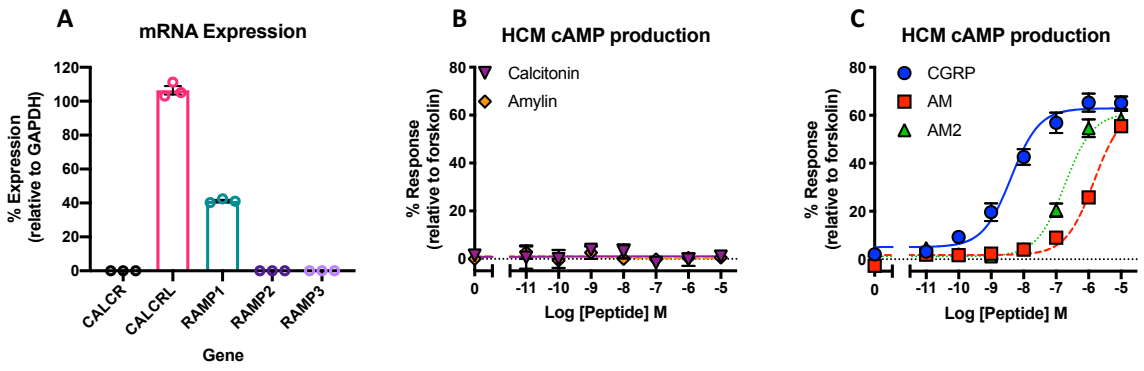

Figure 3.16: Receptor expression, and CGRP family Peptide cAMP accumulation in Human Cardiomyocytes (HCMs). Expression of CALCR, CALCRL, RAMP1, RAMP2, and RAMP3 genes in HCMs (**A**) Based on densitometry analysis of RT-PCR (Supplemental Figure 8.1). Data represent mean + SEM of three independent experiments relative to GAPDH expression. Characterisation of cAMP accumulation in response to stimulation by calcitonin and amylin in HUVECs relative to 100μM Forskolin (**B**). Characterisation of cAMP accumulation relative to forskolin (100 μM)(**C**).

Antagonising CGRP, AM and AM2 cAMP responses in human cardiac myocytes

As in the HUVECs it was important to confirm the cAMP responses observed were due to the suspected receptor, for all three ligands. This was confirmed using well established antagonists; AM22-52 – the CLR/RAMP2 antagonist had no significant effect on any of the CGRP, AM or AM2 responses (**Figure 3.17**). On the other hand, the CLR-RAMP1 antagonist suppressed all three peptide responses to varying degrees of significance. In the case of CGRP reduction in pEC50 and Emax were both significant, for AM, the smallest response, only the Emax reduction was significant. The same was true for AM2 although to a greater extent. Overall the CLR-RAMP1 antagonist had the greatest effect on Emax values, as demonstrated by the Emax suppression for CGRP and AM2 having a significance value < 0.001. Whereas the shift in potency produced in the AM and AM2 scenarios were not significant (**Figure 3.17**).

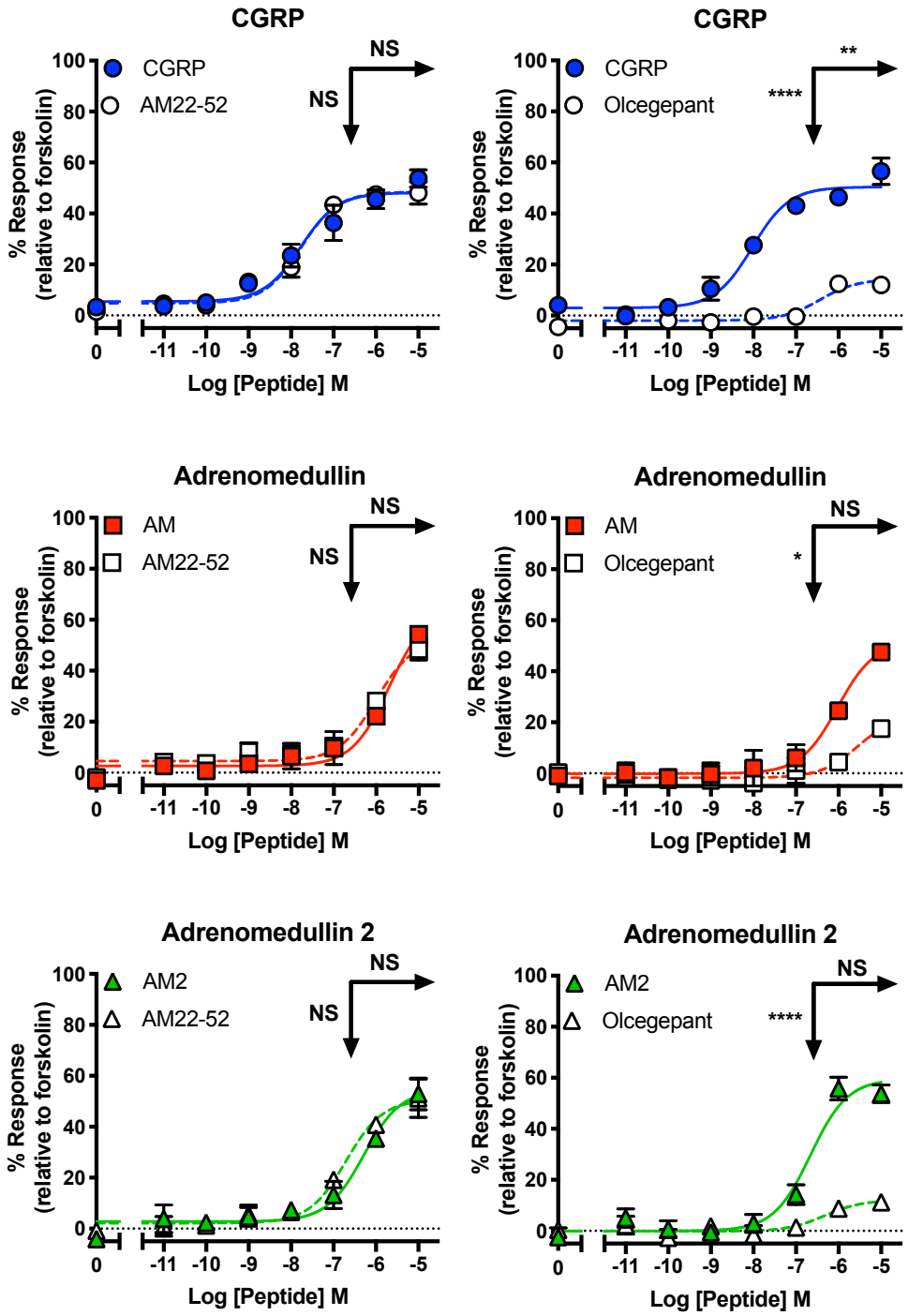

Figure 3.17. Antagonism of cAMP signalling in HCMs with CLR-RAMP2 and CLR RAMP1 antagonists. Characterisation of cAMP accumulation in response to stimulation by CGRP, adrenomedullin (AM) and adrenomedullin 2 (AM2) in HCMs in the presence and absence of 100 nM AM22-52 or Olcegepant respectively. All relative to 100 μM forskolin. Data are analysed using a three-parameter non-linear regression curve. Statistical significance determined compared to control using an unpaired t test with Welch's correction (*, $p<0.05$; **, $p<0.01$; ***, $p<0.001$ ****, $p<0.0001$). NS denotes no statistical significance observed. All values are calculated from at least 3 individual data sets. Horizontal arrows show pEC50, and Vertical arrows show Emax statistical significance.

CGRP family peptide signalling in human cardiac myocytes

Now having profiled the CGRP, AM and AM2 activity through cAMP accumulation and using the antagonists to provide evidence that the CLR/RAMP1 receptor is in these cells, it was important to study how these cells signalling through other signalling pathways. Firstly, intracellular calcium release was recorded in response to the peptides (**Figure 3.18A**). All peptides were noticeably very potent yet still significantly different from the cognate ligand: CGRP which was also most potent. While the rank order of potency in HUVECs and HUAECs in intracellular calcium was reflected in the NO response, it was not the case in HCMs where AM2 was ostensibly the most potent although no parameters significantly differed from each other (**Table 3.12**) and the dose-response curves almost overlaid (**Figure 3.18C**). Moving on to the $ERK_{1/2}$ phosphorylation, remarkably, AM was the most potent (**Figure3.18B, Table 3.12**) at this pathway. This mirrored the HUVEC and HUAEC signalling where the least potent peptide at cAMP accumulation was most potent at causing $ERK_{1/2}$ phosphorylation. The same situation was observed in terms of cell proliferation (**Figure 3.18D**) where AM stimulated the highest level above baseline in HCMs (**Figure 3.18D, Table 3.12**). Again application of the operational model of agonism (Black and Leff 1983) has enabled operation parameters to be determined (**Table 3.12**).

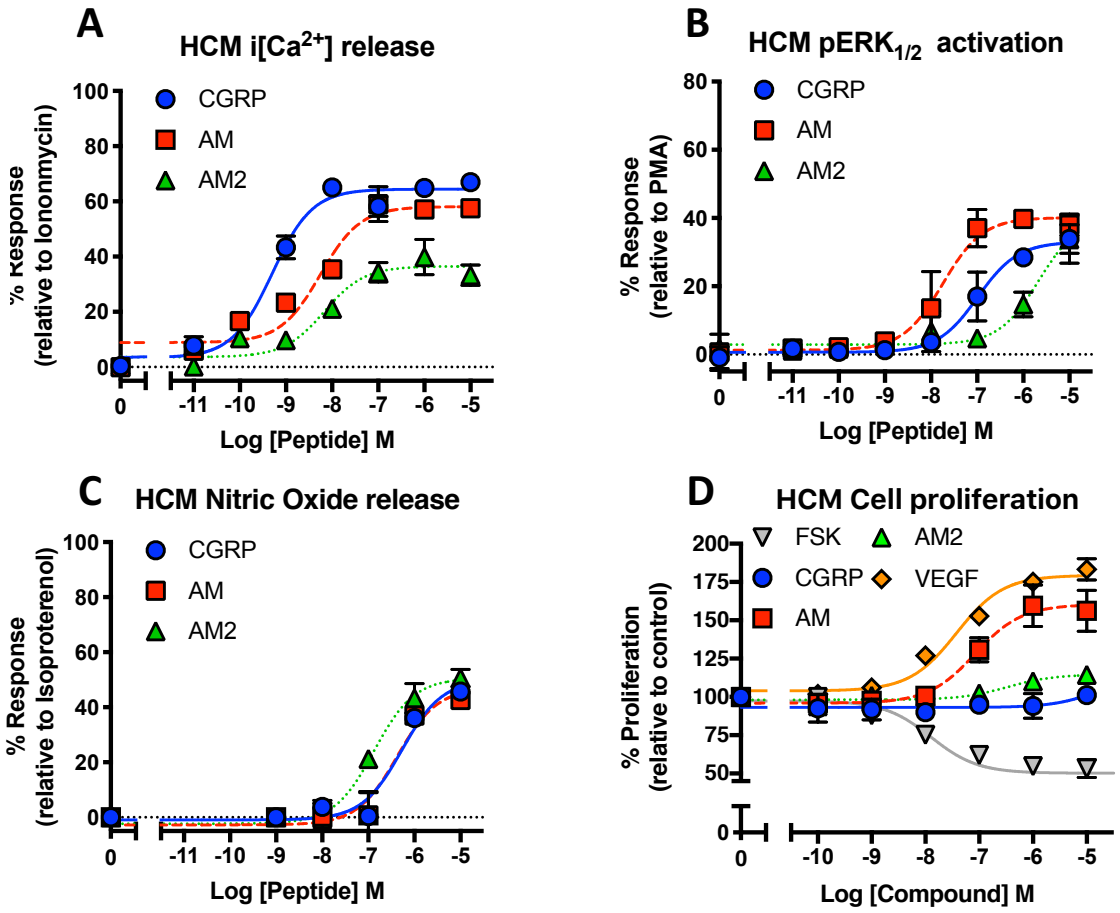

Figure 3.18: CGRP family peptide signalling bias in Human Cardiomyocytes (HCMs). Characterisation of intracellular calcium mobilisation (**A**) relative to ionomycin (10 μM). Characterisation of total nitric oxide production (**B**) relative to acetylcholine (100 μM). Intracellular $ERK_{1/2}$ phosphorylation (**C**) relative to PMA (10μM). Characterisation of cell proliferation (**D**) relative to vector treated control. All pathways measured in response to stimulation by CGRP, adrenomedullin (AM) and adrenomedullin 2 (AM2), with the addition of forskolin (FSK) and VEGF for cell proliferation. Data are analysed using a three-parameter non-linear regression curve. All values are calculated from 3 to 8 independent experiments.

		HCM					
		CGRP		**AM**		**AM2**	
cAMP	pEC50	8.39	0.12	5.84****	0.08	6.73****	0.10
	Emax	62.91	1.85	63.05	3.14	61.04	2.50
	pKa	8.05	0.09	5.38****	0.19	6.29****	0.14
	Logt	0.20	0.03	0.22	0.10	0.18	0.06
	n	10		6		6	
		CGRP		**AM**		**AM2**	
iCa	pEC50	9.30	0.10	8.25*	0.17	8.17*	0.33
	Emax	64.44	1.73	58.12	2.79	36.50***	2.31
	pKa	8.85	0.15	8.10	0.15	7.91	0.35
	Logt	0.22	0.05	0.08	0.04	-0.30***	0.05
	n	3		3		3	
		CGRP		**AM**		**AM2**	
pERK	pEC50	6.99	0.11	7.75*	0.14	5.66**	0.17
	Emax	33.02	1.52	40.13	2.02	40.41	4.17
	pKa	6.77	0.15	7.52*	0.12	5.52**	0.18
	Logt	-0.33	0.04	-0.19	0.03	-0.20	0.08
	n	3		3		3	
		CGRP		**AM**		**AM2**	
NO	pEC50	6.27	0.23	6.37	0.27	6.87	0.11
	Emax	49.97	5.56	46.98	5.85	50.59	2.18
	pKa	-5.99	0.22	-6.07	0.22	-6.55	0.18
	Logt	0.01	0.08	-0.03	0.08	0.03	0.06
	n	3		3		3	
		CGRP		**AM**		**AM2**	
Growth	pEC50	5.32	1.80	7.08	0.23	6.48	0.58
	Emax	108.80	24.20	160.32*	6.82	114.68	3.58
	pKa	5.23	1.90	6.45	0.33	6.38	0.59
	Logt	-0.65	0.80	0.52	0.20	-0.60	0.12
	n	6		6		6	

Table 3.12. pEC50, Emax, pKA, and log tau values for cAMP accumulation, i[Ca^{2+}] mobilisation and $ERK_{1/2}$ activation signalling pathways, nitric oxide release and cell proliferation physiological responses in HCMs. Data are analysed using a three-parameter non-linear regression curve, and are presented here as mean ± S.E.M. of n individual data sets. pEC50: negative logarithm of the agonist concentration required to produce a half-maximal response. Emax: maximal response to ligands expressed as a percentage of positive control. pKa: negative logarithm of the equilibrium dissociation constant for each ligand generated using the operational model of agonism (Black and Leff 1983). Logτ: coupling efficiency parameter of the ligand (Black and Leff 1983). Statistical significance compared to the cognate ligand (CGRP) and determined using one-way ANOVA with Dunnett's post-hoc test, (*, p<0.05; **, p<0.01; ***, p<0.001; ****, p<0.0001).

Endogenous CLR-based signalling bias in primary cells

Bias plots were generated for each of CGRP, AM, and AM2 at each pathway in the HUVEC, HUAEC, and HCM cell models, using the τ and K_A values obtained through the operational model of pharmacological agonism (detailed discussion in Chapter 2). Using the data reported so far in this chapter (**Table 3.1,2,7,9-12**). These are illustrative plots that represent the extent of bias a ligand has towards a certain pathway. It is a relative term, therefore in the $\Delta(\tau/K_A)$ plots all responses are normalised to the reference agonist, this is AM, as it is the cognate ligand in the first cell system studied and normalisation needs to remain consistent so remains the reference agonist for all. Now examining these plots give a clear indication of which pathway ligands are biased towards in different systems: In the CLR-RAMP2 expressing HUVECs (**Figure 3.19A**) it is clear CGRP is biased towards $pERK_{1/2}$ and cell proliferation (growth) whereas AM2 is biased towards $_{i}Ca^{2+}$ and NO, then lastly AM as anticipated is biased towards cAMP. This clearly suggests that each ligand has its own distinct pattern of bias at CLR/RAMP2 in the HUVEC. Intriguingly, in the HUAECs (**Figure 3.19B**) a very similar pattern of bias is observed, in these different cells but that also express CLR-RAMP2. While the bias patterns differ slightly, such as CGRP having a greater bias towards NO in the HUAECs the overall trends are very similar. Moving on to the CLR-RAMP1 expressing HCMs the pattern of bias seen is completely different to the HUVECs and HUAECs (**Figure 3.19C**). Where CGRP is now biased towards cAMP, $_{i}Ca^{2+}$ and NO, while AM is biased towards $pERK_{1/2}$ and cell proliferation. These bias plots provide a neat summary of the bias exhibited by CGRP, AM and AM2 in the different primary cells and enable quick comparison that highlights the similarities between the two CLR-RAMP2 expressing cells and conversely how different the bias patterns of the peptides are in the CLR-RAMP1 expressing HCMs.

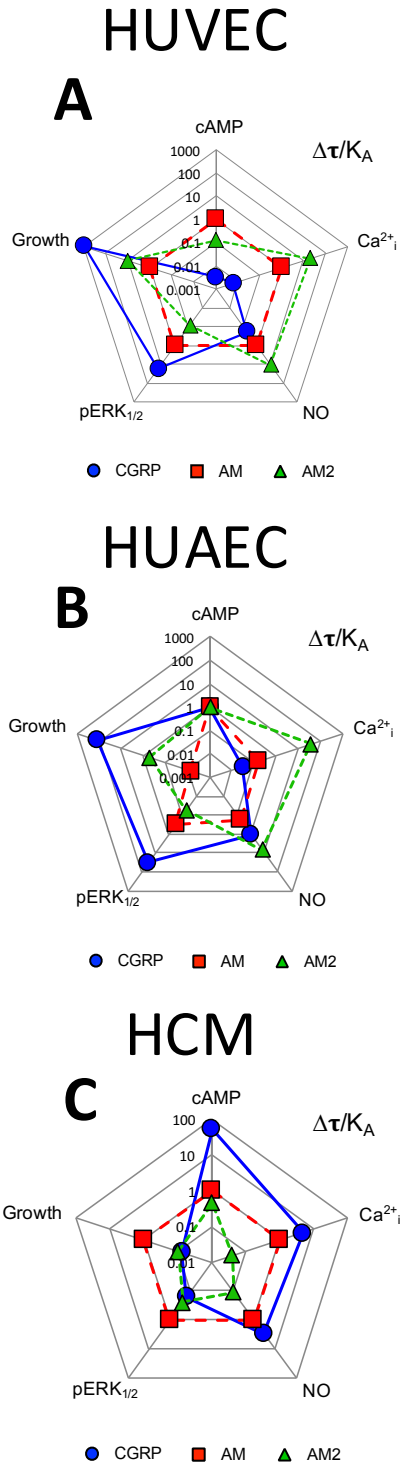

Figure 3.19. Signalling bias of the CGRP family of peptides in HUVECs, HUAECs, and HCMs. Signalling bias plots were calculated as $\Delta(\tau/K_A)$ for HUVECS (**A**), HUAECs (**B**), and HCMs (**C**). Values are on a logarithmic scale for each agonist and for each signalling pathway. Determination of values requires normalisation to a reference agonist (AM) alone in $\Delta(\tau/K_A)$.

Summary

In this chapter It has been shown how initially a primary cell model was established for the study of CLR (+ a single RAMP) and its signalling through various pathways in an endogenous setting. First, the mRNA expression for evidence of the CTR, CLR and 3 RAMP expression was explored in two primary cell lines: HUVECs and HVSMCs. HUVECs were chosen to move forward with as the model of choice as they only expressed CLR and RAMP2 at the mRNA level making them a good candidate for the study of the so called Adrenomedullin receptor endogenously. The fact that CGRP, AM and AM2 were able to activate G_s signalling and cAMP accumulation provided strong evidence that functional receptor is produced in these cells. In the case of cAMP in HUVECs there is a very clear rank order of potency with a logarithmic difference between the EC50s of each. The antagonism data demonstrated that CGRP and AM2 as well as AM signalling is exclusively occurring through the CLR-RAMP2 receptor complex. Then the investigation moved on to profile the signalling of CGRP, AM and AM2 across multiple pathways: $ERK_{1/2}$ phosphorylation, calcium release, NO release and cell proliferation. This unveiled an array of different signalling patterns unique to the specific peptide and pathway. Calcium release produces a stark example of how different the activity of these peptides can be at the same receptor and relative to each other. Where CGRP causes almost no release compared to AM, but AM2 causes almost double the maximal level of release, again compared to AM. Demonstrating the presence of agonism bias through the endogenous CLR-RAMP2 receptor and suggesting interesting and distinct physiological roles for each of the peptide agonists. Although there were no major differences observed over later passage numbers and in the single donor HUVEC peptide signalling responses. Nevertheless, they serve to highlight the importance of considering passage number and where the cells came from when working with primary human cells, as it is of vital importance that these cells remain as relevant and as representative of the cells *in vivo* as possible.

HUAECs are another cell line which has had the receptor expression and signalling profiled, they also express CLR-RAMP2 alone and show remarkable similarities to HUVECs with rank order of potencies for the stimulating peptides mirroring the peptides acting in HUVECs almost exactly. There are subtle differences such as the larger Emax for AM in calcium release and nitric oxide release relative to the positive controls in each cell line respectively, however in other pathways such as cAMP accumulation and $ERK_{1/2}$ phosphorylation the responses are, on the whole, smaller. Demonstrating that in different CLR-RAMP2 expressing primary cell lines the unique signalling profiles seen in HUVECs across multiple pathways can be replicated in another such as the HUAEC albeit another endothelial cell line.

When performing both the RT-PCR and cAMP accumulation assay the evidence suggested that these human cardiac myocyte cells expressed functional CLR-RAMP1. Using antagonists for this and the CLR-RAMP2 receptor confirmed this, allowing research to proceed to explore the responses of the three peptides in the other second messenger and physiological response pathways with confidence that the outcome observed was due to endogenous CLR-RAMP1. Interestingly, the cognate ligand CGRP was most potent at calcium release, but it was AM that was most potent at ERK phosphorylation and proliferation, whereas it was AM2, that was very slightly most potent at NO release.

Chapter 4. Classification of Signalling pathways, and Spatiotemporal aspects of CLR-RAMP2 in a Primary Cell Model

Aims and Hypothesis

In the previous chapter HUVECs were established as a model for studying endogenous CLR function in primary human cells, and observed robust cAMP accumulation reflective of a canonical G_s response indicative of CLR-RAMP2. Although having said that it is not known how much G_i involvement there is in the cAMP response observed. Alongside this cAMP accumulation data, interesting signalling responses were recorded in a number of other pathways, the source of which is much less certain. For $ERK_{1/2}$ phosphorylation it was traditionally considered a downstream product of β-arrestin recruitment. However, there have been many other studies showing at least some degree of activation from GPCR pathways. Therefore the intention was to use established inhibitors of different pathways and effectors to attempt to narrow down where the $ERK_{1/2}$ activation was generated from and if these changes depending on the stimulating ligand. When measuring calcium release the experimental conditions were setup such that the only available calcium was from intracellular sources. This gave the confidence to hypothesise that the intracellular signalling was $G_{q/11}$ and IP_3 mediated, and it was attempted to confirm this using the selective $G_{q/11}$ inhibitor YM-254890. Following this it was also attempted to discover the pathways involved in NO production as well. Another important and recently advanced area of GPCR study is spatiotemporal signalling. This has been explored here in these HUVECs extensively for cAMP signalling. Using a range of internalisation inhibitors to observe the effects these have on signalling response at more than one time point and with or without the pan PDE inhibitor IBMX. The cAMP accumulation assay is utilised as an endpoint assay with the use of a PDE inhibitor to try to measure the maximal cAMP produced by a receptor

stimulated by a specific concentration of ligand. In order to explore temporal cAMP signalling the assay has been modified where the endpoint is adjusted so that for each assay it a time between 0 and 30 min (the normal assay endpoint), moreover IBMX has been omitted to observe natural fluxes in cAMP level to build up and overall picture of temporal cAMP signalling. Combining this with internalisation inhibitors it was hypothesised that it would be possible to build a picture of spatiotemporal cAMP signalling in an endogenous environment.

Results

As outlined in Chapter 3 HUVECs and HCMs provided good primary cell models for the study of CLR-RAMP2 the 'AM receptor' and CLR-RAMP1 the 'CGRP receptor' respectively. In order to interrogate the source of certain signalling pathways further it was important to first establish the G protein and β-arrestin expression of these primary cells and establish which of these proteins they expressed. mRNA expression was explored through the use of RT-PCR which was able to show whether each component was or was not present at the mRNA level. Densitometry analysis was performed on raw gel images shown in (**Supplemental Figure 8.2**). This demonstrated a host of G proteins and both β-arrestin 1 and 2 were present in both HUVECs and HCMs (**Figure 4.1**). There were some notable differences in expression, such as G_z expression in HUVECs but not HCMs. However, there were many more similarities, and one of these was G_s, reassuringly, as this is the only source of GPCR-mediated cAMP production (outside of G_{olf} in the olfactory system). Both of the primary cells expressed other important proteins such as $G_{i1/2/3}$, $G_{q/11/14}$ and β-arrestin 1 and 2 whose contributions to CLR signalling in HUVECs and HCMs will be explored further in this chapter.

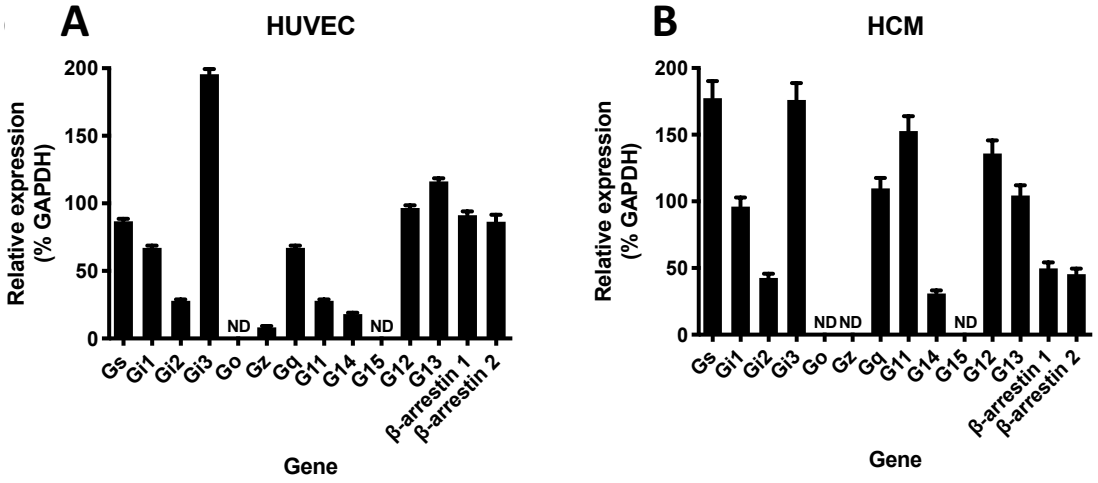

Figure 4.1. RT-PCR assessment of G protein and accessory protein mRNA expression in primary cells. Expression of GCPR accessory protein genes in HUVECs (**A**) and HCMs (**B**). Data represent mean + SEM of three independent experiments relative to GAPDH expression. ND = not detected in all three samples.

Assessing the $G_{i/o}$ component of CGRP family peptide cAMP and $pERK_{1/2}$ signalling in HUVECs

PTX is a well-established $G_{i/o}$ inhibitor (Weston et al. 2016, Malik et al. 2013), taking advantage of this cAMP and $pERK_{1/2}$ assays was performed to assess the contribution of $G_{i/o}$. The presence of $G_{i/o}$ proteins are confirmed by PCR at the mRNA level (**Figure 4.1**) in HUVECs. Performing these assays alongside control experiments and assessing the statistical difference between control and PTX treated responses. In both cAMP and $pERK_{1/2}$ accumulation assays there was no effect from PTX treatment the cognate ligand, AM, induced signalling (**Figure 4.2**). Whereas there was for the other two peptides. For AM2 PTX treatment increased the potency and maximal response for cAMP accumulation, but reduced maximal levels of $ERK_{1/2}$ phosphorylation (**Table 4.1**). PTX treatment had the greatest effect on CGRP signalling causing a strong increase in cAMP signalling potency as well as an equally strong decrease in $pERK_{1/2}$ signalling potency. This suggests that CGRP and AM2, but not AM recruit G_i proteins to the CLR-RAMP2 receptor in HUVECs and that under normal conditions they help supress the cAMP responses from CGRP and AM2, but contribute to $pERK_{1/2}$ signalling.

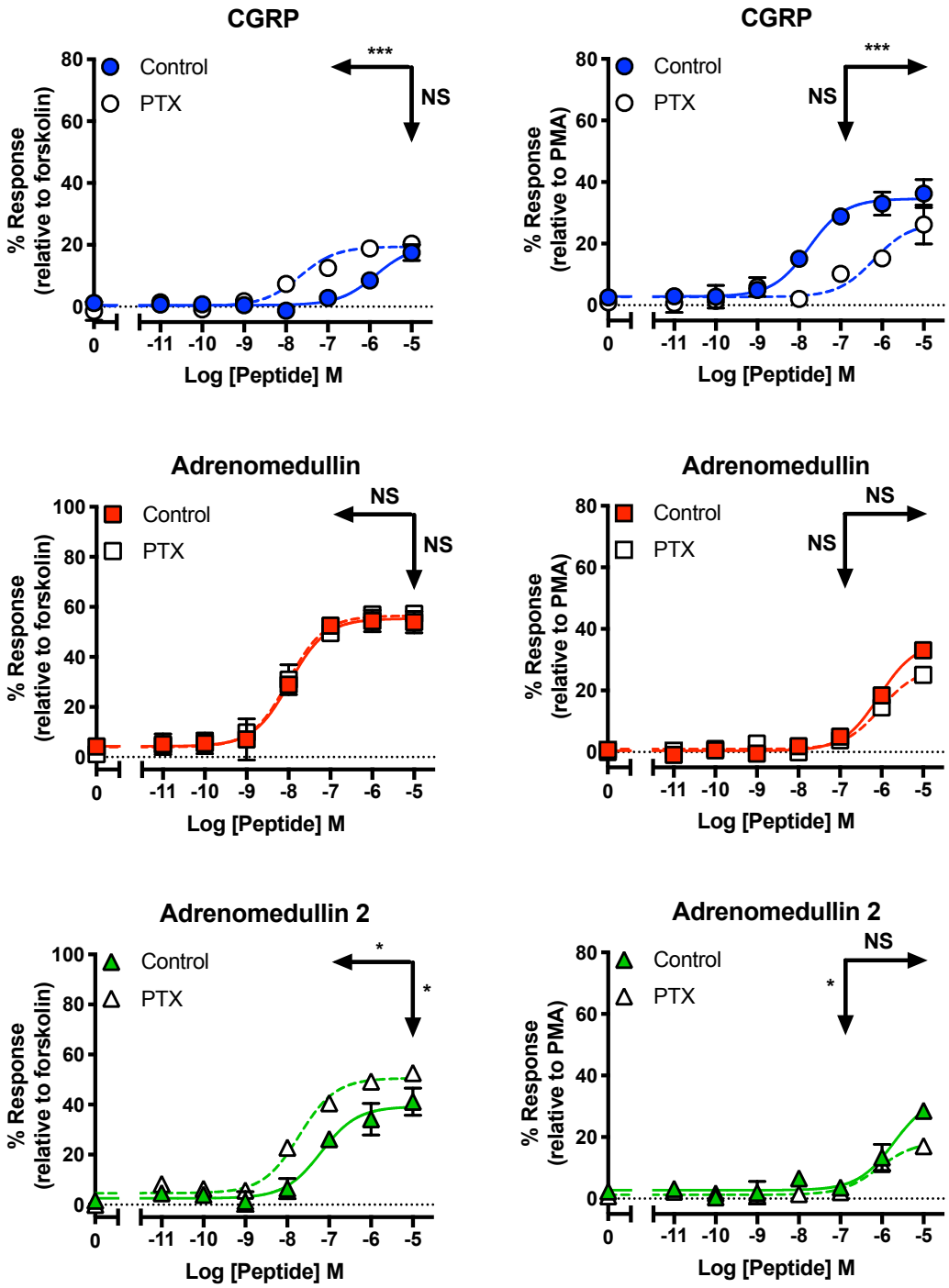

Figure 4.2. cAMP and $ERK_{1/2}$ signalling in HUVECs with and without PTX treatment. Characterisation of cAMP accumulation and ERK phosphorylation in response to stimulation by CGRP, AM and AM2 in HUVECs in the presence and absence of 200 ng/ml PTX. Pre-treated for 16 h with PTX/Control. All relative to 100 μM forskolin or PMA respectively. Data are analysed using a three-parameter non-linear regression curve. Statistical significance determined compared to control using an unpaired t test with Welch's correction (*, p<0.05; **, p<0.01; ***, p<0.001 ****, p<0.0001). NS denotes no statistical significance observed. All values are calculated from at least 3 individual data sets. Horizontal arrows show pEC50, and Vertical arrows show Emax statistical significance.

cAMP + PTX

	CGRP		AM		AM2	
pEC50	7.67***	0.15	8.01	0.05	7.71*	0.09
Emax	19.43	0.98	56.50	0.94	50.59*	1.26
pEC50 (c)	5.86	0.19	7.97	0.09	7.20	0.19
Emax (c)	19.82	2.30	55.31	1.61	39.23	2.76
n	5		5		5	

$pERK_{1/2}$ + PTX

	CGRP		AM		AM2	
pEC50	6.20***	0.18	6.03	0.12	6.09	0.13
Emax	26.76	2.24	27.31	2.02	18.51*	1.27
pEC50 (c)	7.76	0.10	6.06	0.10	5.72	0.21
Emax (c)	34.58	1.09	35.75	1.73	33.45	4.20
n	4		4		4	

Table 4.1. cAMP and $ERK_{1/2}$ signalling in HUVECs with and without PTX treatment. Characterisation of cAMP accumulation in response to stimulation by CGRP, adrenomedullin (AM) and adrenomedullin 2 (AM2) in HUVECs in the presence and absence of 200 ng/ml PTX. Control treatment is denoted by (c). Pre-treated for 16 h with PTX/Control. All relative to 100 μM forskolin or PMA respectively. Data are analysed using a three-parameter non-linear regression curve, and are presented here as mean ± S.E.M. of n individual data sets. Statistical significance determined compared to each individual control using an unpaired t test with Welch's correction: *, $p<0.05$; **, $p<0.01$; ***, $p<0.001$.

Interrogation of $pERK_{1/2}$ signalling by CGRP family peptides in HUVECs

These experiments were conducted to attempt to narrow down the source of $pERK_{1/2}$ signalling in this system. From the PKA inhibitor experiments it is immediately apparent that the cAMP-PKA signalling arm does not lead to an $pERK_{1/2}$ response. Nor does it supress it, as treatment with the PKA inhibitor had no significant effect, either positive or negative on CGRP, AM or AM2 $pERK_{1/2}$ signalling. While there looked to be a small effect of $G_{q/11}$ inhibition on some of the peptide's $pERK_{1/2}$ responses none of these proved to be statistically significant in terms of pEC50 or Emax changes (**Figure 4.3**). Application of the EPAC1/2 inhibitor ESI-09 did significantly reduce the maximal response from AM suggesting it contributes to $pERK_{1/2}$ signalling for these peptides but not CGRP. This suggests overall that multiple pathways contribute to $pERK_{1/2}$ signalling and that it is dependent on the stimulating ligand. However, none of the pathways interrogated individually produce the entire $pERK_{1/2}$ response.

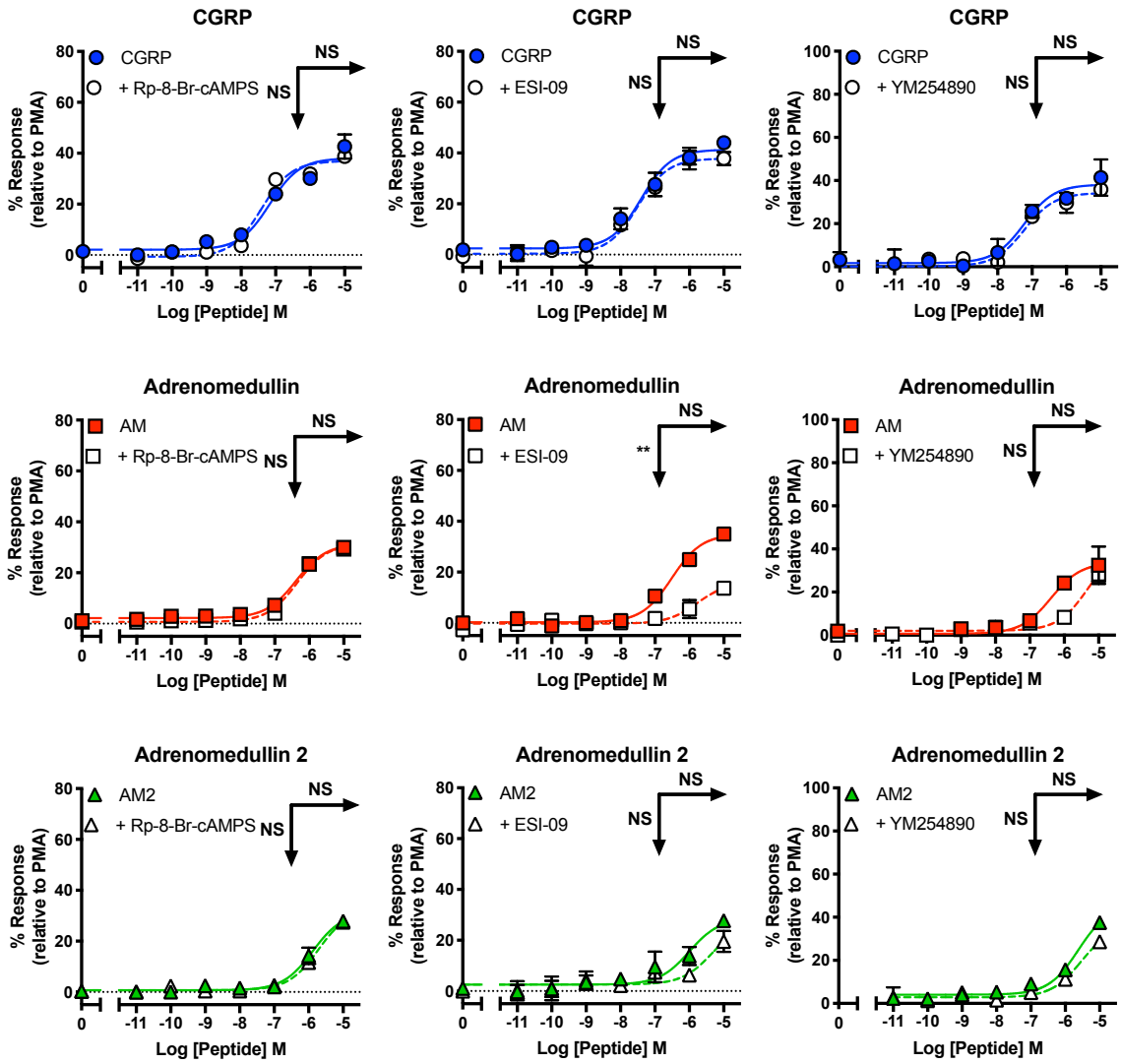

Figure 4.3. $pERK_{1/2}$ signalling in HUVECs with and without PKA, EPAC, and G_q inhibitor treatment. Characterisation of $pERK_{1/2}$ activation in response to stimulation by CGRP, AM, and AM2 in HUVECs in the presence and absence of Rp-8-Br-cAMPs (PKAi), ESI-09 (EPACi), and YM254890 (G_qi) respectively. Pre-treated for 30 min with inhibitor/Control. All relative to 100 μM PMA. Data are analysed using a three-parameter non-linear regression curve. Statistical significance determined compared to control using an unpaired t test with Welch's correction (*, p<0.05; **, p<0.01; ***, p<0.001 ****, p<0.0001). NS denotes no statistical significance observed. All values are calculated from at least 3 individual data sets. Horizontal arrows show pEC50, and Vertical arrows show Emax statistical significance.

Interrogation of intracellular calcium and NO signalling by CGRP family peptides in HUVECs and HCMs

Here the aim was to discover the source of intracellular calcium (i[Ca^{2+}]) and nitric oxide signalling in HUVECs. The canonical pathway for i[Ca^{2+}] release through GPCR activation is via $G_{q/11}$-IP_3-IP_3R and release of calcium from the endoplasmic reticulum. Therefore, the effect of the $G_{q/11}$ selective inhibitor was tested on i[Ca^{2+}] release from HUVECs in response to the CGRP family peptides (**Figure 4.4A**). The effects of YM-254890 was explored on the maximal concentration of each of the three ligands. With the exception of CGRP where there is little to no calcium signalling in the control scenario the inhibitor produced a complete knockdown of response. Thus, confirming that $G_{q/11}$ is recruited to the CLR-RAMP2 in HUVECs and that it directly leads to the i[Ca^{2+}] release observed. To determine the source of NO signalling in HUVECs AM2 was used as a model compound initially due to cell number limitations and as it produced the greatest response and therefore largest window for observing inhibitor effects (**Figure 4.4B**). The adenylyl cyclase inhibitor: SQ22536 and PKA inhibitor: Rp-8-Br-cAMPs were used to see whether the NO was a result of G_s and cAMP, however neither had any effect on the maximal level of NO production. Whereas the NOS inhibitor knocked down the response completely verifying that the NO measured was indeed coming from NOS. Further to this complete knockdown of the response was observed with YM-254890 treatment for AM2 as well as AM and CGRP (**Figure 4.4C**). Showing the response was downstream of $G_{q/11}$ and may also be a consequence of i[Ca^{2+}] signalling.

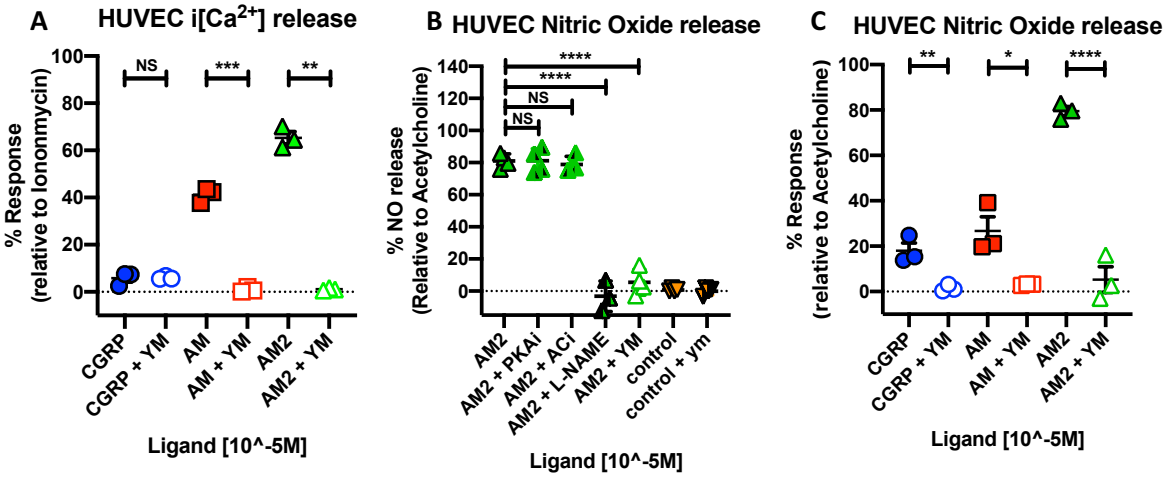

Figure 4.4. Inhibitor effects on i[Ca^{2+}] and NO. Characterisation of intracellular calcium mobilisation with and without YM-254890 relative to Ionomycin (10 μM) (**A**). Characterisation of AM2 mediated Nitric Oxide release with and without Rp-8-Br-cAMPs, SQ22536, L-NAME, and YM-254890 alongside control treated cells with/without YM-254890 (**B**). Characterisation of Nitric Oxide release with/without YM-254890 relative to Ach (10 μM) (**C**). Statistical significance determined compared to control using an unpaired t test with Welch's correction (*, $p<0.05$; **, $p<0.01$; ***, $p<0.001$ ****, $p<0.0001$). NS denotes no statistical significance observed. All values are calculated from at least 3 individual data sets.

From the above results in HUVECs exploring whether the calcium and nitric oxide responses were due to $G_{q/11}$ signalling it seemed plausible that the same could be the case for HCMs, indeed this proved to be the case. Using the $G_{q/11}$ selective inhibitor YM-254890 the complete ablation of intracellular calcium release and NO release was observed for CGRP, AM and AM2 (**Figure 4.5A,B**). Overall this work suggests that regardless of the cell type or RAMP present CLR appears to be a strong recruiter of $G_{q/11}$ signalling and seems to mediate all if its i[Ca^{2+}] through this pathway.

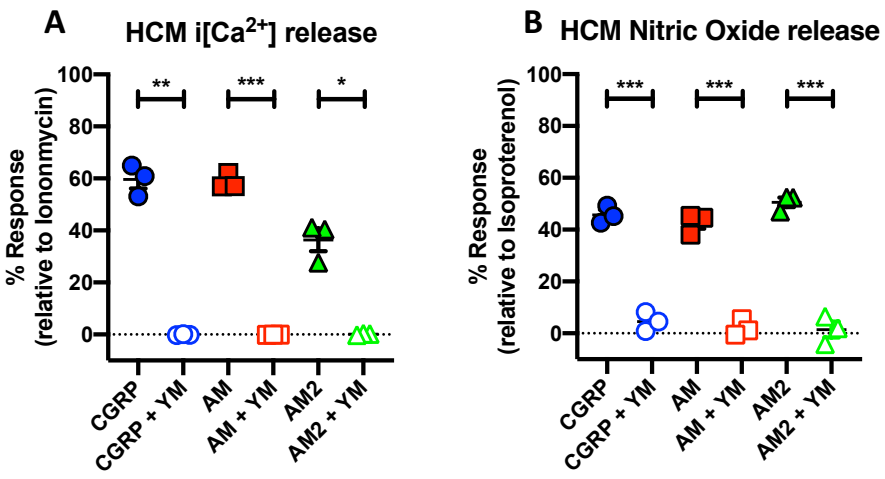

Figure 4.5. Inhibitor effects on i[Ca^{2+}] and NO. Characterisation of intracellular Calcium mobilisation with and without YM-254890 relative to ionomycin (10 μM) (**A**). Characterisation of nitric oxide release with/without YM-254890 relative to Ach (10 μM) (**B**). Statistical significance determined compared to control using an unpaired t test with Welch's correction (*, $p<0.05$; **, $p<0.01$; ***, $p<0.001$ ****, $p<0.0001$). All values are calculated from 3 individual data sets.

Interrogation of spatiotemporal cAMP accumulation in HUVECs using internalisation inhibitors

The next challenge was to try and determine whether spatiotemporal signalling could be observed at the endogenous CLR-RAMP2 in HUVECs. Barbadin is a reported inhibitor of the β-arrestin-AP2 interaction (Beautrait et al. 2017), and therefore is able to prevent β-arrestin mediated internalisation. First a standard cAMP accumulation assay was performed with barbadin vs control **(Figure 4.6**). Upon analysing the results barbadin caused an increase in potency in the pEC50 of CGRP and AM2, although only the CGRP potency change was significant, and the AM results overlaid well suggesting there was no effect of barbadin on AM cAMP accumulation response; confirmed by statistical analysis of the pEC50 and Emax values. The effect of barbadin on CGRP seemed to suggest prevention of internalisation could enhance CGRP mediated cAMP signalling. This and the inconclusive effect on AM2 provided motivation for further exploration of this aspect of cAMP signalling. Therefore a cAMP assay was designed whereby the endpoint (and therefore stimulation time) of individual assay points varied from 0min to 30min so that a 'time-course' for cAMP signalling in response to CGRP, AM and AM2 could be observed, in the absence of IBMX so that cAMP levels could fluctuate 'naturally'. For the three ligands there looked to be an early phase and late phase of signalling, which is particularly pronounced in AM (but not seen at all for CGRP) before reaching a plateau of sorts by 8/10min, and cAMP ligands in the presence of each of the 3 ligands remaining relatively constant until the assay endpoint at 30 min (Figure 4.5). The same experiments were performed in the presence of barbadin. The overall shape of the response remained the same, however the CGRP response was higher and the plateau level of the 3 peptides appeared closer together prompting further exploration.

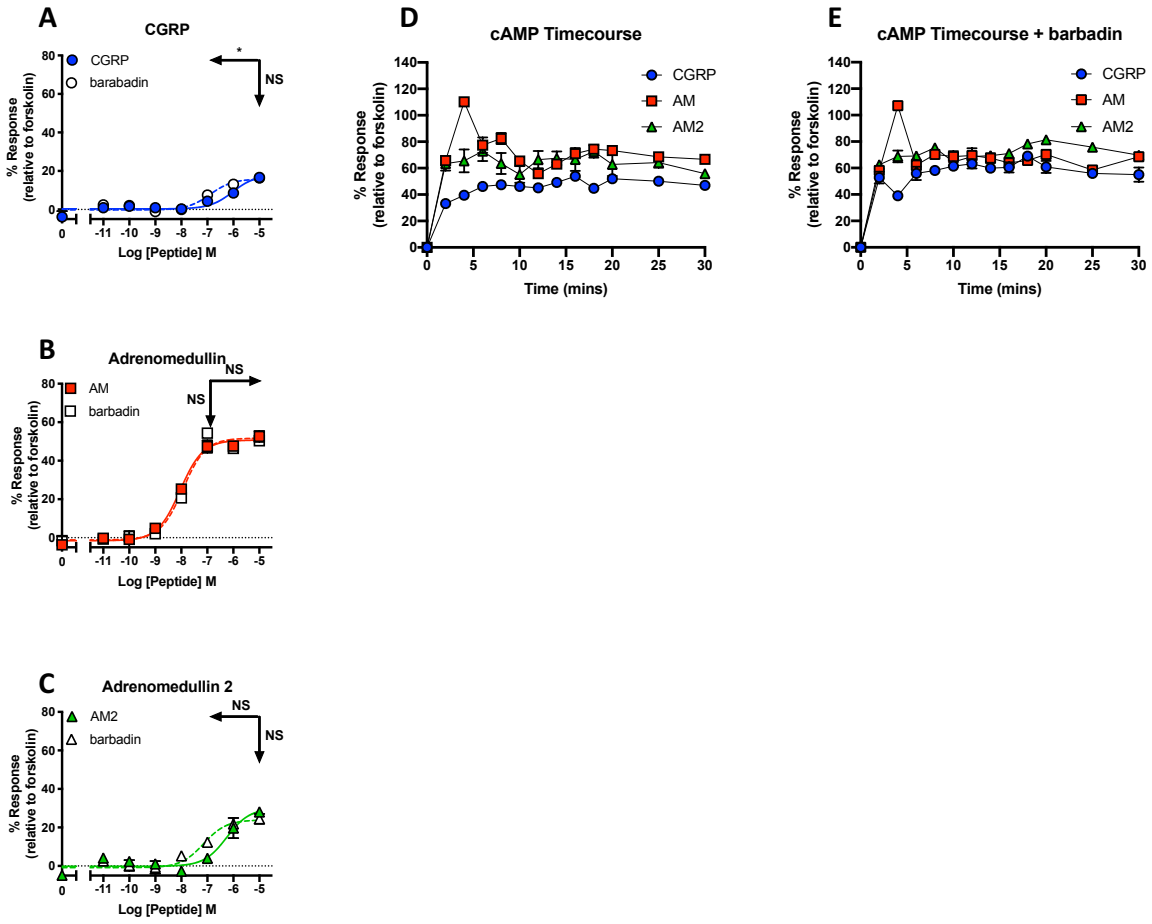

Figure 4.6. Barbadin effects on cAMP accumulation and time-course for cAMP accumulation in HUVECs. Characterisation of cAMP accumulation with and without barbadin (100 μM) In response to stimulation by CGRP (**A**), AM (**B**) and AM2 (**C**). relative to forskolin (10 μM). Characterisation of cAMP accumulation in response to the 3 peptides at 10 μM over time (**D**) relative to forskolin (10 μM). Characterisation of cAMP accumulation in response to the 3 peptides over time (**E**) in the presence of barbadin relative to forskolin (10 μM). Statistical significance determined compared to control using an unpaired t test with Welch's correction (*, $p<0.05$; **, $p<0.01$; ***, $p<0.001$ ****, $p<0.0001$). NS denotes no statistical significance observed. All values are calculated from at least 3 individual data sets. Horizontal arrows show pEC50, and vertical arrows show Emax statistical significance.

These two possible phases of the response provided impetus to explore this in more detail (in terms of full dose-response experiments). Therefore, the effect of multiple internalisation inhibitors on CGRP, AM and AM2 signalling responses were observed at different time points: 8 or 30 min, with and without IBMX. Firstly, the 30 min + IBMX response was studied (**Figure 4.7**). Repeating the barbadin vs control experiment now alongside compound 101, a GRK2/3 inhibitor (Lowe et al. 2015), dynasore (Macia et al. 2006), and pitstop2 (May et al. 2014) both inhibitors of internalisation complex formation. All with the exception of dynasore reinforced the initial CGRP observations by causing a significant increase in pEC50, there was again no increase from barbadin or any of the other on AM, but on this occasion the barbadin induced shift in AM2 was significant, and although an approximate half-log leftward shift could be seen with pitstop2 and compound 101 treatment these were not significant. Interestingly while no effect on CGRP Emax was observed, at least two of the inhibitors for both AM and AM2 saw an increase in their Emax values.

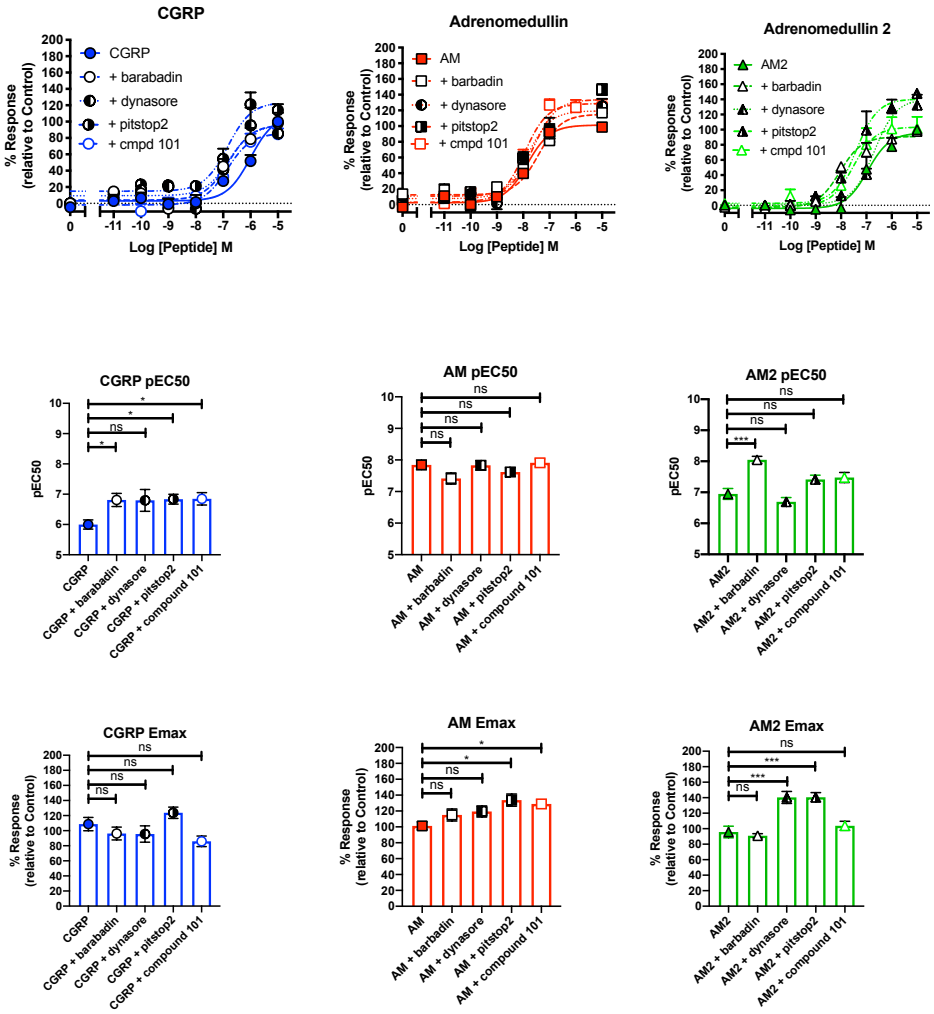

Figure 4.7. Internalisation inhibitor effects on cAMP accumulation and time-course for cAMP accumulation in HUVECs. Characterisation of cAMP accumulation with and without barbadin (100 μM), dynasore (100 μM), pitstop (100 μM), and compound 101 (100 μM), In response to stimulation by CGRP (**A**), AM (**B**) and AM2 (**C**). relative to forskolin (100 μM) for 30 min stimulation time in the presence of IBMX. Also shown are pEC50 and Emax values with statistical significance in relation to control treated cells. Data are analysed using a three-parameter non-linear regression curve, and are presented here as mean ± S.E.M. of 4 individual data sets. Statistical significance compared to the cognate ligand (AM) and determined using one-way ANOVA with Dunnett's post-hoc test, (*, $p<0.05$; **, $p<0.01$; ***, $p<0.001$; ****, $p<0.0001$).

Next, how these inhibitors influenced the responses after 30min stimulation without PDE inhibition (no IBMX) was studied and at a much-reduced stimulation time of 8min with and without PDE inhibition (**Figure 4.8**) to assess whether there was a temporal component to the signalling and whether PDE inhibition was masking any of these potential spatiotemporal aspects. At the 30min time-point the significant barbadin effect on CGRP pEC50 remained however the increases produced by the other inhibitors were not significant. Likewise, there was again no effect from any on AM or AM2 pEC50s. While an increase by barbadin on AM2 was observable it was not significant. The removal of PDE inhibition appeared to abolish the Emax effects seen for AM and AM2, with none of the inhibitors having a significant effect on the Emax of any of the stimulating ligands. At the 8min time-point for ligand stimulation, in the presence of PDE inhibition there was no significant change for any of the peptides at any of the measured parameters. However, moving across to the 8min stimulation time experiments there is a noticeable effect from the inhibitors on CGRP potency, and in one case the Emax increases. In terms of significance only barbadin and compound 101 reach an appreciable level. Again, for AM there are minimal changes between the responses with none of statistical relevance. For AM2 it is interesting to note that barbadin now causes a significant pEC50 change (**Table 4.2**).

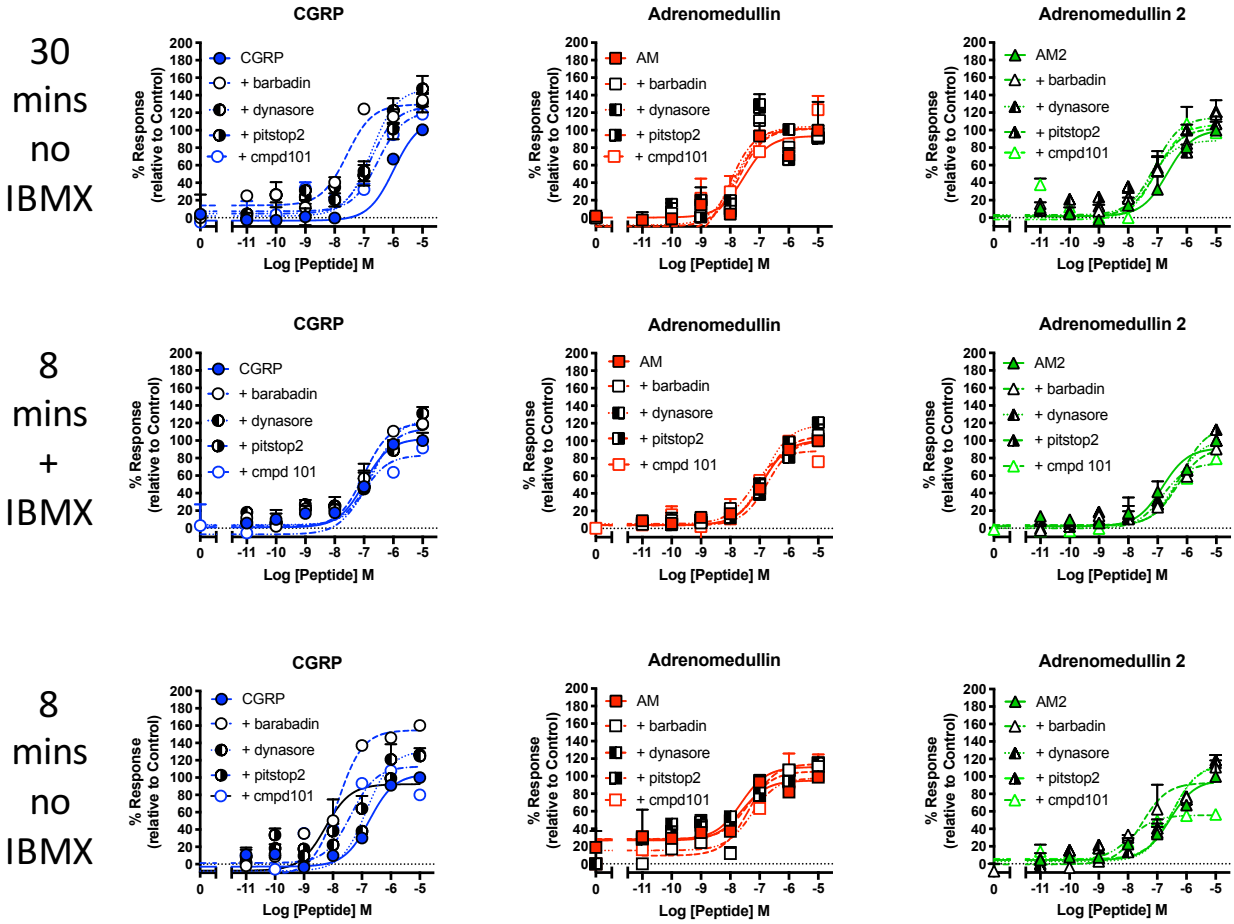

Figure 4.8. Internalisation inhibitor effects on cAMP accumulation and time-course for cAMP accumulation in HUVECs. Characterisation of cAMP accumulation with and without barbadin (100μM), dynasore (100 μM), pitstop2 (100 μM), and compound 101 (100 μM), In response to stimulation by CGRP (**A**), AM (**B**) and AM2 (**C**). relative to forskolin (100 μM). At different time points and with/without IBMX.

30mins + IBMX

Control	CGRP		AM		AM2	
pEC50	6.00	0.15	7.84	0.15	6.95	0.18
Emax	108.68	8.83	101.31	4.94	95.76	7.44
Span	105.62	9.06	98.89	5.67	99.80	8.24
n	4		4		4	

+ barbadin	CGRP		AM		AM2	
pEC50	6.81*	0.22	7.41	0.18	8.05***	0.11
Emax	96.27	8.46	115.06	7.58	90.83	2.82
Span	92.25	9.49	102.50	8.39	93.36	3.62
n	4		4		4	

+dynasore	CGRP		AM		AM2	
pEC50	6.80	0.36	7.83	0.15	6.69	0.14
Emax	95.59	10.81	119.41	6.93	140.35***	7.69
Span	86.17	11.79	111.65	7.87	138.79**	8.52
n	4		4		4	

+pitstop2	CGRP		AM		AM2	
pEC50	6.84*	0.16	7.62	0.14	7.41	0.14
Emax	123.72	7.46	133.78*	7.68	140.60***	6.06
Span	108.73	8.29	122.94	8.25	137.82**	7.42
n	4		4		4	

+compound101	CGRP		AM		AM2	
pEC50	6.85*	0.20	7.95	0.12	7.52	0.15
Emax	85.87	7.03	128.72*	4.90	103.39	5.38
Span	87.76	7.67	125.58	6.25	104.26	6.29
n	4		4		4	

30mins no IBMX

Control	CGRP		AM		AM2	
pEC50	5.98	0.31	7.52	0.35	6.66	0.22
Emax	113.33	17.66	93.36	11.46	100.51	9.54
Span	116.58	17.77	93.13	13.02	98.76	10.16
n	4		4		4	

+ barbadin	CGRP		AM		AM2	
pEC50	7.58**	0.17	7.70	0.25	7.05	0.18
Emax	129.54	6.48	101.68	10.52	102.19	8.66
Span	115.42	7.71	111.78	12.63	100.59	9.28
n	4		4		4	

+dynasore	CGRP		AM		AM2	
pEC50	6.75	0.23	7.80	0.26	7.26	0.32
Emax	147.52	14.78	104.24	11.26	88.21	11.83
Span	145.62	15.97	112.56	13.76	87.35	12.85
n	4		4		4	

+pitstop2	CGRP		AM		AM2	
pEC50	6.78	0.25	7.81	0.25	7.09	0.21
Emax	127.20	13.30	101.65	10.58	114.72	9.42
Span	122.50	14.42	117.10	12.98	111.55	10.58
n	4		4		4	

+compound101	CGRP		AM		AM2	
pEC50	6.52	0.30	8.05	0.29	7.05	0.32
Emax	121.37	13.44	101.95	13.67	106.50	14.14
Span	113.92	14.14	129.64	16.78	108.59	15.82
n	4		4		4	

8 mins + IBMX

Control	CGRP		AM		AM2	
pEC50	7.00	0.26	6.91	0.15	6.84	0.29
Emax	102.35	10.95	100.80	6.01	91.60	11.22
Span	101.36	12.19	96.79	6.63	89.49	12.28
n	4		4		4	

+ barbadin	CGRP		AM		AM2	
pEC50	7.01	0.26	6.87	0.17	6.35	0.25
Emax	120.07	12.75	105.39	7.35	91.71	10.91
Span	118.82	14.22	101.56	8.07	88.49	11.25
n	4		4		4	

+dynasore	CGRP		AM		AM2	
pEC50	6.66	0.25	6.85	0.09	6.37	0.13
Emax	124.14	13.26	118.12	4.22	101.27	6.15
Span	120.20	14.14	114.55	4.63	99.06	6.35
n	4		4		4	

+pitstop2	CGRP		AM		AM2	
pEC50	6.79	0.21	6.73	0.09	6.21	0.18
Emax	114.14	9.99	101.07	3.94	115.95	10.41
Span	110.98	10.86	97.67	4.24	112.32	10.67
n	4		4		4	

+compound101	CGRP		AM		AM2	
pEC50	7.08	0.28	7.24	0.22	6.84	0.14
Emax	83.43	10.12	88.59	7.09	74.37	4.55
Span	90.44	11.94	83.28	8.05	74.55	4.98
n	4		4		4	

8 mins no IBMX

Control	CGRP		AM		AM2	
pEC50	6.74	0.24	7.60	0.43	6.57	0.30
Emax	104.05	9.03	95.06	9.98	96.37	12.11
Span	106.89	9.88	68.32	11.83	91.95	12.82
n	4		4		4	

+ barbadin	CGRP		AM		AM2	
pEC50	7.87*	0.26	7.36	0.24	7.53	0.21
Emax	167.10*	17.67	114.15	8.86	92.77	6.67
Span	161.61	18.39	104.80	10.55	93.41	7.81
n	4		4		4	

+dynasore	CGRP		AM		AM2	
pEC50	6.85	0.24	7.63	0.20	6.49	0.21
Emax	131.03	12.87	110.51	5.50	114.35	10.67
Span	138.94	14.59	82.55	6.65	111.68	11.17
n	4		4		4	

+pitstop2	CGRP		AM		AM2	
pEC50	7.37	0.29	7.39	0.24	6.48	0.22
Emax	112.98	11.04	105.52	6.68	113.65	10.69
Span	111.65	12.70	77.08	7.68	108.03	11.13
n	4		4		4	

+compound101	CGRP		AM		AM2	
pEC50	8.26**	0.35	7.28	0.35	7.92*	0.45
Emax	92.45	11.56	97.95	10.50	55.70*	7.83
Span	100.01	14.71	82.62	12.31	51.37	9.79
n	4		4		4	

Table 4.2. Internalisation inhibitor effects on cAMP accumulation and time-course for cAMP accumulation in HUVECs. Characterisation of cAMP accumulation with and without barbadin (100 μM), dynasore (100 μM), pitstop2 (100 μM), and compound 101 (100 μM), In response to stimulation by CGRP, AM and AM2. relative to forskolin (100 μM). At different time points and with/without IBMX. Data are analysed using a three-parameter non-linear regression curve, and are presented here as mean ± S.E.M. of 4 individual data sets. Statistical significance compared to the cognate ligand (AM) and determined using one-way ANOVA with Dunnett's post-hoc test, (*, p<0.05; **, p<0.01; ***, p<0.001; ****, p<0.0001).

Parallel to this in-depth analysis at specific time points more time course experiments were performed to see if there were observable changes to the natural pattern/shape of the cAMP response (**Figure 4.9**). Looking at CGRP alone alongside treatment + barbadin or + compound 101 it is interesting that over the course of 30 min the inhibitor containing time-courses produce slightly larger responses in terms of amount of cAMP correlating with the dose-response data. In contrast the inhibitor containing time courses for AM and AM2 seem to overlay the control time-course, with the notable exception of the sharp initial peak for AM which is ablated by compound 101 treatment. Although this does not pan through to significant shifts in the responses recorded in the dose-response experiments for AM stimulation without IBMX treatment. Then plotting the compound 101 time-courses together for all three ligands the responses are much closer together than the control responses are relative to each other. When experiments were performed at 4°C this flattened the appearance of the data as well as reducing AM and AM2 responses such that they are now below CGRP and at this temperature CGRP produced the greatest response which was sustained over the 30min. When performing this experiment in the presence of barbadin the same trends were observed suggesting cold inhibited internalisation. This experiment was performed as the literature suggests low temperatures prevent GPCR internalisation from the cell surface (Sorkin and Carpenter 1993, Penheiter et al. 2002).

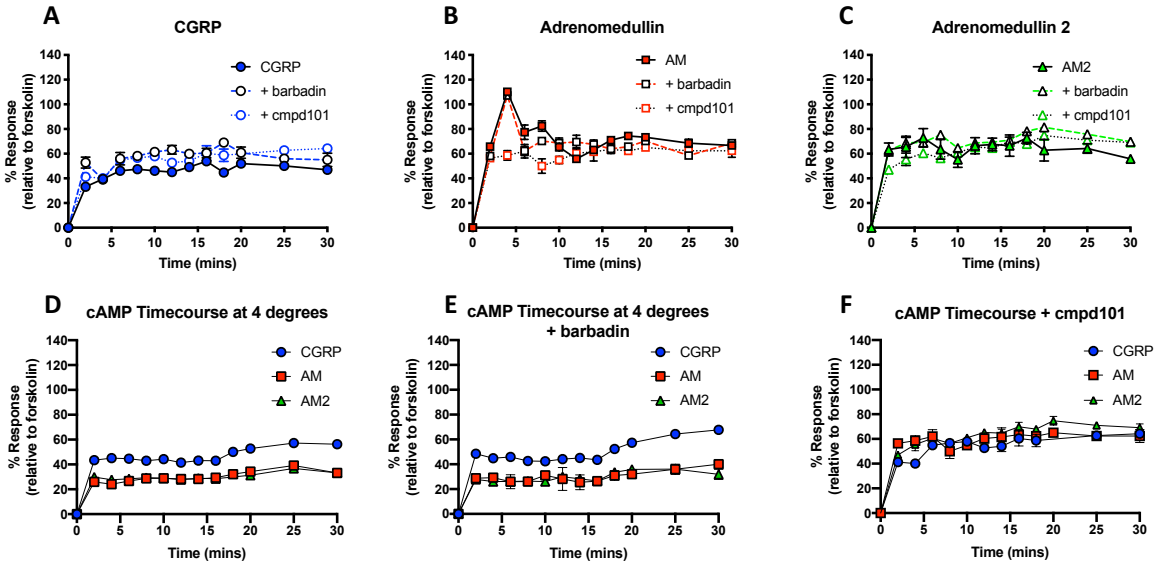

Figure 4.9. Time-course for cAMP accumulation in HUVEC under different conditions. Characterisation of cAMP accumulation over time with and without barbadin (100 μM), and compound 101 (100 μM), In response to stimulation by CGRP (**A**), AM (**B**) and AM2 (**C**). relative to forskolin (100 μM). Characterisation of cAMP accumulation over time at 4°C (**D**), at 4 °C with barbadin (**E**), and in the presence of compound 101 (**F**).

Interrogation of spatiotemporal $pERK_{1/2}$ signalling in HUVECs using an internalisation inhibitor

The next step was to study the effect of internalisation on $pERK_{1/2}$ signalling. Looking at the dose-response relationship barbadin caused a strong decrease in CGRP pEC50 and a strong reduction in AM Emax, although had no effect on the small AM2 response (**Figure 4.10**). Suggesting that internalisation plays an important part in both CGRP and AM $ERK_{1/2}$ activation. This, as outlined previously is initial $pERK_{1/2}$ and there are likely multiple phases. This was explored by performing a time-course experiment. This showed whilst initial $pERK_{1/2}$ response decreases after the initial peak at 5min for all three peptides it does plateau and is sustained right up the final 60min time-point. The time-course in the presence of barbadin showed small reductions of initial $pERK_{1/2}$ and then complete ablation of $pERK_{1/2}$ almost immediately after that. This provides strong evidence that there are multiple phases of $pERK_{1/2}$ and that they are dependent on internalisation. Particularly after 20min where there was little or no $pERK_{1/2}$ recorded from any of CGRP, AM or AM2.

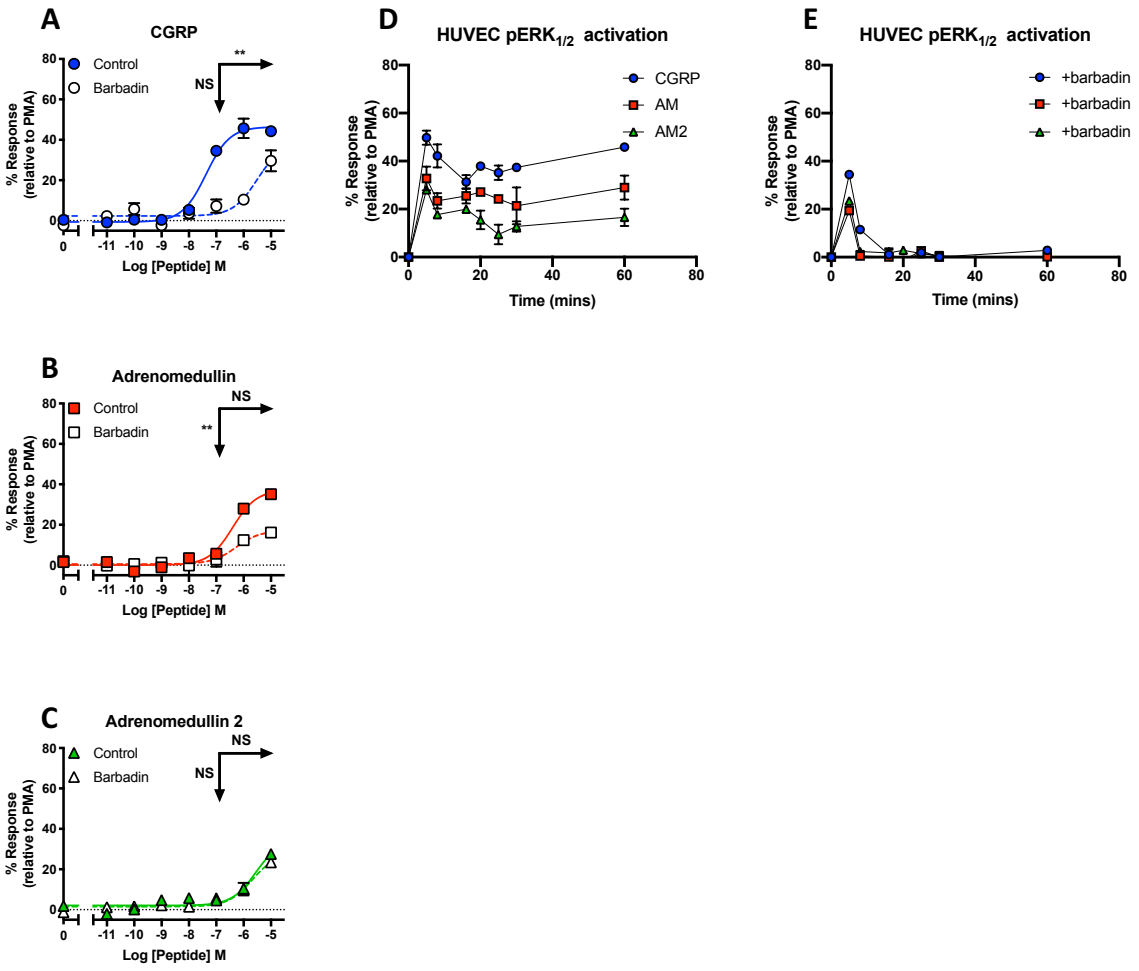

Figure 4.10. Barbadin effects on pERK$_{1/2}$ activation and time-course for pERK$_{1/2}$ activation in HUVECs. Characterisation of pERK$_{1/2}$ activation with and without barbadin (100 μM) In response to stimulation by CGRP (**A**), AM (**B**) and AM2 (**C**). relative to PMA (10 μM). Characterisation of pERK$_{1/2}$ activation in response to the 3 peptides over time (**D**) relative to PMA (10 μM). Characterisation of pERK$_{1/2}$ activation in response to the 3 peptides over time (**E**) in the presence of Barbadin relative to PMA (10 μM). Statistical significance determined compared to control using an unpaired t test with Welch's correction (*, p<0.05; **, p<0.01; ***, p<0.001 ****, p<0.0001). NS denotes no statistical significance observed. All values are calculated from at least 3 individual data sets. Horizontal arrows show pEC50, and Vertical arrows show Emax statistical significance.

Assessing the $G_{i/o}$ component of CGRP family peptide cAMP accumulation in HCMs

Following the successful observation of $G_{i/o}$ signalling from CLR-RAMP2 in HUVECs, and with the conformation that multiple $G_{i/o}$ proteins were expressed in the HCMs (**Figure 4.1**)(**Supplemental Figure 8.2**) It was assessed whether there was a $G_{i/o}$ component to CGRP, AM and AM2 cAMP signalling at the CLR-RAMP1 in HCMs. In each case PTX pre-treatment caused little or no change in cAMP accumulation compared to control (**Figure 4.11**). This was confirmed through statistical analysis of the pEC50 and Emax values, in all cases there was no change (**Figure 4.11**), therefore providing no evidence that there is $G_{i/o}$ coupling to the CLR-RAMP1 in this cell system.

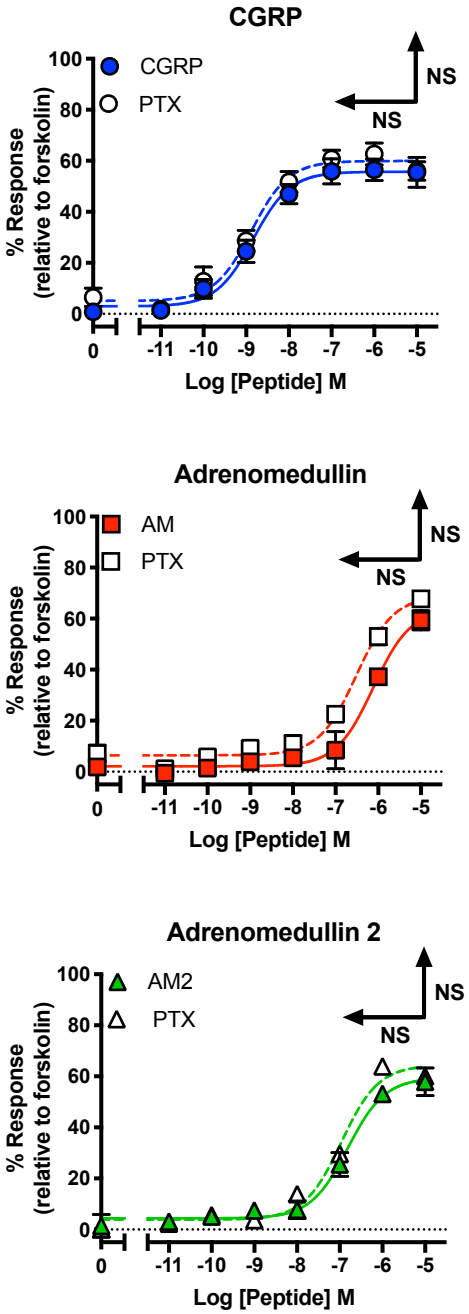

Figure 4.11. cAMP signalling in HCMs with and without PTX treatment. Characterisation of cAMP accumulation in response to stimulation by CGRP, AM, and AM2 in HCMs in the presence and absence of 200 ng/ml PTX. Pre-treated for 16 h with PTX/Control. All relative to 100 µM forskolin. Data are analysed using a three-parameter non-linear regression curve. Statistical significance determined compared to control using an unpaired t test with Welch's correction (*, $p<0.05$; **, $p<0.01$; ***, $p<0.001$ ****, $p<0.0001$). NS denotes no statistical significance observed. All values are calculated from at least 3 individual data sets. Horizontal arrows show pEC50, and Vertical arrows show Emax statistical significance.

Interrogation of spatiotemporal cAMP and $pERK_{1/2}$ signalling in HCMs using an internalisation inhibitor

Previous reports have demonstrated CGRP at the CLR-RAMP1 (co-expressed) continues to signal via cAMP endosomaly (Yarwood et al. 2017). It was therefore unsurprising to see in the presence of the internalisation inhibitor CGRP signalling is significantly supressed (**Figure 4.12A**). Interestingly however, none of the other ligands are significantly affected by the presence of barbadin in terms of cAMP signalling (**Figure 4.12A**). Then the $pERK_{1/2}$ response of the three peptides was profiled with and without barbadin. All of which were significantly affected in different ways. The CGRP and AM responses were significantly enhanced and their potency at this pathway was enhanced, CGRP to the greatest extent as the increase in potency was over ten-fold. The maximum response of AM was also enhanced however unlike the others the response was less potent (**Figure 4.12B**).

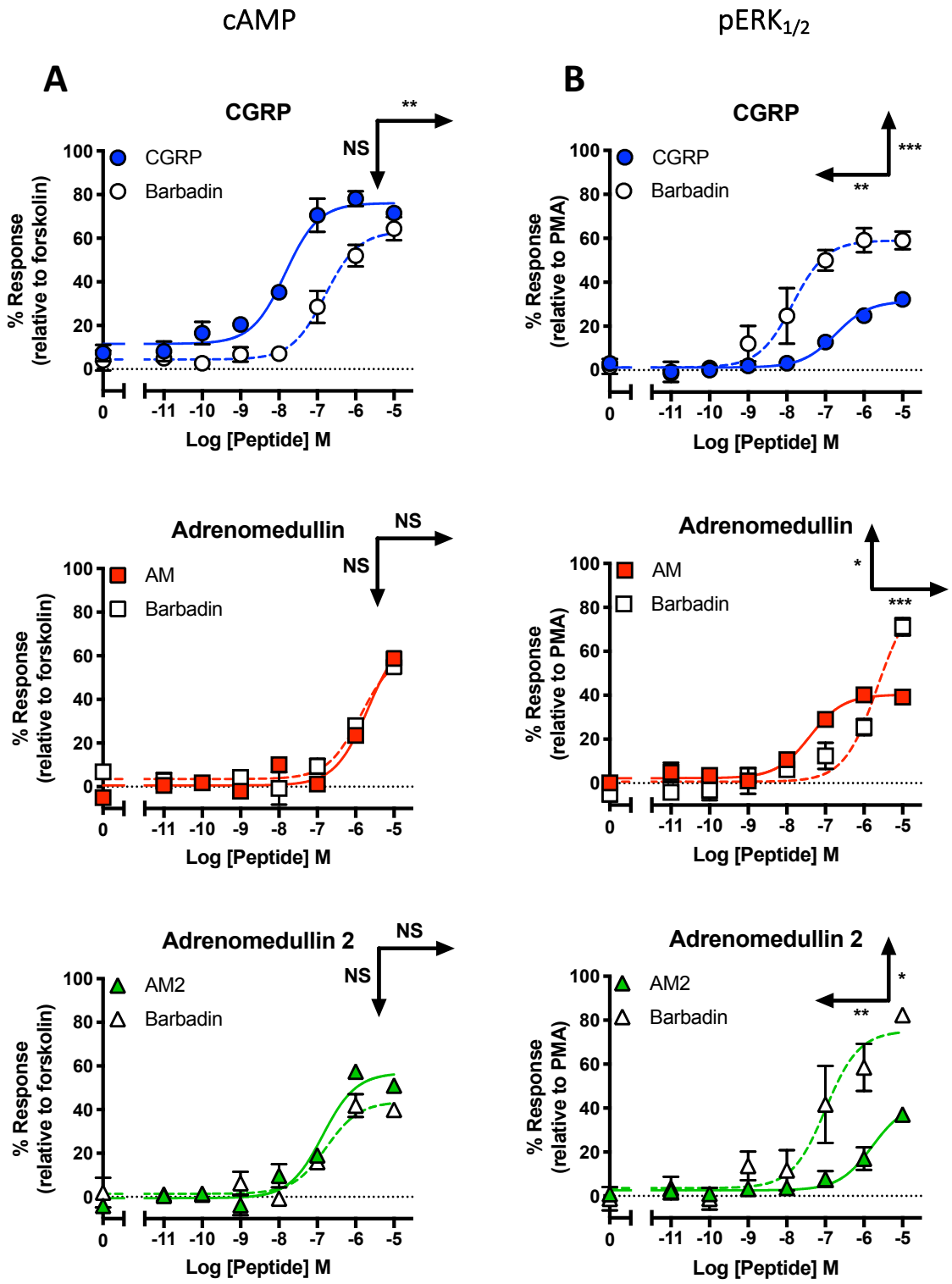

Figure 4.12. Barbadin effects on cAMP accumulation and pERK$_{1/2}$ activation in HCMs. Characterisation of cAMP accumulation (**A**) and pERK$_{1/2}$ activation (**B**) with and without barbadin (10 0μM) In response to stimulation by CGRP, AM and AM2. relative to forskolin (100 μM) and PMA (10 μM) respectively. Statistical significance determined compared to control using an unpaired t test with Welch's correction (*, p<0.05; **, p<0.01; ***, p<0.001 ****, p<0.0001). NS denotes no statistical significance observed. All values are calculated from at least 3 individual data sets. Horizontal arrows show pEC50, and vertical arrows show Emax statistical significance.

Summary

When PTX effects on signalling were assessed the results proved fascinating; they suggest that AM does not recruit $G_{i/o}$ proteins. As this has long been considered the cognate ligand in terms of cAMP signalling and also produces the most potent and largest response it makes sense that it does not recruit the cAMP inhibitory G proteins to the receptor. What is particularly interesting is that the other peptides can recruit these G proteins and that, while the signalling bias suggests this, this may be the first evidence presented here that these peptides differentially recruit G proteins to the same receptor to affect their unique signalling responses. For CGRP this shows that its response is clearly biased away from cAMP compared to the other peptides. Moreover, that these $G_{i/o}$ proteins also contribute to enhancing the CGRP $pERK_{1/2}$ response.

In terms of assessing the contribution of other pathways to $ERK_{1/2}$ signalling it is clear cAMP-PKA does not play a role for any of the peptides. Similarly, there is little or no contribution from the $G_{q/11}$ pathway to $ERK_{1/2}$ signalling. Interestingly there appears to be an EPAC contribution to AM and AM2 $ERK_{1/2}$ signalling suggesting that one arm of signalling from cAMP feeds into $ERK_{1/2}$ phosphorylation but the other does not. Overall it is apparent that there is not one simple source of $pERK_{1/2}$ as no one inhibitor completed knocked out signalling but that many pathways contribute to the $pERK_{1/2}$ response. While these data disputes the assumption that β-arrestins are the sole source of GPCR mediated $pERK_{1/2}$ activation it does not rule out the possibility that they provide some of the response observed. Indeed, this is supported by the experiments using barbadin which inhibits β-arrestin mediated internalisation. As inhibiting this internalisation reduces the ERK responses from CGRP and AM. This confirms that β-arrestins are recruited to CLR-RAMP2 endogenously. It is not direct evidence that they are mediating the $pERK_{1/2}$ response but the fact that they are recruited to the receptor and that the $pERK_{1/2}$ response occurs after they mediate internalisation is good evidence that they are involved to some degree.

It was hypothesised that removal of PDE inhibition would enhance all internalisation inhibitor effects. As it would allow the natural breakdown of cAMP, if internalisation did halt signalling. Then without IBMX to maintain cAMP levels there might be a larger difference between control and Inhibitor treatment. While this was supported by barbadin treatment on CGRP at 30 min, the effect of the other inhibitors became less significant. In the case of AM2 the significance was lost entirely. Therefore, it is hard to come to a general conclusion about the effect of removing PDE inhibition. Or for that matter, about the effects of the internalisation inhibitors with each in some cases changing from ligand to ligand, short vs long stimulation time and IBMX vs no IBMX. The lack of effect at 8min with IBMX for all of them did perhaps show that over this limited time span coupled with prevention of the natural breakdown of cAMP it is not possible to observe any effects of internalisation. Summarising the effects of internalisation on cAMP for each peptide, in the case of AM, excluding two cases where there was a significant increase in Emax, on the whole regardless of stimulation time or PDE inhibition status, the internalisation inhibitors had no real effect on AM induced cAMP suggesting that all cAMP signalling occurs at the surface with this peptide bound to the CLR-RAMP2, and it may not internalise as rapidly as others. This leads on to AM2 where inhibiting internalisation across multiple conditions increased the cAMP response suggesting that it may internalise faster than AM and produce less cAMP at the surface. This leaves CGRP, which was by far the most heavily influenced by the internalisation inhibitors, producing strong increases in cAMP production. CGRP as previously established does not produce much cAMP relative to the other and in fact couples to $G_{i/o}$ as well to reduce cAMP. What this work now shows is that CGRP also seems to internalise rapidly possibly also to reduce its cAMP response. As chemical intervention to prevent this natural internalisation markedly increases the cAMP recorded from CGRP stimulation.

Chapter 5. Functional outcomes of CLR-RAMP complexes in cardiac myocytes and HUVECs

Aims and hypothesis

In this chapter, there are two overarching aims both made possible through the use of industrial (AstraZeneca) facilities and equipment: The first aim was to explore the effects of the CGRP family peptides on cardiac myocyte function. Then the second was to perform CRISPR-cas9 gene editing in HUVECs.

The opportunity was taken to work on some induced pluripotent stem cells (IPSC) derived icell human cardiac myocytes as these cells have been established for use as an *in vitro* cell model for cardiac function. This is because they beat spontaneously, and although they do not proliferate, provide a model for studying how drugs affect cardiac function, and therefore they have primarily been used as model in drug safety screening. These cells have been used to study cell beat rate and intracellular calcium fluxes in 2D cell monolayers, as well as to study 3D spheroid beat rate; when grown together with cardiac fibroblasts (Chapter 2). It was hypothesised, based on previous work here in primary proliferating cardiac myocytes, that CGRP, AM and AM2 may influence cardiac function to differing extents and that this might be detectable as effects on cardiac beat rate. Therefore, it was first attempted to confirm, in the author's hands, the successful functioning of assays for intracellular calcium and beat rate in 2D as well as beat rate studies in 3D; before moving to study the influence of CGRP family peptides on the function of cardiac myocytes in these assays.

Following this the aim was to perform CRISPR-cas9 gene editing in HUVEC cells. In co-expression studies, it is well established that for the CLR to traffic and function it has an absolute requirement for co-expression of one of the three RAMPs. Having explored the signalling function of endogenous CLR

in primary human cells in previous chapters, the aim was to use CRISPR-cas9 gene editing to knock-out RAMP2 expression in HUVECs in order to determine the importance of RAMP expression on signalling in an endogenous cell system. If successful, this could be explored in multiple ways: One way was to see whether the CLR could produce a signalling response without RAMP expressed. With the hypothesis being that it would not be able to. Another was to explore how the expression of a different RAMP could alter the signalling profiles of CGRP, AM and AM2. In the case where RAMP-KO HUVEC cells could be established the purpose of re-expressing a different RAMP (RAMP1) was twofold: The first was to demonstrate that, if it could rescue CLR signalling function, gene editing that had led to a loss of CLR signalling, had done so through affecting RAMP2 gene expression exclusively. Therefore, if RAMP re-expression rescued receptor function this could confirm there were no detrimental off target effects. Secondly, by re-expressing a RAMP different from the endogenous one, it could be observe how much of an effect the RAMP had on the distinct patterns of signalling observed in a HUVEC. As, finding another cell line (HUAECs) that expressed CLR-RAMP2 and showed similar signalling patterns to CLR-RAMP2 in HUVECs, and finding a CLR-RAMP1 cell line (HCMs) that demonstrated different patterns of signalling all suggests it is the RAMP that is crucial in governing signalling patterns through the CLR, only by changing the RAMP in an identical primary background could it be shown with certainty that it is the RAMP (together with the stimulating peptide) that directs signalling patterns. Alongside attempting to knock-out the expression of RAMP2, identical viral machinery, and methods, were utilised directed towards knocking out the unrelated house-keeping gene HPRT1 to ensure that cells could survive the CRISPR process and that this did not prevent cell survival or function. There are not many reports of CRISPR-cas9 gene editing in primary cells, nor for CRISPR-cas9 editing of GPCR components. To the best of the authors knowledge there are no reports of gene editing of GPCR components in primary human cells and therefore of CLR or RAMP proteins in these cells so it was not known whether it would be possible to successfully knockout the RAMP2, and whether HUVECs would survive this. Lentiviral gene editing techniques were used as this has been shown previously in primary cells and is suggested for primary or hard to transfect cell lines.

Results

Establishing beta-adrenoreceptor agonist influence on cardiac function in a 2D beating cell model

First it was attempted to record IPSC derived icell human cardiac myocyte beat rates in response to isoproterenol, an established β-adrenoreceptor agonist known to stimulate an increase in beat rate in this 2D cell model. A sharp rise in beat rate was observed directly post-stimulation from resting beat rate to approximately 80 beats per minute (BPM), which is sustained for the duration of the 60min assay, with only a s all drop towards the end (**Figure 5.1A**). Then the percentage increase in beat rate was recorded in response to isoproterenol over vector treatment in control assays at the corresponding time points: These were; directly prior to stimulation, then at the peak of the ligand response and lastly at the final point before the assay end-point (**Figure 5.1B**). Just as the myocyte response to Isoproterenol was clear to observe in the time-course (**Figure 5.1A**) statistical analysis of the percentage increase in beat rate caused by Isoproterenol compared to the beat rate in the control assays confirmed that increase was strongly significant.

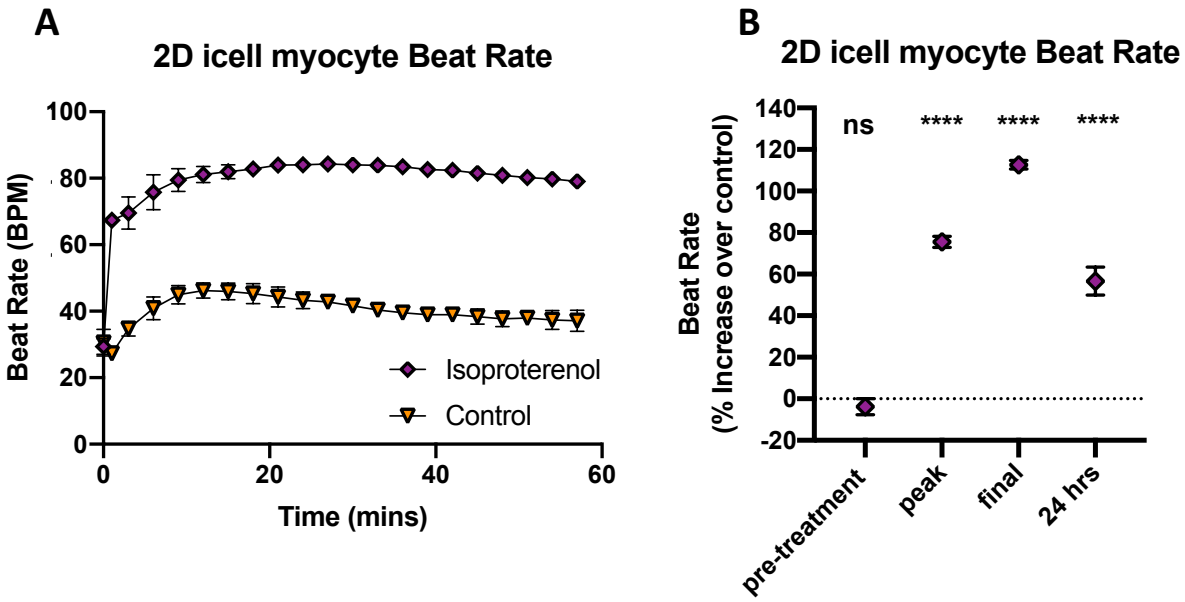

Figure 5.1. icell cardiac myocytes beat rate grown in response to Isoproterenol and Control treatment. Measurement of IPSC derived icell human cardiac myocyte beat rates in response to isoproterenol (100 nM) and control treatment (**A**). Percentage increase in beat rate in response to Isoproterenol and relative to control treatment at multiple time points (**B**). Statistical significance determined compared to control using an unpaired t test with Welch's correction (*, $p<0.05$; **, $p<0.01$; ***, $p<0.001$ ****, $p<0.0001$). NS denotes no statistical significance observed. All values are calculated from 4 individual data sets.

Exploring CGRP family peptide influence on cardiac function in a 2D beating cell model

Having confirmed observable increases in beat rate produced by an established agonist then it was tested whether CGRP, AM and AM2 had any influence on cardiac beat rate: In **Figure 5.2A-C** all three ligands cause the beat rate to rise above level reached in the control cell assays and then maintain a higher beat rate for the duration of the assays. Plotting selected time points as percentage increase over baseline shows subtle differences between the peptide responses (**Figure 5.2D-F**). Firstly, it shows that at the peak response the order of magnitude of response is AM2>AM>CGRP with CGRP producing a response that is not significantly greater than control as determined by statistical analysis. Interestingly, by the final time point in the assay the order of magnitude is reversed: CGRP>AM>AM2. Due to the nature of this assay setup, it was possible to record the beat rate 24 h post-stimulation. This revealed that CGRP produced an even greater increase over control. While AM and AM2 also maintained their effects the difference between them and CGRP was further enhanced ay this time-point. The effects on the amplitude of cell beating was also profiled, however there were no observable changes from control (**Supplemental Figure 8.5**).

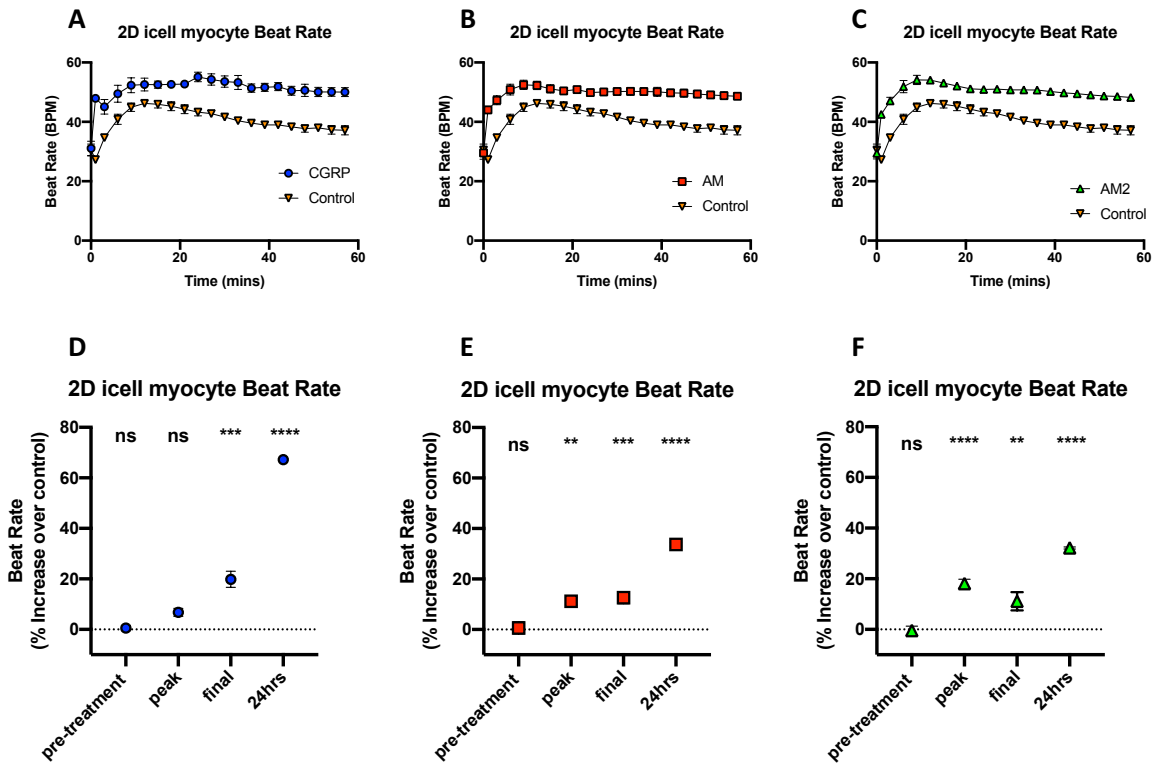

Figure 5.2. Beat rate of icell cardiac myocytes grown in monolayers in response to CGRP family peptide treatment. Measurement of IPSC derived icell human cardiac myocyte beat rates in response to CGRP (**A**), AM (**B**), and AM2 (**C**) (10 μM) and control treatment. Percentage increase in beat rate in response to CGRP (**D**), AM (**E**), and AM2 (**F**) and relative to control treatment at multiple time points (**B**). Statistical significance determined compared to control using an unpaired t test with Welch's correction (*, p<0.05; **, p<0.01; ***, p<0.001 ****, p<0.0001). NS denotes no statistical significance observed. All values are calculated from 4 individual data sets.

Exploring CLR-RAMP1 contribution to CGRP family peptide mediated effects on beat rate in a 2D beating cell model

It was possible to use the known CLR-RAMP1 antagonist Olcegepant to determine whether the beating response caused by CGRP, AM, and AM2 was mediated through CLR-RAMP1 on the surface of these cells. Co-treatment with this antagonist completely ablated all responses from all three peptides relative to control, for the duration of the assay. This suggested that CGRP, AM, and AM2 were mediating the entirety of their functional effects through the CLR-RAMP1 receptor (**Figure 5.3**).

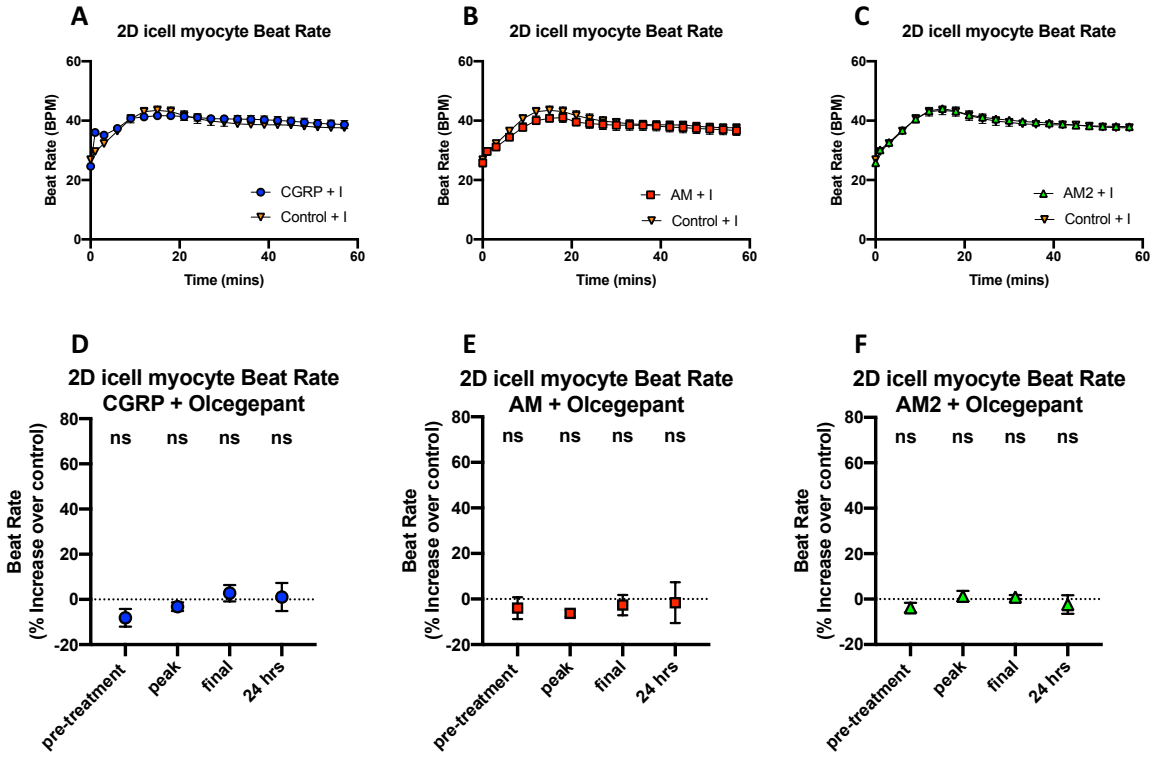

Figure 5.3. icell cardiac myocytes intrinsic calcium beat width, rate, and size in response to Isoproterenol and Control treatment. Measurement of IPSC derived icell human cardiac myocyte calcium peak width (**A**) beat rate (**B**) and beat size (**C**) in response to isoproterenol (100 nM) and Control treatment. Percentage increase in calcium peak width (**D**) beat rate (**E**) and beat size (**F**) beat rate in response to Isoproterenol and relative to control treatment at multiple time points. Statistical significance determined compared to control using an unpaired t test with Welch's correction (*, $p<0.05$; **, $p<0.01$; ***, $p<0.001$ ****, $p<0.0001$). NS denotes no statistical significance observed. All values are calculated from 4 individual data sets.

Establishing beta-adrenoreceptor agonist influence on intracellular calcium release in a 2D beating cell model

Due to the integral role intracellular calcium fluxes play in cardiac myocyte beating and function the research moved to establish whether in the first instance isoproterenol produced an observable difference. Here is plotted the three parameters recorded: calcium peak width, rate and size. The FLIPR (fluorescent imaging plate reader) system is able to record the intrinsic intracellular calcium spikes that occur within the icell myocytes, and this can then be measured and reported as a 'Peak rate' - the number of calcium peaks over a given time interval. It also records the width of these calcium peaks and their size (calculated as maximum – minimum fluorescence). All of these parameters were recorded per minute over the course of 60 min assays in response to isoproterenol treatment as well as vector control treatment. It is clear to see that isoproterenol shortens the peak width, slightly increases the peak size, and most importantly significantly increases the peak frequency (**Figure 5.4**) confirming it is possible in this system to observe a GPCR mediated influence on the intrinsic calcium fluxes.

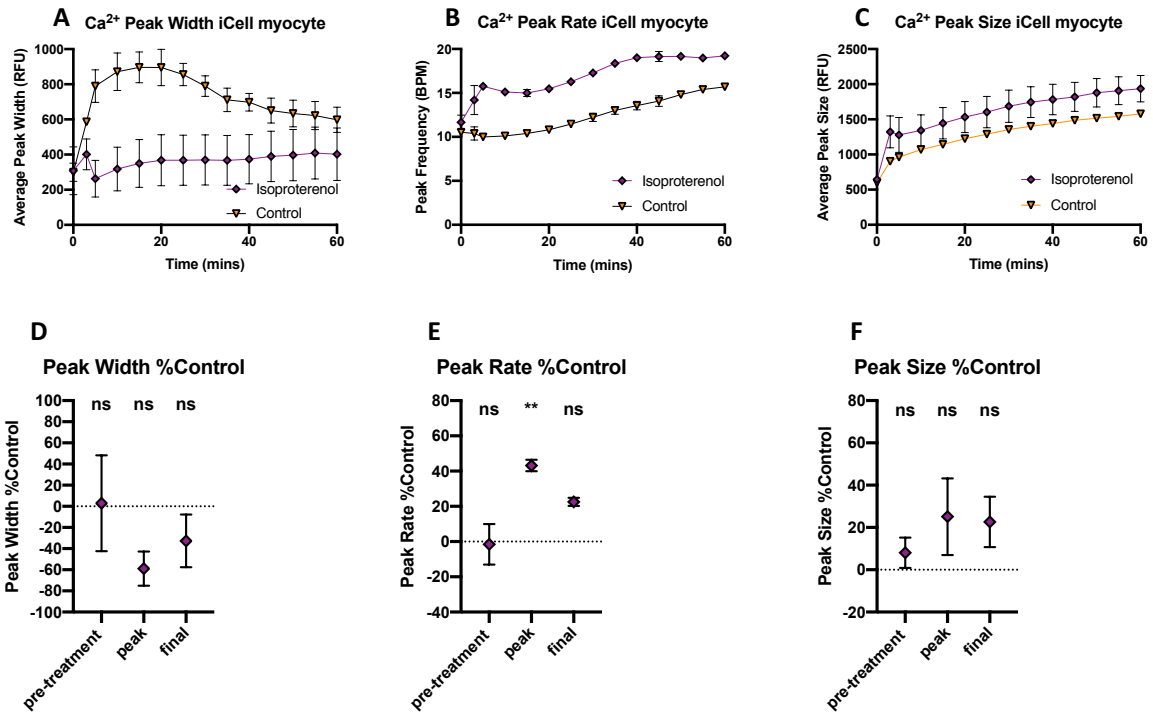

Figure 5.4. icell cardiac myocytes intrinsic calcium beat width, rate, and size in response to Isoproterenol and Control treatment. Measurement of IPSC derived icell human cardiac myocyte calcium peak width (**A**) beat rate (**B**) and beat size (**C**) in response to Isoproterenol (100 nM) and Control treatment. Percentage increase in calcium peak width (**D**) beat rate (**E**) and beat size (**F**) beat rate in response to isoproterenol and relative to control treatment at multiple time points. Statistical significance determined compared to control using an unpaired t test with Welch's correction (*, $p<0.05$; **, $p<0.01$; ***, $p<0.001$ ****, $p<0.0001$). NS denotes no statistical significance observed. All values are calculated from 4 individual data sets.

Exploring CGRP family peptide influence on intracellular calcium release in a 2D beating cell model

Following the successful observation of isoproterenol mediated changes in the intrinsic calcium peaks in icell myocytes then the myocyte calcium responses were profiled in terms of width, peak rate and size changes when stimulated by CGRP (**Figure 5.5**), AM (**Figure 5.6**) and AM2 (**Figure 5.7**). These were calculated from individual calcium traces examples of which are shown in (**Supplemental Figure 8.4**). Immediately it was clear they all influenced the calcium fluxes within the myocytes through decreasing the peak width, increasing peak rate and increasing peak size. However in comparing the percentage changes over control at different time-points (**Figure 5.5,6,7;A**) this reveals subtle differences between the peptide effects on intracellular calcium. Taking changes in the calcium peaks first while none of CGRP, AM, or AM2 produced significant increases over the control at any time point, of the three CGRP stimulated the highest calcium peaks. Moving on to calcium peak frequency, at their peak all three peptides stimulated a statistically significant increase over control (**Figure 5.5,6,7;B**). Although of these the CGRP was the smallest and appeared the most biphasic (**Figure 5.5A**): The peak rate dropped quickly after the peak before rising back up by the end of the assay. In comparison AM and AM2 produced sustained rises in peak rate throughout the assay, of the two AM2 caused the greatest increase. By the assay end-point only AM2 still caused a significant increase above the control. The final parameter was peak width, and all of the ligands at their peak caused a significant shortening, in the order of significance: AM2>AM>CGRP and as with peak frequency by the assay end-point only AM2 caused significant shortening (**Figure 5.7A**).

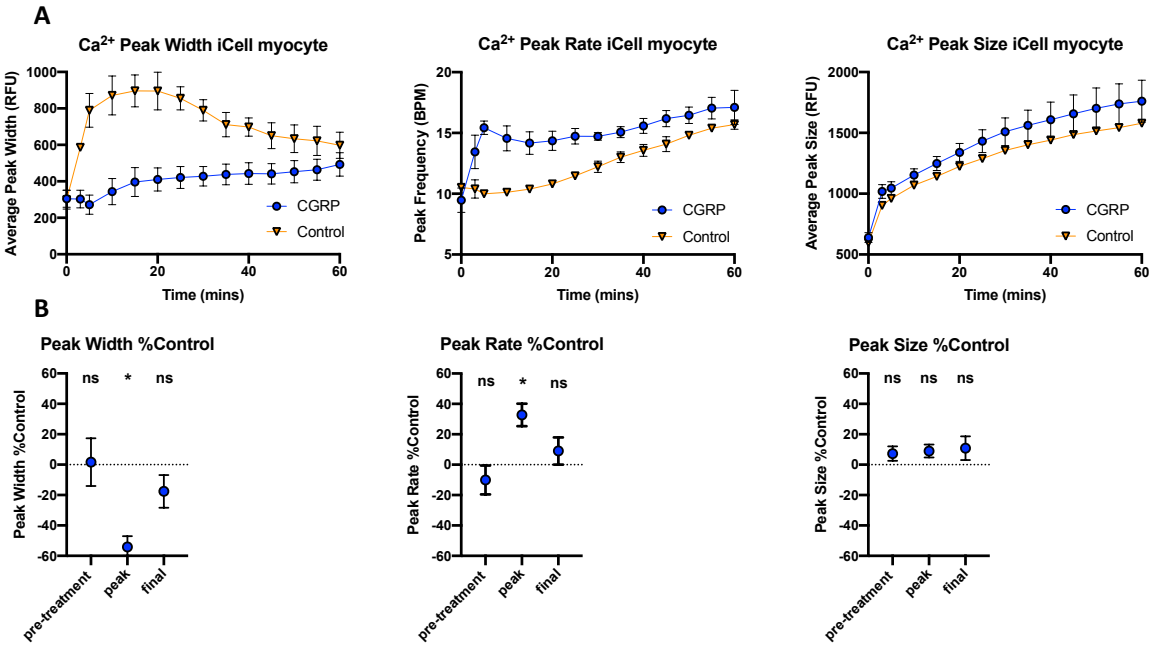

Figure 5.5. icell cardiac myocytes intrinsic calcium beat width, rate, and size in response to CGRP treatment. Measurement of IPSC derived icell human cardiac myocyte calcium peak width, beat rate, and beat size, in response to CGRP (**A**) (10 μM) and control treatment. Percentage increase in calcium peak width, beat rate, and beat size, in response to CGRP (**B**) relative to control treatment at multiple time points. Statistical significance determined compared to control using an unpaired t test with Welch's correction (*, p<0.05). NS denotes no statistical significance observed. All values are calculated from 4 individual data sets.

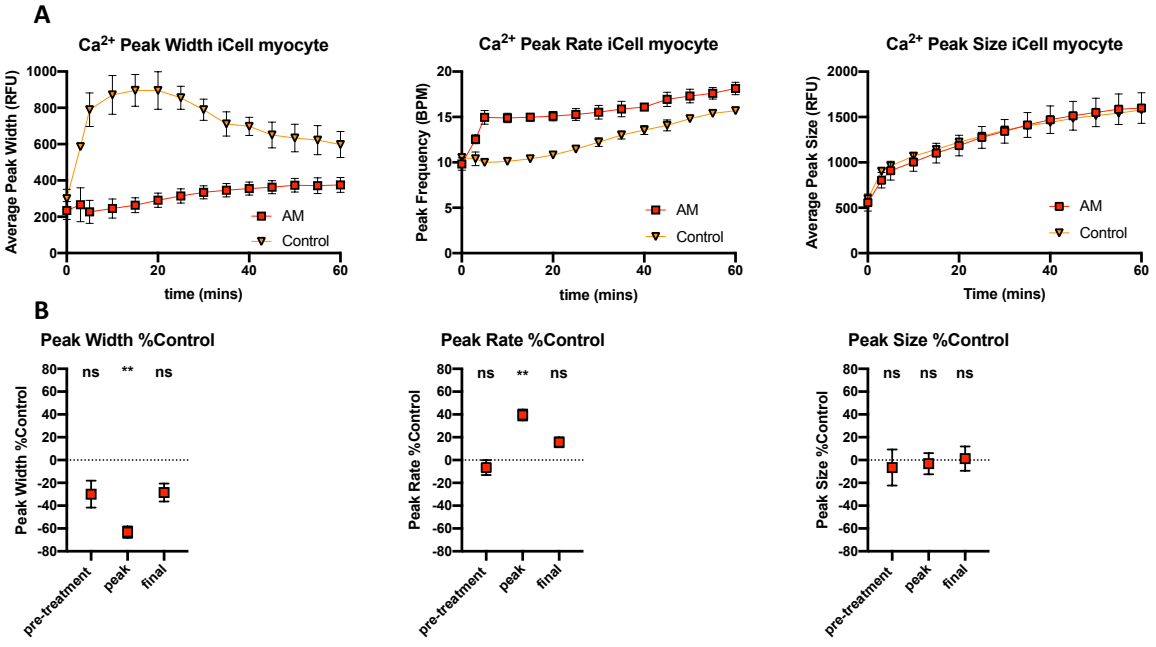

Figure 5.6. icell cardiac myocytes intrinsic calcium beat width, rate, and size in response to AM treatment. Measurement of IPSC derived icell human cardiac myocyte calcium peak width, beat rate, and beat size, in response to AM (**A**) (10 μM) and control treatment. Percentage increase in calcium peak width, beat rate, and beat size, in response to AM (**B**) relative to control treatment at multiple time points. Statistical significance determined compared to control using an unpaired t test with Welch's correction (*, p<0.05; **, p<0.01). NS denotes no statistical significance observed. All values are calculated from 4 individual data sets.

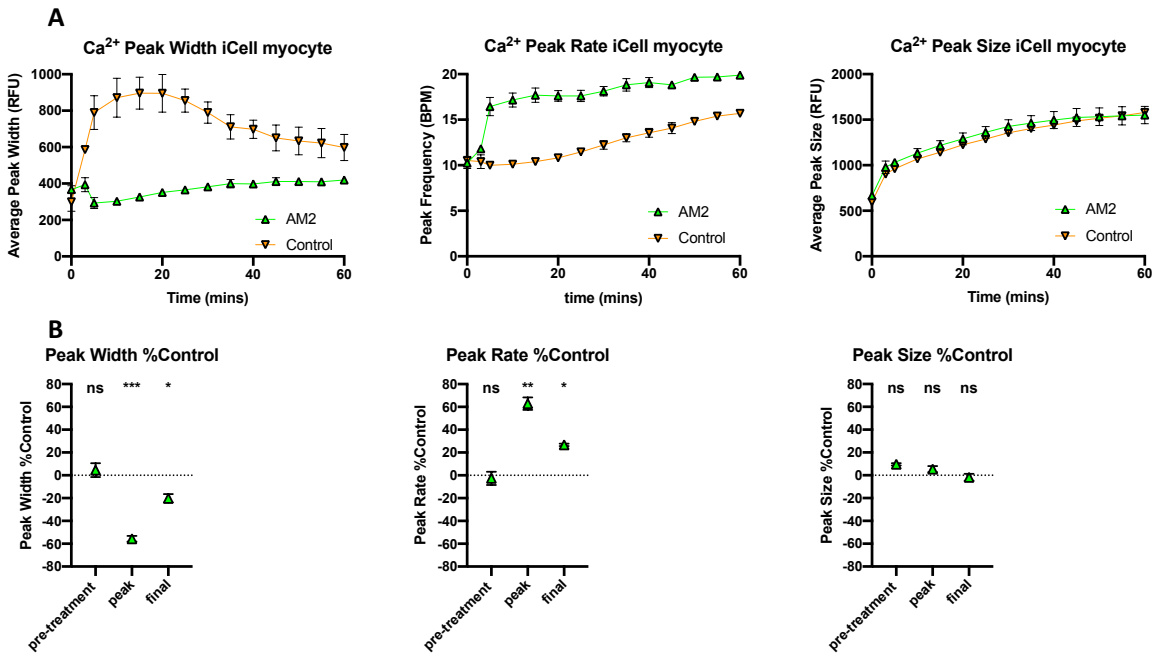

Figure 5.7. icell cardiac myocytes intrinsic calcium beat width, rate, and size in response to AM2 treatment. Measurement of IPSC derived icell human cardiac myocyte calcium peak width, beat rate, and beat size, in response to AM2 (**A)** (10 μM) and control treatment. Percentage increase in calcium peak width, beat rate, and beat size, in response to AM2 (**B**) relative to control treatment at multiple time points. Statistical significance determined compared to control using an unpaired t test with Welch's correction (*, $p<0.05$; **, $p<0.01$; ***, $p<0.001$). NS denotes no statistical significance observed. All values are calculated from 4 individual data sets.

CLR receptor expression, signalling, and function 2D beating cell model

The next aim was to look at the calcium flux and whole cell beat rate effects of CGRP, AM and AM2 in more detail by constructing whole dose-response curves in a number of assays. This was achieved in the whole cell beat rate assay and in the intracellular peak frequency assay. Beyond this profiled here is the cAMP accumulation produced by the three ligands and the CTR receptor family and RAMP family gene expression. This gene expression study demonstrated that of the receptors iCell myocytes expressed only the CLR, however expressed both RAMP1 and RAMP2, although RAMP1 expression was almost three times higher (**Figure 5.8A**). Following this the cAMP accumulation assays were performed and the peptide response varied: In all experiments AM and AM2 did not produce a dose dependant response. CGRP did on the other hand, although the response was small relative to the positive control (**Figure 5.8C**). Then following on from the above experiments in this chapter a full dose response curve was produced for the calcium peak frequency increases produced by the peptides (**Figure 5.8B**). Here it was interesting to observe that AM2 produced the highest maximal response (As seen in **Figure 5.7A** above) but the full dose response revealed that CGRP was more potent at lower concentrations. Moving onto the dose-response curve produced for myocyte cell beating increases stimulated by CGRP, AM and AM2. AM2 as above (**Figure 5.8D**) produces the greatest increase, this follows through to potency at the lower concentrations and the rank order of potency observed was AM2>CGRP>AM.

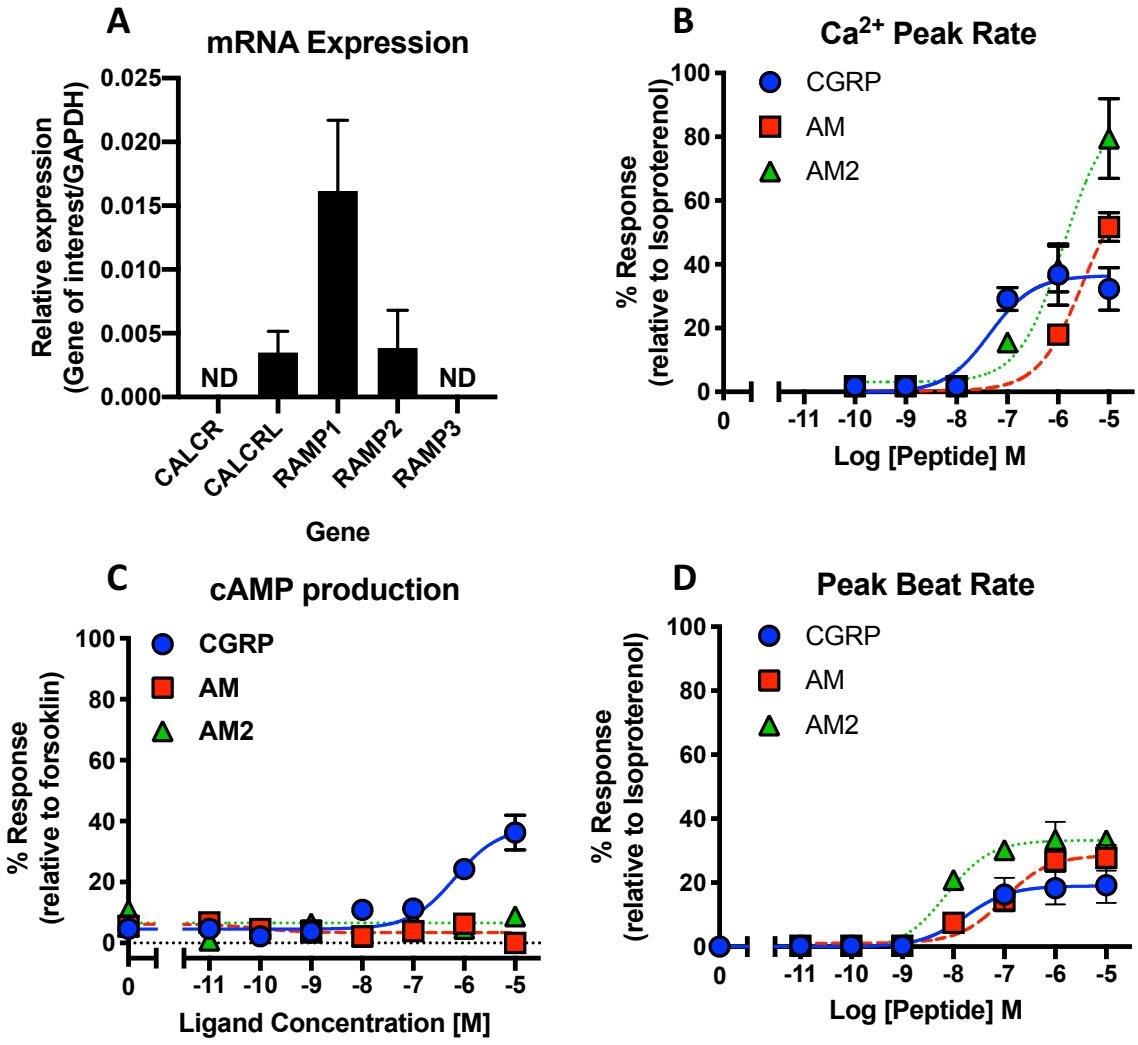

Figure 5.8. icell cardiac myocytes Gene expression and CGRP family peptide dose-response in cAMP accumulation, Ca^{2+} peak rate, and peak beat rate. Expression of CALCR, CALCRL, RAMP1, RAMP2, and RAMP3 genes in icell myocytes determined by qRT-PCR. Data represent mean + SEM of three independent experiments relative to GAPDH expression. ND = not detected in all three samples (**A**). Dose-response curves were constructed for myocytes stimulated with CGRP, AM or AM2 and the cAMP levels quantified relative to forskolin (100 μM) (**B**), peak calcium rate produced relative to isoproterenol (100 nM) (**C**), and the peak whole cell beat rate produced relative to isoproterenol (100 nM) (**D**). All data represent mean + SEM of at least three independent experiments. Data are analysed using a three-parameter non-linear regression curve.

Establishing beta-adrenoreceptor agonist influence on cardiac function in a 3D beating spheroid model

Next an assay for the study of 3D cardiac spheroid beating was utilised to explore whether the effects profiled above were also observable in a more physiological 3D model. These spheroids contained the iCell myocytes profiled above as well as human cardiac fibroblasts; enabling the study of ligand stimulation on individual cardiac spheroids in suspension. As with the 2D iCell monolayer assay above it was important to first confirm that ligand stimulated effects could be recorded in the system and isoproterenol was used to do so (**Figure 5.9**). Experiments with isoproterenol demonstrated a clear increase in spheroid beat rate upon ligand stimulation compared to control from immediately after drug addition (zero time-point). This was strongly evident in the statistical analysis of the peak response and final response showing a potent and sustained response to isoproterenol in terms of beat frequency in this assay (**Figure 5.9B**).

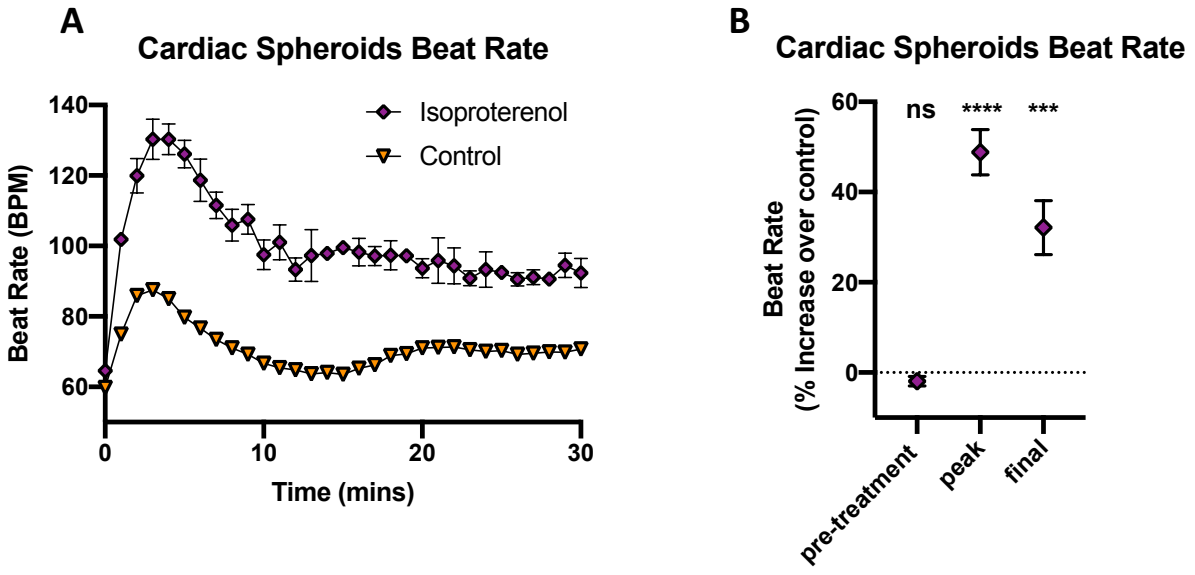

Figure 5.9. Beat rate of icell cardiac myocytes grown in 3D spheroids in response to isoproterenol and control treatment. Measurement of IPSC derived icell human cardiac myocyte spheroid beat rates in response to isoproterenol (100 nM) and control treatment (**A**). Percentage increase in beat rate in response to Isoproterenol and relative to control treatment at multiple time points (**B**). Statistical significance determined compared to control using an unpaired t test with Welch's correction (***; $p<0.001$ ****, $p<0.0001$). NS denotes no statistical significance observed. All values are calculated from 4 individual data sets.

Exploring CGRP family peptide influence on cardiac function in a 3D beating cell model

Up to this point observations of the effects of CGRP, AM and AM2 on iCell beat rates in a 2D system, the 3D system involves a 3D co-culture system using human cardiac fibroblasts (Receptor expression and signalling responses to CGRP family peptides in (**Supplemental Figure 8.6**). This enables an even more physiologically relevant study of peptide effects on cardiac function. Having confirmed that positive effects could be observed on the intrinsic beat rate of the spheroids by isoproterenol then CGRP, AM and AM2 were tested in the spheroid model: In (**Figure 5.10A**) all three ligands cause the beat rate to rise above level reached in the control cell assays and then maintain a higher beat rate for the duration of the assays. The increase is to a lesser extent than the positive control isoproterenol. Interestingly, when plotting peak and final beat rates as percentage increase over baseline this shows the peptides produced their greatest effects at different times compared to each other and that each produces a significant increase at some point over control. The peak responses follow the same trend as that observed in the 2D model system: AM2>AM>CGRP with CGRP producing a response that is not significantly greater than control responses (**Figure 5.10B**). Again, at the final time point in the assay the order of magnitude is reversed: CGRP>AM>AM2 although due the variability of the AM responses the AM2 response is more statistically significant. It was also possible to record the beat rate 24 h post-stimulation. This revealed that CGRP and AM2 sustained the increase in beat rate over control (**Figure 5.10D-F**). While AM showed a very slight increase above the control at 24 h it was not statistically significant. Again, there were also experiments to profile the effects on the amplitude of cell beating, however the peptides showed no difference over control in these assays (**Supplemental Figure 8.5**).

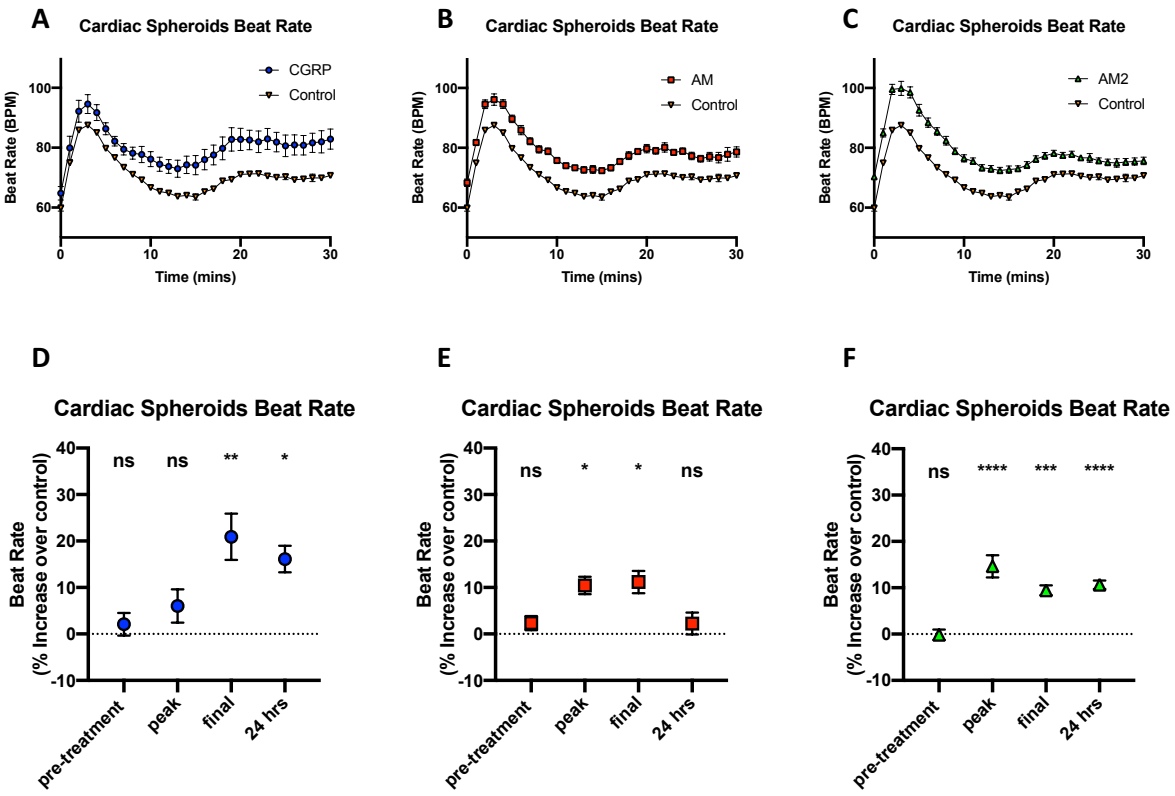

Figure 5.10. Beat rate of icell cardiac myocytes grown in 3D spheroids in response to CGRP family peptide treatment. Measurement of IPSC derived icell human cardiac myocyte spheroid beat rates in response to CGRP (**A**), AM (**B**), and AM2 (**C**) (10 μM) and Control treatment. Percentage increase in beat rate in response to CGRP (**D**), AM (**E**), and AM2 (**F**) and relative to control treatment at multiple time points (**B**). Statistical significance determined compared to control using an unpaired t test with Welch's correction (*, p<0.05; **, p<0.01; ***, p<0.001 ****, p<0.0001). NS denotes no statistical significance observed. All values are calculated from 4 individual data sets.

Establishing protocols for selection of transformed HUVECs

In order to perform CRISPR in HUVECs a kill curve needs to be generated for the antibiotics that will be used as selection markers in the generation of CRISPR cells. Therefore, cells were dosed with a range of concentrations of antibiotic to determine a reasonable minimum concentration needed to cause complete cell death. The aim of this study was to investigate the levels of cell death caused by a range of antibiotic concentrations. A 10-point compound response was chosen and nuclei staining (Hoechst) identified cell population. The initial antibiotic concentrations used were too high (2.5 μg/ml to 30 μg/ml), all of which killing cells completely in the case of puromycin, and almost completely with blasticidin, without producing the gradient of cell death that was hoped for (**Figure 5.11A,B**). Although the blasticidin results showed promise with there seeming to be some cell survival at the lowest concentration used (2.5 μg/ml) (**Figure 5.11B**). Next using a lower range from 0.25 μg/ml to 5 μg/ml. This still caused complete cell death at all concentrations in the case of puromycin (**Figure 5.11C**). However, blasticidin over this range produced a good gradient of cell death (**Figure 5.11D**) showing a dose response ranging from minimal reduction in cell number at the lowest concentration to complete cell death at the highest. Therefore, an even lower range of concentrations was tested (0.025 μg/ml to 0.5 μg/ml) for puromycin only (**Figure 5.11E**). This then produced the desired gradient of cell death: 0.025 μg/ml caused very little death, whereas 0.5 μg/ml (as shown in **Figure 5.11C**) again caused complete cell death. Together these data suggest that the minimum concentration needed for puromycin to cause complete cell death is 0.5 μg/ml (**Figure 5.11E**) and for blasticidin this concentration is 4 μg/ml (**Figure 5.11D**). Therefore, moving forward, 1 μg/ml puromycin and 5 μg/ml blasticidin was used to select for antibiotic resistance in HUVECs.

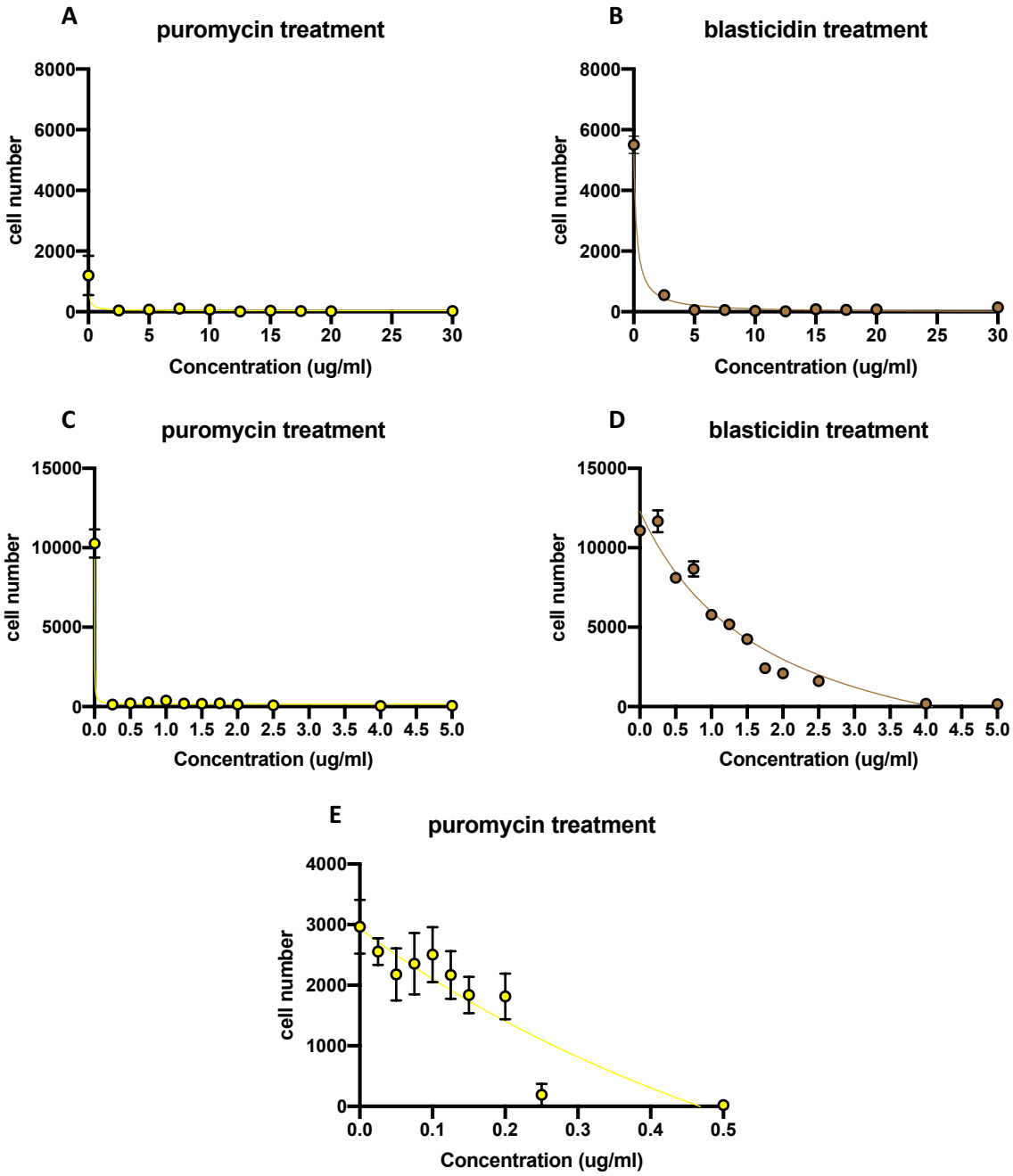

Figure 5.11. Kill curve generation in HUVECs with puromycin and blasticidin. Cells are plated 24 h before being treated with either puromycin or blasticidin with media/antibiotic changed every 2 days. A range of 10 concentrations were used: 2.5 μg/ml to 30 μg/ml (**A-B**) 0.25 μg/ml to 5 μg/ml (**C-D**) 0.025 μg/ml to 0.5 μg/ml (**E**). Cells were then imaged and counted before dose-response curves were constructed for each antibiotic and concentration range. All data represent mean + SEM of three independent experiments. Data are analysed using a three-parameter non-linear inhibitor vs response regression curve.

CRISPR-cas9 control vector transduction in HUVECs

The experiments shown in (**Figure 5.12A**) were performed to provide a control cell pool, that had been through the CRIPSR and antibiotic selection process using the same viral vector but that did not target the gene of interest (RAMP2). The supplier provided a vector targeted to the unrelated Hypoxanthine-guanine phosphoribosyltransferase (HPRT) housekeeping gene (**Figure 5.12A**). HUVECs were transduced at a range of viral MOIs from 0 (Mock transduction) to a multiplicity of infection (MOI) of 10. Cell were selected with antibiotic for the time needed to observe complete cell death in mock transduction wells. Cell survival was then assessed through a cell count of a random field of view during confocal imaging (**Figure 5.12B**). Cells were then stained for cas9 protein expression (**Figure 5.12C**) and GFP expression (**Figure 5.12D**), this was quantified and the sum plotted for all MOIs. As expression is coded for both on the viral expression vector. From the cell survival data it can be seen that higher levels of viral transduction leads to greater cell survival. Transducing 5 or 10 viral particles per cell lead to the highest number of cells remaining after antibiotic selection. Interestingly there is considerable cell survival at levels of transduction that are less than one viral particle per HUVEC plated. Although it is noticeable that total levels of fluorescence from antibody staining for cas9 and intrinsic fluorescence from GFP, both coded for by the viral vector is highest at viral transduction ratios of equal or greater than the number of cells plated. Particularly in the case of GFP (**Figure 5.12D**). These data demonstrate clearly that the virus has successfully integrated into the HUVEC genome, and can do so in concentration dependent manner, using three different methods of confirmation. The first was cell survival, whereby the virus clearly conferred antibiotic resistance, secondly it enabled cellular translation of the cas9 protein, and thirdly translation of GFP, both of which again in a viral concentration dependent manner. Demonstrating that this viral vector was capable of successful uptake in HUVEVCs enabled the research to move on to attempting to use this to method to knockout the RAMP2 gene.

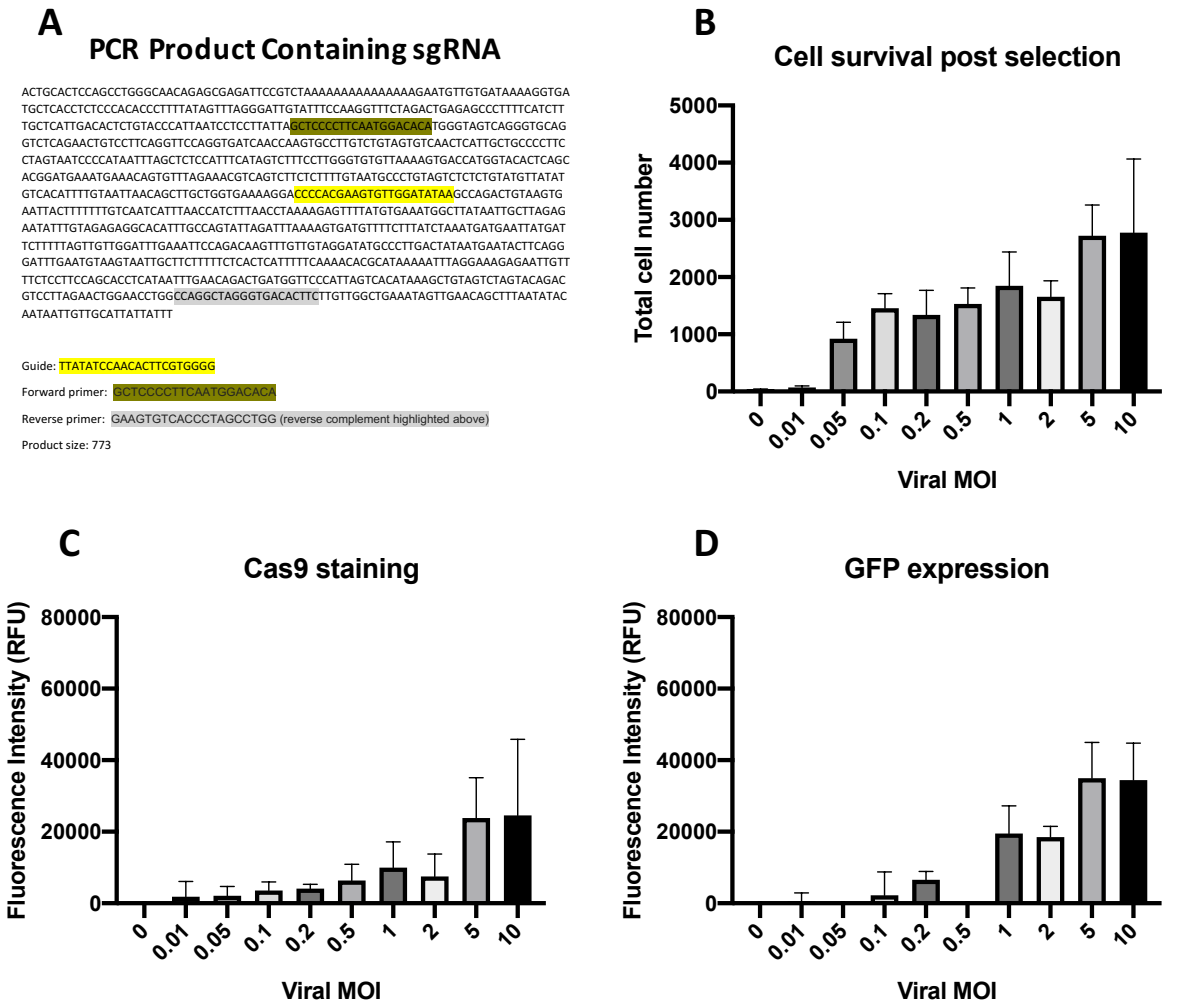

Figure 5.12. Assessment of viral control guide integration. Section of genome targeted by sgRNA and region amplified by primers targeted to the HPRT gene (**A**). After antibiotic selection cells were stained with nuclear marker, quantified and plotted over range of viral MOIs (**B**). After antibiotic selection cells were stained with an antibody for cas9 protein, fluorescent antibody staining was then quantified and plotted over range of viral MOIs (**C**). After antibiotic selection cells were imaged for GFP fluorescence, fluorescence was then quantified and plotted over range of viral MOIs (**D**). All data represents mean + S.E.M. of 3 individual data sets.

CRISPR-cas9 knock-out of RAMP2 gene in HUVECs

The task now was to transduce HUVECs with the same viral vector except each containing one of three different sgRNAs targeted to exon 1 of the RAMP2 gene generated by Sigma (**Figure 5.13A**). These were pooled and transduced into HUVECs at a range of MOIs to again ascertain whether (as in the control) the virus could confer antibiotic resistance and lead to synthesis of cas9 and GFP. Unsurprisingly this was the case, the virus caused concentration dependent antibiotic resistance (**Figure 5.13B**), cas9 production (**Figure 5.13C**) and GFP production (**Figure 5.13D**). Then a sample of the cells was taken that had been transduced and selected for successful integration with an MOI of 1 and using the primers outlined in (**Figure 5.13A**) amplified the guide targeting region of the RAMP2 gene. This was alongside isolating and amplifying the same region from control transduced cells, The resultant DNA was sent to Eurofins for Sanger sequencing, and Tide analysis revealed a knockout efficiency of 39%. This was not sufficient to take the cells forward for further experiments. Therefore the same experiments were performed and DNA amplification transducing the HUVECs with the highest MOI that had been previously optimised for, which was an MOI of 10. Subsequent DNA extraction and Sequencing revealed a knockout efficiency of 97.5%. Further confocal images were also captured to demonstrate the extent of antibiotic resistance conferred by MOI 10 (**Figure 5.14A-C**) (or not without viral transduction) and the extend of cas9 and GFP production (**Figure 5.14D-F**). Interestingly the localisation of these proteins can be seen; with cas9 predominantly nuclear, reassuring as nuclear localisation is required for its function, and GFP seems predominantly cytoplasmic. Further to this the extent of genomic disruption is observable in the chromatograms of the sequencing (provided by Eurogentecs) of the control cells RAMP2 gene (**Figure 5.15A**) vs the MOI10 transduced cells section of sequenced section of the RAMP2 gene (**Figure 5.15B**). The great extent of disruption observed is consistent with expectations for a pool of gene knockout cells treated

with multiple different sgRNAs at many times the ratio of virus to cells causing multiple separate cutting events and DNA damage repair events (**Figure 5.15B**).

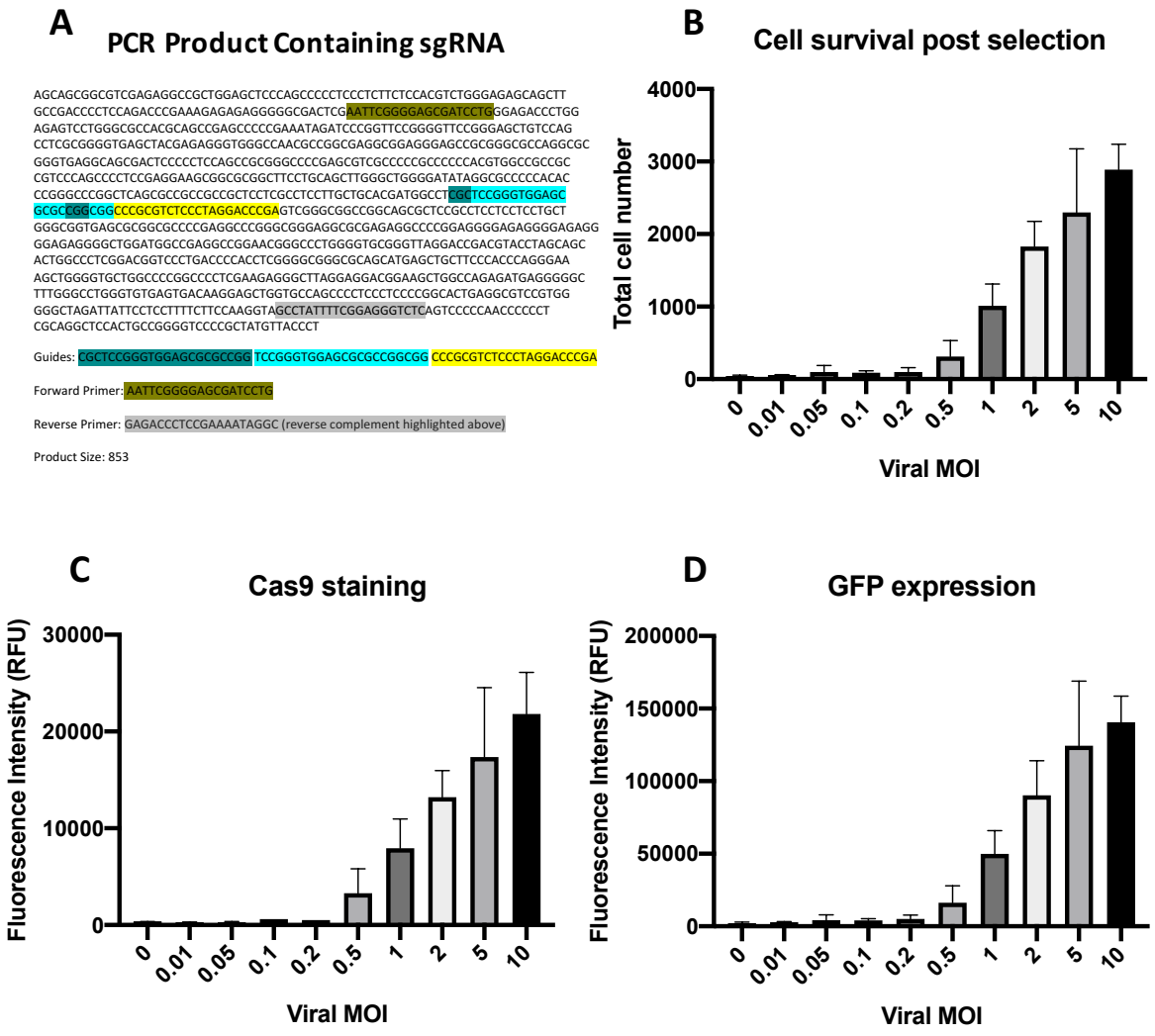

Figure 5.13. Assessment of RAMP2 targeting virus integration. Section of genome targeted by sgRNAs and region amplified by primers targeted to the RAMP2 gene (**A**). After antibiotic selection cells were stained with nuclear marker, quantified and plotted over range of viral MOIs (**B**). After antibiotic selection cells were stained with an antibody for cas9 protein, fluorescent antibody staining was then quantified and plotted over range of viral MOIs (**C**). After antibiotic selection cells were imaged for GFP fluorescence, fluorescence was then quantified and plotted over range of viral MOIs (**D**). All data represents mean + S.E.M. of 3 individual data sets.

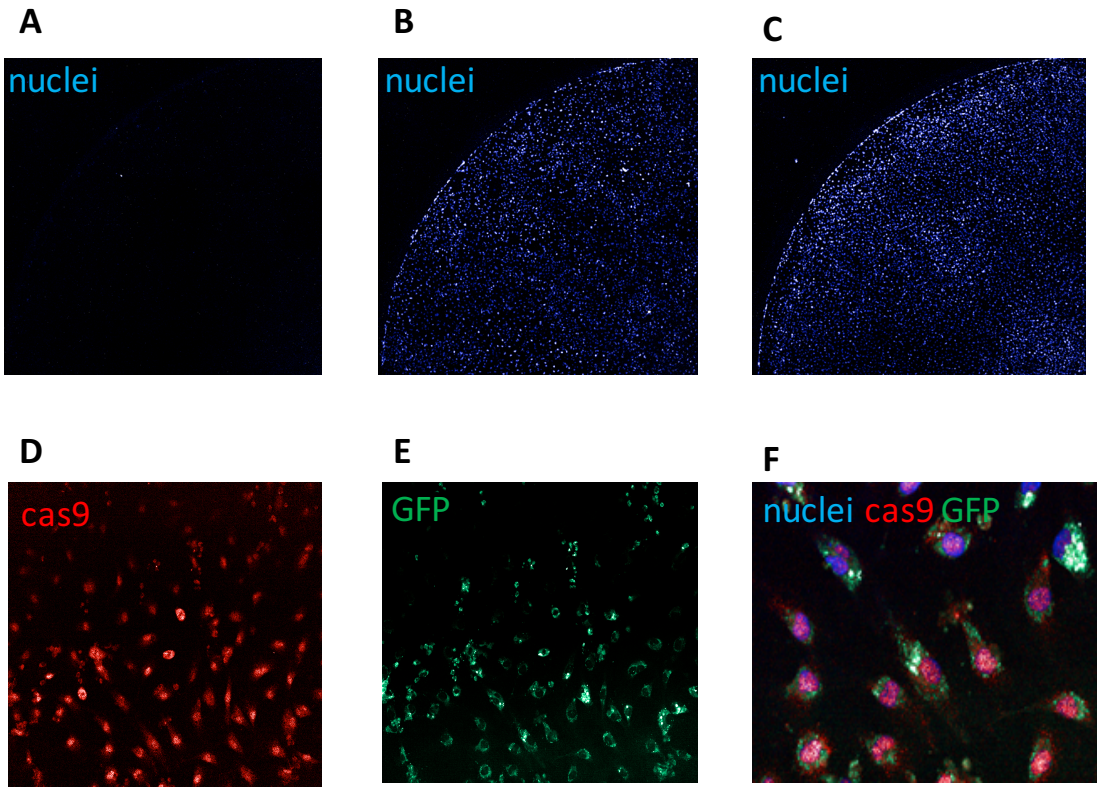

Figure 5.14. Confocal assessment of virus integration. Cell survival post-selection with mock transduction (MOI 0) + puromycin (**A**), Virus transduction (MOI 10) + puromycin (**B**), and mock transduction (MOI 0) no puromycin (**C**). Nuclei stained for with Hoechst imaged using 4x objective (**A-C**). Confocal images of cells treated with virus (MOI 10) and post selection showing cas9 alone (**D**), GFP alone (**E**) and nuclei staining with all three fluorescence channels overlaid and image manually zoomed for single cell clarity (**F**). Cells treated with cas9 protein antibody, and Hoechst nuclear stain imaged using 20x objective (**D-F**).

A

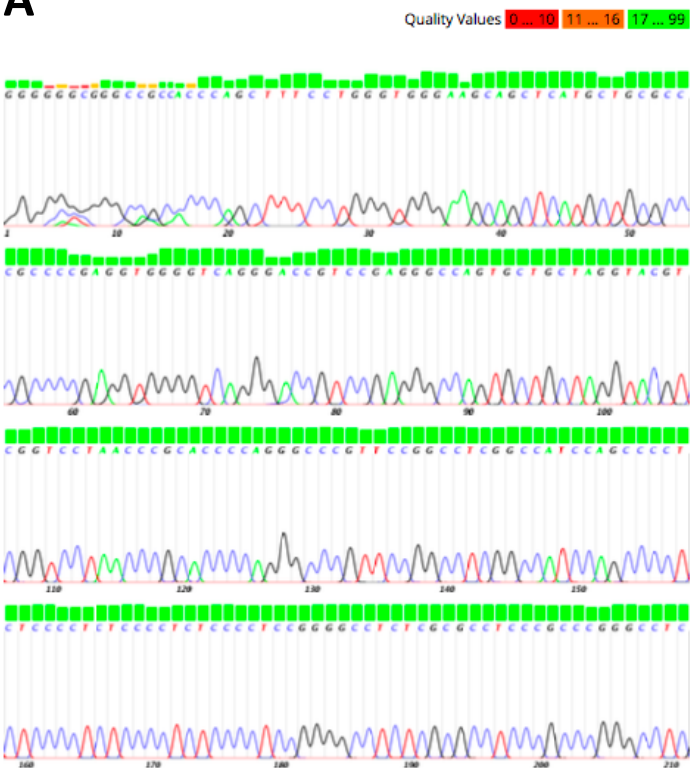

B

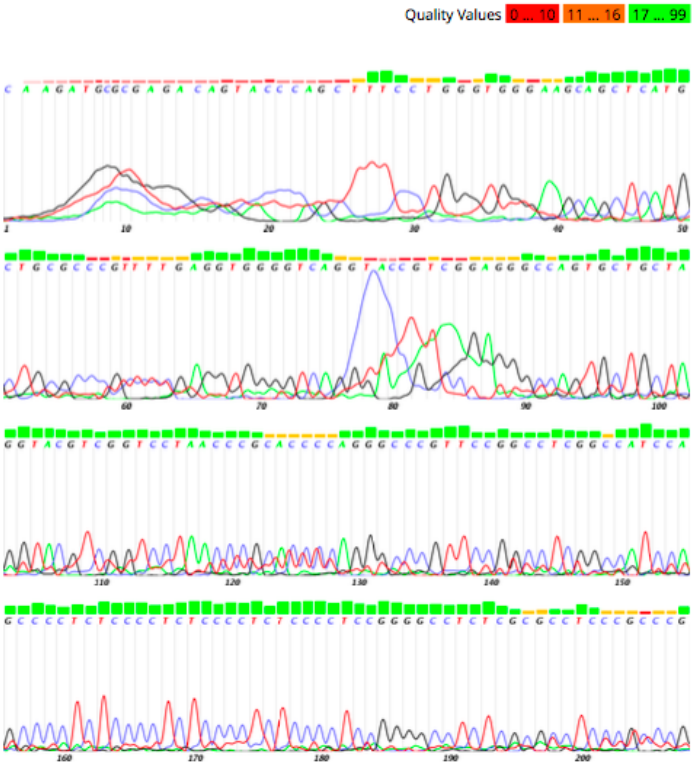

Figure 5.15. Sequencing results for Control HUVECs vs RAMP2 KO HUVECs. Genomic Sequencing results provided by Euorgentics for section of exon 1 of RAMP2 gene containing sgRNA target sites for Control HUVECs (**A**) vs same section in CRISPR-cas9 KO HUVECs (**B**) both sequenced using the RAMP2 primer: GCCTATTTTCGGAGGGTCTC.

Assessment of RAMP2 knock-out HUVECs through functional assays

These RAMP2 knockout HUVECs were then used to observe how the knockout influenced the transcription and then signalling function of RAMP2. Firstly, the qRT-PCR experiments performed on these cells, in these experiments RAMP2 mRNA no longer appeared above detection threshold (**Figure 5.16A**). This loss of RAMP2 transcript detection suggests degradation through nonsense-mediated mRNA decay (NMD). Importantly however the expression of CLR remained, suggesting, at the mRNA level at least, that CLR expression was unaffected by RAMP2 knockout (**Figure 5.16A**). It is also important to note that the gene editing did not have any impact upon the cells rate of proliferation (**Supplemental Figure 8.7**) or that the Gα subunit/β-arrestin profile also remained consistent with the wild type HUVECs (**Supplemental Figure 8.7**). The maximal intracellular signalling responses that the CGRP family of peptides could evoke in these RAMP2 knockout HUVECs vs the Control treated HUVECs were recorded. This was measured at each of the signalling pathways previously profiled in these HUVECs: $_{i}Ca^{2+}$ mobilisation (**Figure 5.16B**), $ERK_{1/2}$ phosphorylation (**Figure 5.16C**), cAMP accumulation (**Figure 5.16D**). As well as the more physiological responses: Nitric Oxide release (**Figure 5.16E**) and cell proliferation (**Figure 5.16F**). In all pathways responses were normalised to the positive controls which signalled as before, and in the case of the control cells; CGRP, AM and AM2 signalling responses mirrored all those outlined previously. However, in contrast in the RAMP2 knockouts all responses in all pathways measured were abolished (**Figure 5.16B-F**). Demonstrating, unsurprisingly given the overwhelming data from recombinant studies, that without a RAMP present CLR does not function (McLatchie et al. 1998), and this is indeed the case here in the HUVECs where RAMP2 has been knocked out.

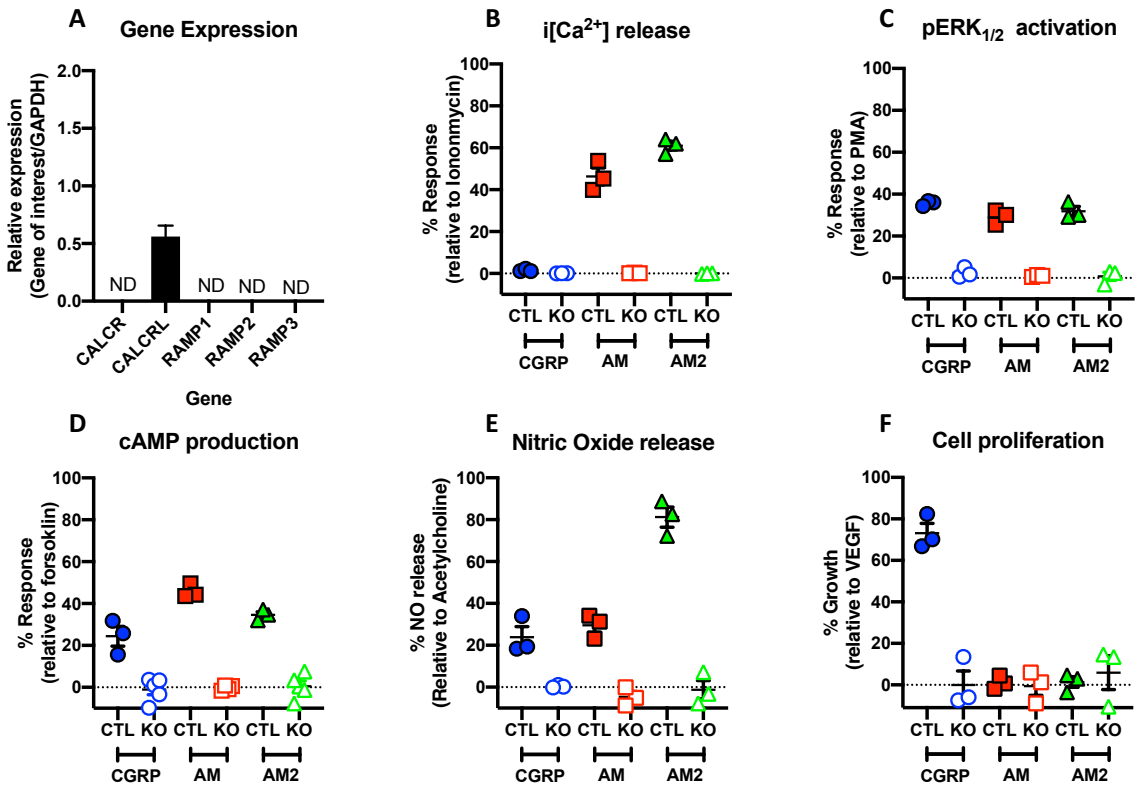

Figure 5.16. Receptor expression, cAMP accumulation, i[Ca^{2+}] mobilisation and $pERK_{1/2}$ activation pathways, nitric oxide release and cell proliferation physiological responses in control transduced HUVECs wild-type for RAMP2 expression (CTL) vs RAMP2 Knockout (KO) HUVECs. Expression of CALCR, CALCRL, RAMP1, RAMP2, and RAMP3 genes in. RAMP2 KO HUVECs (**A**). Data represent mean + SEM of three independent experiments relative to GAPDH expression. ND = not detected in all three samples. Characterisation of intracellular calcium mobilisation in CTL vs KO HUVECs relative to 10 μM ionomycin (**B**). Intracellular $ERK_{1/2}$ phosphorylation in CTL vs KO HUVECs relative to 10 μM PMA (**C**). Characterisation of cAMP accumulation in CTL vs KO HUVECs relative to 100 μM forskolin (**D**). Characterisation of total nitric oxide production in CTL vs KO HUVECs relative to 10 μM acetylcholine (**E**). Characterisation of cell proliferation in CTL vs KO HUVECs relative to 10 μM VEGF (**F**). All pathways measured in response to stimulation by CGRP, AM, and AM2. Data are analysed using a three-parameter non-linear regression curve. All data represent Emax + SEM of 3 to 5 independent experiments.

Characterisation of RAMP1 expressing HUVECs

In order to ascertain whether CLR function could be rescued in the RAMP knockout HUVECs, The aim was to re-express RAMP1 in these cells, and observe whether CGRP peptide signalling could be rescued. Then if so profile in detail the signalling patterns of the peptides and how they might differ with a different CLR-RAMP complex. Again using lentiviral transduction, this time containing a RAMP1 ORF and blasticidn selection, to overexpress RAMP1 in the RAMP2 knockout HUVECs (further details in Chapter 2). The presence of transcripts for RAMP1 post-selection was confirmed by qRT-PCR in the HUVECs (**Figure 5.17A**). The next step was to ascertain whether functional CLR-RAMP complexes were now formed in these cells. This was first assessed through cAMP accumulation as this pathway was once seen as the canonical CLR signalling pathway and most well understood. In these RAMP1-HUVECs CGRP, AM and AM2 are now able evoke a dose-dependent increase in cAMP accumulation. Strikingly for HUVECs, but as would be expected of the CLR-RAMP1 receptor complex (or 'CGRP receptor). CGRP was now the most potent ligand (**Figure 5.17B**), and by a significant margin (**Figure 5.17C**). It has an EC50 of 9.03±0.12 (**Table 5.1**). This is over a hundred times more potent than CGRP was in wt-HUVECs. AM is the next most potent ligand, followed by AM2, making the rank order of potencies: CGRP>AM>AM2. These rescue data not only confirm that RAMP2 knockout had no adverse side effects on CLR or other components of GPCR signalling but that by expressing a different RAMP1 you can dramatically alter the signalling pattern observed in terms of cAMP accumulation.

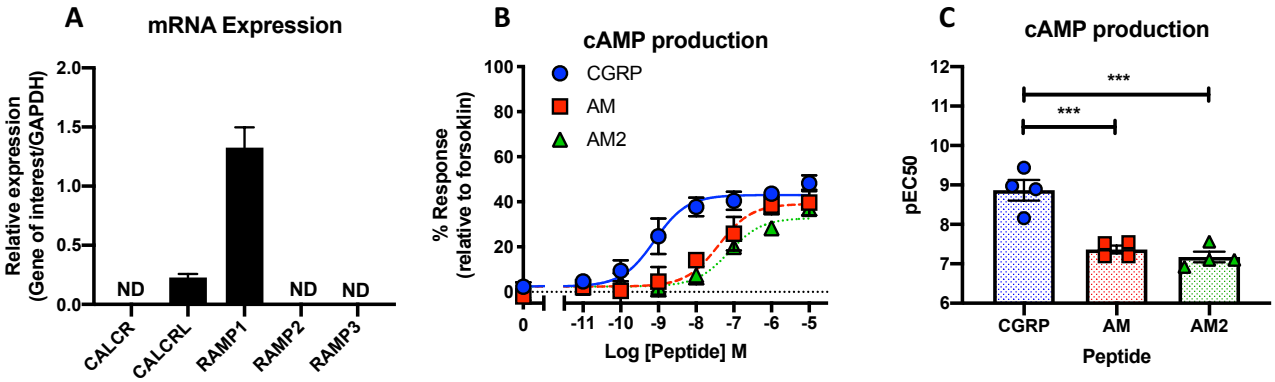

Figure 5.17. Receptor expression and cAMP accumulation in HUVECs transduced with a RAMP1 ORF, in response to the calcitonin peptide family and CGRP peptide family. Expression of CALCR, CALCRL, RAMP1, RAMP2, and RAMP3 genes determined by qRT-PCR (**A**). Data represent mean + SEM of three independent experiments relative to GAPDH expression. ND = not detected in all three samples. Characterisation of cAMP accumulation in response to stimulation by CGRP, AM, and AM2 in RAMP1-HUVECs relative to 100 μM forskolin (**B**). Data are analysed using a three-parameter non-linear regression curve. Individual pEC50 values + S.E.M. are the plotted for HUVECs **(C).** All values are calculated from 6 individual data sets. Statistical significance compared to the cognate ligand (CGRP) and determined using one-way ANOVA with Dunnett's post-hoc test, (*, $p<0.05$; **, $p<0.01$; ***, $p<0.001$; ****, $p<0.0001$).

Further characterisation of CGRP family peptide signalling in RAMP1-HUVECs

The next step was to explore whether the CGRP peptide family could signal through the other pathways explored thus far in this body of work, and how their signalling profiles now compare to each other. In the case of intracellular calcium signalling CGRP is again now the most potent peptide, followed by AM and AM2 (**Figure 5.18A**). This is in sharp contrast to the results seen in wt-HUVECs where CGRP barely evokes a response. Then for $pERK_{1/2}$ signalling AM is now the most potent ligand. Perhaps surprising for the CLR-RAMP1 receptor but in fact reflective of the work in chapter 3 (**Figure 3.18**) in another primary cell: the human cardiac myocytes which also expressed CLR-RAMP1 and there too the intriguing $ERK_{1/2}$ response was seen; where the non-cognate ligand displays a strong potency. Then in nitric oxide signalling all three ligands produce a response with a rank order of potency: CGRP>AM>AM2 (**Figure 5.18C**), this order is identical to that of intracellular calcium signalling mirroring a trend seen in wild type HUVECs and HUAECs. Lastly all three peptides also promoted cell proliferation (**Figure 5.18D**), a difference from all previous cell models, moreover the potencies were less distinct from one another – none were statistically different from CGRP (**Table 5.1**). However, AM was the most potent which reflected the HCM results and therefore this proliferation result is consistent with the CLR-RAMP1 receptor in another primary cell type (HCM). As the comparisons above suggest these results would benefit from further analysis of CGRP peptide family signalling at these CLR-RAMP complexes across the multiple primary cells studied in this body of work. Therefore, in the subsequent sections the overall bias plots for the peptides have been assessed in each model and how their signalling between the cell models correlate to enable side-by-side comparison.

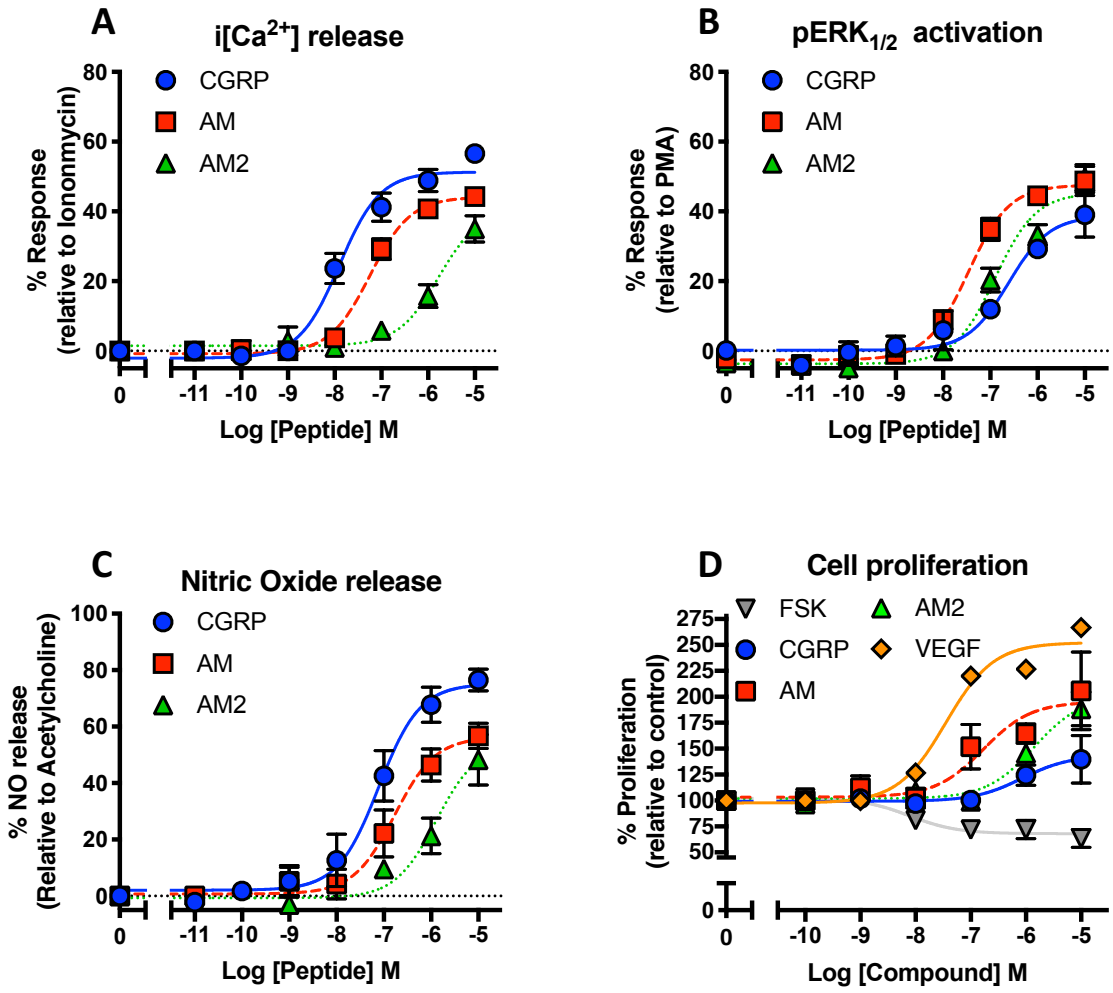

Figure 5.18. i[Ca^{2+}] mobilisation and $pERK_{1/2}$ activation signalling pathways, nitric oxide release and cell proliferation physiological responses in RAMP1-HUVECs. Characterisation of intracellular calcium mobilisation in RAMP1-HUVECs relative to 10 μM ionomycin (**A**). Intracellular $ERK_{1/2}$ phosphorylation in RAMP1-HUVECs relative to 10 μM PMA (**B**). Characterisation of total nitric oxide production in RAMP1-HUVECs relative to 10 μM acetylcholine (**C**). Characterisation of cell proliferation RAMP1-HUVECs relative to 10 μM VEGF (**D**). All pathways measured in response to stimulation by CGRP, AM, and AM2. Data are analysed using a three-parameter non-linear regression curve. All data represent Emax + SEM of 3 to 5 independent experiments.

		HUVEC RAMP1					
		CGRP		AM		AM2	
cAMP	pEC50	9.03	0.12	7.43****	0.17	7.16****	0.11
	Emax	43.20	1.29	38.95	2.08	32.66**	1.57
	pKa	8.87	0.11	7.20****	0.14	6.97****	0.16
	Logt	-0.15	0.02	-0.22	0.03	-0.344**	0.05
	n	4		4		4	
		CGRP		AM		AM2	
iCa	pEC50	7.90	0.12	7.24***	0.09	5.78****	0.10
	Emax	51.30	2.06	44.13*	1.42	40.46**	2.26
	pKa	7.52	0.09	6.97*	0.10	5.64****	0.18
	Logt	0.03	0.03	-0.10	0.03	-0.18**	0.06
	n	6		6		6	
		CGRP		AM		AM2	
pERK	pEC50	6.62	0.20	7.47*	0.08	6.90	0.14
	Emax	38.69	3.40	47.57	1.48	45.35	2.89
	pKa	6.52	0.17	7.16*	0.13	6.56	0.14
	Logt	-0.19	0.05	-0.02	0.04	-0.06	0.05
	n	3		3		3	
		CGRP		AM		AM2	
NO	pEC50	7.11	0.16	6.77	0.19	5.90**	0.23
	Emax	75.15	4.51	56.30	4.50	53.96	7.60
	pKa	6.54	0.18	6.43	0.21	5.51*	0.29
	Logt	0.47	0.09	0.11	0.08	0.08	0.14
	n	3		3		3	
		CGRP		AM		AM2	
Growth	pEC50	6.07	0.49	6.77	0.40	5.85	0.17
	Emax	143.61	12.20	195.27*	14.23	201.29*	11.45
	pKa	5.89	0.70	5.84	0.81	5.02	0.44
	Logt	-0.09	0.30	1.10	0.64	0.71	0.34
	n	4		4		4	

Table 5.1. pEC50, Emax, pKa, and log tau values for cAMP accumulation, i[Ca^{2+}] mobilisation and $ERK_{1/2}$ activation pathways, nitric oxide release and cell proliferation physiological responses in RAMP1-HUVECs. Data are analysed using a three-parameter non-linear regression curve, and are presented here as mean ± S.E.M. of n individual data sets. pEC50: negative logarithm of the agonist concentration required to produce a half-maximal response. Emax: maximal response to ligands expressed as a percentage of forskolin. pKa: negative logarithm of the equilibrium dissociation constant for each ligand generated using the operational model of agonism (Black and Leff 1983). Logτ: coupling efficiency parameter of the ligand (Black and Leff 1983). Statistical significance compared to the cognate ligand (CGRP) and determined using one-way ANOVA with Dunnett's post-hoc test, (*, p<0.05; **, p<0.01; ***, p<0.001; ****, p<0.0001).

Comparison of CGRP family peptide signalling bias across primary cells

Here are reported the bias plots generated in chapter 3 for each of CGRP, AM, and AM2 at each pathway in the different cell models here again for comparison alongside new plots for HUVEC-RAMP1s, as well as other bias new plots. These additional bias plots represent the $\Delta\Delta(\tau/K_A)$: this is achieved by normalising the date to a reference ligand and reference pathway. In this case all data were normalised to AM an as well as being normalised to cAMP. The reason for this additional level of normalisation to cAMP is so it is possible to visualise bias also relative to a reference pathway (**Figure 5.19**). Another addition is the generation of bias plots for HUVEC RAMP1s (**Figure 5.19D**). The bias plots for HUVEC-RAMP1s exemplify the remarkable effect that switching the RAMP has had on bias in these HUVECs (**Figure 5.19A vs D**), as the bias patterns now reflect the cells that endogenously express CLR-RAMP1 (HCMs) (**Figure 5.19C**). They are not identical with large differences between the ligand bias at NO, and smaller ones at $pERK_{1/2}$ and cell proliferation. However, the strongest displays of ligand bias such as CGRP at cAMP, and the strong bias of AM towards $pERK_{1/2}$ and cell proliferation are seen in both systems reflecting the integral role that the CLR-RAMP combination plays in directing signalling bias. The $\Delta\Delta(\tau/K_A)$ exemplify CGRP's bias towards proliferation in HUVECs and AM's bias characteristics in HCMs and HUVEC RAMP1, showing that AM has a strong bias towards all pathways except cAMP, which is representative of the very weak potency observed for AM at that pathway.

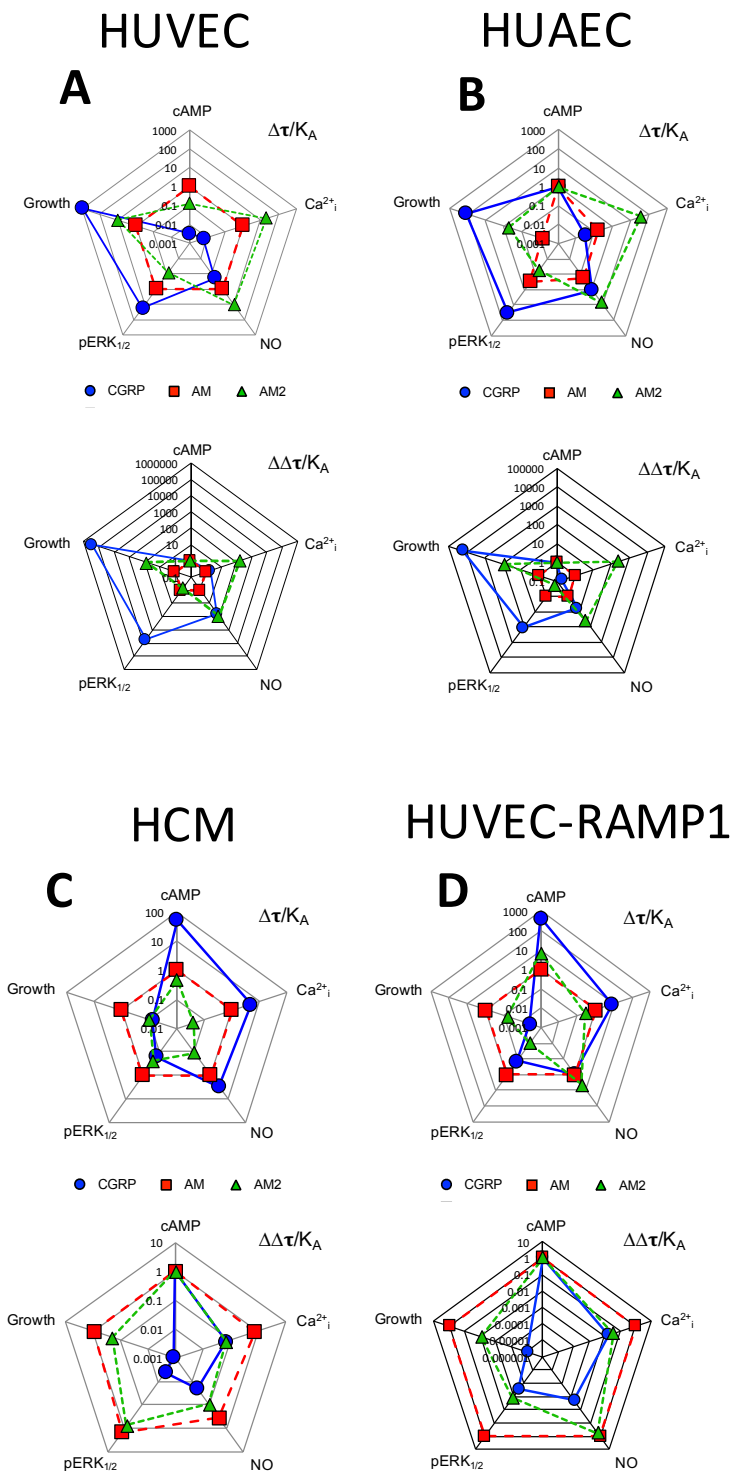

Figure 5.19. Signalling bias of the CGRP family of peptides in primary human cells. Signalling bias plots were calculated as $\Delta(\tau/K_A)$ or $\Delta\Delta(\tau/K_A)$ for HUVECS (**A**), HUAECs (**B**), HCMs (**C**), and HUVEC-RAMP1s (**D**). Values are on a logarithmic scale for each agonist and for each signalling pathway. Determination of values requires normalisation to a reference agonist (AM) alone in $\Delta(\tau/K_A)$, while for $\Delta\Delta(\tau/K_A)$ values were normalised to both a reference agonist (AM) and a reference pathway (cAMP).

Assessment of the correlation in CGRP family peptide signalling of primary cells expressing the same or different RAMPs

This work aims to analyse the correlation between the responses of the CGRP peptide family in different cell types To provide more direct comparisons between them the degree of correlation was determined for the potencies induced by all three peptide agonists at all five signalling pathways, and producing four separate cell type comparisons (**Figure 5.2A-D**). Firstly, analysis of the correlation between peptide agonist potency in RAMP1-HUVECs and HCMs for the five different signalling pathways revealed a positive correlation: ($r = 0.55$ (95% confidence interval, 0.051 to 0.82; $p < 0.05$)(**Figure 5.20A**) showing how closely aligned the signalling properties in RAMP1-HUVECs and HCMs are. In contrast, when performing the same analysis of the correlation between HUVECs and HCMs (**Figure 5.20B**), and then HUVECs and RAMP1-HUVECs there was no detectable correlation (**Figure 5.20C**). In both these comparisons one cell type expresses CLR-RAMP1 and the other CLR-RAMP2. Lastly for the two wild-type endothelial cells (HUVECs and HUAECs), where there was a strong similarity in the bias plots across the five different pathways. This was then further supported by a significant correlation in potency when comparing all ligands in all pathways ($r = 0.73$ – 95% confidence interval 0.35 – 0.90; $p < 0.01$)(**Figure 5.20D**).

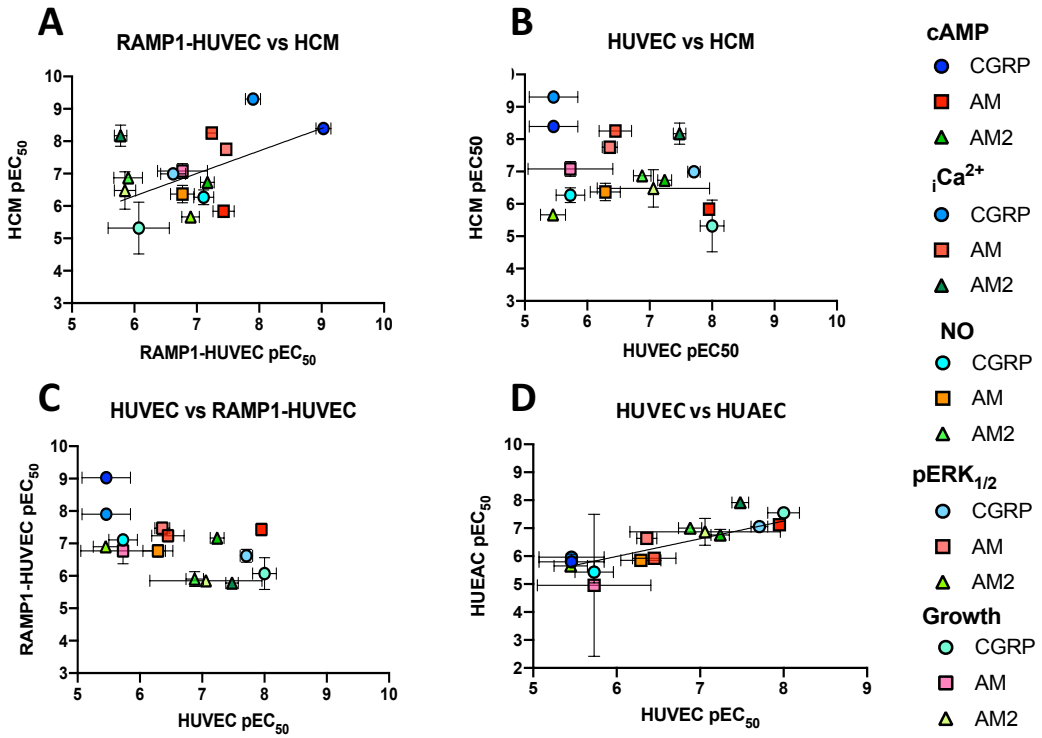

Figure 5.20. CGRP family peptide signalling bias in RAMP1 expressing HUVECs correlates with that in human cardiac myocytes. The correlation of log agonist potencies ± SEM for CGRP, AM, and AM2 stimulated cAMP accumulation, mobilisation of Ca^{2+}, NO production, intracellular $pERK_{1/2}$ and cell proliferation in RAMP1 expressing HUVECs and HCMs (**A**), HUVECs and HCMs (**B**), HUVECs and RAMP1 expressing HUVECs (**C**), and HUVECs and HUEACs (**D**) was analysed by a scatter plot and Pearson's correlation coefficients (*r*) were calculated. A significant positive correlation was observed for RAMP1-HUVECs vs HCMs (**A**), and HUVECs vs HUEACs (**D**). The presence of a line indicates a positive correlation.

Summary

This chapter started with research designed to further explore whether the CGRP family of peptides were capable of differentially influencing physiologically relevant, functional cellular outcomes. The was explored through assessing their impact on IPSC derived cardiac myocyte beat rates, in 2D and 3D models, and intracellular calcium fluxes. It was reported that all three peptides had a positive impact on myocyte beat rate, but there were subtle differences in their effects at different time points. Then it was reported that they could also increase the rate of intracellular calcium release, both these systems revealed an intriguing role for AM2, as the most potent stimulator of these effects. While there appeared to be the presence of two RAMPs, at least at the mRNA level in these stem cell derived myocytes, there appeared to be only one functional receptor exerting the beat rate effects seem upon agonist addition. This was determined through the use of the CLR-RAMP1 receptor antagonist Olcegepant. Then the effects of CGRP, AM and AM2 on myocyte beat rate in a 3D model were studied. The trends observed in the 2D system could be seen again in the 3D model with AM2 producing a strong increase in beat rate short term, and CGRP appearing to exert its effect in a more long term manner.

Next the aim was to use CRISPR-cas9 gene editing techniques to manipulate RAMP expression in HUVECs. First a control lentiviral construct was used to provide a proof of principle for the successful integration of lentivirus in HUVECs, and having shown this was possible through conferring antibiotic resistance and lentiviral vector contained protein expression (GFP and cas9). This viral vector, now containing sgRNAs specifically targeted to the RAMP2 gene was used to attempt to knockout RAMP2 expression. A pooled guide system was used, and found that a high ratio of virus:cell (MOI) was required to produce the desired level of gene knockout. Then using these cells it was confirmed that in the HUVECs CLR was unable to function without RAMP co-expression. Following this it was possible to rescue CLR function through the expression of RAMP1 in the knockout HUVECs. This rescued CLR

function in all pathways measured, and then enable CGRP, AM and AM2 to evoke subtly different signalling patterns in the RAMP1-HUVECs. To more directly compare these RAMP1-HUVECs with wt HUVECs, and the other CLR-RAMP1 expressing primary cell line that have been profiled here (HCM), as well as comparing the non-genetically altered primary cell types with each other bias and correlation plots were generated. These helped illuminate the similarities and differences seen in CGRP peptide family signalling between the different cell types, as well as reinforcing the importance of CLR-RAMP expression and how it dictates CGRP, AM and AM2 signalling.

Chapter 6. Discussion

CLR based Receptors in Primary Human cardiovascular cells

In order to best understand the signalling properties of CGRP, Adrenomedullin and Adrenomedullin 2 in primary cells an integral part of this was to discover which of the calcitonin family of GPCRs were expressed and which of the RAMP accessory proteins. The CLR was the object of this body of work and the receptor for the three ligands. However, as mentioned previously the CTR can form a high affinity receptor for CGRP through co-expression with RAMP1 (AMY_1R) (Walker et al. 2015). Therefore, it was crucial to confirm whether CTR was present in the primary cells of interest to ensure that the CGRP response observed was purely due to CLR-RAMP receptor complexes not a mixed population. Furthermore, it was also important to discern between the different CLR-RAMP complexes was present in each cell as each receptor-RAMP complex forms unique and distinct receptors with their own signalling properties (Hay et al. 2003). The first primary cells studied included HUVECs and VSMCs. Comparing purely their receptor expression at an mRNA level both expressed solely the CLR (no CTR), and the HUVECs expressed only one RAMP: RAMP2 however the SMCs expressed two RAMPs: RAMP1 and RAMP2. Having a potentially mixed pool of receptors can limit the insights that can be gained into the receptor itself, and produce difficulties in targeting one particular receptor (Walker et al. 2015) For this reason the choice was made to proceed with investigations in primary cells where only one CLR-RAMP complex was detectable at the mRNA level, firstly HUVECs, and then later HUAECs and HCMs. This enabled conclusions to be made about the signalling properties of a single endogenous receptor.

CGRP, AM and AM2 G_s signalling at the CLR in primary cells

In heterologous cell systems $G\alpha_s$ signalling at the CLR was the first signalling pathway discovered from the receptor and by far the most well studied, with the CGRP, AM and AM2 signalling patterns at each of the CLR-RAMP combinations well established in these systems (Weston et al. 2016, Hay et al. 2018), however what had not been established is how individual CLR receptor complexes signalled in primary cell human cell systems where there are endogenous expressed as opposed to over-expressed in their non-native environment. In HUVECs, the first cell line of interest the CLR-RAMP2 receptor was discovered in these cells. This does not mean to say a functional receptor is produced in these cells. Therefore, the endogenous peptide ligands for the CLR: CGRP, AM and AM2 were used to assess whether a functional response could be observed. They were capable of producing distinct dose dependent cAMP responses. As the CLR-RAMP2 is known as the AM receptor, and the relevance of other peptides acting at it endogenously is uncertain receptor specific inhibitors were used to provide further evidence that the receptor being studied was in fact the AM receptor. Reassuringly, all peptide responses were suppressed by an AM antagonist but the CGRP receptor antagonist had no effect on any of the responses. Moreover, calcitonin and amylin could not evoke a cAMP response in these cells giving two insights, the first more evidence that there is no calcitonin receptor in HUVECs, and the second that the endogenous CLR-RAMP2 does not respond at a detectable level to these two peptides. Returning to the cAMP responses produced by CGRP, AM and AM2. These represent a closer representation of the cAMP profile these peptides will be producing in these endothelial cells *in vivo*, than has been produced up until now. This makes the comparison of these responses with data from co-expression models interesting. The rank order of the peptides at the CLR-RAMP2 as an average of multiple studies is: AM(9.19)> AM2(7.91)>CGRP(7.16) (Hay et al. 2018). Then looking at the rank order of potencies for the endogenous CLR-RAMP2 AM (7.95)>AM2(7.24)>CGRP(5.46); immediately it is clear that in both cases it is a CLR/RAMP2 response, with AM the most potent and CGRP the least,

interestingly the differences arise in the potencies, all of the literature data shows much higher potencies, this could be a result of receptor over-expression and signalling, as well as the much greater signalling capacity of an immortalised cell such as a HEK-293, COS-7 or CHO-K1 cells compared to a primary HUVEC. There is also the possibility of background receptor expression; many immortalised cell lines express the calcitonin receptor (Eglen, Gilchrist, and Reisine 2008) and RAMPs that may not be screened for. Given the knowledge that the CTR, CLR and RAMP1 all form potent CGRP receptors (Walker et al. 2015) if there is any background expression in the cells used for co-expression studies it could explain the almost hundred fold greater potency of CGRP in these cells vs HUVECs: 7.16 vs 5.46.

Recruitment of G proteins and pathways beyond $G\alpha_s$ in primary cells

In the literature there is some suggestion that the CLR can couple to G proteins and pathways beyond $G\alpha_s$, with reports that G_i coupling can be seen in some cell types, and that G_q mediated calcium release is also possible (Weston et al. 2016) all in co-expression systems, but the question remains, does this coupling exist in physiologically relevant cell systems, and to what end? It has been demonstrated that G_i, G_q, and $pERK_{1/2}$ (discussed further later) signalling as well as Nitric Oxide (discussed below). PTX was used as a known specific inhibitor of G_i proteins to assess their involvement in cAMP accumulation, and intracellular calcium fluxes as an indirect measure of G_q protein coupling, but also in combination with a G_q specific inhibitor which was able to directly link calcium release to G_q protein activity. G_i coupling is the next G protein revealed here to directly couple to the CLR in primary HUVECs. The coupling upon stimulation by CGRP is particularly interesting – CGRP is weak promoter of cAMP accumulation at CLR-RAMP2 in HUVECs these could be attributed at first glance to a relative inability to recruit G_s. However, the PTX revelation that G_i inhibition can significantly increase CGRP mediated cAMP production shows that under natural conditions CGRP recruits G_i proteins and actively moves the receptor's signalling away from cAMP production and inhibits adenylyl cyclase. Moreover, the observation that PTX also inhibits the CGRP mediated ERK response suggests that the purpose of G_i recruitment is twofold: to suppress cAMP production and to promote $ERK_{1/2}$ phosphorylation this is also likely to be mediated separately by the G protein components; as $G\alpha$ subunit inhibits AC and the $G_{\beta\gamma}$ subunit has previously been implicated in G_i mediated ERK activation (Koch et al. 1994). There is no evidence from the data here that AM recruits G_i proteins to the CLR-RAMP2. This is perhaps unsurprising as it is the cognate ligand for the receptor and produces such a potent cAMP response. AM2 does seem to recruit G_i to a limited extent, both pathways show similar patterns to the CGRP mediated recruitment, but to a lesser extent. PTX based

studies in the human cardiac myocytes revealed more interesting differences between the CLR-RAMP2 and CLR-RAMP1 in that none of the peptides seemed able to recruite G_i proteins which is markedly different from the scenario just described at the CLR-RAMP2. It is interesting as the initial prediction may have been that there would be a parallel scenario where the non-cognate ligand, so AM, might recruit G_i proteins to some extent, but it did not, and neither did CGRP or AM highlighting the differences between RAMP1 and RAMP2 and their influences on G protein recruitment. Together these results from the PTX studies gives us a greater overall understanding of how the three peptides mediate their cAMP and $pERK_{1/2}$ signalling effects endogenously.

Another protein of importance in the CLR signalling field is Receptor Component Protein (RCP), It is thought to be important in the signalling of some CLR based receptors although no effects from knocking down this protein in the HUVEC system could be observed (**Supplemental Figure 8.8**). Although much controversy accompanies the discussion of RCP as it is also a component of human RNA polymerase III. Throwing into question the cause of effects seen from knockdown studies (Routledge et al. 2020).

Further exploration of this ERK signalling in HUVECs suggested that ERK phosphorylation is a signalling event that ultimately multiple pathways may converge on. This is a concept that has been explored previously (Belcheva and Coscia 2002). The contribution that G_i makes to CGRP mediated $pERK_{1/2}$ through CLR-RAMP2 in the primary setting has already been discussed here. When using inhibitors of other GPCR signalling components it was discovered that inhibition of EPAC1/2 supressed AM mediated $pERK_{1/2}$ slightly, but significantly, suggesting that EPAC partly contributes to AM's ERK response, but not to CGRP or AM2's. This may make sense due to AM's bias towards, and reliance upon, cAMP production relative to the other peptides, to mediate its signalling. Interestingly however PKA, which is also downstream of cAMP did not contribute to ERK phosphorylation, stating the importance of signalling divergence further downstream from the second messenger. PKA also does

not contribute to any of the other peptides ERK response, neither does the G_q pathway to any of the ERK responses ruling out that G protein pathway as a contributor.

Importantly the revelation that AM2 is the most potent ligand at eliciting calcium release at the AM receptor demonstrates a previously unknown signalling role for AM2 at this receptor. If this is then considered alongside the CGRP bias towards, and potency at $pERK_{1/2}$ this begins to suggest that the nomenclature referring to CLR-RAMP2 as the AM receptor is over-simplified and based entirely on G_s receptor coupling. Whereas this work beings to show that CLR-RAMP2 has many more signalling properties beyond AM stimulated cAMP production (**Figure 6.1**).

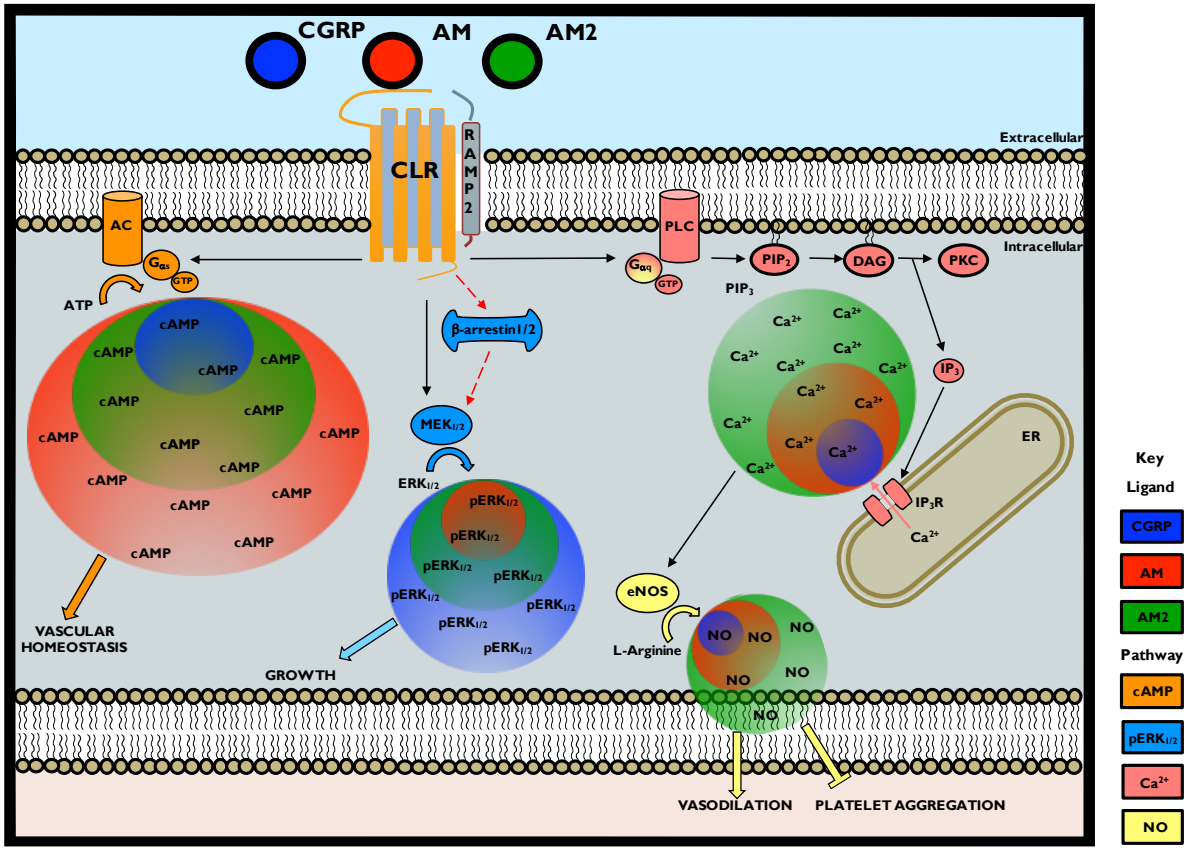

Figure 6.1. Representation of the signalling outcomes downstream of CLR-RAMP2 stimulated by CGRP, Adrenomedullin or Adrenomedullin 2 in a HUVEC. Including G proteins known to couple to CLR-RAMP2 and their signalling pathways as a result of peptide mediated receptor activation. Solid arrows indicate known pathways. Dashed arrows represent possible pathways.

Physiological Outcomes and Relevance of signalling through CLR in primary human cells

The two pathways investigated here to attempt to undercover whether CGRP, AM, and AM2 have a more physiological roles in the cells in question, as well as whether signalling bias plays a part in dictating these roles are: NO and proliferation. NO is a direct mediator of vasodilation and an important regulator of vascular homeostasis and observing cell proliferation is a direct measure of growth and the overall effects of these peptide hormones on cellular physiology. It has been well studied in reports of the systemic actions of CGRP, AM and AM2 that they all have vasodilatory roles, all though how they compare to each other, the mechanisms and involvement of bias all remain to be established. Equally NO is a molecule released by endothelial cells in order to promote and regulate vasodilation through direct actions of vascular smooth muscles cells or myocytes: acting predominantly in a paracrine manner, it diffuses into cardiac myocytes and VSMCs where it stimulates cGMP production, which itself activates PKG and in VSMCs. This kinase reduces vascular tone, VSMC proliferation, and therefore dilates blood vessels. PKG-Iα (the isoform present in VSMCs and myocytes) dilates vessels by reducing intracellular calcium concentrations reducing myosin light chain kinase activity. It can do this by inhibiting voltage operated calcium channels and increasing calcium reuptake by SERCA into the SR in VSMCs (Farah, Michel, and Balligand 2018). Therefore, there was a desire to see whether CGRP, AM and AM2 could promote NO release in human endothelial cells. They were all cable of doing so, and at levels statistically distinct from one another demonstrating they through NO they could mediate vasodilation to differing extents. Moreover, the rank orders of potency, with the interesting potency of AM2 in particular was reminiscent of the calcium mobilisation results achieved previously, therefore it was tested whether G_q signalling was linked to NO release. The use of YM-254890 confirmed that G_q coupling and signalling was responsible for NO production from all three peptide ligands. While there is no direct link in this study between calcium and NO much

work has shown that calcium can promote NOS activity, primarily eNOS in endothelial cells (Farah, Michel, and Balligand 2018), and as both molecules are produced downstream of G_q it seems reasonable to suggest that NO production through the CLR-RAMP2 and these peptides is also mediated by intracellular calcium signalling.

The next physiological pathway studied was cell proliferation. This was measured after 72 h and was relative to control treated cells therefore it could be observed whether compounds promoted or inhibited cell proliferation. Indeed, of the controls tested: VEGF and Forskolin, the first promoted growth and the second inhibited it, intriguingly AM and AM2 did not promote or inhibit growth, having no particularly discernible effect, but CGRP on the other hand produced a potent increase. Speculating on why these results might be the case it is clear AM produces a potent cAMP response, as does AM2, although not to the same extent as the positive control for cAMP: Forskolin, but if cAMP inhibits growth then ligands which produce primarily this second messenger may be less likely to have a role in promoting growth. Equally they both produce relatively weak $pERK_{1/2}$ responses. $pERK_{1/2}$ is a known promotor of cellular proliferation (Chang and Karin 2001, Pagès et al. 1993, Lefloch et al. 2009) and as was revealed above, CGRP has a novel role in promoting a potent $pERK_{1/2}$ response at the CLR-RAMP2 in endothelial cells this could go some way to explaining a possible mechanism for CGRP's promotion of growth. Nevertheless, it is clear from these results that CGRP could have an important role on the physiology of these endothelial cells that is unique from the other peptide agonists. As stated previously the G_s coupling to the CLR and any of the RAMPs has been well studied - the physiological importance of this signalling pathway has also been looked at in some detail in endothelial cells, with a report showing that AM is important for endothelial barrier stabilisation and protect against infection (S. aureus α-toxin) mediated loss of VE-cadherin, it also blocked toxin related junctional protein disappearance. It was also shown that and therefore cAMP forskolin induced protection against thrombin or α-toxin induced loss of VE-cadherin disassembly of endothelial barriers (Hocke et

al. 2006). Now this work begins to shed light on the signalling roles of the other peptides beyond AM in endothelial cells.

CLR signalling in other primary cell models

A question arising from the study of CGRP family peptide signalling at the CLR-RAMP2 in HUVECs is how much of the responses can be attributed to the receptor and how much to the cell background. In order to address this, another primary cell expressing CLR-RAMP2 was discovered and had its signalling profiled in this system. These were the HUAECs, and the trends in each pathway showed strong similarities to the HUVEC system. Taking cAMP as an example the rank order of potencies was AM>AM2>CGRP in both cases and the rank order of potencies was the same in other pathways such as $pERK_{1/2}$ and intracellular calcium release. There were however some differences, such as in the overall magnitude of response – In most cases the Emax values were lower in HUAECs. In the previous chapter when bias plots and correlation plots were compared, the data there confirmed the similarity between the two systems. Suggesting that the intrinsic coupling abilities of CGRP, AM and AM2 when bound to CLR-RAMP2 govern the second messenger outcomes observed. However, there is the caveat that both these cells are endothelial cells, therefore in order to remove background as a variable later CRISPR-cas9 is used to switch RAMPs in HUVECs to most directly see how the RAMP effects signalling outcomes. Another way to explore the effect of having a different RAMP in a primary cell system was to find a cell that expressed a RAMP other than RAMP2 and Human cardiac myocytes proved to be that cell type.

The first important step in using a new cell system was to establish the receptors and RAMPs present. The mRNA analysis indicated that the CLR and RAMP1 were expressed in these HCMs, and that there was no CTR, RAMP2 or RAMP3. This was confirmed through mRNA analysis showing no trace of the CTR and functional cAMP assays using both CT the cognate ligand for the CTR and amylin the cognate

ligand for the amylin receptors which displayed no cAMP response upon CT/AMY stimulation as the mRNA analysis predicted. This provided confidence that the response seen was due to a single receptor population, and the insights gained were into CLR-RAMP1 signalling and function. Further to this CGRP is the most potent mediator of cAMP production which is expected of a CGRP receptor from the heterologous studies (Weston et al. 2016), it was then confirmed that all peptides were signalling through the CLR-RAMP1 receptor complex with the use of the clinically approved CGRP receptor antagonist Olcegepant. This then enabled the research to explore further signalling pathways beyond cAMP: one of which was G_q mediated intracellular calcium release, all three peptides produced a potent response but CGRP was again the most potent. Then there was $G_{q/11}$ mediated NO production, this avenue was explored in myocytes as previous evidence had suggested that it was possible for certain GPCRs to mediate a negative inotropic effect on the heart through NO release, in this case it was the β-3 adrenergic receptor (Gauthier et al. 1998). In this assay it appeared all three ligands could elicit a a NO response however they were neither large not very distinct from one another. This then leaves $pERK_{1/2}$ and cell proliferation, and here again, just as in the HUVECs and HUAECs the intriguing result was seen whereby the non-cognate ligand AM was the most potent producer of $pERK_{1/2}$ and proliferation whereas the cognate ligand CGRP seemed to have little or no role in either. The potential importance of the $pERK_{1/2}$ and proliferation results are discussed further below.

Physiological outcomes and therapeutic potential of the CGRP peptide family

Heart failure is a devastating disease of global importance, with a prognosis that can be worse than multiple cancers (Braunwald 2015, Stewart et al. 2001) Myocardial damage often leads to heart failure because there is not enough cardiomyocyte regeneration, and ground-breaking work has demonstrated a low rate of innate regeneration in the heart (Bergmann et al. 2009), and much research has gone in to attempts to harness this in the hope of therapeutically promoting cardiac repair, including studies into the potential use of VEGF (Taimeh et al. 2013).

New and different approaches are needed as studies into the efficacy of stem cell or cardiac progenitor cell transplantation into the damaged heart have not been successful for a number of reasons. Foremost among them being they were not able to differentiate engraft and survive in a beneficial way. Nonetheless they were aided the failing heart through paracrine effects and the release of molecules from these stem cells(Maghin et al. 2020). One such molecule was pregnancy-associated plasma protein-A (PAPP-A). PAPP-A was demonstrated to instruct vesicle release of insulin-like growth factor-1 (IGF-1) resulting in AKT and ERK1/2 phosphorylation in target cardiomyocytes (Barile et al. 2018) and proved to be cardioprotective. Other extracellular vesicle release has been implicated in promoting cardiomyocyte proliferation (Xuan et al. 2020). Moreover, studies into the use of heart derived decellularised extracellular matrices (dECM) to aid cardiac regeneration highlight the importance of retaining endogenous peptides and growth factors that are likely to enhance cardiac proliferation and survival (Di Meglio et al. 2017, Sarig et al. 2016).

Therefore, there has been a reinvigorated focus on myocyte regeneration. It has been suggested that mature myocytes have the ability to regenerate in the adult heart (Anversa and Nadal-Ginard 2002). The (Bergmann et al. 2009) study shows there is no overall increase in myocyte number over a lifetime

but a replacement of myocytes over time. However, this study was not able to predict whether the replacement came from duplication or myocyte production from a stem/progenitor pool. A later study (albeit in mice) concluded that pre-existing cardiomyocytes are the dominant source of cardiomyocyte replacement in normal mammalian hearts and after injury (Senyo et al. 2013). Stimulation of cardiomyocytes has been proposed, and is currently a much explored therapeutic strategy (Becker and Hesse 2020). Growth factors such as neuregulin 1 have been shown in vivo to promote cardiomyocyte proliferation (Bersell et al. 2009). As well as other potential pro-proliferative factors (Mills et al. 2019, Eulalio et al. 2012) as well as VEGF mentioned above. Proliferating human ventricular myocytes were utilised and demonstrated that through signalling bias AM, the pERK1/2 biased agonist (but not CGRP or AM2) can enhance proliferation in these cells. This work highlights AM as a novel peptide hormone that may promote cardiac regeneration naturally in vivo, and as a model for the design of small molecules that could mimic AM's signalling bias to promote cardiomyocyte proliferation.

Since cardiomyocytes comprise only about 20% of all cells within the human myocardium (Rubart and Field 2006). This means the heart is made up of many cell types including; myocytes, fibroblasts, smooth muscle cells, endothelial cells or hematopoietic cells, this makes it very difficult for studies of drug/hormone/peptide overall effect on heart function to narrow down how precisely an effect is brought about. Particularly in the case of CGRP/AM/AM2. This is further complicated by observations of the vastly different receptor composition (**Figure 6.2**) and signalling outcomes these peptides have on ECs vs SMCs vs HCMs. However, this work should help to elucidate the effects these peptide hormones have on the different cell types and aid in attempts to specifically target these. While also highlighting the need to improve our understanding of where these peptides are acting to exert the effects seen during systemic administration.

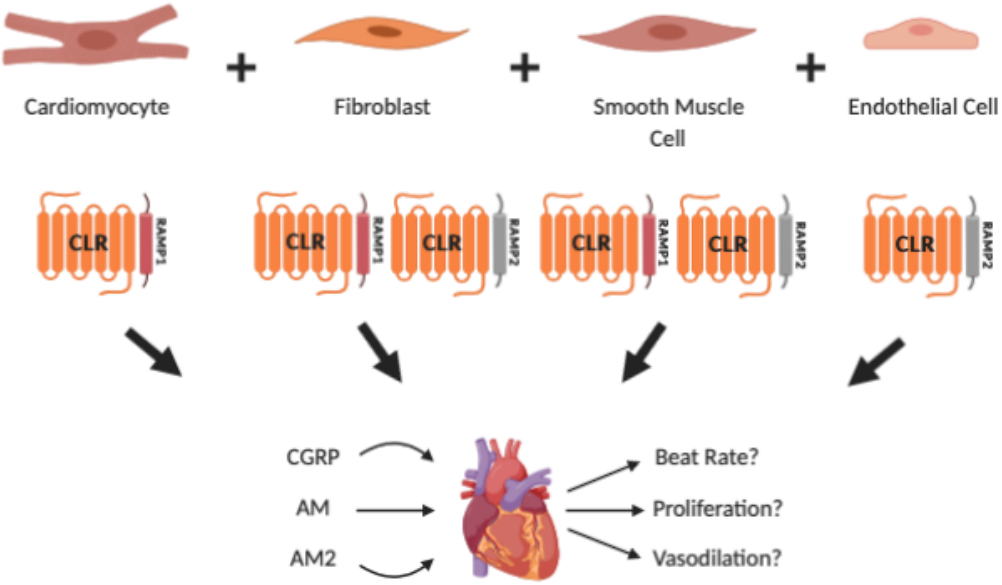

Figure 6.2. Representation of CLR expression and potential contribution to heart function. Graphic showing cell types making up the human heart and their respective mRNA expression of CLR receptor subtypes, as well as the CGRP family of peptides and their possible actions on the heart

Spatiotemporal signalling of CLR and its complexity

It was demonstrated recently that GPCR signalling and in particular CLR signalling goes far beyond the cell surface, figuratively and literally. A study into CGRP receptor trafficking showed how CGRP continues to signal from within the endosome (Yarwood et al. 2017). The internalisation inhibitor barbadin (Beautrait et al. 2017) was used to explore the role of internalisation on CGRP family peptide signalling in the primary cell models. In the case of the HCMs and CGRP mediated cAMP, barbadin suppressed the response and corroborated the results seen by (Beautrait et al. 2017). Initial experiments in HUVECs and on cAMP signalling suggested barbadin may have had some effect. As well as performing traditional dose-response experiments Time courses were performed to observe whether there were different phases of the response. These appeared to show an early peak in the cAMP response at about 8 minutes after stimulation, and then the responses levelled out until the end-point at 30 minutes. This in itself provided an interesting insight into the signalling profile of the three peptides over time. There was then further investigation to uncover how this might be dictated by internalisation using barbadin as well as a host of other internalisation inhibitors, also with and without the pan-PDE inhibitor IBMX to allow for the natural recycling of cAMP. Overall it was clear that without IBMX it was easier to observe the influence of the internalisation inhibitors, however the results were varied, for instance in terms of AM signalling there were no cases where any of the inhibitors could influence AM signalling. This suggests that the majority, if not all of AM's cAMP production through the CLR-RAMP2 receptor occurs at the cell surface. All inhibitors tested at at least one condition were able to influence AM2, whereby they were able to increase the cAMP produced by this peptide. Although compound 101 and barbadin also influenced the pEC50, the inhibitors predominantly raised AM2's Emax at the 30 min time point. This suggests that rather than influencing acute cAMP production by AM2, preventing internalisation increases sustained cAMP and prolongs the cAMP signalling at the surface. Then with CGRP almost all the inhibitors could increase the potency

of CGRP at producing cAMP, this occurred at both the 8 and 30 min time point, and of all three peptides CGRP was the most frequently influenced peptide across all conditions. This seems to imply that internalisation plays the greatest role in CGRP's cAMP signalling, and that by preventing it in both the short and long term you can enhance the level of cAMP produced by CGRP

Next this body of research investigated the effects of barbadin on $pERK_{1/2}$ signalling. There has been much work to suggest that $pERK_{1/2}$ signalling occurs intracellularly and downstream of β-arrestins (Shenoy et al. 2006, Strungs and Luttrell 2014), therefore it seemed logical to assess the contribution of of β-arrestin mediated internalisation on CLR-RAMP2 $pERK_{1/2}$ signalling in the primary cell setting. The effects in these HUVECs were remarkable, barbadin suppressed the short term ERK response of all peptides except AM2, and had the greatest effect on CGRP, however it was in the long term that the effects were most pronounced with the time course experiments showing that after a small initial peak all $ERK_{1/2}$ responses from all peptides returned effectively to baseline. This seems to demonstrate that from this receptor there is a portion of initial $ERK_{1/2}$ phosphorylation that happens at the cell surface (or downstream of signalling mediated by the receptor at the surface as well as after internalisation. But that after this initial wave all subsequent $ERK_{1/2}$ phosphorylation takes place intracellularly. Then in the human cardiomyocyte scenario where the peptides signal through CLR-RAMP1 it appeared that inhibiting internalisation enhanced some of the $ERK_{1/2}$ responses suggesting they are mediated from the surface, while further work may be required in the future to elucidate which precise signalling pathways from endogenous CLR-RAMP1 leads to $ERK_{1/2}$ phosphorylation it is clear from this assessment of the contribution of internalisation to the ERK response that CLR-RAMP1 and CLR-RAMP2 have vastly different patterns of internalisation and signalling when stimulated by the same peptides.

Functional outcomes of CLR-agonist bias observed in spontaneously beating IPSC derived myocytes

Systemic administration of CGRP, AM and AM2 in humans, as discussed previously, has a variety of effects, but one that is consistently noted is the effect on the heart, and this has been overwhelming reported as positive inotropic effects (Gennari and Fischer 1985, Bisping et al. 2007, Fujisawa et al. 2007), although it has been uncertain how much of this effect is a response to the vasodilatory effects, and how the peptide effects directly compare to one another. Using spontaneously beating IPSC derived myocytes the direct effects of CGRP, AM and AM2 on myocyte beat rate were investigated in 2D and 3D. The 2D beat rate experiments revealed interesting differences between the peptides whereby there was a time dependence in their differences: AM2 caused the highest initial increase in beat rate, but decreased more rapidly than the other peptides such that by 60min it had the smallest increase over control. On the other hand CGRP produced the smallest initial increase, but sustained this increase much better than the other peptides so that by the final time point its beat rate was higher than the other peptides. Compared to the other peptides AM stayed in the middle in both the early and late phase of the response. This difference was then enhanced at 24 h where the CGRP mediated increase was even greater. In order to see whether these effects were mediated through a single receptor they were also performed in the presence of the CLR-RAMP1 inhibitor Olcegepant which completely prevented all three ligands exerting an effect. Then moving to myocyte intracellular calcium, having shown isoproterenol could again stimulate a response the effects of CGRP, AM and AM2 on the calcium responses were recorded. They all stimulated changes however it was AM2 that produced the greatest response at its peak as in the beat rate studies. Although in in terms of peak size it was CGRP that increased it the most, with the caveat that this increase with still too small to be of statistical significance. The dose-response curves provided some interesting insights in that these cells expressed two RAMPs in an interesting change from proliferating myocytes profiled in previous

chapters However the experiments above utilising a CLR-RAMP1 antagonist suggests that functionally at least, there is likely to be only one receptor responsible for the responses observed. The other dose-responses also produced some interesting differences compared to other pathways and cell types profiled in previous chapters. Such as in intracellular calcium measurements in these iCell myoctes where the ligand producing the greatest response (AM2) is not the most potent, CGRP is. Then in cell beating dose response curves the rank order of potency is different again with AM2 the most potent then CGRP then AM a previously unseen order. Adding more evidence to the observation that these peptides produce interesting and varied effects on beating myocytes were the 3D spheroid experiments where similar rank orders of magnitude were seen in terms of peak and final responses. However, the 24hr result differed from the 2D system. Overall the beat-rate of the spheroids was faster and more physiologically relevant although in some cases the effects of the peptides on the spheroids was less pronounced compared to the control. It is the author's belief that this could relate a lack of penetration from the peptides. In the 2D system all the cells in their monolayer were directly exposed all at once to agonist when it was added to the media. Whereas in the 3D scenario only the cells around the surface of the spheroid are directly and initially exposed to agonist, there may be some penetration over time, or it is likely many cells in the centre of the spheroid never 'see' agonist over the course of the assay. This of course *in vivo* is resolved by the circulatory system, which the organoids did not have. Therefore, in the case of these *in vitro* assays this may contribute to the differences seen in 2D vs 3D.

Another noteworthy point is the lack of amplitude effects seen in the iCell myoctyes this seems to be a curious quirk of these cells, in that even with compounds known to alter the amplitude of heart beats *in vivo* are reported not to do so on the stem cell derived myocytes (Pillekamp et al. 2012, Yang, Pabon, and Murry 2014). These reason for this is unclear, and has been suggested potentially to be due to an underdeveloped sarcoplasmic reticulum. However, this does serve to highlight that

conclusions drawn from work using these cells should be made with this cautionary example that they do not exactly replicate a human myocyte *in vivo*.

Insights gained from CRISPR-cas9, and comparing signalling bias at the CLR across multiple primary cell systems

This experimental avenue was pursued with the knowledge that exploring the signalling of CLR and each RAMP combination in multiple different primary cell line gave fascinating and novel insights into its endogenous function. But with the caveat that in order to truly compare how the RAMP itself governs signalling, comparing RAMP1 and RAMP2 the cell background needed to be the same. Therefore, there was a strong desire to create the RAMP1-HUVEC cell to enable such a comparison. The first task was to attempt to knockout the expression of the RAMP2 gene in the HUVECs, once this had been achieved it was vital to assess how this influenced cell signalling of the three peptides. Whilst all previous heterologous studies agreed that RAMP expression was vital for CLR function(McLatchie et al. 1998), this could not be taken for granted in the endogenous setting and so all pathways were assessed for peptide function. In each tested there was no response recorded above baseline. This confirmed that RAMP was essential for CLR function. However, as always the case for CRISPR-cas9 off target effects from the RAMP2 knockout could have caused the loss of function. Therefore, equally vital to this set of experiments was the rescue of CLR function by the re-expression of a RAMP protein. Re-expressing RAMP1, if it rescued function, as it did, would then allow for exploration of the subtle differences in signalling that having a different RAMP protein would produce. It was remarkable to then to observe thes subtle differences, while seeing CGRP as the most potent at causing cAMP production was to be expected from the literature, all following observations in terms of calcium, NO, $pERK_{1/2}$, and proliferation were unprecedented. But bore some similarities to the responses observed in the primary HCMs that expressed RAMP1 – this is discussed further below. Assessing side-by-side

the signalling bias in HUVECs either expressing RAMP1 or RAMP2 emphasised the remarkable influence the single transmembrane RAMP has on CLR signalling: Using CGRP as an example the peptide shows strong bias towards $pERK_{1/2}$ and proliferation at the CLR-RAMP2, but then at the CLR-RAMP1 its bias profile is completely switched such that it is now biased towards cAMP and intracellular calcium mobilisation

Using primary cells however does have its limitations, most prominent among them is the limited lifespan of these cells, this would limit their utility in large scale screening of compounds and the potential development of biased agonists, which is a shame as the study of future therapeutics in a physiologically relevant system where the effects of the endogenous peptides has been established could be particularly enlightening. Another limitation was the tools available, currently there is a lack of good antibodies targeting, GPCRs such as the CLR and the RAMPs specifically (Hay et al. 2018). Indeed there are two commercial antibodies that were recently designed for use in Immunofluorescence, but when it was attempted to optimise them for use in this study they did not appear very selective for one RAMP over another (**Supplemental Figure 8.9**)

A potential downside of the CRISPR-cas9 mediated gene editing and re-expression of RAMP1 in HUVECs is that it involves the creation of an artificial expression system. Something there was a strong desire to avoid in starting these studies of endogenous receptor, and whilst the cell background remains physiologically relevant, and cell growth/survival remains similar (**Supplemental Figure 8.7**) the expression levels of RAMP1 may not be. At the mRNA level for instance they were much higher than the levels of RAMP2 in the wt-HUVECs. Therefore, having compared the differences in signalling RAMP1 expression produced in HUVECs vs wt-HUVECs. It was thought important to compare the bias patterns observed back to the bias seen in HCMs endogenously expressing RAMP1. As well as analysing how the responses from each peptide at each pathway correlated with each other in the two systems. It is clear to see, upon comparison of the bias plots from the HUVEC-RAMP1s vs the HCMs that in both scenarios CGRP has a clear bias towards cAMP and calcium mobilisation, whereas

AM is biased towards pERK and proliferation. The correlation analysis then confirms that there is a strong positive correlation between all the pEC50 values showing overall that the RAMP1-HUVECs generated produce signalling responses reflective of another primary cell expressing CLR and RAMP1 endogenously. There were some interesting differences such as in the bias of the peptides towards the more physiological NO response, this may relate more to the cell type and their purposes with endothelial cells and myocytes having vastly different functions and therefore potentially different needs in terms of NO.

Then all the different signalling outcomes measured have been summarised (**Figure 6.3**) from CGRP, AM, and AM2 in the wt-HUVECs, RAMP1-HUVECs, and HCMs in order to visually highlight the trends and differences discussed above, that really emphasise the absolute importance of RAMPs in governing CLR signalling and function.

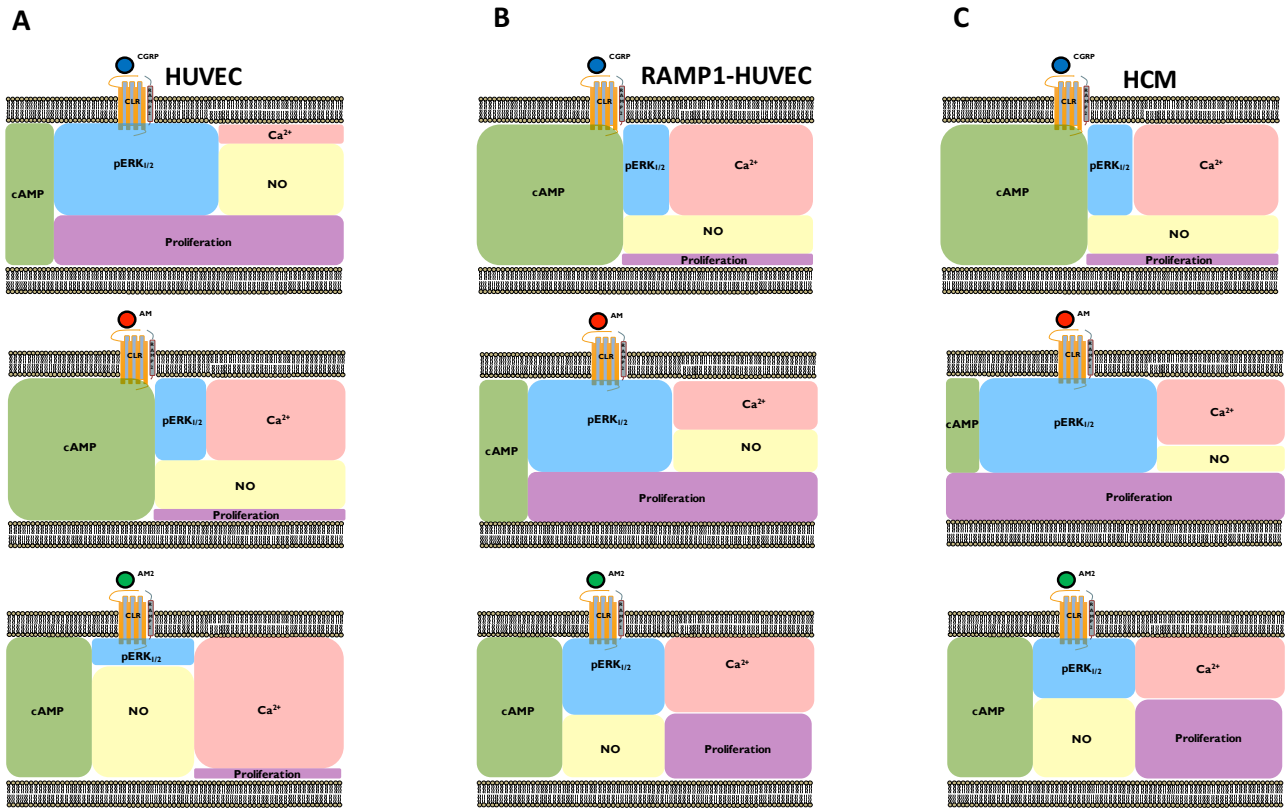

Figure 6.3. Schematic representation of the signalling bias produced by CGRP, AM, and AM2 in a variety of primary cell types. Schematic representation of CGRP peptide signalling cardiovascular cells and the intracellular 'signalling codes' they bring about based on the potencies recorded at individual pathways in HUVECs (**A**), RAMP1-HUVECs (**B**), and HCMs (**C**).

Future Directions

Future work in this field could go down many avenues: more work could be done to explore other signalling pathways downstream of the CLR and into the bias patterns of these, whether these be second messengers or pathways downstream of the messengers already studied here. Future work could also explore further the spatiotemporal aspects of signalling how does it relate to physiological function - which stage and location of each signal is the most important for downstream signalling. Another exciting pathway to explore would be expanding on the organoid work or looking into using whole tissue samples. Particularly bloody vessels; here the process by which many cardiovascular cells signal and function when grown as single cell monolayers has been profiled extensively. How these cells behave in whole vessels and how the signalling bias of CGRP, AM and AM2 contribute to their function will be fascinating to explore as well as vitally important to further our understanding of how GPCRs function *in vivo*. As well as aiding in targeting the CLR in cardiovascular drug discovery. Another future direction could be identifying and exploring a primary cell system that expresses the illusive RAMP3. This is the only RAMP not explored here and future work could look at how the signalling of the peptides through the CLR-RAMP3 compares to the work here on CLR-RAMP1 and CLR-RAMP2. Further work could also be performed using these CRISPR-cas9 gene editing techniques: this could include looking at the contribution of the RAMPs to the pathophysiology of disease, such as cardiovascular disease through comparing models cells for disease with and without RAMP knockout to assess their contribution to disease progression and cell function. Equally in these models the action of CGRP, AM and AM2 in these cells could also be assessed, as discussed previously they are thought to have protective effects in heart failure. Using models of heart failure work could look at which pathways contribute to this protection with the aim of therapeutically targeting them in the future. Recently there has also been ground-breaking work that looks into CRISPR-cas9 gene editing in humans (Baylis and McLeod 2017). As this becomes more commonplace as a therapeutic option work

could be done to explore elucidate RAMP involvement and therefore potentially targeting them in these kinds of ways. Looking back at this body of work and the potential physiological roles of CGRP and AM2 in particular, that this work may have revealed, this could be explored further *in vivo*. It is the author's belief that this work also highlights the importance and rewards gained from studying a GPCR in its endogenous setting, and therefore the scientific community's knowledge of many other RAMP interacting GPCRs and beyond could benefit from this kind of study in the future.

Chapter 7. References

Aittaleb, M., C. A. Boguth, and J. J. Tesmer. 2010. "Structure and function of heterotrimeric G protein-regulated Rho guanine nucleotide exchange factors." *Mol Pharmacol* 77 (2):111-25. doi: 10.1124/mol.109.061234.

Alevizaki, M., A. Shiraishi, F. V. Rassool, G. J. Ferrier, I. MacIntyre, and S. Legon. 1986. "The calcitonin-like sequence of the beta CGRP gene." *FEBS Lett* 206 (1):47-52. doi: 10.1016/0014-5793(86)81338-2.

Alexander, S. P., A. Christopoulos, A. P. Davenport, E. Kelly, N. V. Marrion, J. A. Peters, E. Faccenda, S. D. Harding, A. J. Pawson, J. L. Sharman, C. Southan, J. A. Davies, and Cgtp Collaborators. 2017. "THE CONCISE GUIDE TO PHARMACOLOGY 2017/18: G protein-coupled receptors." *Br J Pharmacol* 174 Suppl 1:S17-S129. doi: 10.1111/bph.13878.

Alexander, S. P. H., A. Christopoulos, A. P. Davenport, E. Kelly, A. Mathie, J. A. Peters, E. L. Veale, J. F. Armstrong, E. Faccenda, S. D. Harding, A. J. Pawson, J. L. Sharman, C. Southan, J. A. Davies, and Cgtp Collaborators. 2019. "THE CONCISE GUIDE TO PHARMACOLOGY 2019/20: G protein-coupled receptors." *Br J Pharmacol* 176 Suppl 1:S21-S141. doi: 10.1111/bph.14748.

Almahariq, M., T. Tsalkova, F. C. Mei, H. Chen, J. Zhou, S. K. Sastry, F. Schwede, and X. Cheng. 2013. "A novel EPAC-specific inhibitor suppresses pancreatic cancer cell migration and invasion." *Mol Pharmacol* 83 (1):122-8. doi: 10.1124/mol.112.080689.

Amara, S. G., V. Jonas, M. G. Rosenfeld, E. S. Ong, and R. M. Evans. 1982. "Alternative RNA processing in calcitonin gene expression generates mRNAs encoding different polypeptide products." *Nature* 298 (5871):240-4. doi: 10.1038/298240a0.

Anand, I. S., J. Gurden, G. S. Wander, P. O'Gara, S. E. Harding, R. Ferrari, A. Cornacchiari, A. Panzali, P. L. Wahi, and P. A. Poole-Wilson. 1991. "Cardiovascular and hormonal effects of calcitonin gene-related peptide in congestive heart failure." *J Am Coll Cardiol* 17 (1):208-17. doi: 10.1016/0735-1097(91)90729-s.

Anversa, P., and B. Nadal-Ginard. 2002. "Myocyte renewal and ventricular remodelling." *Nature* 415 (6868):240-3. doi: 10.1038/415240a.

Archbold, J. K., J. U. Flanagan, H. A. Watkins, J. J. Gingell, and D. L. Hay. 2011. "Structural insights into RAMP modification of secretin family G protein-coupled receptors: implications for drug development." *Trends Pharmacol Sci* 32 (10):591-600. doi: 10.1016/j.tips.2011.05.007.

Ashina, M., P. J. Goadsby, U. Reuter, S. Silberstein, D. Dodick, G. A. Rippon, J. Klatt, F. Xue, V. Chia, F. Zhang, S. Cheng, and D. D. Mikol. 2019. "Long-term safety and tolerability of erenumab: Three-plus year results from a five-year open-label extension study in episodic migraine." *Cephalalgia* 39 (11):1455-1464. doi: 10.1177/0333102419854082.

Aslam, M., U. Pfeil, D. Gündüz, A. Rafiq, W. Kummer, H. M. Piper, and T. Noll. 2012. "Intermedin (adrenomedullin2) stabilizes the endothelial barrier and antagonizes thrombin-induced barrier failure in endothelial cell monolayers." *Br J Pharmacol* 165 (1):208-22. doi: 10.1111/j.1476-5381.2011.01540.x.

Ayad, S., M. A. Demitrack, D. A. Burt, C. Michalsky, L. Wase, M. J. Fossler, and A. K. Khanna. 2020. "Evaluating the Incidence of Opioid-Induced Respiratory Depression Associated with Oliceridine and Morphine as Measured by the Frequency and Average Cumulative Duration of Dosing Interruption in Patients Treated for Acute Postoperative Pain." *Clin Drug Investig*. doi: 10.1007/s40261-020-00936-0.

Ayling, L. J., S. J. Briddon, M. L. Halls, G. R. Hammond, L. Vaca, J. Pacheco, S. J. Hill, and D. M. Cooper. 2012. "Adenylyl cyclase AC8 directly controls its micro-environment by recruiting the actin cytoskeleton in a cholesterol-rich milieu." *J Cell Sci* 125 (Pt 4):869-86. doi: 10.1242/jcs.091090.

Baltos, J. A., K. J. Gregory, P. J. White, P. M. Sexton, A. Christopoulos, and L. T. May. 2016. "Quantification of adenosine A(1) receptor biased agonism: Implications for drug discovery." *Biochem Pharmacol* 99:101-12. doi: 10.1016/j.bcp.2015.11.013.

Barbash, S., E. Lorenzen, T. Persson, T. Huber, and T. P. Sakmar. 2017. "GPCRs globally coevolved with receptor activity-modifying proteins, RAMPs." *Proc Natl Acad Sci U S A* 114 (45):12015-12020. doi: 10.1073/pnas.1713074114.

Barbash, S., T. Persson, E. Lorenzen, M. A. Kazmi, T. Huber, and T. P. Sakmar. 2019. "Detection of Concordance between Transcriptional Levels of GPCRs and Receptor-Activity-Modifying Proteins." *iScience* 11:366-374. doi: 10.1016/j.isci.2018.12.024.

Barile, L., E. Cervio, V. Lionetti, G. Milano, A. Ciullo, V. Biemmi, S. Bolis, C. Altomare, M. Matteucci, D. Di Silvestre, F. Brambilla, T. E. Fertig, T. Torre, S. Demertzis, P. Mauri, T. Moccetti, and G. Vassalli. 2018. "Cardioprotection by cardiac progenitor cell-secreted exosomes: role of pregnancy-associated plasma protein-A." *Cardiovasc Res* 114 (7):992-1005. doi: 10.1093/cvr/cvy055.

Baylis, F., and M. McLeod. 2017. "First-in-human Phase 1 CRISPR Gene Editing Cancer Trials: Are We Ready?" *Curr Gene Ther* 17 (4):309-319. doi: 10.2174/1566523217666171121165935.

Beautrait, A., J. S. Paradis, B. Zimmerman, J. Giubilaro, L. Nikolajev, S. Armando, H. Kobayashi, L. Yamani, Y. Namkung, F. M. Heydenreich, E. Khoury, M. Audet, P. P. Roux, D. B. Veprintsev, S. A. Laporte, and M. Bouvier. 2017. "A new inhibitor of the β-arrestin/AP2 endocytic complex reveals interplay between GPCR internalization and signalling." *Nat Commun* 8:15054. doi: 10.1038/ncomms15054.

Becker, C., and M. Hesse. 2020. "Role of Mononuclear Cardiomyocytes in Cardiac Turnover and Regeneration." *Curr Cardiol Rep* 22 (6):39. doi: 10.1007/s11886-020-01289-y.

Belcheva, M. M., and C. J. Coscia. 2002. "Diversity of G protein-coupled receptor signaling pathways to ERK/MAP kinase." *Neurosignals* 11 (1):34-44. doi: 10.1159/000057320.

Bell, D., B. J. Gordon, A. Lavery, K. Megaw, M. O. Kinney, and M. T. Harbinson. 2016. "Plasma levels of intermedin (adrenomedullin-2) in healthy human volunteers and patients with heart failure." *Peptides* 76:19-29. doi: 10.1016/j.peptides.2015.12.003.

Bell, D., and B. J. McDermott. 2008. "Intermedin (adrenomedullin-2): a novel counter-regulatory peptide in the cardiovascular and renal systems." *Br J Pharmacol* 153 Suppl 1:S247-62. doi: 10.1038/sj.bjp.0707494.

Bell, D., Y. Zhao, F. P. McCoy, A. Devine, and B. J. McDermott. 2008. "Expression of the counter-regulatory peptide intermedin is augmented in the presence of oxidative stress in hypertrophied cardiomyocytes." *Cell Physiol Biochem* 21 (5-6):409-20. doi: 10.1159/000129633.

Benovic, J. L., R. H. Strasser, M. G. Caron, and R. J. Lefkowitz. 1986. "Beta-adrenergic receptor kinase: identification of a novel protein kinase that phosphorylates the agonist-occupied form of the receptor." *Proc Natl Acad Sci U S A* 83 (9):2797-801. doi: 10.1073/pnas.83.9.2797.

Bergmann, O., R. D. Bhardwaj, S. Bernard, S. Zdunek, F. Barnabe-Heider, S. Walsh, J. Zupicich, K. Alkass, B. A. Buchholz, H. Druid, S. Jovinge, and J. Frisen. 2009. "Evidence for cardiomyocyte renewal in humans." *Science* 324 (5923):98-102. doi: 10.1126/science.1164680.

Bersell, K., S. Arab, B. Haring, and B. Kuhn. 2009. "Neuregulin1/ErbB4 signaling induces cardiomyocyte proliferation and repair of heart injury." *Cell* 138 (2):257-70. doi: 10.1016/j.cell.2009.04.060.

Bisping, E., G. Tenderich, P. Barckhausen, B. Stumme, S. Bruns, D. von Lewinski, and B. Pieske. 2007. "Atrial myocardium is the predominant inotropic target of adrenomedullin in the human heart." *Am J Physiol Heart Circ Physiol* 293 (5):H3001-7. doi: 10.1152/ajpheart.01276.2006.

Bjarnadottir, T. K., R. Fredriksson, P. J. Hoglund, D. E. Gloriam, M. C. Lagerstrom, and H. B. Schioth. 2004. "The human and mouse repertoire of the adhesion family of G-protein-coupled receptors." *Genomics* 84 (1):23-33. doi: 10.1016/j.ygeno.2003.12.004.

Bjarnadottir, T. K., D. E. Gloriam, S. H. Hellstrand, H. Kristiansson, R. Fredriksson, and H. B. Schioth. 2006. "Comprehensive repertoire and phylogenetic analysis of the G protein-coupled

receptors in human and mouse." *Genomics* 88 (3):263-73. doi: 10.1016/j.ygeno.2006.04.001.
Black, J. W., and P. Leff. 1983. "Operational models of pharmacological agonism." *Proc R Soc Lond B Biol Sci* 220 (1219):141-62. doi: 10.1098/rspb.1983.0093.
Boularan, C., and C. Gales. 2015. "Cardiac cAMP: production, hydrolysis, modulation and detection." *Front Pharmacol* 6:203. doi: 10.3389/fphar.2015.00203.
Brain, S. D., and A. D. Grant. 2004. "Vascular actions of calcitonin gene-related peptide and adrenomedullin." *Physiol Rev* 84 (3):903-34. doi: 10.1152/physrev.00037.2003.
Brain, S. D., T. J. Williams, J. R. Tippins, H. R. Morris, and I. MacIntyre. 1985. "Calcitonin gene-related peptide is a potent vasodilator." *Nature* 313 (5997):54-6. doi: 10.1038/313054a0.
Braunwald, E. 2015. "The war against heart failure: the Lancet lecture." *Lancet* 385 (9970):812-24. doi: 10.1016/S0140-6736(14)61889-4.
Chang, C. P., R. V. Pearse, 2nd, S. O'Connell, and M. G. Rosenfeld. 1993. "Identification of a seven transmembrane helix receptor for corticotropin-releasing factor and sauvagine in mammalian brain." *Neuron* 11 (6):1187-95.
Chang, L., and M. Karin. 2001. "Mammalian MAP kinase signalling cascades." *Nature* 410 (6824):37-40. doi: 10.1038/35065000.
Charles, C. J., M. T. Rademaker, and A. M. Richards. 2006. "Hemodynamic, hormonal, and renal actions of adrenomedullin-2 in normal conscious sheep." *Endocrinology* 147 (4):1871-7. doi: 10.1210/en.2005-1403.
Chauhan, M., M. Balakrishnan, A. Vidaeff, U. Yallampalli, F. Lugo, K. Fox, M. Belfort, and C. Yallampalli. 2016. "Adrenomedullin2 (ADM2)/Intermedin (IMD): A Potential Role in the Pathophysiology of Preeclampsia." *J Clin Endocrinol Metab* 101 (11):4478-4488. doi: 10.1210/jc.2016-1333.
Chen, H., X. Wang, M. Tong, D. Wu, S. Wu, J. Chen, X. Wang, X. Wang, Y. Kang, H. Tang, C. Tang, and W. Jiang. 2013. "Intermedin suppresses pressure overload cardiac hypertrophy through activation of autophagy." *PLoS One* 8 (5):e64757. doi: 10.1371/journal.pone.0064757.
Chen, L., B. Kis, H. Hashimoto, D. W. Busija, Y. Takei, H. Yamashita, and Y. Ueta. 2006. "Adrenomedullin 2 protects rat cerebral endothelial cells from oxidative damage in vitro." *Brain Res* 1086 (1):42-9. doi: 10.1016/j.brainres.2006.02.128.
Coleman, D. E., A. M. Berghuis, E. Lee, M. E. Linder, A. G. Gilman, and S. R. Sprang. 1994. "Structures of active conformations of Gi alpha 1 and the mechanism of GTP hydrolysis." *Science* 265 (5177):1405-12. doi: 10.1126/science.8073283.
Crossman, D. C., M. R. Dashwood, S. D. Brain, J. McEwan, and J. D. Pearson. 1990. "Action of calcitonin gene-related peptide upon bovine vascular endothelial and smooth muscle cells grown in isolation and co-culture." *Br J Pharmacol* 99 (1):71-6. doi: 10.1111/j.1476-5381.1990.tb14656.x.
Davenport, A. P., C. C. G. Scully, C. de Graaf, A. J. H. Brown, and J. J. Maguire. 2020. "Advances in therapeutic peptides targeting G protein-coupled receptors." *Nat Rev Drug Discov* 19 (6):389-413. doi: 10.1038/s41573-020-0062-z.
de Graaf, C., G. Song, C. Cao, Q. Zhao, M. W. Wang, B. Wu, and R. C. Stevens. 2017. "Extending the Structural View of Class B GPCRs." *Trends Biochem Sci* 42 (12):946-960. doi: 10.1016/j.tibs.2017.10.003.
Depre, C., L. Antalik, A. Starling, M. Koren, O. Eisele, R. A. Lenz, and D. D. Mikol. 2018. "A Randomized, Double-Blind, Placebo-Controlled Study to Evaluate the Effect of Erenumab on Exercise Time During a Treadmill Test in Patients With Stable Angina." *Headache* 58 (5):715-723. doi: 10.1111/head.13316.
DeVree, B. T., J. P. Mahoney, G. A. Velez-Ruiz, S. G. Rasmussen, A. J. Kuszak, E. Edwald, J. J. Fung, A. Manglik, M. Masureel, Y. Du, R. A. Matt, E. Pardon, J. Steyaert, B. K. Kobilka, and R. K. Sunahara. 2016. "Allosteric coupling from G protein to the agonist-binding pocket in GPCRs." *Nature* 535 (7610):182-6. doi: 10.1038/nature18324.

Di Meglio, F., D. Nurzynska, V. Romano, R. Miraglia, I. Belviso, A. M. Sacco, V. Barbato, M. Di Gennaro, G. Granato, C. Maiello, S. Montagnani, and C. Castaldo. 2017. "Optimization of Human Myocardium Decellularization Method for the Construction of Implantable Patches." *Tissue Eng Part C Methods* 23 (9):525-539. doi: 10.1089/ten.TEC.2017.0267.

Dixon, R. A., B. K. Kobilka, D. J. Strader, J. L. Benovic, H. G. Dohlman, T. Frielle, M. A. Bolanowski, C. D. Bennett, E. Rands, R. E. Diehl, R. A. Mumford, E. E. Slater, I. S. Sigal, M. G. Caron, R. J. Lefkowitz, and C. D. Strader. 1986. "Cloning of the gene and cDNA for mammalian beta-adrenergic receptor and homology with rhodopsin." *Nature* 321 (6065):75-9. doi: 10.1038/321075a0.

Doerr, L., U. Thomas, D. R. Guinot, C. T. Bot, S. Stoelzle-Feix, M. Beckler, M. George, and N. Fertig. 2015. "New easy-to-use hybrid system for extracellular potential and impedance recordings." *J Lab Autom* 20 (2):175-88. doi: 10.1177/2211068214562832.

Dohlman, H. G., J. Thorner, M. G. Caron, and R. J. Lefkowitz. 1991. "Model systems for the study of seven-transmembrane-segment receptors." *Annu Rev Biochem* 60:653-88. doi: 10.1146/annurev.bi.60.070191.003253.

Doi, Y., H. Kudo, T. Nishino, K. Kayashima, H. Kiyonaga, T. Nagata, S. Nara, M. Morita, and S. Fujimoto. 2001. "Synthesis of calcitonin gene-related peptide (CGRP) by rat arterial endothelial cells." *Histol Histopathol* 16 (4):1073-9. doi: 10.14670/HH-16.1073.

Dong, F., M. M. Taylor, W. K. Samson, and J. Ren. 2006. "Intermedin (adrenomedullin-2) enhances cardiac contractile function via a protein kinase C- and protein kinase A-dependent pathway in murine ventricular myocytes." *J Appl Physiol (1985)* 101 (3):778-84. doi: 10.1152/japplphysiol.01631.2005.

Dong, Y. L., S. Vegiraju, P. R. Gangula, S. B. Kondapaka, S. J. Wimalawansa, and C. Yallampalli. 2002. "Expression and regulation of calcitonin gene-related Peptide receptor in rat placentas." *Biol Reprod* 67 (4):1321-6. doi: 10.1093/biolreprod/67.4.1321.

Dunn, H. A., and S. S. Ferguson. 2015. "PDZ Protein Regulation of G Protein-Coupled Receptor Trafficking and Signaling Pathways." *Mol Pharmacol* 88 (4):624-39. doi: 10.1124/mol.115.098509.

Eglen, R. M., A. Gilchrist, and T. Reisine. 2008. "The use of immortalized cell lines in GPCR screening: the good, bad and ugly." *Comb Chem High Throughput Screen* 11 (7):560-5. doi: 10.2174/138620708785204144.

Eichel, K., and M. von Zastrow. 2018. "Subcellular Organization of GPCR Signaling." *Trends Pharmacol Sci* 39 (2):200-208. doi: 10.1016/j.tips.2017.11.009.

Eto, T., J. Kato, and K. Kitamura. 2003. "Regulation of production and secretion of adrenomedullin in the cardiovascular system." *Regul Pept* 112 (1-3):61-9. doi: 10.1016/s0167-0115(03)00023-5.

Eulalio, A., M. Mano, M. Dal Ferro, L. Zentilin, G. Sinagra, S. Zacchigna, and M. Giacca. 2012. "Functional screening identifies miRNAs inducing cardiac regeneration." *Nature* 492 (7429):376-81. doi: 10.1038/nature11739.

Evans, B. N., M. I. Rosenblatt, L. O. Mnayer, K. R. Oliver, and I. M. Dickerson. 2000. "CGRP-RCP, a novel protein required for signal transduction at calcitonin gene-related peptide and adrenomedullin receptors." *J Biol Chem* 275 (40):31438-43. doi: 10.1074/jbc.M005604200.

Falcone, J. C., D. Lominadze, W. T. Johnson, and D. A. Schuschke. 2008. "Endothelial cell-derived nitric oxide mobilization is attenuated in copper-deficient rats." *Appl Physiol Nutr Metab* 33 (6):1073-8. doi: 10.1139/H08-091.

Farah, C., L. Y. M. Michel, and J. L. Balligand. 2018. "Nitric oxide signalling in cardiovascular health and disease." *Nat Rev Cardiol* 15 (5):292-316. doi: 10.1038/nrcardio.2017.224.

Feng, C. J., B. Kang, A. D. Kaye, P. J. Kadowitz, and B. D. Nossaman. 1994. "L-NAME modulates responses to adrenomedullin in the hindquarters vascular bed of the rat." *Life Sci* 55 (22):PL433-8. doi: 10.1016/0024-3205(94)00347-5.

Fernandez-Sauze, S., C. Delfino, K. Mabrouk, C. Dussert, O. Chinot, P. M. Martin, F. Grisoli, L. Ouafik, and F. Boudouresque. 2004. "Effects of adrenomedullin on endothelial cells in the multistep process of angiogenesis: involvement of CRLR/RAMP2 and CRLR/RAMP3 receptors." *Int J Cancer* 108 (6):797-804. doi: 10.1002/ijc.11663.

Findlay, D. M. 2006. "Regulation of cell growth mediated by the calcitonin receptor." *Cell Mol Biol (Noisy-le-grand)* 52 (3):3-8.

Fisher, L. A., D. O. Kikkawa, J. E. Rivier, S. G. Amara, R. M. Evans, M. G. Rosenfeld, W. W. Vale, and M. R. Brown. 1983. "Stimulation of noradrenergic sympathetic outflow by calcitonin gene-related peptide." *Nature* 305 (5934):534-6. doi: 10.1038/305534a0.

Flock, T., A. S. Hauser, N. Lund, D. E. Gloriam, S. Balaji, and M. M. Babu. 2017. "Selectivity determinants of GPCR-G-protein binding." *Nature* 545 (7654):317-322. doi: 10.1038/nature22070.

Fredriksson, R., M. C. Lagerstrom, P. J. Hoglund, and H. B. Schioth. 2002. "Novel human G protein-coupled receptors with long N-terminals containing GPS domains and Ser/Thr-rich regions." *FEBS Lett* 531 (3):407-14. doi: 10.1016/s0014-5793(02)03574-3.

Fujisawa, Y., Y. Nagai, A. Miyatake, K. Miura, A. Nishiyama, S. Kimura, and Y. Abe. 2007. "Effects of adrenomedullin 2 on regional hemodynamics in conscious rats." *Eur J Pharmacol* 558 (1-3):128-32. doi: 10.1016/j.ejphar.2006.11.043.

Fukuhara, S., H. Chikumi, and J. S. Gutkind. 2000. "Leukemia-associated Rho guanine nucleotide exchange factor (LARG) links heterotrimeric G proteins of the G(12) family to Rho." *FEBS Lett* 485 (2-3):183-8. doi: 10.1016/s0014-5793(00)02224-9.

Gangula, P. R., H. Zhao, S. C. Supowit, S. J. Wimalawansa, D. J. Dipette, K. N. Westlund, R. F. Gagel, and C. Yallampalli. 2000. "Increased blood pressure in alpha-calcitonin gene-related peptide/calcitonin gene knockout mice." *Hypertension* 35 (1 Pt 2):470-5. doi: 10.1161/01.hyp.35.1.470.

Gauthier, C., V. Leblais, L. Kobzik, J. N. Trochu, N. Khandoudi, A. Bril, J. L. Balligand, and H. Le Marec. 1998. "The negative inotropic effect of beta3-adrenoceptor stimulation is mediated by activation of a nitric oxide synthase pathway in human ventricle." *J Clin Invest* 102 (7):1377-84. doi: 10.1172/JCI2191.

Gennari, C., and J. A. Fischer. 1985. "Cardiovascular action of calcitonin gene-related peptide in humans." *Calcif Tissue Int* 37 (6):581-4. doi: 10.1007/BF02554909.

Gennari, C., R. Nami, D. Agnusdei, and J. A. Fischer. 1990. "Improved cardiac performance with human calcitonin gene related peptide in patients with congestive heart failure." *Cardiovasc Res* 24 (3):239-41. doi: 10.1093/cvr/24.3.239.

Gingell, J. J., E. R. Hendrikse, and D. L. Hay. 2019. "New Insights into the Regulation of CGRP-Family Receptors." *Trends Pharmacol Sci* 40 (1):71-83. doi: 10.1016/j.tips.2018.11.005.

Gingell, J. J., T. A. Rees, E. R. Hendrikse, A. Siow, D. Rennison, J. Scotter, P. W. R. Harris, M. A. Brimble, C. S. Walker, and D. L. Hay. 2020. "Distinct Patterns of Internalization of Different Calcitonin Gene-Related Peptide Receptors." *ACS Pharmacol Transl Sci* 3 (2):296-304. doi: 10.1021/acsptsci.9b00089.

Goadsby, P. J., U. Reuter, Y. Hallstrom, G. Broessner, J. H. Bonner, F. Zhang, S. Sapra, H. Picard, D. D. Mikol, and R. A. Lenz. 2017. "A Controlled Trial of Erenumab for Episodic Migraine." *N Engl J Med* 377 (22):2123-2132. doi: 10.1056/NEJMoa1705848.

Goodman, O. B., Jr., J. G. Krupnick, F. Santini, V. V. Gurevich, R. B. Penn, A. W. Gagnon, J. H. Keen, and J. L. Benovic. 1996. "Beta-arrestin acts as a clathrin adaptor in endocytosis of the beta2-adrenergic receptor." *Nature* 383 (6599):447-50. doi: 10.1038/383447a0.

Gray, D. W., and I. Marshall. 1992. "Human alpha-calcitonin gene-related peptide stimulates adenylate cyclase and guanylate cyclase and relaxes rat thoracic aorta by releasing nitric oxide." *Br J Pharmacol* 107 (3):691-6. doi: 10.1111/j.1476-5381.1992.tb14508.x.

Gregory, K. J., N. E. Hall, A. B. Tobin, P. M. Sexton, and A. Christopoulos. 2010. "Identification of orthosteric and allosteric site mutations in M2 muscarinic acetylcholine receptors that

contribute to ligand-selective signaling bias." *J Biol Chem* 285 (10):7459-74. doi: 10.1074/jbc.M109.094011.

Halls, M. L., and D. M. F. Cooper. 2017. "Adenylyl cyclase signalling complexes - Pharmacological challenges and opportunities." *Pharmacol Ther* 172:171-180. doi: 10.1016/j.pharmthera.2017.01.001.

Hanyu, R., V. L. Wehbi, T. Hayata, S. Moriya, T. N. Feinstein, Y. Ezura, M. Nagao, Y. Saita, H. Hemmi, T. Notomi, T. Nakamoto, E. Schipani, S. Takeda, K. Kaneko, H. Kurosawa, G. Karsenty, H. M. Kronenberg, J. P. Vilardaga, and M. Noda. 2012. "Anabolic action of parathyroid hormone regulated by the beta2-adrenergic receptor." *Proc Natl Acad Sci U S A* 109 (19):7433-8. doi: 10.1073/pnas.1109036109.

Hay, D. L., G. Christopoulos, A. Christopoulos, D. R. Poyner, and P. M. Sexton. 2005. "Pharmacological discrimination of calcitonin receptor: receptor activity-modifying protein complexes." *Mol Pharmacol* 67 (5):1655-65. doi: 10.1124/mol.104.008615.

Hay, D. L., M. L. Garelja, D. R. Poyner, and C. S. Walker. 2018. "Update on the pharmacology of calcitonin/CGRP family of peptides: IUPHAR Review 25." *Br J Pharmacol* 175 (1):3-17. doi: 10.1111/bph.14075.

Hay, D. L., S. G. Howitt, A. C. Conner, M. Schindler, D. M. Smith, and D. R. Poyner. 2003. "CL/RAMP2 and CL/RAMP3 produce pharmacologically distinct adrenomedullin receptors: a comparison of effects of adrenomedullin22-52, CGRP8-37 and BIBN4096BS." *Br J Pharmacol* 140 (3):477-86. doi: 10.1038/sj.bjp.0705472.

Hay, D. L., and A. A. Pioszak. 2016. "Receptor Activity-Modifying Proteins (RAMPs): New Insights and Roles." *Annu Rev Pharmacol Toxicol* 56:469-87. doi: 10.1146/annurev-pharmtox-010715-103120.

Hendrikse, E. R., L. P. Liew, R. L. Bower, M. Bonnet, M. A. Jamaluddin, N. Prodan, K. D. Richards, C. S. Walker, G. Pairaudeau, D. M. Smith, R. M. Rujan, R. Sudra, C. A. Reynolds, J. M. Booe, A. A. Pioszak, J. U. Flanagan, M. P. Hay, and D. L. Hay. 2020. "Identification of Small-Molecule Positive Modulators of Calcitonin-like Receptor-Based Receptors." *ACS Pharmacol Transl Sci* 3 (2):305-320. doi: 10.1021/acsptsci.9b00108.

Hilairet, S., C. Belanger, J. Bertrand, A. Laperriere, S. M. Foord, and M. Bouvier. 2001. "Agonist-promoted internalization of a ternary complex between calcitonin receptor-like receptor, receptor activity-modifying protein 1 (RAMP1), and beta-arrestin." *J Biol Chem* 276 (45):42182-90. doi: 10.1074/jbc.M107323200.

Hilairet, S., C. Bélanger, J. Bertrand, A. Laperrière, S. M. Foord, and M. Bouvier. 2001. "Agonist-promoted internalization of a ternary complex between calcitonin receptor-like receptor, receptor activity-modifying protein 1 (RAMP1), and beta-arrestin." *J Biol Chem* 276 (45):42182-90. doi: 10.1074/jbc.M107323200.

Hilger, D., M. Masureel, and B. K. Kobilka. 2018. "Structure and dynamics of GPCR signaling complexes." *Nat Struct Mol Biol* 25 (1):4-12. doi: 10.1038/s41594-017-0011-7.

Hill, R., A. Disney, A. Conibear, K. Sutcliffe, W. Dewey, S. Husbands, C. Bailey, E. Kelly, and G. Henderson. 2018. "The novel mu-opioid receptor agonist PZM21 depresses respiration and induces tolerance to antinociception." *Br J Pharmacol* 175 (13):2653-2661. doi: 10.1111/bph.14224.

Hoare, S. R. 2005. "Mechanisms of peptide and nonpeptide ligand binding to Class B G-protein-coupled receptors." *Drug Discov Today* 10 (6):417-27. doi: 10.1016/S1359-6446(05)03370-2.

Hocke, A. C., B. Temmesfeld-Wollbrueck, B. Schmeck, K. Berger, E. M. Frisch, M. Witzenrath, B. Brell, N. Suttorp, and S. Hippenstiel. 2006. "Perturbation of endothelial junction proteins by Staphylococcus aureus alpha-toxin: inhibition of endothelial gap formation by adrenomedullin." *Histochem Cell Biol* 126 (3):305-16. doi: 10.1007/s00418-006-0174-5.

Holton, M., T. M. Mohamed, D. Oceandy, W. Wang, S. Lamas, M. Emerson, L. Neyses, and A. L. Armesilla. 2010. "Endothelial nitric oxide synthase activity is inhibited by the plasma

membrane calcium ATPase in human endothelial cells." *Cardiovasc Res* 87 (3):440-8. doi: 10.1093/cvr/cvq077.

Hong, Y., D. L. Hay, R. Quirion, and D. R. Poyner. 2012. "The pharmacology of adrenomedullin 2/intermedin." *Br J Pharmacol* 166 (1):110-20. doi: 10.1111/j.1476-5381.2011.01530.x.

Hu, P., S. Wu, Y. Sun, C. C. Yuan, R. Kobayashi, M. P. Myers, and N. Hernandez. 2002. "Characterization of human RNA polymerase III identifies orthologues for Saccharomyces cerevisiae RNA polymerase III subunits." *Mol Cell Biol* 22 (22):8044-55. doi: 10.1128/mcb.22.22.8044-8055.2002.

Ichiki, Y., K. Kitamura, K. Kangawa, M. Kawamoto, H. Matsuo, and T. Eto. 1994. "Distribution and characterization of immunoreactive adrenomedullin in human tissue and plasma." *FEBS Lett* 338 (1):6-10. doi: 10.1016/0014-5793(94)80106-1.

Jacobsen, L. B., S. A. Calvin, K. E. Colvin, and M. Wright. 2004. "FuGENE 6 Transfection Reagent: the gentle power." *Methods* 33 (2):104-12. doi: 10.1016/j.ymeth.2003.11.002.

Jaffe, E. A., R. L. Nachman, C. G. Becker, and C. R. Minick. 1973. "Culture of human endothelial cells derived from umbilical veins. Identification by morphologic and immunologic criteria." *J Clin Invest* 52 (11):2745-56. doi: 10.1172/JCI107470.

Jersmann, H. P., C. S. Hii, G. L. Hodge, and A. Ferrante. 2001. "Synthesis and surface expression of CD14 by human endothelial cells." *Infect Immun* 69 (1):479-85. doi: 10.1128/IAI.69.1.479-485.2001.

Jolly, L., J. E. March, P. A. Kemp, T. Bennett, and S. M. Gardiner. 2009. "Mechanisms involved in the regional haemodynamic effects of intermedin (adrenomedullin 2) compared with adrenomedullin in conscious rats." *Br J Pharmacol* 157 (8):1502-13. doi: 10.1111/j.1476-5381.2009.00306.x.

Kamato, D., P. Mitra, F. Davis, N. Osman, R. Chaplin, P. J. Cabot, R. Afroz, W. Thomas, W. Zheng, H. Kaur, M. Brimble, and P. J. Little. 2017. "Gaq proteins: molecular pharmacology and therapeutic potential." *Cell Mol Life Sci* 74 (8):1379-1390. doi: 10.1007/s00018-016-2405-9.

Kataoka, Y., S. Miyazaki, S. Yasuda, N. Nagaya, T. Noguchi, N. Yamada, I. Morii, A. Kawamura, K. Doi, K. Miyatake, H. Tomoike, and K. Kangawa. 2010. "The first clinical pilot study of intravenous adrenomedullin administration in patients with acute myocardial infarction." *J Cardiovasc Pharmacol* 56 (4):413-9. doi: 10.1097/FJC.0b013e3181f15b45.

Kato, J., and K. Kitamura. 2015. "Bench-to-bedside pharmacology of adrenomedullin." *Eur J Pharmacol* 764:140-8. doi: 10.1016/j.ejphar.2015.06.061.

Kawase, T., K. Okuda, C. H. Wu, H. Yoshie, K. Hara, and D. M. Burns. 1999. "Calcitonin gene-related peptide acts as a mitogen for human Gin-1 gingival fibroblasts by activating the MAP kinase signalling pathway." *J Periodontal Res* 34 (3):160-8. doi: 10.1111/j.1600-0765.1999.tb02237.x.

Kenakin, T. 2017. "Theoretical Aspects of GPCR-Ligand Complex Pharmacology." *Chem Rev* 117 (1):4-20. doi: 10.1021/acs.chemrev.5b00561.

Kitamura, K., K. Kangawa, M. Kawamoto, Y. Ichiki, S. Nakamura, H. Matsuo, and T. Eto. 1993. "Adrenomedullin: a novel hypotensive peptide isolated from human pheochromocytoma." *Biochem Biophys Res Commun* 192 (2):553-60. doi: 10.1006/bbrc.1993.1451.

Klein, K. R., and K. M. Caron. 2015. "Adrenomedullin in lymphangiogenesis: from development to disease." *Cell Mol Life Sci* 72 (16):3115-26. doi: 10.1007/s00018-015-1921-3.

Kliewer, A., A. Gillis, R. Hill, F. Schmiedel, C. Bailey, E. Kelly, G. Henderson, M. J. Christie, and S. Schulz. 2020. "Morphine-induced respiratory depression is independent of beta-arrestin2 signalling." *Br J Pharmacol* 177 (13):2923-2931. doi: 10.1111/bph.15004.

Kliewer, A., F. Schmiedel, S. Sianati, A. Bailey, J. T. Bateman, E. S. Levitt, J. T. Williams, M. J. Christie, and S. Schulz. 2019. "Phosphorylation-deficient G-protein-biased mu-opioid receptors improve analgesia and diminish tolerance but worsen opioid side effects." *Nat Commun* 10 (1):367. doi: 10.1038/s41467-018-08162-1.

Koch, W. J., B. E. Hawes, L. F. Allen, and R. J. Lefkowitz. 1994. "Direct evidence that Gi-coupled receptor stimulation of mitogen-activated protein kinase is mediated by G beta gamma activation of p21ras." *Proc Natl Acad Sci U S A* 91 (26):12706-10. doi: 10.1073/pnas.91.26.12706.

Kourlas, P. J., M. P. Strout, B. Becknell, M. L. Veronese, C. M. Croce, K. S. Theil, R. Krahe, T. Ruutu, S. Knuutila, C. D. Bloomfield, and M. A. Caligiuri. 2000. "Identification of a gene at 11q23 encoding a guanine nucleotide exchange factor: evidence for its fusion with MLL in acute myeloid leukemia." *Proc Natl Acad Sci U S A* 97 (5):2145-50. doi: 10.1073/pnas.040569197.

Kozasa, T., and A. G. Gilman. 1996. "Protein kinase C phosphorylates G12 alpha and inhibits its interaction with G beta gamma." *J Biol Chem* 271 (21):12562-7. doi: 10.1074/jbc.271.21.12562.

Kraenzlin, M. E., J. L. Ch'ng, P. K. Mulderry, M. A. Ghatei, and S. R. Bloom. 1985. "Infusion of a novel peptide, calcitonin gene-related peptide (CGRP) in man. Pharmacokinetics and effects on gastric acid secretion and on gastrointestinal hormones." *Regul Pept* 10 (2-3):189-97. doi: 10.1016/0167-0115(85)90013-8.

Kuwasako, K., Y. Shimekake, M. Masuda, K. Nakahara, T. Yoshida, M. Kitaura, K. Kitamura, T. Eto, and T. Sakata. 2000. "Visualization of the calcitonin receptor-like receptor and its receptor activity-modifying proteins during internalization and recycling." *J Biol Chem* 275 (38):29602-9. doi: 10.1074/jbc.M004534200.

Lee, M. H., K. M. Appleton, E. G. Strungs, J. Y. Kwon, T. A. Morinelli, Y. K. Peterson, S. A. Laporte, and L. M. Luttrell. 2016. "The conformational signature of beta-arrestin2 predicts its trafficking and signalling functions." *Nature* 531 (7596):665-8. doi: 10.1038/nature17154.

Lefkowitz, R. J. 2004. "Historical review: a brief history and personal retrospective of seven-transmembrane receptors." *Trends Pharmacol Sci* 25 (8):413-22. doi: 10.1016/j.tips.2004.06.006.

Lefkowitz, R. J. 2007. "Seven transmembrane receptors: something old, something new." *Acta Physiol (Oxf)* 190 (1):9-19. doi: 10.1111/j.1365-201X.2007.01693.x.

Lefloch, R., J. Pouysségur, and P. Lenormand. 2009. "Total ERK1/2 activity regulates cell proliferation." *Cell Cycle* 8 (5):705-11. doi: 10.4161/cc.8.5.7734.

Lewis, L. K., M. W. Smith, T. G. Yandle, A. M. Richards, and M. G. Nicholls. 1998. "Adrenomedullin(1-52) measured in human plasma by radioimmunoassay: plasma concentration, adsorption, and storage." *Clin Chem* 44 (3):571-7.

Li, J., S. P. Levick, D. J. DiPette, J. S. Janicki, and S. C. Supowit. 2013. "Alpha-calcitonin gene-related peptide is protective against pressure overload-induced heart failure." *Regul Pept* 185:20-8. doi: 10.1016/j.regpep.2013.06.008.

Liang, Y. L., M. Khoshouei, G. Deganutti, A. Glukhova, C. Koole, T. S. Peat, M. Radjainia, J. M. Plitzko, W. Baumeister, L. J. Miller, D. L. Hay, A. Christopoulos, C. A. Reynolds, D. Wootten, and P. M. Sexton. 2018. "Cryo-EM structure of the active, Gs-protein complexed, human CGRP receptor." *Nature* 561 (7724):492-497. doi: 10.1038/s41586-018-0535-y.

Lowe, J. D., H. S. Sanderson, A. E. Cooke, M. Ostovar, E. Tsisanova, S. L. Withey, C. Chavkin, S. M. Husbands, E. Kelly, G. Henderson, and C. P. Bailey. 2015. "Role of G Protein-Coupled Receptor Kinases 2 and 3 in mu-Opioid Receptor Desensitization and Internalization." *Mol Pharmacol* 88 (2):347-56. doi: 10.1124/mol.115.098293.

Lu, J. T., Y. J. Son, J. Lee, T. L. Jetton, M. Shiota, L. Moscoso, K. D. Niswender, A. D. Loewy, M. A. Magnuson, J. R. Sanes, and R. B. Emeson. 1999. "Mice lacking alpha-calcitonin gene-related peptide exhibit normal cardiovascular regulation and neuromuscular development." *Mol Cell Neurosci* 14 (2):99-120. doi: 10.1006/mcne.1999.0767.

Macia, E., M. Ehrlich, R. Massol, E. Boucrot, C. Brunner, and T. Kirchhausen. 2006. "Dynasore, a cell-permeable inhibitor of dynamin." *Dev Cell* 10 (6):839-50. doi: 10.1016/j.devcel.2006.04.002.

Maghin, E., P. Garbati, R. Quarto, M. Piccoli, and S. Bollini. 2020. "Young at Heart: Combining Strategies to Rejuvenate Endogenous Mechanisms of Cardiac Repair." *Front Bioeng Biotechnol* 8:447. doi: 10.3389/fbioe.2020.00447.

Malik, R. U., M. Ritt, B. T. DeVree, R. R. Neubig, R. K. Sunahara, and S. Sivaramakrishnan. 2013. "Detection of G protein-selective G protein-coupled receptor (GPCR) conformations in live cells." *J Biol Chem* 288 (24):17167-78. doi: 10.1074/jbc.M113.464065.

Marinissen, M. J., and J. S. Gutkind. 2001. "G-protein-coupled receptors and signaling networks: emerging paradigms." *Trends Pharmacol Sci* 22 (7):368-76.

Matson, B. C., and K. M. Caron. 2014. "Adrenomedullin and endocrine control of immune cells during pregnancy." *Cell Mol Immunol* 11 (5):456-9. doi: 10.1038/cmi.2014.71.

Matteoli, M., C. Haimann, F. Torri-Tarelli, J. M. Polak, B. Ceccarelli, and P. De Camilli. 1988. "Differential effect of alpha-latrotoxin on exocytosis from small synaptic vesicles and from large dense-core vesicles containing calcitonin gene-related peptide at the frog neuromuscular junction." *Proc Natl Acad Sci U S A* 85 (19):7366-70. doi: 10.1073/pnas.85.19.7366.

May, V., T. R. Buttolph, B. M. Girard, T. A. Clason, and R. L. Parsons. 2014. "PACAP-induced ERK activation in HEK cells expressing PAC1 receptors involves both receptor internalization and PKC signaling." *Am J Physiol Cell Physiol* 306 (11):C1068-79. doi: 10.1152/ajpcell.00001.2014.

McLatchie, L. M., N. J. Fraser, M. J. Main, A. Wise, J. Brown, N. Thompson, R. Solari, M. G. Lee, and S. M. Foord. 1998. "RAMPs regulate the transport and ligand specificity of the calcitonin-receptor-like receptor." *Nature* 393 (6683):333-9. doi: 10.1038/30666.

Mills, R. J., B. L. Parker, G. A. Quaife-Ryan, H. K. Voges, E. J. Needham, A. Bornot, M. Ding, H. Andersson, M. Polla, D. A. Elliott, L. Drowley, M. Clausen, A. T. Plowright, I. P. Barrett, Q. D. Wang, D. E. James, E. R. Porrello, and J. E. Hudson. 2019. "Drug Screening in Human PSC-Cardiac Organoids Identifies Pro-proliferative Compounds Acting via the Mevalonate Pathway." *Cell Stem Cell* 24 (6):895-907 e6. doi: 10.1016/j.stem.2019.03.009.

Mizuno, N., and H. Itoh. 2009. "Functions and regulatory mechanisms of Gq-signaling pathways." *Neurosignals* 17 (1):42-54. doi: 10.1159/000186689.

Morimoto, R., F. Satoh, O. Murakami, K. Totsune, T. Suzuki, H. Sasano, S. Ito, and K. Takahashi. 2007. "Expression of adrenomedullin2/intermedin in human brain, heart, and kidney." *Peptides* 28 (5):1095-103. doi: 10.1016/j.peptides.2007.01.018.

Muff, R., K. Leuthauser, N. Buhlmann, S. M. Foord, J. A. Fischer, and W. Born. 1998. "Receptor activity modifying proteins regulate the activity of a calcitonin gene-related peptide receptor in rabbit aortic endothelial cells." *FEBS Lett* 441 (3):366-8.

Mukherjee, R., M. M. Multani, J. A. Sample, K. B. Dowdy, J. L. Zellner, D. B. Hoover, and F. G. Spinale. 2002. "Effects of adrenomedullin on human myocyte contractile function and beta-adrenergic response." *J Cardiovasc Pharmacol Ther* 7 (4):235-40. doi: 10.1177/107424840200700406.

Nagaya, N., and K. Kangawa. 2004. "Adrenomedullin in the treatment of pulmonary hypertension." *Peptides* 25 (11):2013-8. doi: 10.1016/j.peptides.2004.07.007.

Nagaya, N., T. Nishikimi, M. Uematsu, T. Satoh, H. Oya, S. Kyotani, F. Sakamaki, K. Ueno, N. Nakanishi, K. Miyatake, and K. Kangawa. 2000. "Haemodynamic and hormonal effects of adrenomedullin in patients with pulmonary hypertension." *Heart* 84 (6):653-8. doi: 10.1136/heart.84.6.653.

Nagaya, N., T. Satoh, T. Nishikimi, M. Uematsu, S. Furuichi, F. Sakamaki, H. Oya, S. Kyotani, N. Nakanishi, Y. Goto, Y. Masuda, K. Miyatake, and K. Kangawa. 2000. "Hemodynamic, renal, and hormonal effects of adrenomedullin infusion in patients with congestive heart failure." *Circulation* 101 (5):498-503. doi: 10.1161/01.cir.101.5.498.

Naot, D., and J. Cornish. 2008. "The role of peptides and receptors of the calcitonin family in the regulation of bone metabolism." *Bone* 43 (5):813-8. doi: 10.1016/j.bone.2008.07.003.

Nelson, M. T., Y. Huang, J. E. Brayden, J. Hescheler, and N. B. Standen. 1990. "Arterial dilations in response to calcitonin gene-related peptide involve activation of K+ channels." *Nature* 344 (6268):770-3. doi: 10.1038/344770a0.

Neves, S. R., P. T. Ram, and R. Iyengar. 2002. "G protein pathways." *Science* 296 (5573):1636-9. doi: 10.1126/science.1071550.

Nikitenko, L. L., N. Blucher, S. B. Fox, R. Bicknell, D. M. Smith, and M. C. Rees. 2006. "Adrenomedullin and CGRP interact with endogenous calcitonin-receptor-like receptor in endothelial cells and induce its desensitisation by different mechanisms." *J Cell Sci* 119 (Pt 5):910-22. doi: 10.1242/jcs.02783.

Nikitenko, L. L., R. Leek, S. Henderson, N. Pillay, H. Turley, D. Generali, S. Gunningham, H. R. Morrin, A. Pellagatti, M. C. Rees, A. L. Harris, and S. B. Fox. 2013. "The G-protein-coupled receptor CLR is upregulated in an autocrine loop with adrenomedullin in clear cell renal cell carcinoma and associated with poor prognosis." *Clin Cancer Res* 19 (20):5740-8. doi: 10.1158/1078-0432.ccr-13-1712.

Njuki, F., C. G. Nicholl, A. Howard, J. C. Mak, P. J. Barnes, S. I. Girgis, and S. Legon. 1993. "A new calcitonin-receptor-like sequence in rat pulmonary blood vessels." *Clin Sci (Lond)* 85 (4):385-8.

Oakley, R. H., S. A. Laporte, J. A. Holt, L. S. Barak, and M. G. Caron. 1999. "Association of beta-arrestin with G protein-coupled receptors during clathrin-mediated endocytosis dictates the profile of receptor resensitization." *J Biol Chem* 274 (45):32248-57. doi: 10.1074/jbc.274.45.32248.

Offermanns, S., Y. H. Hu, and M. I. Simon. 1996. "Galpha12 and galpha13 are phosphorylated during platelet activation." *J Biol Chem* 271 (42):26044-8. doi: 10.1074/jbc.271.42.26044.

Oldham, W. M., and H. E. Hamm. 2008. "Heterotrimeric G protein activation by G-protein-coupled receptors." *Nat Rev Mol Cell Biol* 9 (1):60-71. doi: 10.1038/nrm2299.

Olesen, J., H. C. Diener, I. W. Husstedt, P. J. Goadsby, D. Hall, U. Meier, S. Pollentier, L. M. Lesko, and Bibn Bs Clinical Proof of Concept Study Group. 2004. "Calcitonin gene-related peptide receptor antagonist BIBN 4096 BS for the acute treatment of migraine." *N Engl J Med* 350 (11):1104-10. doi: 10.1056/NEJMoa030505.

Onaran, H. O., S. Rajagopal, and T. Costa. 2014. "What is biased efficacy? Defining the relationship between intrinsic efficacy and free energy coupling." *Trends Pharmacol Sci* 35 (12):639-47. doi: 10.1016/j.tips.2014.09.010.

Onat, D., D. Brillon, P. C. Colombo, and A. M. Schmidt. 2011. "Human vascular endothelial cells: a model system for studying vascular inflammation in diabetes and atherosclerosis." *Curr Diab Rep* 11 (3):193-202. doi: 10.1007/s11892-011-0182-2.

Ostrovskaya, A., C. Hick, D. S. Hutchinson, B. W. Stringer, P. J. Wookey, D. Wootten, P. M. Sexton, and S. G. B. Furness. 2019. "Expression and activity of the calcitonin receptor family in a sample of primary human high-grade gliomas." *BMC Cancer* 19 (1):157. doi: 10.1186/s12885-019-5369-y.

Pagès, G., P. Lenormand, G. L'Allemain, J. C. Chambard, S. Meloche, and J. Pouysségur. 1993. "Mitogen-activated protein kinases p42mapk and p44mapk are required for fibroblast proliferation." *Proc Natl Acad Sci U S A* 90 (18):8319-23. doi: 10.1073/pnas.90.18.8319.

Palczewski, K., T. Kumasaka, T. Hori, C. A. Behnke, H. Motoshima, B. A. Fox, I. Le Trong, D. C. Teller, T. Okada, R. E. Stenkamp, M. Yamamoto, and M. Miyano. 2000. "Crystal structure of rhodopsin: A G protein-coupled receptor." *Science* 289 (5480):739-45. doi: 10.1126/science.289.5480.739.

Pandy-Szekeres, G., C. Munk, T. M. Tsonkov, S. Mordalski, K. Harpsoe, A. S. Hauser, A. J. Bojarski, and D. E. Gloriam. 2018. "GPCRdb in 2018: adding GPCR structure models and ligands." *Nucleic Acids Res* 46 (D1):D440-D446. doi: 10.1093/nar/gkx1109.

Pavlos, N. J., and P. A. Friedman. 2017. "GPCR Signaling and Trafficking: The Long and Short of It." *Trends Endocrinol Metab* 28 (3):213-226. doi: 10.1016/j.tem.2016.10.007.

Penheiter, S. G., H. Mitchell, N. Garamszegi, M. Edens, J. J. Dore, Jr., and E. B. Leof. 2002. "Internalization-dependent and -independent requirements for transforming growth factor beta receptor signaling via the Smad pathway." *Mol Cell Biol* 22 (13):4750-9. doi: 10.1128/mcb.22.13.4750-4759.2002.

Perez-Villa, F., A. Leivas, E. Roig, W. Jimenez, and G. Sanz. 2004. "Adrenomedullin messenger RNA expression is increased in myocardial tissue of patients with idiopathic dilated cardiomyopathy." *J Heart Lung Transplant* 23 (11):1297-300. doi: 10.1016/j.healun.2003.09.002.

Perret, M., H. Broussard, T. LeGros, A. Burns, J. K. Chang, W. Summer, A. Hyman, and H. Lippton. 1993. "The effect of adrenomedullin on the isolated heart." *Life Sci* 53 (22):PL377-9. doi: 10.1016/0024-3205(93)90213-m.

Petersen, K. A., S. Birk, L. H. Lassen, C. Kruuse, O. Jonassen, L. Lesko, and J. Olesen. 2005. "The CGRP-antagonist, BIBN4096BS does not affect cerebral or systemic haemodynamics in healthy volunteers." *Cephalalgia* 25 (2):139-47. doi: 10.1111/j.1468-2982.2004.00830.x.

Peterson, Y. K., and L. M. Luttrell. 2017. "The Diverse Roles of Arrestin Scaffolds in G Protein-Coupled Receptor Signaling." *Pharmacol Rev* 69 (3):256-297. doi: 10.1124/pr.116.013367.

Pike, L. J., X. Han, K. N. Chung, and R. W. Gross. 2002. "Lipid rafts are enriched in arachidonic acid and plasmenylethanolamine and their composition is independent of caveolin-1 expression: a quantitative electrospray ionization/mass spectrometric analysis." *Biochemistry* 41 (6):2075-88. doi: 10.1021/bi0156557.

Pillekamp, F., M. Haustein, M. Khalil, M. Emmelheinz, R. Nazzal, R. Adelmann, F. Nguemo, O. Rubenchyk, K. Pfannkuche, M. Matzkies, M. Reppel, W. Bloch, K. Brockmeier, and J. Hescheler. 2012. "Contractile properties of early human embryonic stem cell-derived cardiomyocytes: beta-adrenergic stimulation induces positive chronotropy and lusitropy but not inotropy." *Stem Cells Dev* 21 (12):2111-21. doi: 10.1089/scd.2011.0312.

Pires, A. L., M. Pinho, C. M. Sena, R. Seica, and A. F. Leite-Moreira. 2012. "Intermedin elicits a negative inotropic effect in rat papillary muscles mediated by endothelial-derived nitric oxide." *Am J Physiol Heart Circ Physiol* 302 (5):H1131-7. doi: 10.1152/ajpheart.00877.2011.

Poyner, D. R., P. M. Sexton, I. Marshall, D. M. Smith, R. Quirion, W. Born, R. Muff, J. A. Fischer, and S. M. Foord. 2002. "International Union of Pharmacology. XXXII. The mammalian calcitonin gene-related peptides, adrenomedullin, amylin, and calcitonin receptors." *Pharmacol Rev* 54 (2):233-46.

Qi, T., M. Dong, H. A. Watkins, D. Wootten, L. J. Miller, and D. L. Hay. 2013. "Receptor activity-modifying protein-dependent impairment of calcitonin receptor splice variant Delta(1-47)hCT((a)) function." *Br J Pharmacol* 168 (3):644-57. doi: 10.1111/j.1476-5381.2012.02197.x.

Qin, C. X., L. T. May, R. Li, N. Cao, S. Rosli, M. Deo, A. E. Alexander, D. Horlock, J. E. Bourke, Y. H. Yang, A. G. Stewart, D. M. Kaye, X. J. Du, P. M. Sexton, A. Christopoulos, X. M. Gao, and R. H. Ritchie. 2017. "Small-molecule-biased formyl peptide receptor agonist compound 17b protects against myocardial ischaemia-reperfusion injury in mice." *Nat Commun* 8:14232. doi: 10.1038/ncomms14232.

Quallo, T., C. Gentry, S. Bevan, L. M. Broad, and A. J. Mogg. 2015. "Activation of transient receptor potential ankyrin 1 induces CGRP release from spinal cord synaptosomes." *Pharmacol Res Perspect* 3 (6):e00191. doi: 10.1002/prp2.191.

Raehal, K. M., C. L. Schmid, C. E. Groer, and L. M. Bohn. 2011. "Functional selectivity at the mu-opioid receptor: implications for understanding opioid analgesia and tolerance." *Pharmacol Rev* 63 (4):1001-19. doi: 10.1124/pr.111.004598.

Raehal, K. M., J. K. Walker, and L. M. Bohn. 2005. "Morphine side effects in beta-arrestin 2 knockout mice." *J Pharmacol Exp Ther* 314 (3):1195-201. doi: 10.1124/jpet.105.087254.

Rajagopal, S., K. Rajagopal, and R. J. Lefkowitz. 2010. "Teaching old receptors new tricks: biasing seven-transmembrane receptors." *Nat Rev Drug Discov* 9 (5):373-86. doi: 10.1038/nrd3024.

Ran, F. A., P. D. Hsu, J. Wright, V. Agarwala, D. A. Scott, and F. Zhang. 2013. "Genome engineering using the CRISPR-Cas9 system." *Nat Protoc* 8 (11):2281-2308. doi: 10.1038/nprot.2013.143.

Ranjan, R., H. Dwivedi, M. Baidya, M. Kumar, and A. K. Shukla. 2017. "Novel Structural Insights into GPCR-beta-Arrestin Interaction and Signaling." *Trends Cell Biol* 27 (11):851-862. doi: 10.1016/j.tcb.2017.05.008.

Ravnskjaer, K., A. Madiraju, and M. Montminy. 2016. "Role of the cAMP Pathway in Glucose and Lipid Metabolism." *Handb Exp Pharmacol* 233:29-49. doi: 10.1007/164_2015_32.

Roh, J., C. L. Chang, A. Bhalla, C. Klein, and S. Y. Hsu. 2004. "Intermedin is a calcitonin/calcitonin gene-related peptide family peptide acting through the calcitonin receptor-like receptor/receptor activity-modifying protein receptor complexes." *J Biol Chem* 279 (8):7264-74. doi: 10.1074/jbc.M305332200.

Rosenfeld, M. G., J. J. Mermod, S. G. Amara, L. W. Swanson, P. E. Sawchenko, J. Rivier, W. W. Vale, and R. M. Evans. 1983. "Production of a novel neuropeptide encoded by the calcitonin gene via tissue-specific RNA processing." *Nature* 304 (5922):129-35. doi: 10.1038/304129a0.

Routledge, S. J., J. Simms, A. Clark, H. Y. Yeung, M. J. Wigglesworth, I. M. Dickerson, P. Kitchen, G. Ladds, and D. R. Poyner. 2020. "Receptor component protein, an endogenous allosteric modulator of family B G protein coupled receptors." *Biochim Biophys Acta Biomembr* 1862 (3):183174. doi: 10.1016/j.bbamem.2019.183174.

Rubart, M., and L. J. Field. 2006. "Cardiac regeneration: repopulating the heart." *Annu Rev Physiol* 68:29-49. doi: 10.1146/annurev.physiol.68.040104.124530.

Safitri, D., M. Harris, H. Potter, H. Yan Yeung, I. Winfield, L. Kopanitsa, F. Svensson, T. Rahman, M. T. Harper, D. Bailey, and G. Ladds. 2020. "Elevated intracellular cAMP concentration mediates growth suppression in glioma cells." *Biochem Pharmacol* 174:113823. doi: 10.1016/j.bcp.2020.113823.

Santiago, J. A., E. Garrison, W. L. Purnell, R. E. Smith, H. C. Champion, D. H. Coy, W. A. Murphy, and P. J. Kadowitz. 1995. "Comparison of responses to adrenomedullin and adrenomedullin analogs in the mesenteric vascular bed of the cat." *Eur J Pharmacol* 272 (1):115-8. doi: 10.1016/0014-2999(94)00693-2.

Sarig, U., H. Sarig, E. de-Berardinis, S. Y. Chaw, E. B. Nguyen, V. S. Ramanujam, V. D. Thang, M. Al-Haddawi, S. Liao, D. Seliktar, T. Kofidis, F. Y. Boey, S. S. Venkatraman, and M. Machluf. 2016. "Natural myocardial ECM patch drives cardiac progenitor based restoration even after scarring." *Acta Biomater* 44:209-20. doi: 10.1016/j.actbio.2016.08.031.

Sata, M., M. Kakoki, D. Nagata, H. Nishimatsu, E. Suzuki, T. Aoyagi, S. Sugiura, H. Kojima, T. Nagano, K. Kangawa, H. Matsuo, M. Omata, R. Nagai, and Y. Hirata. 2000. "Adrenomedullin and nitric oxide inhibit human endothelial cell apoptosis via a cyclic GMP-independent mechanism." *Hypertension* 36 (1):83-8. doi: 10.1161/01.hyp.36.1.83.

Schaeffer, C., D. Vandroux, L. Thomassin, P. Athias, L. Rochette, and J. L. Connat. 2003. "Calcitonin gene-related peptide partly protects cultured smooth muscle cells from apoptosis induced by an oxidative stress via activation of ERK1/2 MAPK." *Biochim Biophys Acta* 1643 (1-3):65-73. doi: 10.1016/j.bbamcr.2003.09.005.

Schioth, H. B., and R. Fredriksson. 2005. "The GRAFS classification system of G-protein coupled receptors in comparative perspective." *Gen Comp Endocrinol* 142 (1-2):94-101. doi: 10.1016/j.ygcen.2004.12.018.

Schonauer, R., A. Kaiser, C. Holze, S. Babilon, J. Kobberling, B. Riedl, and A. G. Beck-Sickinger. 2015. "Fluorescently labeled adrenomedullin allows real-time monitoring of adrenomedullin receptor trafficking in living cells." *J Pept Sci* 21 (12):905-12. doi: 10.1002/psc.2833.

Schwede, F., E. Maronde, H. Genieser, and B. Jastorff. 2000. "Cyclic nucleotide analogs as biochemical tools and prospective drugs." *Pharmacol Ther* 87 (2-3):199-226. doi: 10.1016/s0163-7258(00)00051-6.

Senyo, S. E., M. L. Steinhauser, C. L. Pizzimenti, V. K. Yang, L. Cai, M. Wang, T. D. Wu, J. L. Guerquin-Kern, C. P. Lechene, and R. T. Lee. 2013. "Mammalian heart renewal by pre-existing cardiomyocytes." *Nature* 493 (7432):433-6. doi: 10.1038/nature11682.

Serafin, D. S., N. R. Harris, N. R. Nielsen, D. I. Mackie, and K. M. Caron. 2020. "Dawn of a New RAMPage." *Trends Pharmacol Sci* 41 (4):249-265. doi: 10.1016/j.tips.2020.01.009.

Shenoy, S. K., M. T. Drake, C. D. Nelson, D. A. Houtz, K. Xiao, S. Madabushi, E. Reiter, R. T. Premont, O. Lichtarge, and R. J. Lefkowitz. 2006. "beta-arrestin-dependent, G protein-independent ERK1/2 activation by the beta2 adrenergic receptor." *J Biol Chem* 281 (2):1261-73. doi: 10.1074/jbc.M506576200.

Sheykhzade, M., B. Abdolalizadeh, C. Koole, D. S. Pickering, K. Dreisig, S. E. Johansson, B. K. Abboud, R. Dreier, J. O. Berg, J. L. Jeppesen, P. M. Sexton, L. Edvinsson, D. Wootten, and A. Sams. 2018. "Vascular and molecular pharmacology of the metabolically stable CGRP analogue, SAX." *Eur J Pharmacol* 829:85-92. doi: 10.1016/j.ejphar.2018.04.007.

Shukla, A. K., G. H. Westfield, K. Xiao, R. I. Reis, L. Y. Huang, P. Tripathi-Shukla, J. Qian, S. Li, A. Blanc, A. N. Oleskie, A. M. Dosey, M. Su, C. R. Liang, L. L. Gu, J. M. Shan, X. Chen, R. Hanna, M. Choi, X. J. Yao, B. U. Klink, A. W. Kahsai, S. S. Sidhu, S. Koide, P. A. Penczek, A. A. Kossiakoff, V. L. Woods, Jr., B. K. Kobilka, G. Skiniotis, and R. J. Lefkowitz. 2014. "Visualization of arrestin recruitment by a G-protein-coupled receptor." *Nature* 512 (7513):218-22. doi: 10.1038/nature13430.

Singer, W. D., R. T. Miller, and P. C. Sternweis. 1994. "Purification and characterization of the alpha subunit of G13." *J Biol Chem* 269 (31):19796-802.

Singla, N. K., F. Skobieranda, D. G. Soergel, M. Salamea, D. A. Burt, M. A. Demitrack, and E. R. Viscusi. 2019. "APOLLO-2: A Randomized, Placebo and Active-Controlled Phase III Study Investigating Oliceridine (TRV130), a G Protein-Biased Ligand at the mu-Opioid Receptor, for Management of Moderate to Severe Acute Pain Following Abdominoplasty." *Pain Pract* 19 (7):715-731. doi: 10.1111/papr.12801.

Sit, S. T., and E. Manser. 2011. "Rho GTPases and their role in organizing the actin cytoskeleton." *J Cell Sci* 124 (Pt 5):679-83. doi: 10.1242/jcs.064964.

Slusarski, D. C., V. G. Corces, and R. T. Moon. 1997. "Interaction of Wnt and a Frizzled homologue triggers G-protein-linked phosphatidylinositol signalling." *Nature* 390 (6658):410-3. doi: 10.1038/37138.

Smith, J. S., R. J. Lefkowitz, and S. Rajagopal. 2018. "Biased signalling: from simple switches to allosteric microprocessors." *Nat Rev Drug Discov* 17 (4):243-260. doi: 10.1038/nrd.2017.229.

Sorkin, A., and G. Carpenter. 1993. "Interaction of activated EGF receptors with coated pit adaptins." *Science* 261 (5121):612-5. doi: 10.1126/science.8342026.

Sriram, K., and P. A. Insel. 2018. "G Protein-Coupled Receptors as Targets for Approved Drugs: How Many Targets and How Many Drugs?" *Mol Pharmacol* 93 (4):251-258. doi: 10.1124/mol.117.111062.

Stewart, S., K. MacIntyre, D. J. Hole, S. Capewell, and J. J. McMurray. 2001. "More 'malignant' than cancer? Five-year survival following a first admission for heart failure." *Eur J Heart Fail* 3 (3):315-22. doi: 10.1016/s1388-9842(00)00141-0.

Strungs, E. G., and L. M. Luttrell. 2014. "Arrestin-dependent activation of ERK and Src family kinases." *Handb Exp Pharmacol* 219:225-57. doi: 10.1007/978-3-642-41199-1_12.

Sugo, S., N. Minamino, K. Kangawa, K. Miyamoto, K. Kitamura, J. Sakata, T. Eto, and H. Matsuo. 1994. "Endothelial cells actively synthesize and secrete adrenomedullin." *Biochem Biophys Res Commun* 201 (3):1160-6. doi: 10.1006/bbrc.1994.1827.

Taimeh, Z., J. Loughran, E. J. Birks, and R. Bolli. 2013. "Vascular endothelial growth factor in heart failure." *Nat Rev Cardiol* 10 (9):519-30. doi: 10.1038/nrcardio.2013.94.

Takasaki, J., T. Saito, M. Taniguchi, T. Kawasaki, Y. Moritani, K. Hayashi, and M. Kobori. 2004. "A novel Galphaq/11-selective inhibitor." *J Biol Chem* 279 (46):47438-45. doi: 10.1074/jbc.M408846200.

Takei, Y., K. Inoue, M. Ogoshi, T. Kawahara, H. Bannai, and S. Miyano. 2004. "Identification of novel adrenomedullin in mammals: a potent cardiovascular and renal regulator." *FEBS Lett* 556 (1-3):53-8. doi: 10.1016/s0014-5793(03)01368-1.

Temmesfeld-Wollbrück, B., A. C. Hocke, N. Suttorp, and S. Hippenstiel. 2007. "Adrenomedullin and endothelial barrier function." *Thromb Haemost* 98 (5):944-51. doi: 10.1160/th07-02-0128.

Thal, D. M., R. Y. Yeow, C. Schoenau, J. Huber, and J. J. Tesmer. 2011. "Molecular mechanism of selectivity among G protein-coupled receptor kinase 2 inhibitors." *Mol Pharmacol* 80 (2):294-303. doi: 10.1124/mol.111.071522.

Theocharis, A. D., S. S. Skandalis, C. Gialeli, and N. K. Karamanos. 2016. "Extracellular matrix structure." *Adv Drug Deliv Rev* 97:4-27. doi: 10.1016/j.addr.2015.11.001.

Thillaiappan, N. B., P. Chakraborty, G. Hasan, and C. W. Taylor. 2019. "IP3 receptors and Ca(2+) entry." *Biochim Biophys Acta Mol Cell Res* 1866 (7):1092-1100. doi: 10.1016/j.bbamcr.2018.11.007.

Thomsen, A. R. B., B. Plouffe, T. J. Cahill, A. K. Shukla, J. T. Tarrasch, A. M. Dosey, A. W. Kahsai, R. T. Strachan, B. Pani, J. P. Mahoney, L. Huang, B. Breton, F. M. Heydenreich, R. K. Sunahara, G. Skiniotis, M. Bouvier, and R. J. Lefkowitz. 2016. "GPCR-G Protein-β-Arrestin Super-Complex Mediates Sustained G Protein Signaling." *Cell* 166 (4):907-919. doi: 10.1016/j.cell.2016.07.004.

Tsuruda, T., J. Kato, K. Kuwasako, and K. Kitamura. 2019. "Adrenomedullin: Continuing to explore cardioprotection." *Peptides* 111:47-54. doi: 10.1016/j.peptides.2018.03.012.

Tsvetanova, N. G., and M. von Zastrow. 2014. "Spatial encoding of cyclic AMP signaling specificity by GPCR endocytosis." *Nat Chem Biol* 10 (12):1061-5. doi: 10.1038/nchembio.1665.

Van der Schueren, B. J., A. Rogiers, F. H. Vanmolkot, A. Van Hecken, M. Depre, S. A. Kane, I. De Lepeleire, S. R. Sinclair, and J. N. de Hoon. 2008. "Calcitonin gene-related peptide8-37 antagonizes capsaicin-induced vasodilation in the skin: evaluation of a human in vivo pharmacodynamic model." *J Pharmacol Exp Ther* 325 (1):248-55. doi: 10.1124/jpet.107.133868.

Vaniotis, G., I. Glazkova, C. Merlen, C. Smith, L. R. Villeneuve, D. Chatenet, M. Therien, A. Fournier, A. Tadevosyan, P. Trieu, S. Nattel, T. E. Hébert, and B. G. Allen. 2013. "Regulation of cardiac nitric oxide signaling by nuclear β-adrenergic and endothelin receptors." *J Mol Cell Cardiol* 62:58-68. doi: 10.1016/j.yjmcc.2013.05.003.

Verin, A. D., F. Liu, N. Bogatcheva, T. Borbiev, M. B. Hershenson, P. Wang, and J. G. Garcia. 2000. "Role of ras-dependent ERK activation in phorbol ester-induced endothelial cell barrier dysfunction." *Am J Physiol Lung Cell Mol Physiol* 279 (2):L360-70. doi: 10.1152/ajplung.2000.279.2.L360.

Violin, J. D., and R. J. Lefkowitz. 2007. "Beta-arrestin-biased ligands at seven-transmembrane receptors." *Trends Pharmacol Sci* 28 (8):416-22. doi: 10.1016/j.tips.2007.06.006.

Walker, C. S., S. Eftekhari, R. L. Bower, A. Wilderman, P. A. Insel, L. Edvinsson, H. J. Waldvogel, M. A. Jamaluddin, A. F. Russo, and D. L. Hay. 2015. "A second trigeminal CGRP receptor: function and expression of the AMY1 receptor." *Ann Clin Transl Neurol* 2 (6):595-608. doi: 10.1002/acn3.197.

Wei, H., S. Ahn, S. K. Shenoy, S. S. Karnik, L. Hunyady, L. M. Luttrell, and R. J. Lefkowitz. 2003. "Independent beta-arrestin 2 and G protein-mediated pathways for angiotensin II activation of extracellular signal-regulated kinases 1 and 2." *Proc Natl Acad Sci U S A* 100 (19):10782-7. doi: 10.1073/pnas.1834556100.

Wei, P., X. J. Yang, Q. Fu, B. Han, L. Ling, J. Bai, B. Zong, and C. Y. Jiang. 2015. "Intermedin attenuates myocardial infarction through activation of autophagy in a rat model of ischemic heart failure via both cAMP and MAPK/ERK1/2 pathways." *Int J Clin Exp Pathol* 8 (9):9836-44.

Weston, C., I. Winfield, M. Harris, R. Hodgson, A. Shah, S. J. Dowell, J. C. Mobarec, D. A. Woodlock, C. A. Reynolds, D. R. Poyner, H. A. Watkins, and G. Ladds. 2016. "Receptor Activity-modifying Protein-directed G Protein Signaling Specificity for the Calcitonin Gene-related Peptide Family of Receptors." *J Biol Chem* 291 (42):21925-21944. doi: 10.1074/jbc.M116.751362.

Willoughby, D., and D. M. Cooper. 2007. "Organization and Ca2+ regulation of adenylyl cyclases in cAMP microdomains." *Physiol Rev* 87 (3):965-1010. doi: 10.1152/physrev.00049.2006.

Wimalawansa, S. J. 1997. "Amylin, calcitonin gene-related peptide, calcitonin, and adrenomedullin: a peptide superfamily." *Crit Rev Neurobiol* 11 (2-3):167-239. doi: 10.1615/critrevneurobiol.v11.i2-3.40.

Wisler, J. W., K. Xiao, A. R. Thomsen, and R. J. Lefkowitz. 2014. "Recent developments in biased agonism." *Curr Opin Cell Biol* 27:18-24. doi: 10.1016/j.ceb.2013.10.008.

Wootten, D., A. Christopoulos, M. Marti-Solano, M. M. Babu, and P. M. Sexton. 2018. "Mechanisms of signalling and biased agonism in G protein-coupled receptors." *Nat Rev Mol Cell Biol* 19 (10):638-653. doi: 10.1038/s41580-018-0049-3.

Wootten, D., L. J. Miller, C. Koole, A. Christopoulos, and P. M. Sexton. 2017. "Allostery and Biased Agonism at Class B G Protein-Coupled Receptors." *Chem Rev* 117 (1):111-138. doi: 10.1021/acs.chemrev.6b00049.

Xuan, W., M. Khan, and M. Ashraf. 2020. "Extracellular Vesicles From Notch Activated Cardiac Mesenchymal Stem Cells Promote Myocyte Proliferation and Neovasculogenesis." *Front Cell Dev Biol* 8:11. doi: 10.3389/fcell.2020.00011.

Yang, J. H., C. S. Pan, Y. X. Jia, J. Zhang, J. Zhao, Y. Z. Pang, J. Yang, C. S. Tang, and Y. F. Qi. 2006. "Intermedin1-53 activates L-arginine/nitric oxide synthase/nitric oxide pathway in rat aortas." *Biochem Biophys Res Commun* 341 (2):567-72. doi: 10.1016/j.bbrc.2006.01.010.

Yang, X., L. Pabon, and C. E. Murry. 2014. "Engineering adolescence: maturation of human pluripotent stem cell-derived cardiomyocytes." *Circ Res* 114 (3):511-23. doi: 10.1161/CIRCRESAHA.114.300558.

Yarwood, R. E., W. L. Imlach, T. Lieu, N. A. Veldhuis, D. D. Jensen, C. Klein Herenbrink, L. Aurelio, Z. Cai, M. J. Christie, D. P. Poole, C. J. H. Porter, P. McLean, G. A. Hicks, P. Geppetti, M. L. Halls, M. Canals, and N. W. Bunnett. 2017. "Endosomal signaling of the receptor for calcitonin gene-related peptide mediates pain transmission." *Proc Natl Acad Sci U S A* 114 (46):12309-12314. doi: 10.1073/pnas.1706656114.

Yoshida, S., and S. Plant. 1992. "Mechanism of release of Ca2+ from intracellular stores in response to ionomycin in oocytes of the frog Xenopus laevis." *J Physiol* 458:307-18.

Zaidi, M., S. D. Brain, J. R. Tippins, V. Di Marzo, B. S. Moonga, T. J. Chambers, H. R. Morris, and I. MacIntyre. 1990. "Structure-activity relationship of human calcitonin-gene-related peptide." *Biochem J* 269 (3):775-80. doi: 10.1042/bj2690775.

Zhang, B., A. Albaker, B. Plouffe, C. Lefebvre, and M. Tiberi. 2014. "Constitutive activities and inverse agonism in dopamine receptors." *Adv Pharmacol* 70:175-214. doi: 10.1016/B978-0-12-417197-8.00007-9.

Zhao, P., Y. L. Liang, M. J. Belousoff, G. Deganutti, M. M. Fletcher, F. S. Willard, M. G. Bell, M. E. Christe, K. W. Sloop, A. Inoue, T. T. Truong, L. Clydesdale, S. G. B. Furness, A. Christopoulos, M. W. Wang, L. J. Miller, C. A. Reynolds, R. Danev, P. M. Sexton, and D. Wootten. 2020. "Activation of the GLP-1 receptor by a non-peptidic agonist." *Nature* 577 (7790):432-436. doi: 10.1038/s41586-019-1902-z.

Chapter 8. Appendices

Supplemental Figures

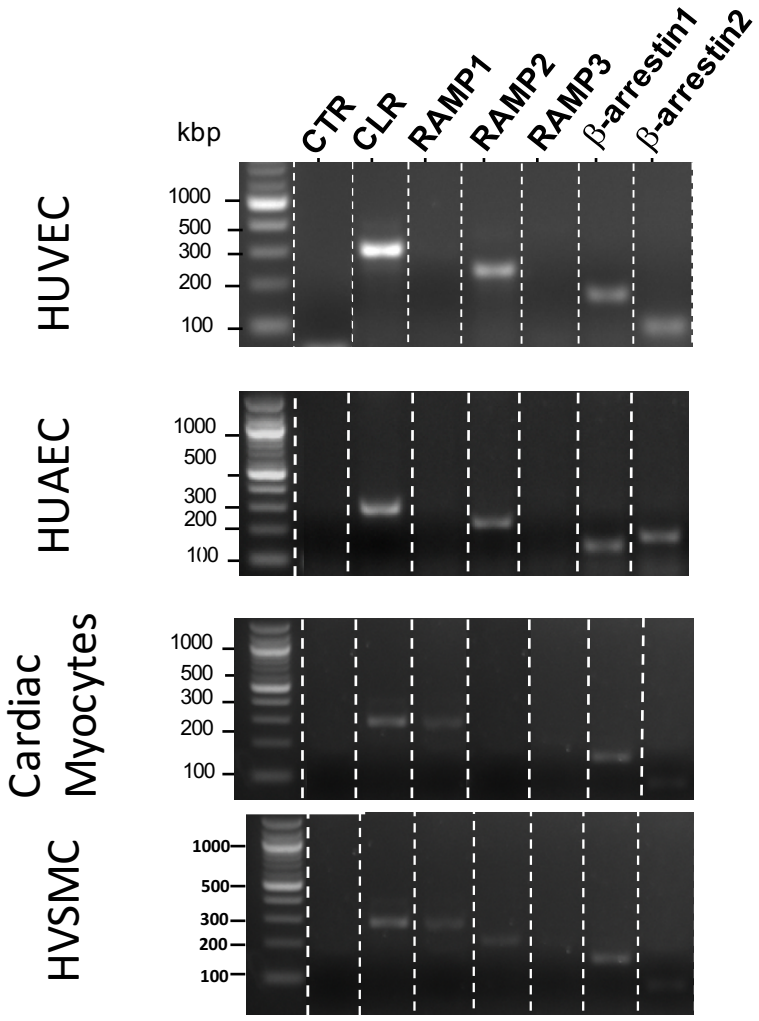

Supplemental Figure 8.1. RT-PCR Gel Images for CGRP receptors. Raw image examples of RT-PCR to determine mRNA expression of CGRP receptor components in a variety of human primary cells

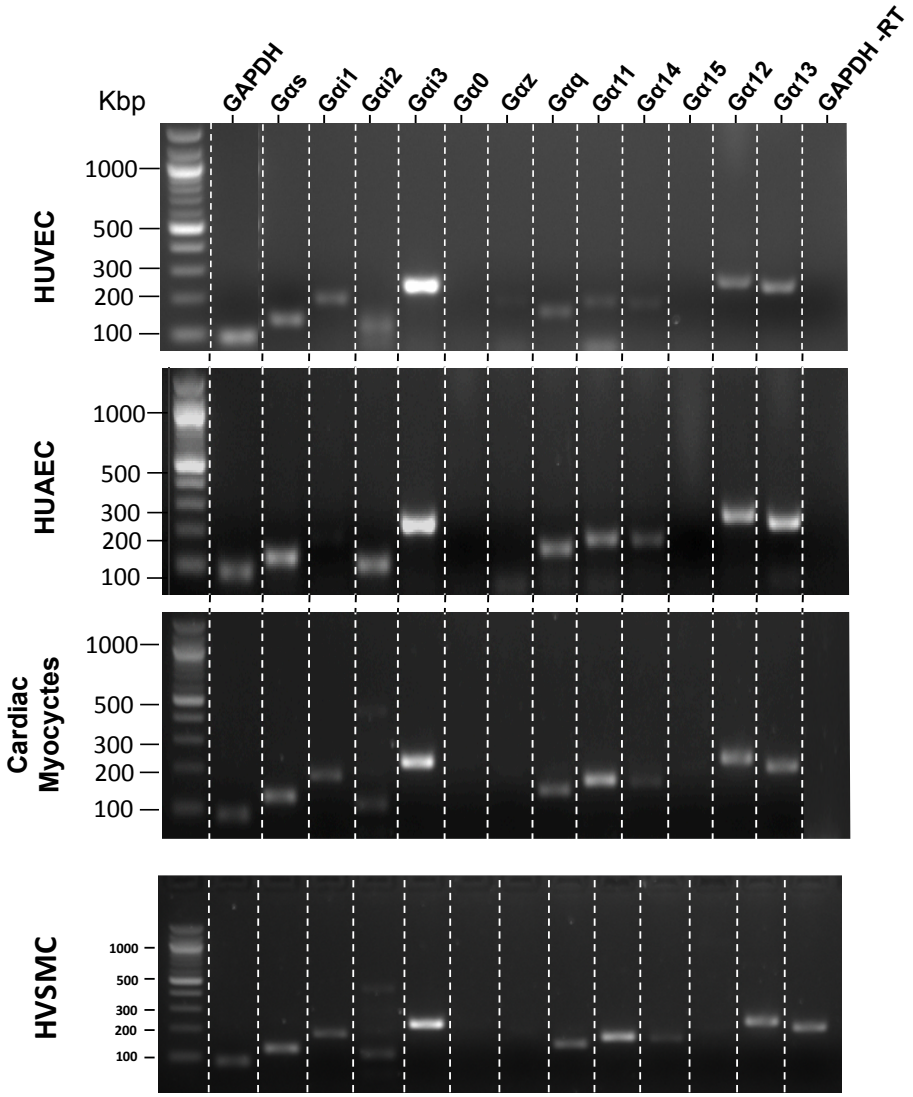

Supplemental Figure 8.2. RT-PCR Gel Images for GPCR components. Raw image examples of RT-PCR to determine mRNA expression of GPCR signaling components in a variety of human primary cells.

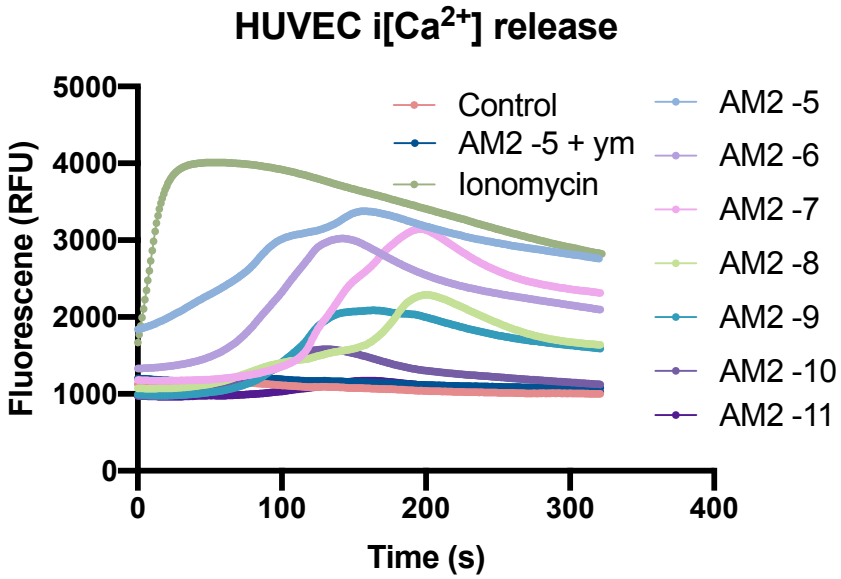

Supplemental Figure 8.3. Example raw intracellular calcium release trace. This trace shows over time the fluorescence output from fluo4 binding to intracellular calcium upon stimulation by a range of concentrations of AM2 as well as Ionomycin, Control solution, and AM2 action on HUVECs pre-treated with YM-254890. Measured on a BD pathway

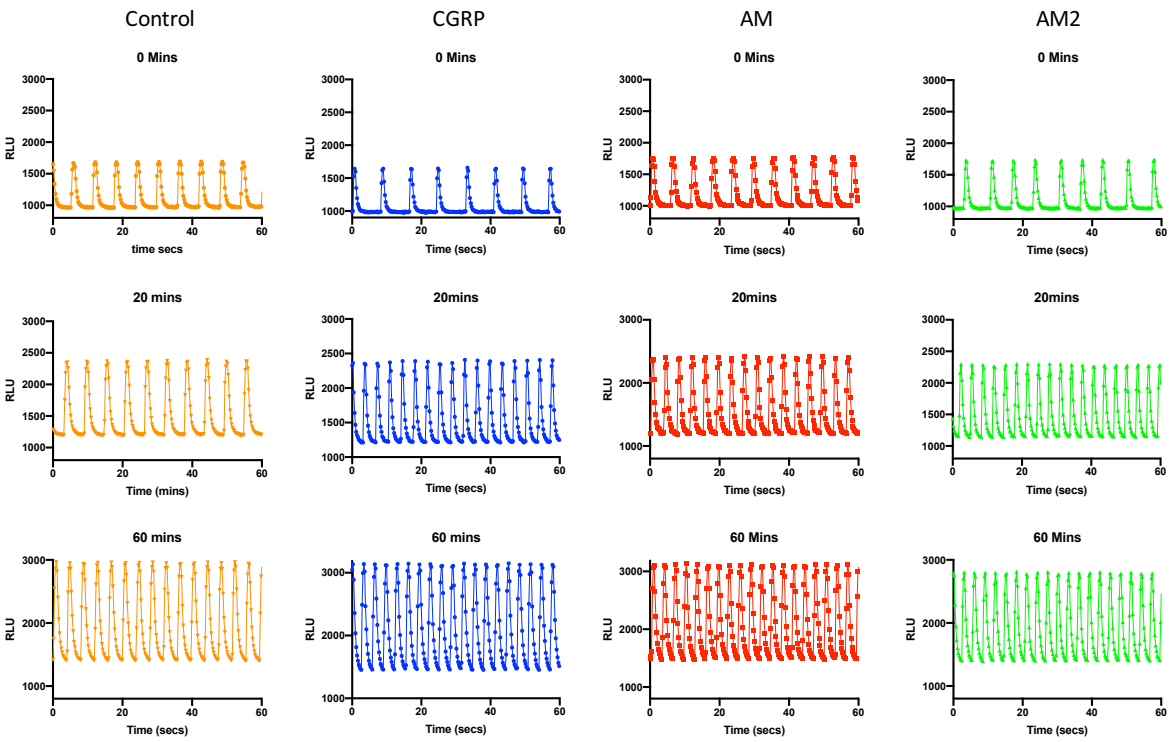

Supplemental Figure 8.4. Example raw calcium release traces. These traces show a snapshot of the intracellular calcium fluxes in a spontaneously beating icell myocyte in response to control solution, CGRP, AM, and AM2. Measured on a FLIPR system.

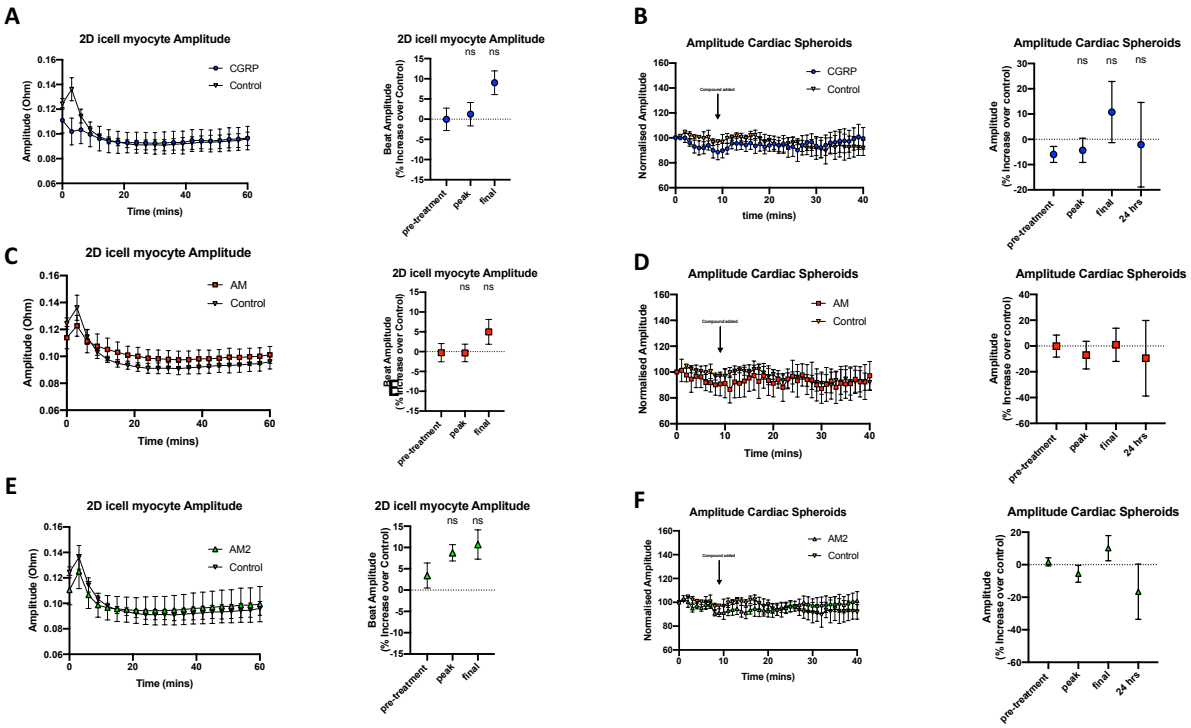

Supplemental Figure 8.5. Beat rate of icell cardiac myocytes grown in 2D (A,C,E) and 3D (B,D,F) spheroids in response to CGRP family peptide treatment. Measurement of IPSC derived icell human cardiac myocyte monolayer spheroid beat amplitudes in response to CGRP (**A,B**), AM (**C,D**), and AM2 (**E,F**) (10μM) and Control treatment. Percentage increase in beat amplitude in response to CGRP, AM, and AM2 and relative to control treatment at multiple time points is shown alongside each set of traces. Statistical significance determined compared to control using an unpaired t test with Welch's correction (*, p<0.05; **, p<0.01; ***, p<0.001 ****, p<0.0001). NS denotes no statistical significance observed. All values are calculated from 4 individual data sets.

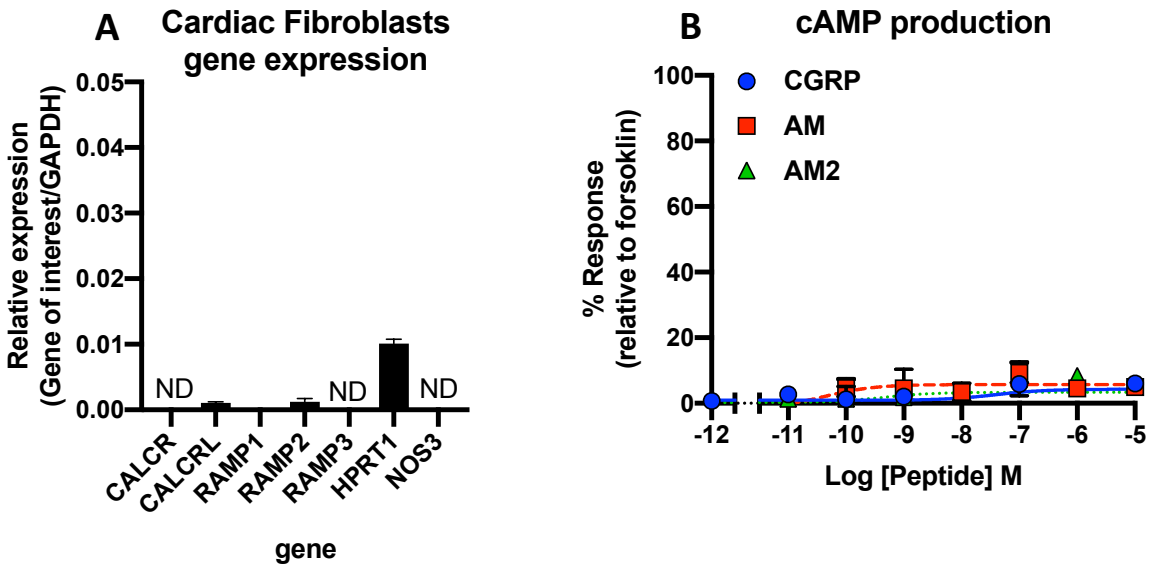

Supplemental Figure 8.6. Receptor Expression and cAMP signalling in human Cardiac Fibroblasts in response to the Calcitonin peptide family and CGRP peptide family. Expression of CALCR, CALCRL, RAMP1, RAMP2, RAMP3, HPRT1 and NOS3 genes determined by qRT-PCR (**A**). Data represent mean + SEM of three independent experiments relative to GAPDH expression. ND = not detected in all three samples. Characterisation of cAMP accumulation in response to stimulation by CGRP, AM, and AM2 in human cardiac fibroblasts to 100μM Forskolin (**B**). Data are analysed using a three-parameter non-linear regression curve.

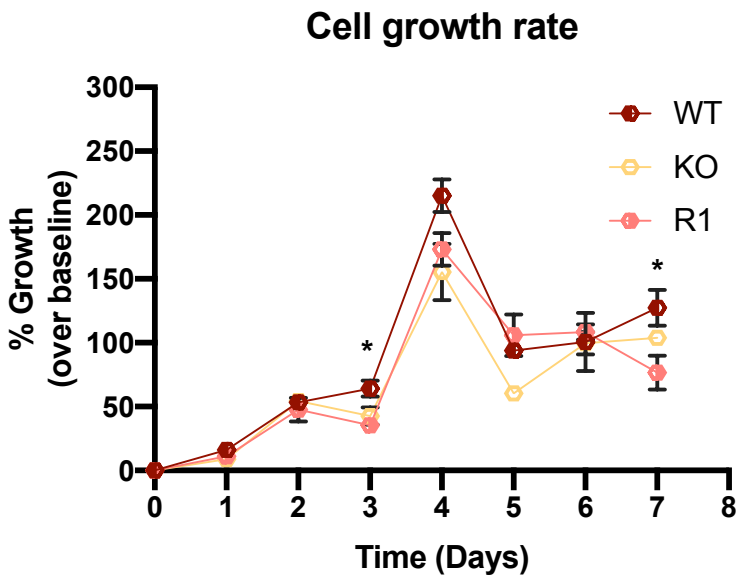

Supplemental Figure 8.7. **Proliferation of different cell populations over 7 days.** Comparison of the proliferative ability of WT-HUVECs, RAMP2 KO HUVECs and RAMP1-HUVECs. Statistical significance calculated using a one way Anova in comparison to the control (WT-HUVECs) for each day. Only RAMP1-HUVECs demonstrated significance on the indicated days.

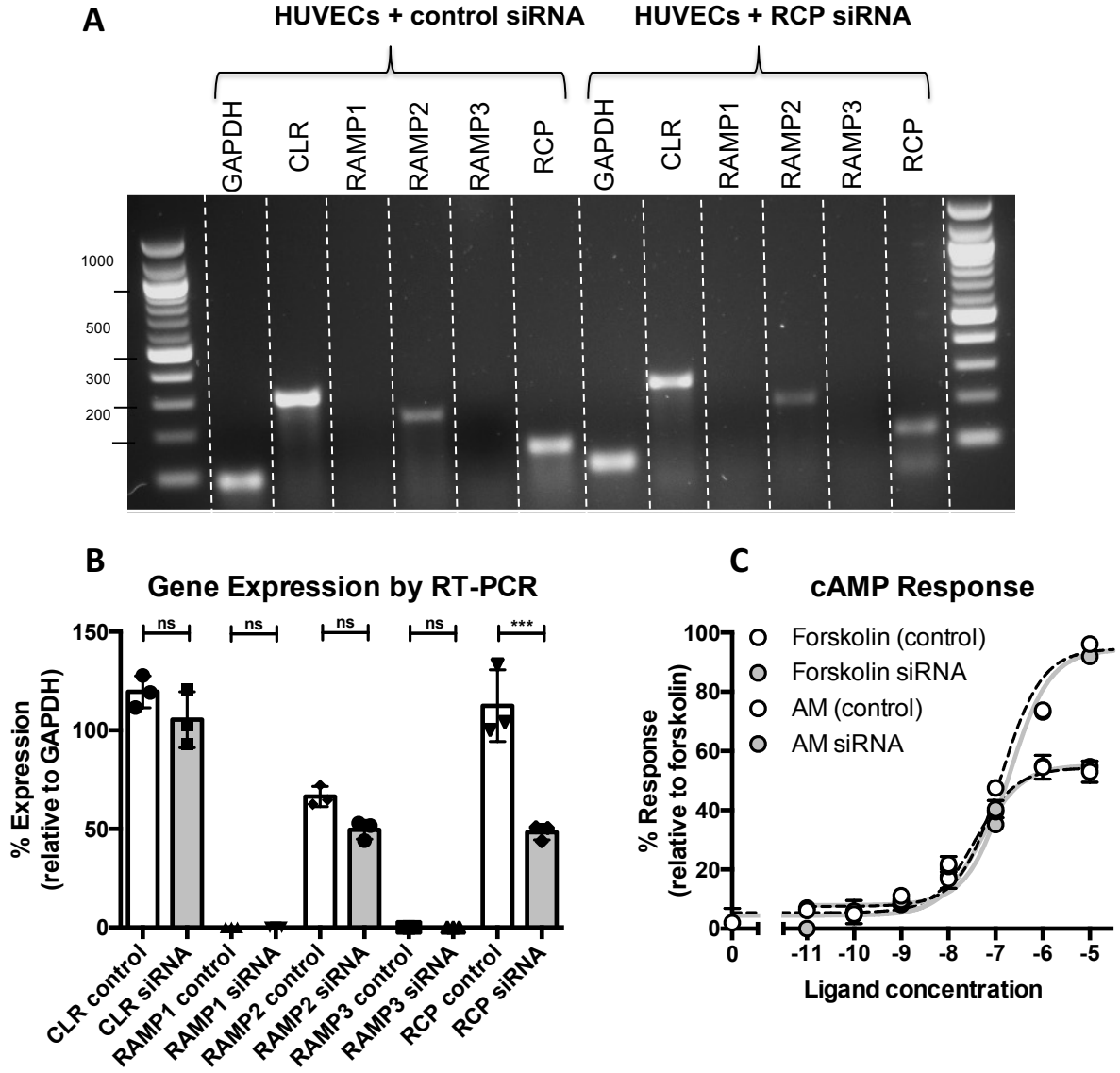

Supplemental Figure 8.8. Influence of RCP on endogenous CLR signalling in HUVECs: RT-PCR Gel showing results of RT-PCR (**A**), Densitometry analysis of RT-PCR expression (**B**) HUVEC cAMP in response to Forskolin and Adrenomedulllin (**C**). All data compares HUVECs treated 100nM RCP siRNA with 100nM scrambled siRNA for 48 h. Statistical significance determined compared to control using an unpaired t test with Welch's correction (*, $p<0.05$; **, $p<0.01$; ***, $p<0.001$ ****, $p<0.0001$). NS denotes no statistical significance observed. All values are calculated from 3 individual data sets

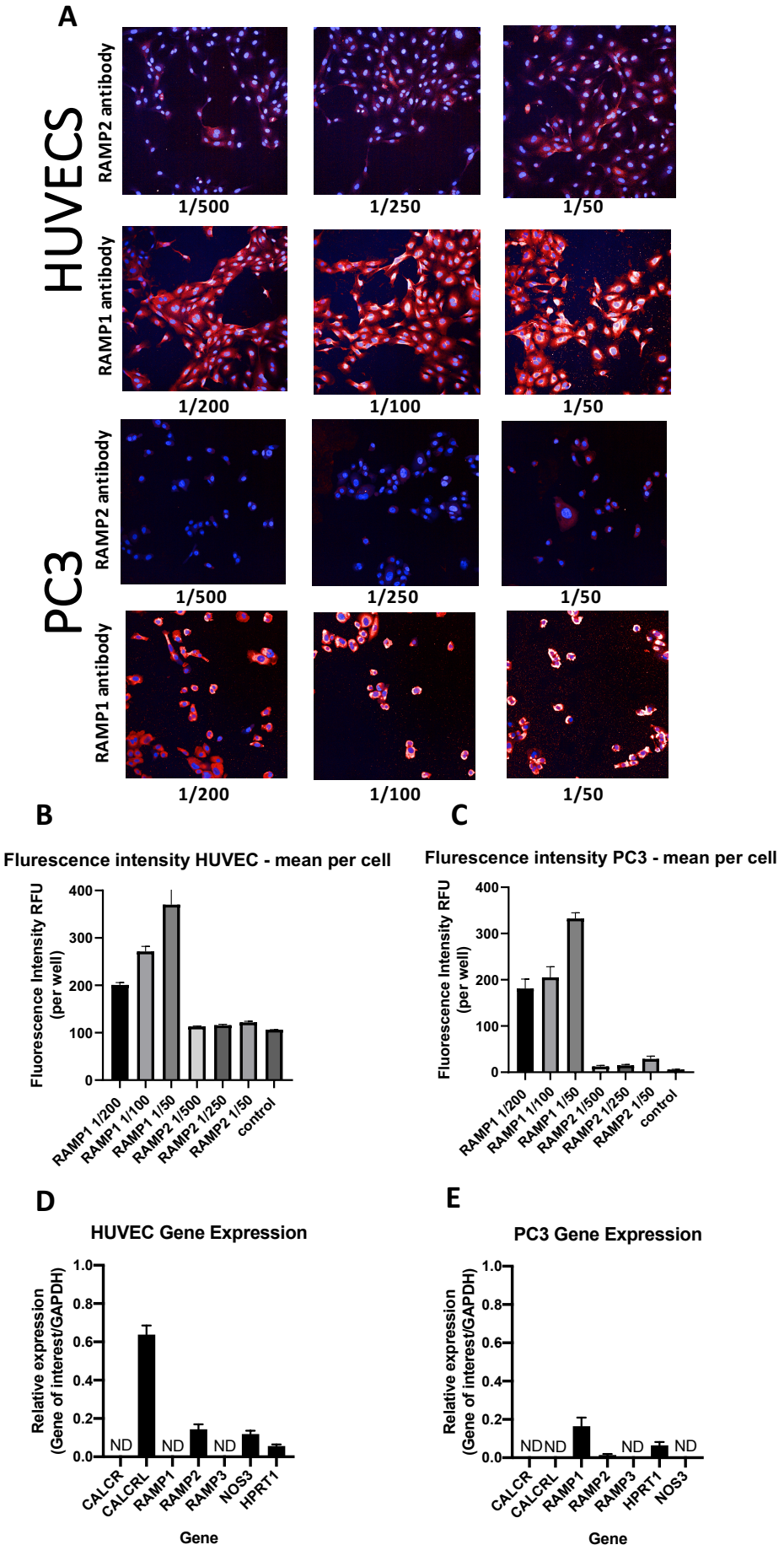

Supplemental Figure 8.9 Confocal antibody validation and qRT-PCR. Optimisation of a range of manufacturer suggested dilutions of antibodies for human RAMP1 and RAMP2 protein in HUVEC and PC3 cells. Cells treated with RAMP1 or RAMP2 protein antibody, and Hoechst nuclear stain imaged using 20x objective with both fluorescence channels overlaid (**A**). Analysis of mean fluorescence intensity/cell/well for each antibody over a range of concentrations in HUVECs (**B**), and PC3 (**C**) data represent mean + SEM of three independent experiments. Expression of CALCR, CALCRL, RAMP1, RAMP2, RAMP3, HPRT1, and NOS3 genes determined by qRT-PCR in HUVECs (**D**) and PC3 cells (**E**). Data represent mean + SEM of three independent experiments relative to GAPDH expression. ND = not detected in all three samples.